NASA Technical Memorandum

NASA TM - 100362

SPACE STATION CMIF EXTENDED DURATION METABOLIC CONTROL TEST FINAL REPORT

By Richard G. Schunk, Robert M. Bagdigian, Robyn L. Carrasquillo, Kathyrn Y. Ogle, and Paul O. Wieland

Structures and Dynamics Laboratory
Science and Engineering Directorate

March 1989

National Aeronautics and Space Administration

George C. Marshall Space Flight Center

TECHNICAL REPORT STANDARD TITLE PAGE

1. REPORT NO.	2. GOVERNMENT ACCESSION NO.	3. RECIPIENT'S CATALOG NO.
NASA TM-100362		

4. TITLE AND SUBTITLE	5. REPORT DATE
Space Station CMIF Extended Duration Metabolic Control Test Final Report	March 1989
	6. PERFORMING ORGANIZATION CODE
7. AUTHOR(S) Richard G. Schunk, Robert M. Bagdigian, Robyn L. Carrasquillo, Kathyrn Y. Ogle, and Paul O. Wieland	8. PERFORMING ORGANIZATION REPORT #
9. PERFORMING ORGANIZATION NAME AND ADDRESS George C. Marshall Space Flight Center Marshall Space Flight Center, Alabama 35812	10. WORK UNIT, NO.
	11. CONTRACT OR GRANT NO.
	13. TYPE OF REPORT & PERIOD COVERED Technical Memorandum
12. SPONSORING AGENCY NAME AND ADDRESS National Aeronautics and Space Administration Washington, D.C. 20546	14. SPONSORING AGENCY CODE

15. SUPPLEMENTARY NOTES

Prepared by Environmental Control and Life Support Branch, Thermal Engineering and Life Support Division, Structures and Dynamics Laboratory, Science and Engineering Directorate.

16. ABSTRACT

This report contains a discussion of the Space Station Extended Duration Metabolic Control Test (EMCT) that was conducted at the MSFC Core Module Integration Facility in November of 1987. The primary objective of the EMCT was to gather performance data from a partially-closed regenerative Environmental Control and Life Support (ECLS) system functioning under steady-state conditions. Included in the report is a description of the EMCT configuration, a summary of events, a discussion of anomalies that occurred during the test, and detailed results and analysis from individual measurements of water and gas samples taken during the test. A comparison of the physical, chemical, and microbiological methods used in the post test laboratory analyses of the water samples is included. The report also details the preprototype ECLS hardware used in the test, providing an overall process description and theory of operation for each hardware item. Analytical results pertaining to a system level mass balance and selected system power estimates are also included in the report.

17. KEY WORDS	18. DISTRIBUTION STATEMENT
Space Station Core Module Integration Facility Metabolic Control Test Environmental Control and Life Support Air Revitalization Water Recovery Regenerative	Unclassified – Unlimited

19. SECURITY CLASSIF. (of this report)	20. SECURITY CLASSIF. (of this page)	21. NO. OF PAGES	22. PRICE
Unclassified	Unclassified	191	NTIS

TABLE OF CONTENTS

TABLE OF CONTENTS (Concluded)

LIST OF ILLUSTRATIONS

LIST OF ILLUSTRATIONS (Continued)

LIST OF ILLUSTRATIONS (Continued)

LIST OF ILLUSTRATIONS (Concluded)

LIST OF TABLES

LIST OF ACRONYMS AND ABBREVIATIONS

BAC	Boeing Aerospace Company
CCA	Coolant Control Assembly (Static Feed Electrolysis)
CEU	Central Electronics Unit (Static Feed Electrolysis)
CFM	Cubic Feet per Minute
cm	Centimeter
CMIF	Core Module Integration Facility
CST	Central Standard Time
DCC	Display and Control Console (TIMES and Sabatier)
ECLSS	Environmental Control and Life Support System
EMCT	Extended Duration Metabolic Control Test
FCA	Fluids Control Assembly (Static Feed Electrolysis)
4BMS	Four Bed Molecular Sieve
ft	Feet
HFM	Hollow Fiber Membrane (TIMES)
hr	Hour
HX	Heat Exchanger
JSC	Johnson Space Center
KOH	Potassium Hydroxide
lb	Pound
MCT	Metabolic Control Test
meq	Milliequivalent
MMC	Martin Marietta Corporation
mmHg	Millimeters of Mercury (pressure)
MSFC	Marshall Space Flight Center
nom	Nominal
OD	Outside Diameter
PC	Personal Computer
PCA	Pressure Control Assembly (Static Feed Electrolysis)
pCO_2	Pressure of Carbon Dioxide
PDU	Performance Diagnostic Unit (Static Feed Electrolysis)
PPM	Parts Per Million
psia	Pounds per Square Inch Absolute
psid	Pounds per Square Inch Difference
psig	Pounds per Square Inch Gauge

REV	Revision
SFES	Static Feed Electrolysis Subsystem
SIT	Simplified Integrated Test
slpm	Standard Liters Per Minute
TCCS	Trace Contaminant Control Subsystem
TDS	Total Dissolved Solids
TED	Thermoelectric Device (TIMES)
TER	Thermoelectric Regenerator (TIMES)
TGA	Trace Gas Analyzer
TIMES	Thermoelectric Membrane Evaporation System
THCS	Temperature and Humidity Control System
TOC	Total Organic Content
TSA	Test Support Accessory (Static Feed Electrolysis)
umho	Micro Mhos (conductivity)
UV	Ultraviolet (light)
UPM	Urine Pretreat Mixer
Vdc	Volts Direct Current

TECHNICAL MEMORANDUM

SPACE STATION CMIF EXTENDED DURATION METABOLIC CONTROL TEST FINAL REPORT

1.0 INTRODUCTION

This report describes the Space Station Environmental Control and Life Support System (ECLSS) Extended Duration Metabolic Control Test (EMCT) that was conducted at the Core Module Integration Facility (CMIF) located in building 4755 of the Marshall Space Flight Center (MSFC). The test, which began on November 18, 1987, was 150 hr in duration with approximately 148 hr of integrated system operation. The EMCT was the final test of three tests making up the phase II system test program. Both of the prior tests were approximately 50 hr in duration. The first test, the Simplified Integrated Test (SIT) was conducted between June 9 and June 11 of 1987, and the second test, the Metabolic Control Test (MCT), was conducted between October 27 and October 29 of 1987. The SIT was primarily an "open-simulator" verification of the ECLS system and facility, while the MCT provided the first experience with testing the ECLS system inside of a "closed-simulator" under a simulated crew metabolic respiration simulation. Accounts of both of the previous tests are contained in separate reports. As the name implies, the EMCT was similar in scope to the MCT except longer in duration. The primary objectives of the EMCT were to gather performance data for a partial ECLS system functioning under steady state conditions and to conduct a system level mass balance under those conditions. The test was conducted inside a closed module simulator with nominal three-man metabolic design loads imposed.

In order to ascertain performance information, 250 measurements were monitored continuously by on-site personnel and archived for later recovery by an automated data acquisition system. Additionally, water and gas samples were taken during the test to aid in determining subsystem performance. All 250 measurements were reviewed. Results from over 70 of these measurements along with the water and gas sample data were selected for inclusion into this report.

2.0 TEST CONFIGURATION AND SCOPE

2.1 General

The EMCT configuration utilized four regenerative ECLS subsystems located inside the MSFC Core Module Simulator. The subsystems used were the Thermoelectric Integrated Membrane Evaporation System (TIMES) water reclamation subsystem, the 4-Bed Molecular Sieve (4BMS) carbon dioxide removal subsystem, the Static Feed Electrolysis (SFE) oxygen generation subsystem, and the Sabatier carbon dioxide reduction subsystem. The Trace Contaminant Control Subsystem (TCCS), which was used in the two previous tests, was not used in the EMCT to allow contaminants to build up for real-time analysis by the Trace Gas Analyzer (TGA). Also internal to the simulator, a temperature and humidity control system provided sensible and latent heat removal and ventilation for the module simulator atmosphere, and a commercial oxygen concentrator was used to simulate

metabolic oxygen consumption. A number of support hardware items were located outside the simulator including the TGA, a metabolic simulator, a Performance Diagnostic Unit (PDU) and a Test Support Accessory (TSA) for the SFE subsystem, and a Display and Control Console (DCC) for the TIMES and the Sabatier subsystems. Facility-provided services included a System and Components Automated Test System (SCATS) computer for data acquisition/management, bottled gases for metabolic simulations and system and subsystem purges, and necessary electrical power services.

Figure 2-1 shows the integrated phase II ECLS system test configuration in schematic detail. The five ECLS (TCCS not used in EMCT) subsystems are denoted as shaded areas while the bold lines represent the boundary of the simulator. A number of components, including the metabolic simulator and supply and product water tanks, were located outside the module simulator. Additionally, much of the SFE/Sabatier hydrogen interface line was routed external to the module simulator for safety reasons. The TGA which is shown in the schematic, was also located external to the simulator. The basic subsystem interfaces included the TIMES waste water input and brine output, the TIMES reclaimed water output to the SFE, the Molecular Sieve concentrated CO_2 and the SFE H_2 inputs to the Sabatier, the Sabatier product gas vent, and the SFE O_2 output. There were also additional interfaces for the addition of CO_2 and the removal of O_2 from the simulator. Referring to the schematic, the TIMES reclaimed water was delivered to a product water tank. This water was then pumped to the SFE through a TSA which was used as the SFE interface to facility services and other subsystems. The water was electrolyzed by the SFE into hydrogen and oxygen. The oxygen could be vented either internal or external to the simulator as shown (the external vent capability was normally used only during system start up). Hydrogen produced by the SFE was mixed with concentrated carbon dioxide from the Molecular Sieve in a mixing chamber located at the inlet to the Sabatier. As shown on the schematic, the Molecular Sieve utilized an accumulator to dampen the effects of the adsorption/desorption cycle. The H_2/CO_2 mixture was reduced to methane and water by the Sabatier. The methane, along with the excess constituent from the H_2/CO_2 reaction, was vented external to the simulator. Water from the reaction was collected in an external tank. Aside from the basic subsystem interfaces, much of the complexity of the system was to support sampling of interconnecting process streams, nitrogen purging of subsystems and gas lines, and a design philosophy that required all subsystems be capable of stand-alone independent operation. An external photograph of the core module simulator and the physical layout of the subsystems inside the simulator are shown in Figures 2-2 and 2-3. Figure 2-4 is a photograph of the internal module simulator as visible from the front. The mechanical interfaces for each of the major components are described in Sections 2.3 and 2.4.

2.2 Major Changes from the SIT and MCT

Several changes were made to the ECLS sytem and subsystems between the EMCT and the previous phase II tests, a number of which were related to the Molecular Sieve subsystem. During the SIT, it was discovered that significant quantities of air were contained in the Molecular Sieve concentrated carbon dioxide output. The problem was isolated to leaks caused by old seals on the five-way valves located on the inlets of the two carbon dioxide sorbent beds. Each five-way valve was replaced with a set of three commercial two-way valves (see Section 5.4 and the SIT Final Report for more information) configured to emulate the function of the original valve. The original five-way valves were scavenged from the Skylab backup flight unit. After the MCT, the Molecular Sieve subsystem air-return duct was routed to just upstream of the simulator heat exchanger in an effort to improve the temperature stability of the internal simulator environment. Prior to this change,

ORIGINAL PAGE IS
OF POOR QUALITY

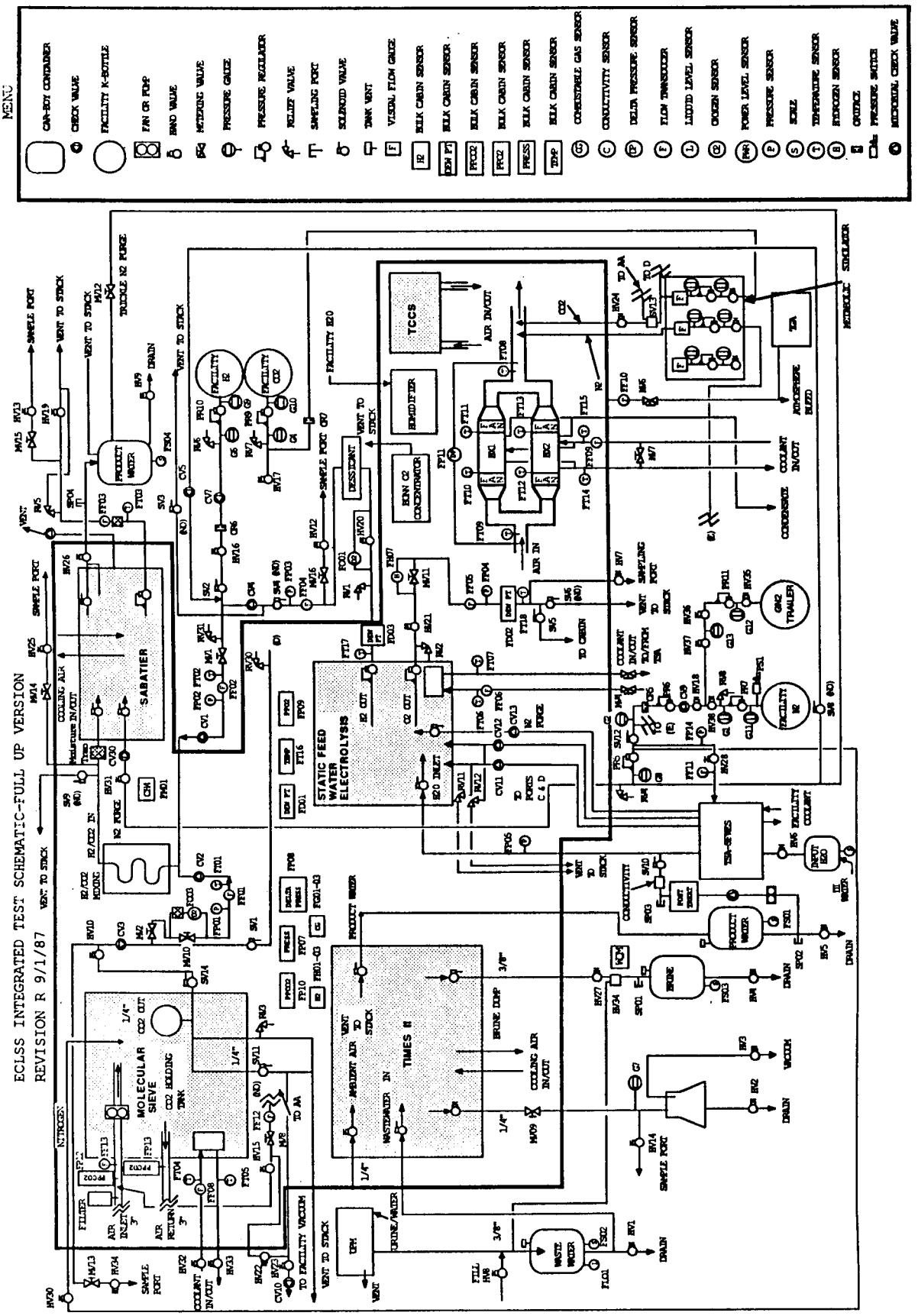

Figure 2-1. ECLS integrated test schematic.

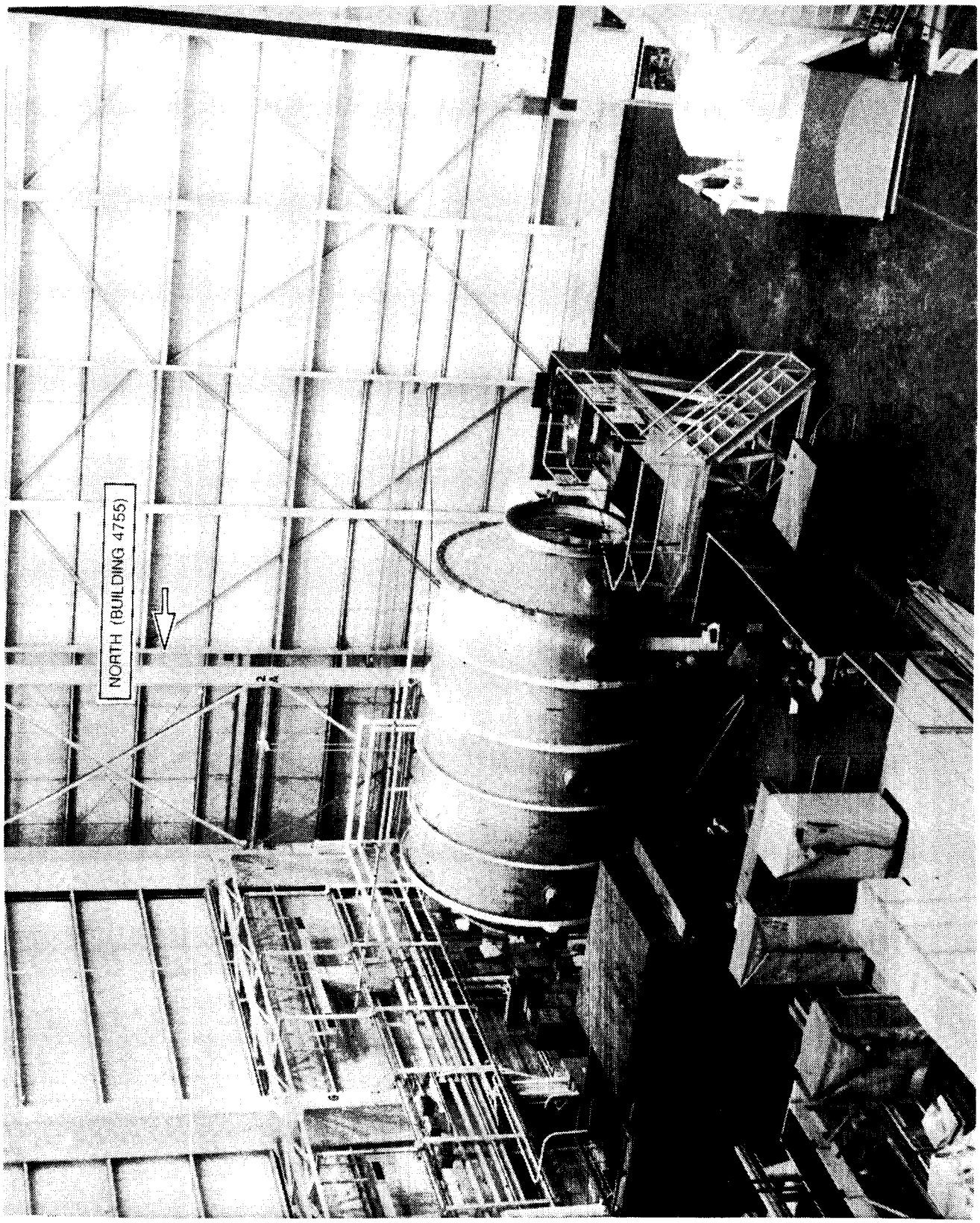

Figure 2-2. CMIF photograph.

ORIGINAL PAGE
BLACK AND WHITE PHOTOGRAPH

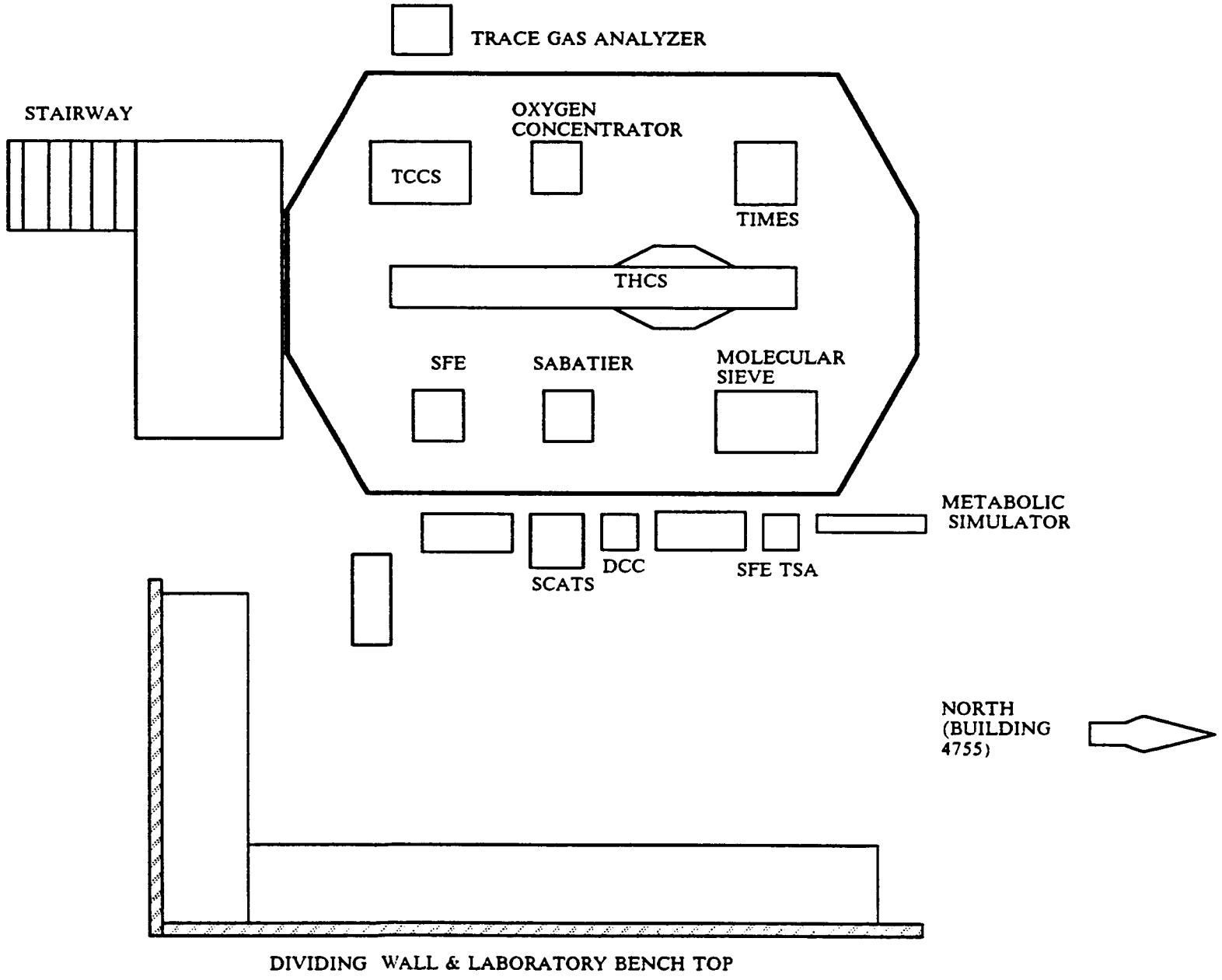

Figure 2-3. Phase II CMIF system test layout.

Figure 2-4. Internal simulator photograph.

the Molecular Sieve return air exhausted directly into the internal simulator environment creating a cyclic variation in the bulk simulator temperature, carbon dioxide partial pressure, and dewpoint. After the SIT, dry-bulb temperature sensors were added to the SFE hydrogen and oxygen output lines. The lines already contained dewpoint sensors. The new instrumentation was added to provide information on the relative humidity of the SFE oxygen and hydrogen output streams. Leakage problems were signficant during the MCT. Much effort was dedicated to reducing the leakage before the EMCT. A typical feed-through plate with "puddy" around the connections to reduce leakage is shown in Figure 2-5.

2.3 Subsystem Interfaces

2.3.1 TIMES

The TIMES achieves the reclamation of water from urine through a distillation process. During the test, pretreated urine was input to the TIMES from an elevated tank located outside the simulator. This tank was positioned on a weighing scale with an analog output to the TIMES. After processing, the reclaimed water was collected in a product water tank which was located on a similar scale. The reclaimed water was pumped from the product tank to the SFE subsystem after passing through a post-treatment bed. (Recycle of the TIMES output was activated by an internal conductivity sensor.) Other facilty interfaces for the TIMES included an overboard dump line for brine and a vent source to vacuum purge noncondensable gases from the TIMES internal steam passage. All internal TIMES measurements were recorded by the facility data management system through an RS-232 data link located on the TIMES controller. The Display and Control Console (DCC) was utilized by the TIMES and the Sabatier subsystem for real-time data display and evaluation and manual subsystem control and is shown in Figure 2-6. The DCC has the capability to display important subsystem data in a schematic format. A menu-oriented touchpad is used to issue commands. Figure 2-7 is a photograph of the TIMES installed inside the simulator. The process package is covered with removable insulation panels to prevent heat loss due to the elevated operating temperature (140°F) of the brine loop. A driver box is mounted on top of the package and houses the subsystem controller.

2.3.2 Four-Bed Molecular Sieve (4BMS)

The 4BMS subsystem removes and concentrates carbon dioxide from air via an adsorption/desorption process. During the test, air was pulled in from the module simulator by a Molecular Sieve internal fan and returned minus the removed carbon dioxide. The concentrated carbon dioxide was first collected in an accumulator before being mixed with hydrogen from the SFE subsystem in a mixing chamber. The CO_2/H_2 mixture was then reduced by the Sabatier. Other interfaces for the 4BMS included cooling water for thermal conditioning of desiccant bed outlet air, nitrogen for the operation of internal valves, and a vacuum source used to evacuate the CO_2 holding tank before filling with CO_2 prior to operation. Instrumentation external to the unit was used to measure inlet air flow, inlet and return air carbon dioxide partial pressure, and the concentrated carbon dioxide pressure, temperature, and flow. A sensor was also located in the carbon dioxide output stream to detect the presence of oxygen prior to hydrogen mixing. All measurements internal to the 4BMS were sent to the facility data management system through an instrumentation scanner. An IBM PC was used to display this information in a graphic format by interfacing with the facility data management

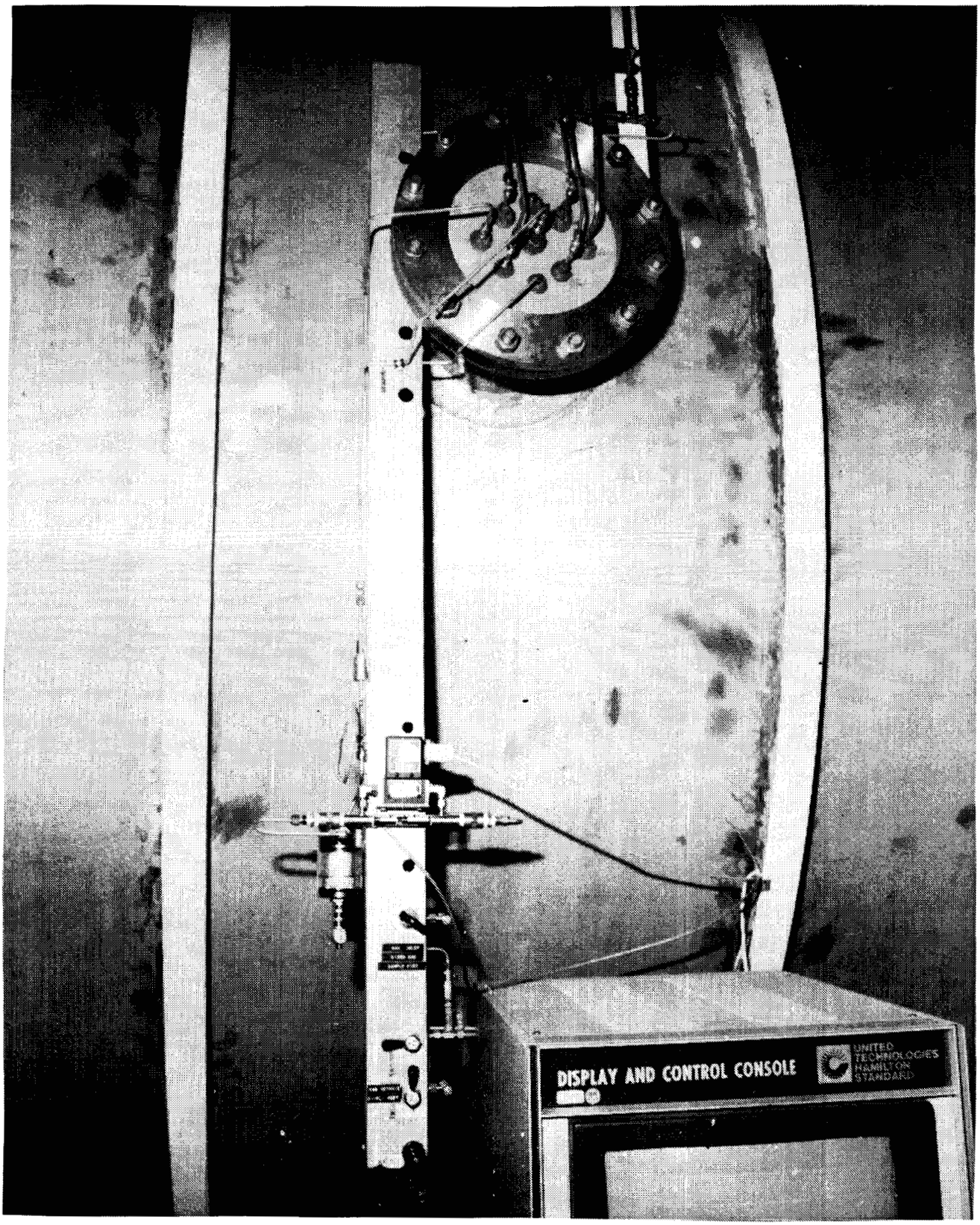

Figure 2-5. Feed-through plate photograph.

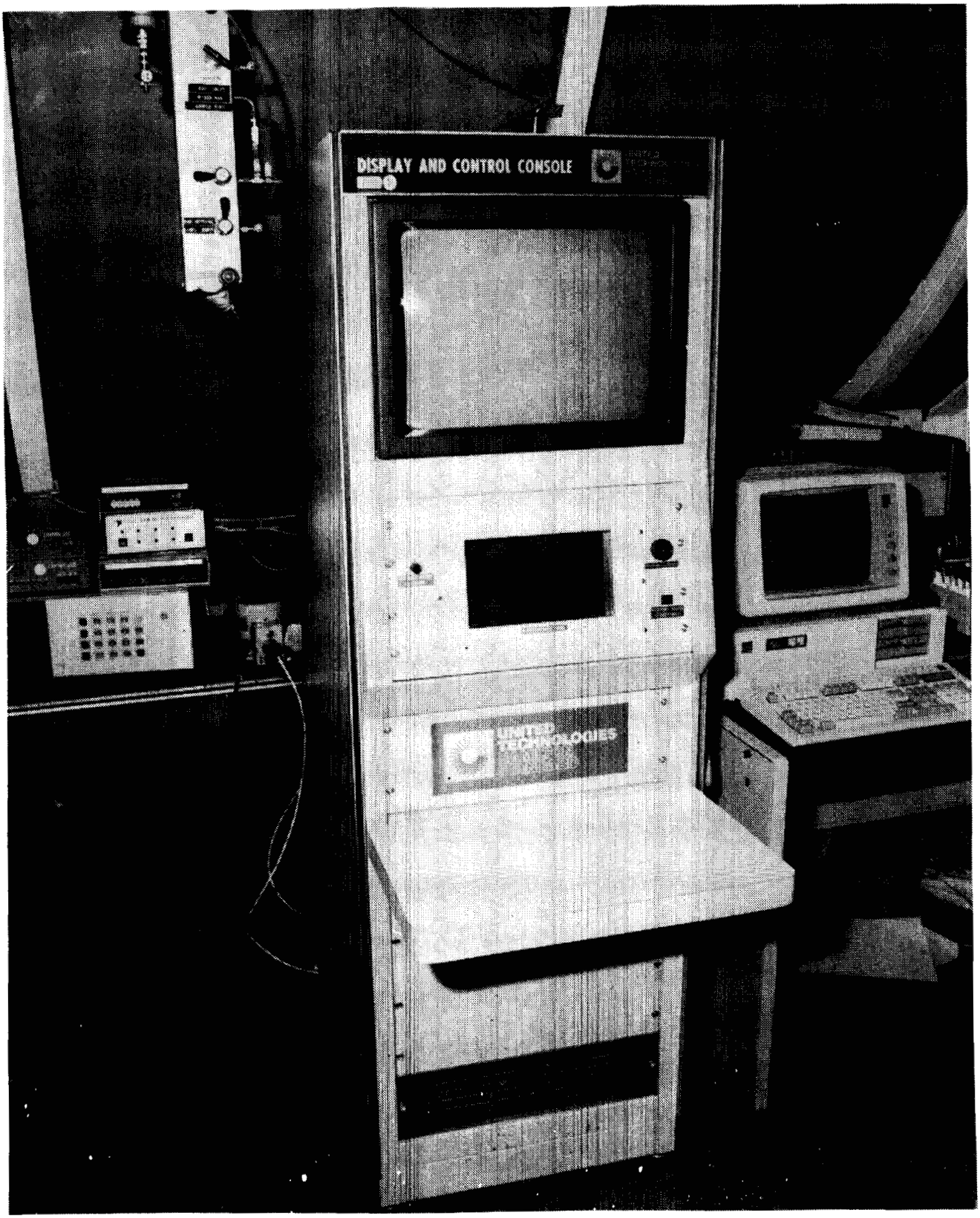

Figure 2-6. Display and control console photograph.

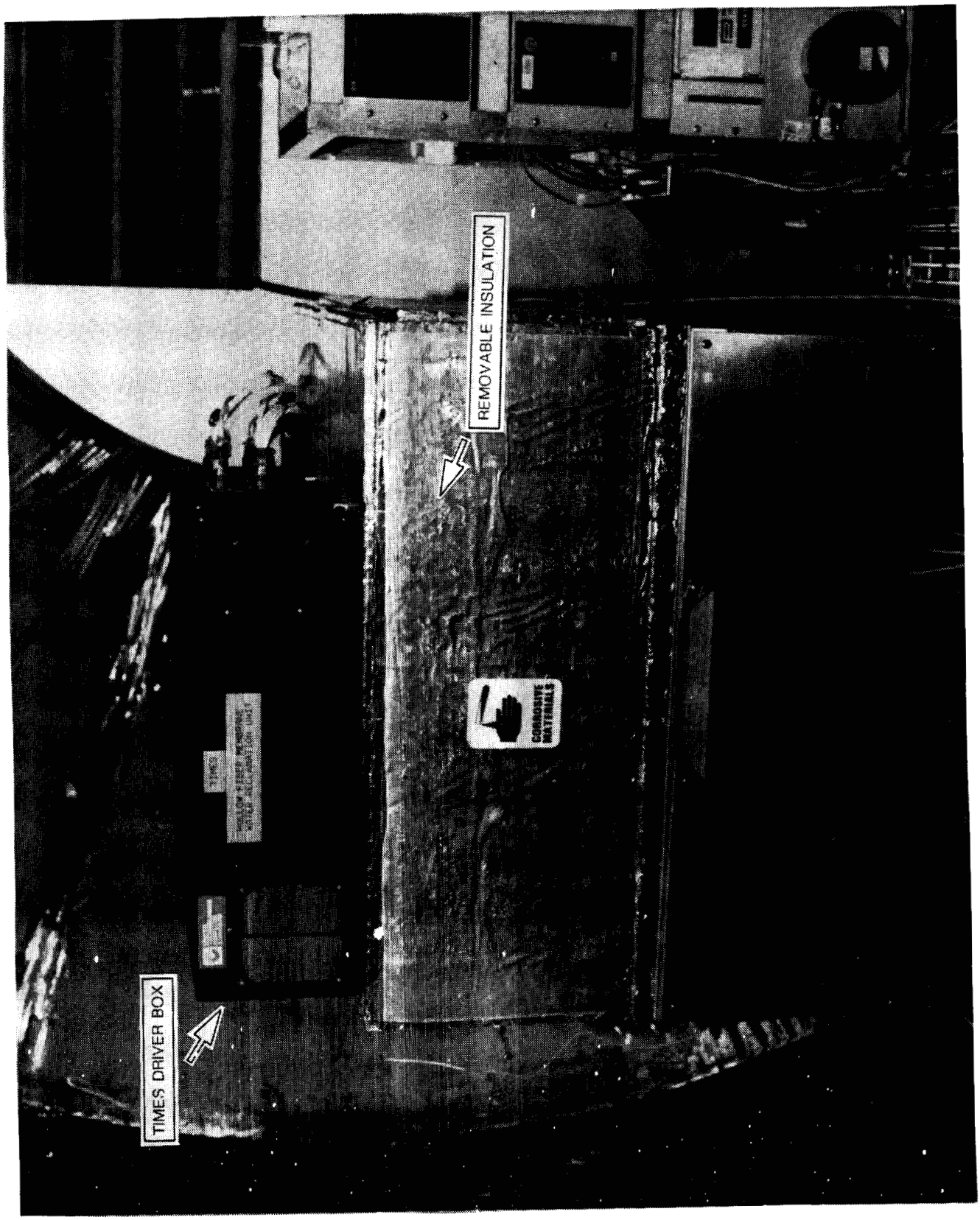

Figure 2-7. TIMES photograph.

ORIGINAL PAGE
BLACK AND WHITE PHOTOGRAPH

system through a serial bus. The 4BMS is shown in Figure 2-8. Air enters the Molecular Sieve through the inlet duct which is connected to the Temperature and Humidity Control System downstream of the condensing heat exchanger. The desiccant beds remove water vapor from the inlet air stream prior to adsorption. The sorbent beds are used to alternately trap and desorb the captured CO_2. Concentrated CO_2 is stored in the CO_2 accumulator, shown mounted underneath the subsystem.

2.3.3 Static Feed Electrolysis (SFE)

The SFE subsystem was designed to electrolyze water into hydrogen and oxygen. The phase II system was designed such that input water could be provided as either reclaimed water from the TIMES or deionized water from the facility. In the EMCT, the SFE TSA holding tank was initially charged with reclaimed water from a previous TIMES operation and thereafter was filled with TIMES product water generated during the EMCT. Except during sampling periods, the SFE subsystem's total oxygen output was directed into the closed simulator environment. The oxygen-output stream contained instrumentation to measure temperature, dewpoint, flow, and pressure as well as to detect the presence of hydrogen. Similarly, the SFE subsystem's total hydrogen output was directed to the Sabatier carbon dioxide reduction subsystem except during sampling. A moisture trap was located in the hydrogen output stream to prevent passage to downsteam components of potentially damaging moisture. Instrumentation on the hydrogen output stream was available to measure temperature, dewpoint, flow, and pressure as well as to detect the presence of oxygen. The SFE subsystem also used nitrogen for purging and facility water for cell stack temperature control. All inputs to the SFE subsystem were interfaced through the TSA. Internal measurements from the SFE were first processed by the PDU, which was used for subsystem control and real-time data display, before being sent to the facility data management system on a serial data bus. A photograph of the SFE mounted inside the simulator is shown in Figure 2-9. As shown in the figure, the SFE is comprised of a number of modular subassemblies designed to perform various subsystem functions such as the regulation of coolant (Coolant Control Assembly) and purge gas flow (Fluids Control Assembly), regulation of internal cell pressure (Pressure Control Assembly), and the electrolysis of water (Electrolysis Module). An external control box is also shown mounted on the support structure. A detailed explanation of the function of each of these components is provided in Section 5.3.1 of this document.

2.3.4 Sabatier

The Sabatier carbon dioxide reduction subsystem reacts a hydrogen/carbon dioxide mixture in the presence of a catalyst to form methane and water. If the hydrogen/carbon dioxide mixture is not balanced stoichiometrically, the excess constituent will pass unreacted into the gaseous output stream. During the test, hydrogen generated by the SFE and carbon dioxide concentrated by the Molecular Sieve were input to the Sabatier after passing through a mixing chamber and a moisture trap external to the unit. Instrumentation was available upstream of the mixing chamber to measure pressure, temperature, and flow of each input stream. The gaseous ouput from the Sabatier was vented outside the building while product water generated in the reaction was collected in a tank which was located on a scale similar to the ones used to weigh the TIMES input and output water. Instrumentation was available to measure temperature and flow of the gaseous output stream, although no real-time measurement was available to determine the composition of the exit stream. Both the gaseous input and

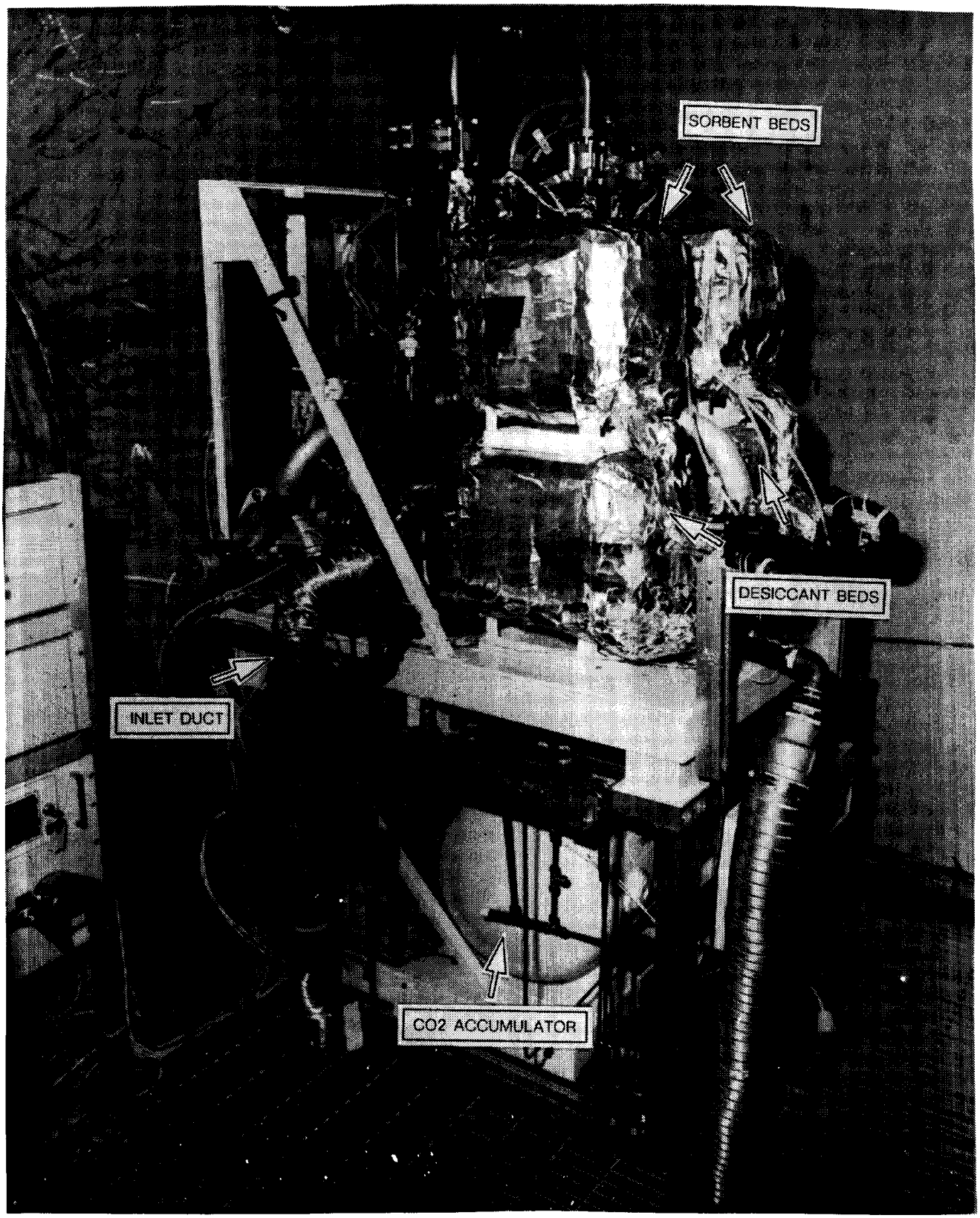

Figure 2-8. 4BMS photograph.

ORIGINAL PAGE
BLACK AND WHITE PHOTOGRAPH

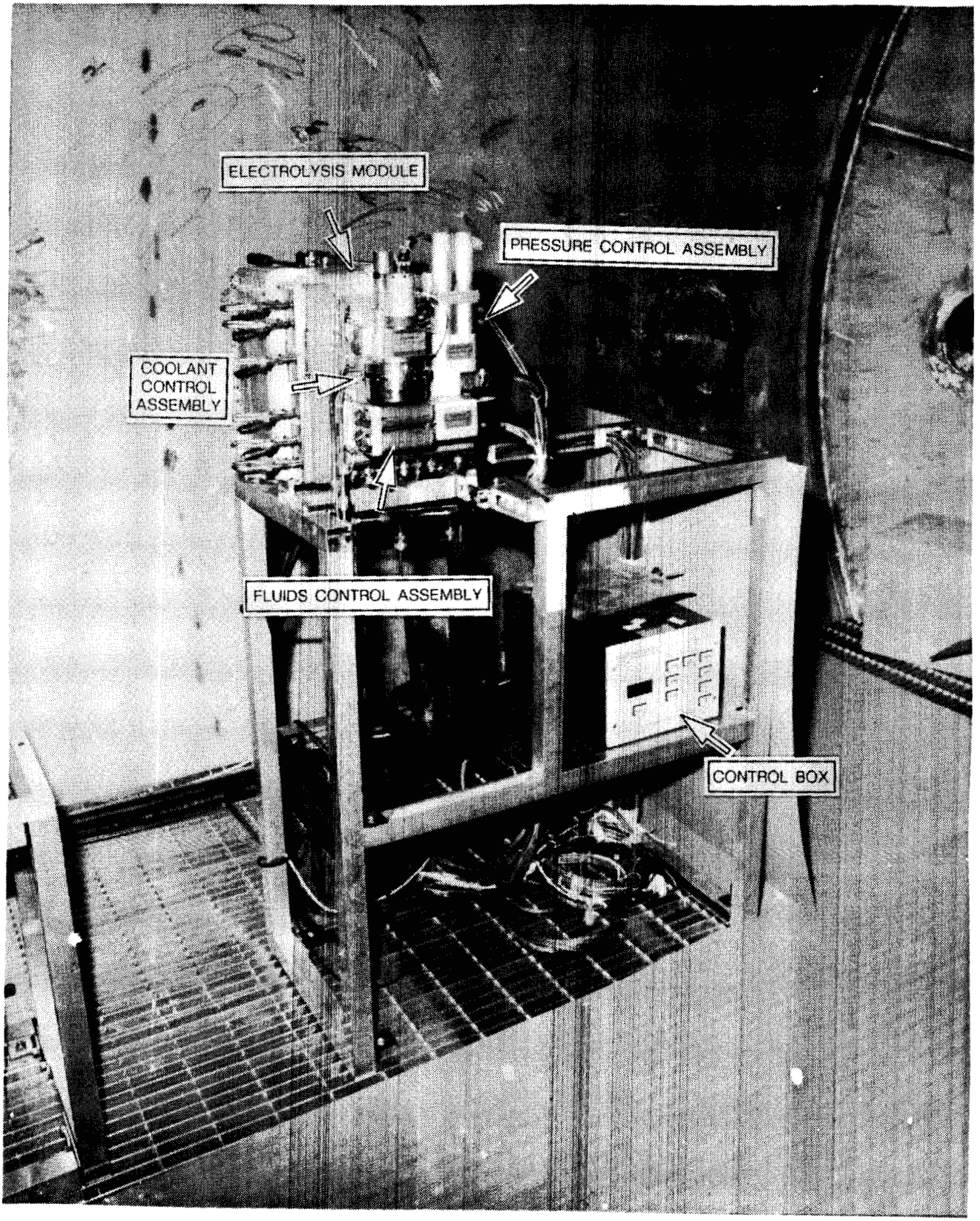

Figure 2-9. SFE photograph.

output streams on the Sabatier subsystem, as well as the product water tank, had provisions for sampling. Nitrogen was used as a purge gas for the unit. A "trickle" purge of nitrogen was also placed on the product water tank to prevent the possibility of dissolved methane from accumulating in the tank. Like the TIMES, internal measurements were sent simultaneously to the DCC and to the facility data management system (SCATS) in the form of serial data streams. The Sabatier subsystem is shown in Figure 2-10. Most of the important Sabatier components are visibly mounted in the frame. The reactor bed is where the carbon dioxide and hydrogen enter to be reacted into methane and water vapor. The hot gases then pass into the fan/condensing HX assembly where the water vapor is condensed out. Water from the reaction is separated from the gaseous stream at the water separator. A driver box, which is mounted on the frame, houses the subsystem controller.

2.4 Temperature and Humidity Control System (THCS), Metabolic Simulator, and Simulator Relief Valve

The internal THCS was built from commercial "off-the-shelf" components and was designed to provide sensible and latent heat removal from the module simulator internal environment as well as ventilation flow. All THCS components were located in the subfloor of the module simulator. An air-supply duct was located at one end of the simulator with the return duct at the opposite end. Condensate was collected in a drip pan located on the bottom of each of the heat exchangers where it was sent to the facility drain. Four fan/hx packages, each containing one heat exchanger and two fans, were used in the design. The THCS is shown in Figure 2-11.

The metabolic simulator was designed to allow for the introduction of various gases, namely carbon dioxide and nitrogen, into the module simulator. The metabolic simulator was constructed in the form of a panel with all components such as gauges, regulators, and valves mounted into the panel. During the EMCT, carbon dioxide was bled into the closed simulator duct at a three-man metabolic rate. Nitrogen was used as a make-up gas during the EMCT to maintain the simulator total pressure above ambient. The simulator also had an adjustable relief valve that would vent if the simulator internal pressure was approximately 3 mm Hg above the ambient pressure. Although highly functional, the relief valve was quite simple in design. Flexible "U" tubes connected to the internal simulator atmosphere were mounted such that their open ends were submerged in a beaker of water. The pressure at which the internal atmosphere would vent was set by the height of water in the beaker. A simplified diagram of the relief valve is shown in Figure 2-12.

Another part of the metabolic simulation was the oxygen concentrator device. This device is normally used in commercial hospital appications, but was adapted for use in the EMCT to simulate crew oxygen consumption. The unit uses an adsorption/desorption process much like the Molecular Sieve to concentrate the oxygen. The trapped oxygen was vented external to the simulator, thus simulating metabolic oxygen consumption. A schematic of the oxygen concentrator is shown in Figure 2-13.

2.5 Test Scope

Since the ECLS subsystems utilized in this test were a "preprototype" level, no effort was made to simulate many of the higher system management functions as well as interactions with other

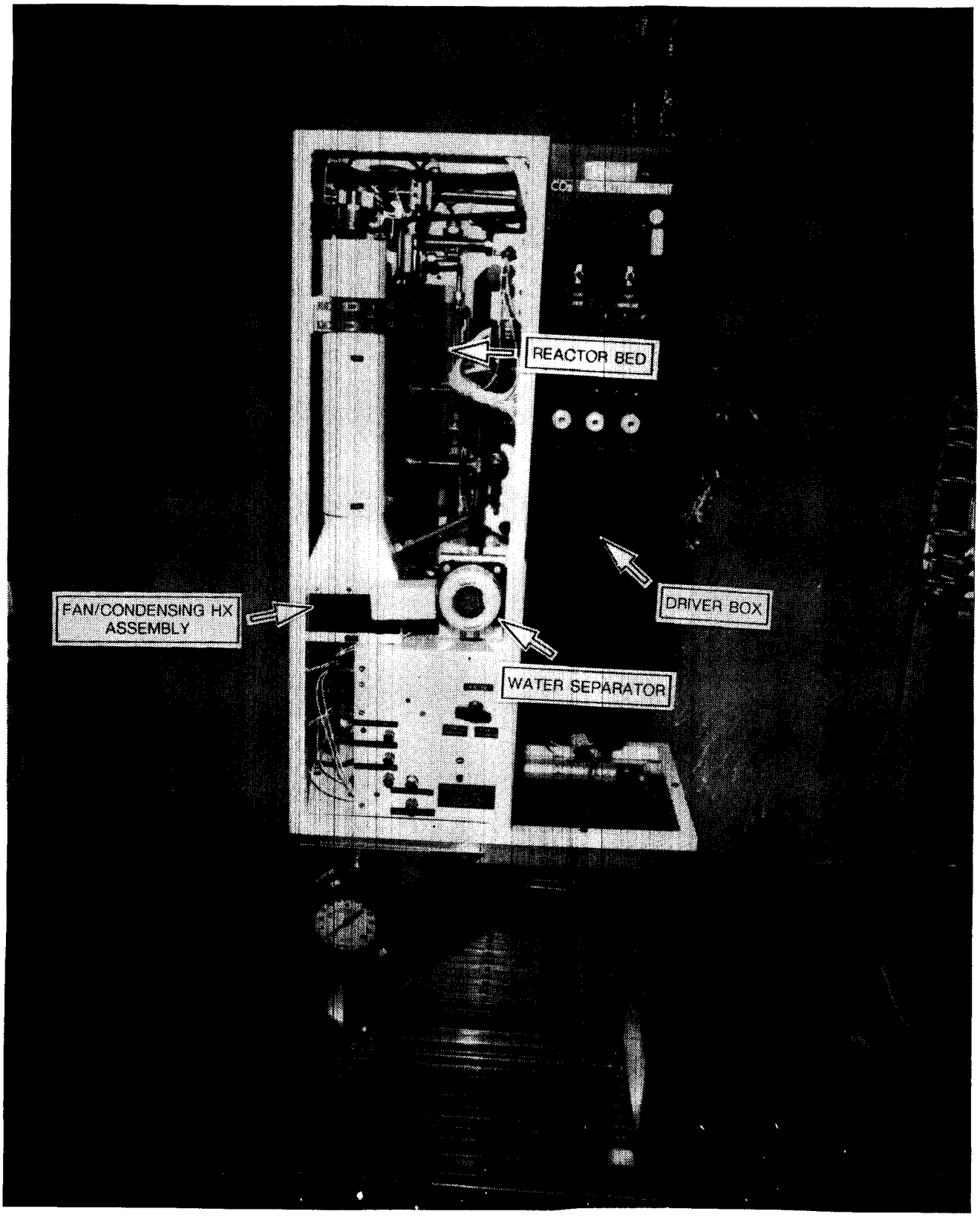

Figure 2-10. Sabatier photograph.

ORIGINAL PAGE
BLACK AND WHITE PHOTOGRAPH

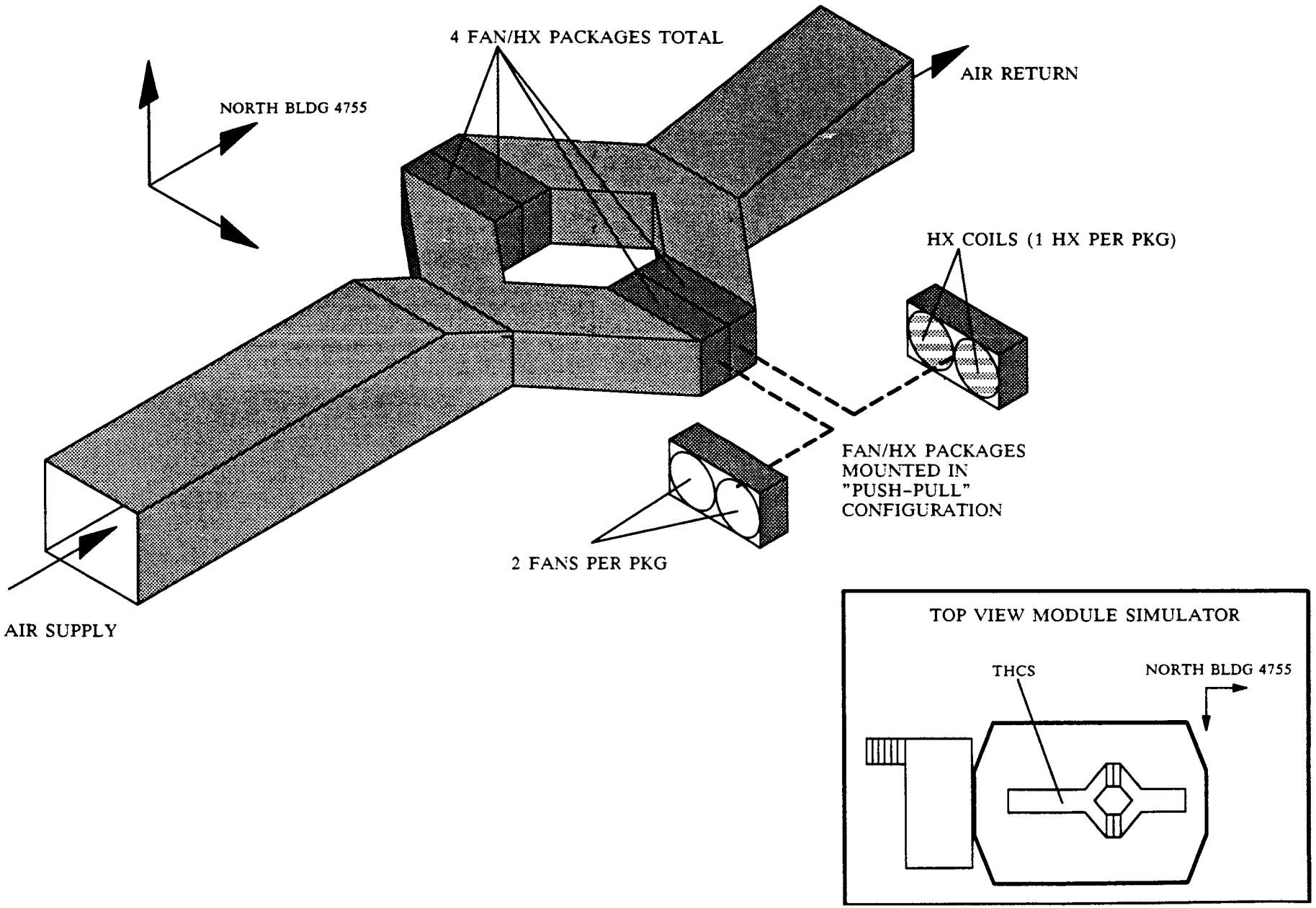

Figure 2-11. Phase II temperature and humidity control system.

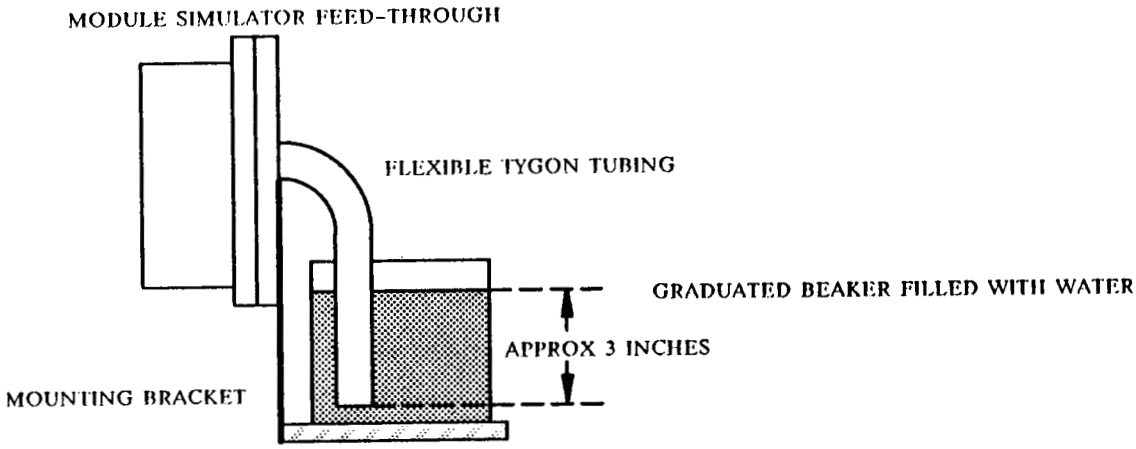

Figure 2-12. Module simulator pressure relief valve.

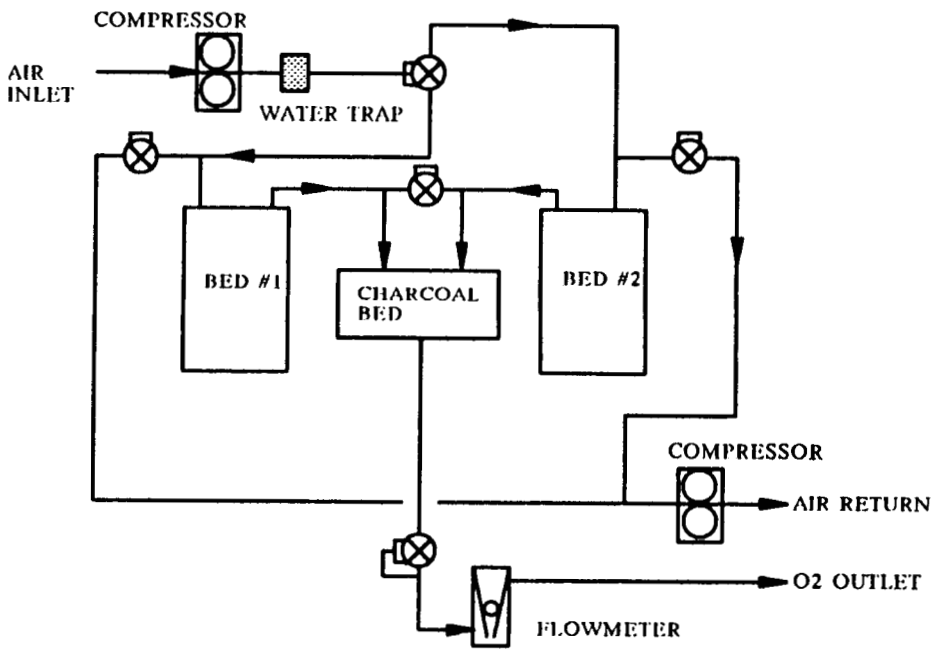

Figure 2-13. Oxygen concentrator.

space station elements such as thermal control and data management. In an actual flight system, many services such as O_2/N_2 supply and control, air distribution and handling, integrated data management and control, hygiene/potable water processing and supply, and thermal control would be present. In the current test scheme, these functions, if provided at all, are available only as a non-flight-like facility service. Data from this and subsequent tests should provide valuable insight to allow the evolution of the ECLS system test program at MSFC into a more flight-like simulation.

3.0 TEST SUMMARY

This section is a narrative of what is contained in the test log (see appendix A). A timeline showing all major events of the EMCT is provided in Figure 3-1. A more detailed explanation of each anomaly that occurred during the test is given in Section 4.0. The absolute times that are given in this section are followed by a number in brackets which is the test elapsed time in hr:min format.

The EMCT began at 1:00 p.m. (00:00) on Wednesday, November 18, 1987. Over the next 41 min the ECLS subsystems were activated in the following order: TIMES, SFE, Molecular Sieve, and Sabatier. At 3:25 p.m. (02:25) on November 18, the simulator door was closed. At 3:26 p.m. (02:26) hydrogen generation by the SFE was at full production and the hydrogen flow was diverted from the facility vent to the Sabatier CO_2 reduction subsystem. Similarly, the SFE-generated oxygen was diverted from the facility vent to the internal simulator. At 3:28 p.m. (02:28) the oxygen concentrator was activated to remove oxygen from the internal simulator at a three-person level. At 3:30 p.m. (02:30) the facility CO_2 input to the Molecular Sieve CO_2 removal subsystem was terminated and switched to the internal simulator. At 3:32 p.m. (02:32) the CO_2 addition rate was increased to a nine-person level to increase the CO_2 partial pressure buildup to 3mm Hg at a quicker rate. At 4:30 p.m. (3:30) the TIMES subsystem was put on standby for activation the next day. (This was a planned action as the TIMES was being cycled to process only a three crew-person amount of urine per day.) Aside from adjustments to the O_2 removal rate and CO_2 addition rate, operation continued nominally through the night.

On Thursday, November 19, at 8:00 a.m. (19:00), the TIMES was activated. Operation continued for the next 4:41 hours until 12:41 p.m. (23:41) when the TIMES was placed in the standby mode for activation the next day. Aside from a TGA sample at 1:27 p.m. (24:27) and an adjustment of O_2 removal rate at 2:55 p.m. (25:55), operation was uneventful during the second day of testing.

At 4:10 a.m. (39:10) on November 20, a low Molecular Sieve CO_2 holding tank pressure condition was discovered. Further investigation revealed that the Molecular Sieve controller was "stuck" in Mode 2 (for a complete discussion of Molecular Sieve operating modes see Section 5.2.1). At 4:19 a.m. (39:19) the Molecular Sieve was manually advanced to Mode 3A. The CO_2 holding tank pressure then began to increase. At 5:15 a.m. (40:15) on November 20 the Molecular Sieve was again manually cycled between modes. Susequently, the Molecular Sieve required manual cycling for every mode change. At 8:03 a.m. (43:03) the TIMES was activated. By 8:45 a.m. (43:45) the ECLS system had begun to recover from the Molecular Sieve controller anomaly. In the succeeding four hours since the anomaly occurred, the simulator partial pressure of CO_2 had reached a maximum of 4.3 mm Hg, but was now 3.8 mm Hg and trending downward. At 12:23 p.m. (47:23) the TIMES was placed in the standby mode after approximately 4 hr and 23 min of operation. A simulator air

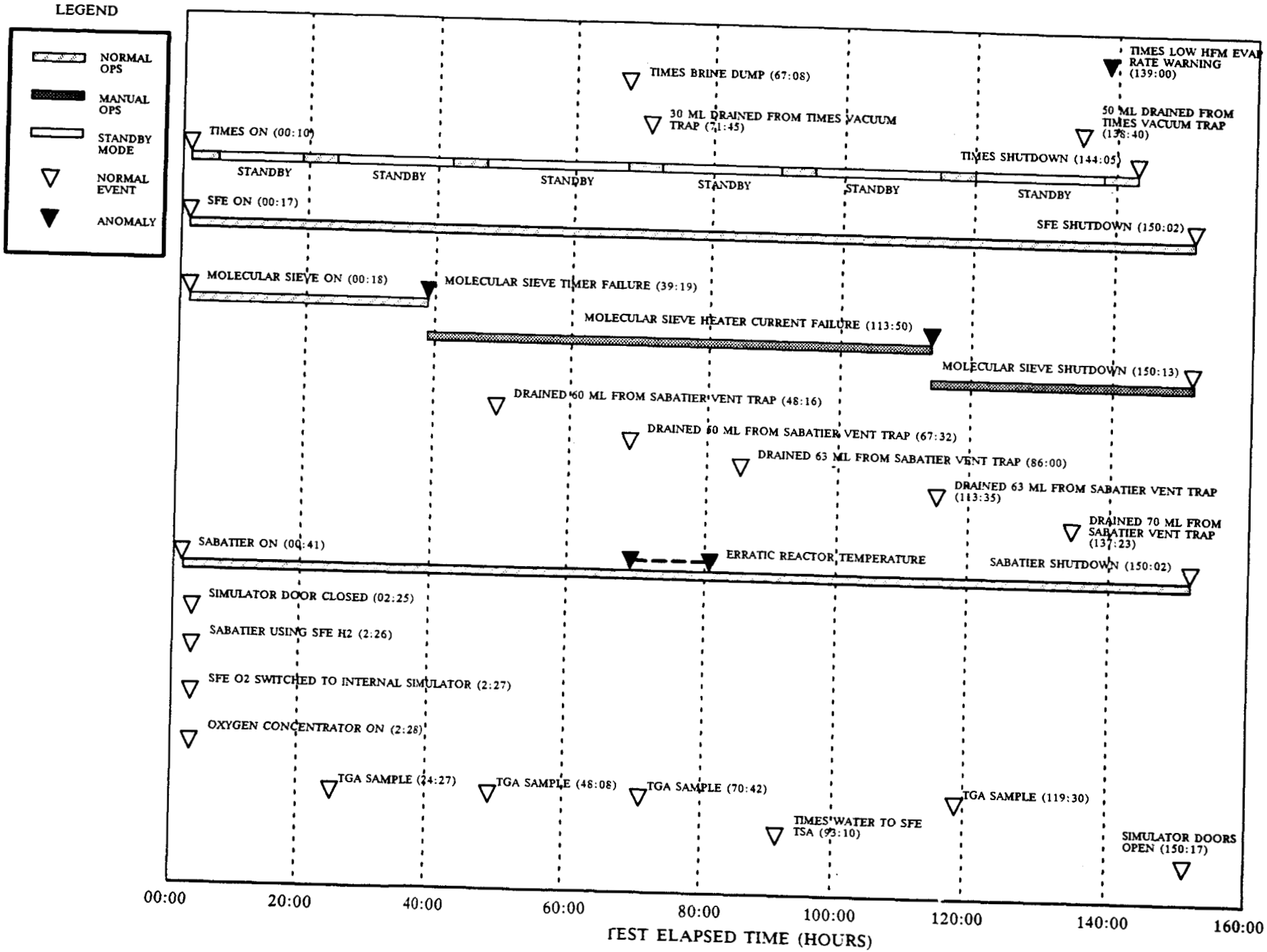

Figure 3-1. Extended duration metabolic control test outline.

sample was initiated at 1:08 p.m. (48:08) and was completed approximately 20 min later. At 1:16 p.m. (48:16) 60 ml of water was drained from the Sabatier water trap. Operation was uneventful through the night with no action taken until the following morning.

At 8:08 a.m. (67:08) on Saturday, November 21, the TIMES was activated. A brine dump was also initiated at this time. At 8:32 a.m. (67:32) 50 ml of water was drained from the Sabatier vent trap. At 10:34 a.m. (69:32) erratic behavior in one of the Sabatier reactor temperature sensors was noted. A TGA air sample was initiated at 11:42 a.m. (70:42). At 12:35 p.m. (71:35) the TIMES was placed in the standby mode after approximately 4 hr and 27 min of operation. Ten minutes later, at 12:45 p.m. (71:45), approximately 30 ml of water was drained from the TIMES vacuum trap. Operation continued normally through the night on November 21 except for erratic behavior of the Sabatier reactor temperature sensor at 6:00 p.m. (77:00).

On November 22 at 3:00 a.m. (86:00), the Sabatier vent trap was drained, recovering approximately 63 ml of water. The TIMES was activated at 8:02 a.m. (91:02). Several hours later at 10:10 a.m. (93:10), water was added to the SFE TSA from the TIMES product water tank. Conductivity measurements taken at that time showed the water to be within specification at 96 micromho/cm (limit = 100 micromho/cm). The TIMES was placed into the standby mode at 12:34 p.m. after 4 hr and 32 min of operation. Between 6:58 p.m. (101:58) and 9:05 p.m. (104:05) on November 22, a slight increase in the SFE O_2/H_2 delta pressure from 1.9 psid to 2.0 psid was observed. The alarm limit for this measurement was 2.5 psid, so no action was taken.

On November 23 at 6:35 a.m. (113:35), the Sabatier water trap was drained, recovering 63 ml of water. At 6:50 a.m. (113:50), a Molecular Sieve heater current failure was detected. Once the unit was powered off and restarted, normal operations resumed. The Molecular Sieve now no longer required the manual mode advances as the power off and restart sequence had apparently reset the faulty controller. At 7:58 a.m. (114:58), the TIMES was activated. At 9:40 a.m. (116:40), the Molecular Sieve timer failed, requiring a return to manual cycling operation. At 12:30 p.m. (119:30), the final TGA sample of the test was initiated. At 1:00 p.m. (120:00), the TIMES was placed in the standby mode.

On November 24 at 6:23 a.m. (137:23), 70 ml of water was drained from the Sabatier vent trap. The TIMES vacuum trap was drained of 50 ml of water at 7:40 a.m. (138:40). At 7:55 a.m. (138.55) the TIMES was activated. A TIMES low Hollow Fiber Membrane (HFM) evaporation rate warning was sounded at 8:00 a.m. (139:00). No action was taken as this was attributed to a transient startup condition. The TIMES was shut down at 1:05 p.m. (114:05). At 7:02 p.m. (150:02) on November 24, 1987, the shutdown sequence for the EMCT was initiated. At 7:17 p.m. (150:17), the simulator doors were opened and the test concluded. The phase II ECLS system had accumulated over 147 hr of integrated operation, the longest integrated ECLS system test at MSFC.

4.0 TEST ANOMALIES

Several anomalies occurred during the EMCT. An account of the anomaly and explanations, where possible, are given in the following sections.

4.1 Molecular Sieve Timer Failure

At 4:10 a.m. on November 20 (test elapsed time = 39:10 hr) it was discovered that the Molecular Sieve holding tank pressure was low at 6.474 psig (nom = 15.0 psig) with flow to the Sabatier diminished at 2.38 lb/day (nom = 6.0 lb/day). Subsequent investigation revealed that the Molecular Sieve was not cycling between modes and, thus, not allowing the adsorption/desorption beds to function properly. At 4:19 a.m. the Molecular Sieve was manually advanced to Mode 3A (see Section 5.2.1 for a complete discussion of Molecular Sieve operating modes) and a decision was made to continue the test while manually advancing the unit between modes. Operation continued for the next 74 hr and 31 min in this fashion with only a slight degradation in performance. Post-test investigation revealed a faulty diode in the control hardware of the Molecular Sieve.

4.2 Molecular Sieve Heater Current Failure

At 6:50 a.m. on November 23 (test elapsed time = 113:50 hr), the Molecular Sieve experienced a heater current failure. The Molecular Sieve uses heaters in its desorption beds to drive off the adsorbed CO_2 during the desorption cycle. With no heater power, the Molecular Sieve could no longer desorb CO_2 and the sorbent beds would become saturated with CO_2, eventually resulting in no capacity to remove CO_2. At the time of the failure, CO_2 partial pressure in the simulator increased due to the diminished performance of the subsystem. At the time the failure was discovered, the unit was shut down and then restarted with a return to normal operations. For approximately 3 hr the Molecular Sieve required no manual cycling until the timer failed again at 9:40 a.m.

4.3 Sabatier Reactor Core Temperature Sensor

At 10:34 a.m. on November 21 (test elapsed time = 69.32 hr), one of two Sabatier reactor core temperature sensors began to behave erratically. Since the CO_2 and H_2 inlet flows to the Sabatier were steady during this time and the other reactor core temperature sensor did not correlate with the erratic sensor, the sensor was believed to be faulty. No action was taken although there was concern that the faulty sensor may initiate a false shutdown of the subsystem if its value deviated too much from normal. This did not happen and the subsystem functioned normally for the remainder of the test. Post-test investigation revealed a faulty connection to the temperature sensor. The connection was repaired and the sensor has behaved normally in several subsequent short duration tests of the Sabatier subsystem.

4.4 TIMES HFM Low Evaporation Rate Warning

At 8:00 a.m. on November 24 (test elapsed time = 139:00 hr), shortly after activation, the TIMES indicated an HFM low evaporation rate warning. Since the warning was only 5 min after activation and no further problems were encountered, the warning was attributed to a transient condition upon startup. During the EMCT, the TIMES was run under a duty cycle where it was in a standby mode approximately 20 hr of every 24-hr period. Once in the standby mode, the TIMES HFM heaters were turned on to allow for a quicker startup when the unit was reactivated. Since the heaters maintain recycle loop temperatures in the vicinity of the HFM close to normal, this probably

forced the controller to issue the warning since the evaporation rate was still low so soon after startup. The anomaly occurred on the last day of testing so there was no opportunity to duplicate the problem.

4.5 Water Tank Scale Data Link Failure

The data link between three of the four product water-tank scales and the data acquisition computer failed shortly after the start of the EMCT. The product-tank weights were recorded manually for the duration of the test. This anomaly has been a recurring problem throughout each of the phase II tests with no solution found. Further study of this problem is planned before the next phase of testing.

5.0 SUBSYSTEM DISCUSSIONS OF RESULTS

The following sections discuss the test results for each individual subsystem in detail. At the beginning of each section is a brief description of each subsystem including theory of operation.

5.1 TIMES

5.1.1 Subsystem Description

A schematic of the TIMES utilized in the EMCT is provided in Figure 5-1.1. The main elements of the subsystem are the dual evaporators and the thermoelectric regenerator (TER). The function of these two elements is to produce a low temperature, purified steam distillate from concentrated wastewater while reducing the inherent power requirement associated with any phase-change process.

Each evaporator consists of three HFM assemblies. Each assembly includes 100 tubes (0.04 in. ID, 0.05 in. OD, 7.5 ft long) made of Nafion, a fluorocarbon-based cation exchange material. The function of the tubes is to control the vapor/liquid interface in microgravity. Heated wastewater, at a temperature of approximately 140°F, flows through the inner diameter of these tubes. Water is transported through the walls of the tubes by diffusion and ion exchange mechanisms. Vaporization occurs at the outer surfaces of the tubes which are maintained at a pressure of 2.7 psia.

The TER is an integrated package consisting of two wastewater heat exchangers and two arrays of thermoelectric devices (TED) as well as a common condensing heat exchanger. The hot sides of the TEDs are in contact with the two wastewater heat exchangers and the cold sides with the condenser. In this arrangement the TEDs are able, through the application of power (28 Vdc, 9 A total), to transfer heat from the condenser to the heat exchangers, thereby effectively recovering the heat of vaporization for reuse.

Wastewater is gravity-fed to the TIMES from a facility storage tank. Within the subsystem, the wastewater feed is preheated via a regenerative heat exchanger and combined with a concentrated

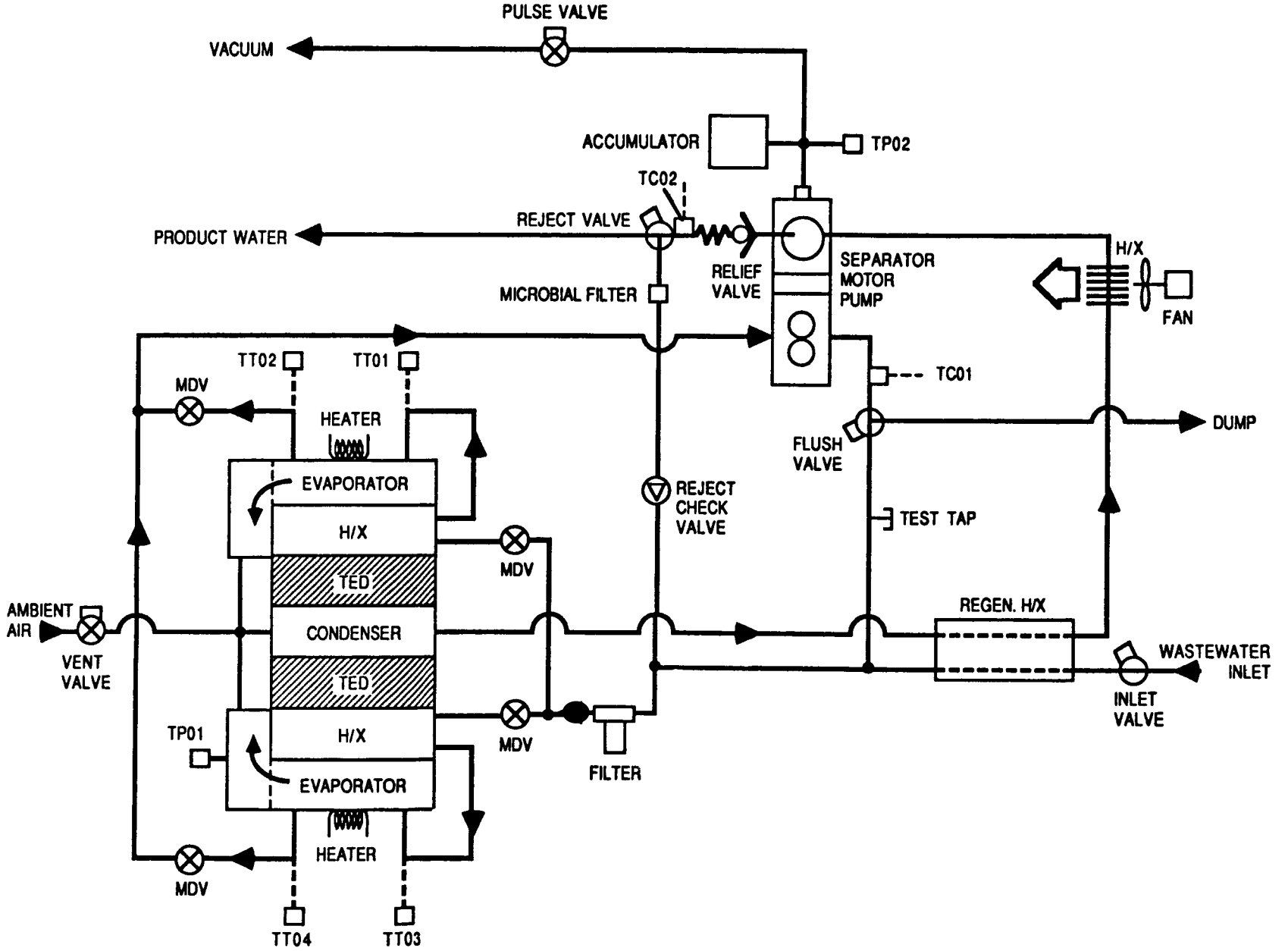

Figure 5-1.1. TIMES schematic.

brine solution that is recirculated internally at a rate of 600 lb/hr. The brine is passed through a 25 micron polypropylene filter which protects the HFMs from gross particulate contamination. Effluent from the filter is split and flows through the wastewater heat exchangers which raise the temperature of the brine to approximately 140°F. The heated brine flows through the two HFMs. The portion of the brine that does not evaporate during a single pass through the HFMs is recirculated via the recycle pump for additional processing.

Steam generated in the evaporators is partially condensed in the condenser. The latent heat that is released is transferred by the TEDs to the wastewater heat exchangers. Additional condensation occurs through heat transfer to the incoming wastewater in the regenerative heat exchanger. Final condensation is accomplished with an air-cooled heat exchanger. Noncondensable gases such as carbon dioxide are removed from the condensate via a centrifugal air/water separator, stored in an accumulator, and periodically purged to a facility vacuum source to maintain a subsystem reference pressure of 1.6 to 20 psia. A check of condensate quality is provided by a conductivity sensor prior to delivery to a facility product water storage tank. Condensate, with a conductivity in excess of 250 umho/cm, triggers an alarm and results in the condensate being returned, via the reject valve, to the recirculation loop for reprocessing.

Heaters are installed on the exterior surfaces of the two evaporators. These heaters are utilized during the initial startup of the unit to prevent excessive condensation from accumulating in the evaporators before steady-state operating temperatures are reached. The heaters are turned off once the temperature of the evaporator, as inferred from the HFM inlet and outlet temperatures, reaches approximately 130°F and remain off under nominal processing conditions.

5.1.2 Post Treatment Module Description

A post treatment sorbent bed was provided to polish the aggregate distillate produced by the TIMES. The bed contained both activated carbon and a mixed ion-exchange resin. The exact specifications of the activated carbon and the resin were not recorded prior to the test. The bed also did not have any provisions (such as the inclusion of iodinated resin or heaters) for microbial control.

The bed was located between the TIMES product water tank and the TSA for the water electrolysis subsystem. A pump was used, on a periodic basis, to pump aggregate distillate from the TIMES product water storage tank, through the post-treatment bed, and into the TSA storage tank or out through a facility sampling port.

5.1.3 Discussion of Results

5.1.3.1 General

Throughout the test the TIMES processed a wastewater mixture comprised of 75 percent pretreated urine and 25 percent deionized water by volume. The addition of deionized water is required to simulate the amount of urinal flush water projected to be required for space station operations. The pretreatment formulation used is listed in Table 5-1. Throughout the remainder of this report, the mixture of pretreated urine and deionized water will be referred to simply as pretreated urine.

TABLE 5-1 PRETREATED URINE COMPOSITION

Pretreatment Chemicals	Dosage (g/l)*
Sulfuric Acid	2.52
Oxone	5.00

Pretreat Urine/Deionized Water Mixture Ratio	
Pretreated Urine	75% v/v
Deionized Water	25% v/v

* refers to grams of chemical per liter of raw urine (i.e., urine without flush water)

The TIMES operated for a total of 31.5 hr over the course of the test. Since the nominal water production rate of the TIMES exceeds that required to process a daily three-man load of urine, the subsystem was operated in a batch mode. Each day, the TIMES was operated for between 3.33 and 5.33 hr until the daily quantity of urine processed approximated a three-man load. In order to facilitate the understanding of the trends shown in the various measurements discussed below, the times associated with each of the seven process cycles are listed in Table 5-2.

Between each process cycle, the subsystem was placed in Off mode. In order to minimize the heat load variations on the simulator and allow for a quicker subsystem startup, the evaporator heaters were powered throughout the entire test. During process cycles, power to the heaters was reduced slightly in an effort to maintain the appropriate process temperatures.

TABLE 5-2 ELAPSED TEST TIME (hrs)

Date	Cycle	Cycle Start	Cycle Stop
11/18	DAY 1	0.2	3.5
11/19	DAY 2	19.0	23.7
11/20	DAY 3	43.0	47.4
11/21	DAY 4	67.1	71.6
11/22	DAY 5	91.0	97.7
11/23	DAY 6	115.0	120.0
11/24	DAY 7	138.9	144.2

5.1.3.2 Pretreated Urine Processing Rate

The TIMES wastewater tank scale is shown in Figure 5-1.2. As derived from the figure, the TIMES processed a total of 83.5 lb of pretreated urine over seven processing cycles totaling 31.52 hr. This translates into an average urine processing rate of 11.9 lb/day of 2.65 lb/hr. A brine dump was initiated manually at approximately 67:00 hr and appears as a sharp drop of approximately 9.7 lb in the wastewater tank scale reading prior to the beginning of the Day 4 processing cycle. This drop is due to the rapid replacement of brine within the internal recycle loop with fresh pretreated urine. The brine dump was initiated inadvertently. As shown in Section 10, the total solids concentration of this brine was later measured to be 71,394 ppm or about 7.2 percent. This is below the maximum concentration typically tolerated by the TIMES during normal operation. Fresh pretreated urine was added to the wastewater storage tank at approximately 25:00 hr, 90:00 hr, and 138:00 hr accounting for the sharp increases evident in Figure 5-1.2 at these times.

The maximum urine processing rate observed during the test was 4.01 lb/hr in the early stages of operation. By Day 3 the urine processing rate had dropped to 2.66 lb/hr due to the normal accumulation of solids within the internal brine loop. Following the brine dump, the urine processing rate on Day 4 was 3.66 lb/hr and gradually decreased to 2.44 lb/hr by the end of the test.

Figures 5-1.3 and 5-1.4 show the quantities of processed distillate and brine in the TIMES product water tank and brine tanks, respectively. These figures were prepared using data recorded manually over the course of the test. Automatic acquisition of this data was not possible due to communications problems between the respective scales and the SCATS data acquisition system. Since data was not recorded until 3 hr into the test, an accurate measure of distillate production on Day 1 is not possible. On Days 2 through 4, distillate production decreased from 2.70 to 2.54 lb/hr. During the process cycle on Day 5, approximately 27.7 lb of distillate was pumped from the TIMES product tank to replenish the water supply in the SFWES feed tank. This accounts for the sharp drop appearing in the middle of Day 5 in Figure 5-3. The drop on Day 6 is attributable to the collection of water samples directly from the TIMES product water tank and from distillate pumped from the tank through the post-treatment module. The total quantity of water samples collected was not recorded and therefore the quantity of distillate produced on Day 6 cannot be determined.

In Figure 5-1.4, the brine dump is clearly shown as an increase of approximately 9.7 lb at 67:00 hr. The drop at approximately 118:00 hr represents the collection of brine for subsequent analysis.

An estimate of the overall water recovery efficiency achieved over the course of the test can be made using the waste and product water quantity data from Days 2 through 5 when such data was most complete. Over the course of these days, a total of 52.25 lb of urine was fed to the TIMES and a total of 46.36 lb of distillate was produced. As described in Section 10.0, an analysis of the total solids concentration of the pretreated urine measured 21.604 ppm or roughly 2.2 percent. The measured total solids concentration of the raw distillate was 61 ppm. Combining the definition of overall water recovery (i.e., total mass of water produced divided by the total mass of water fed) with an overall solids balance yields a calculated overall water recovery efficiency for Days 2 through 5 of 90.7 percent. The water lost with the brine dump is not included in this calculated efficiency since the dump was initiated inadvertently.

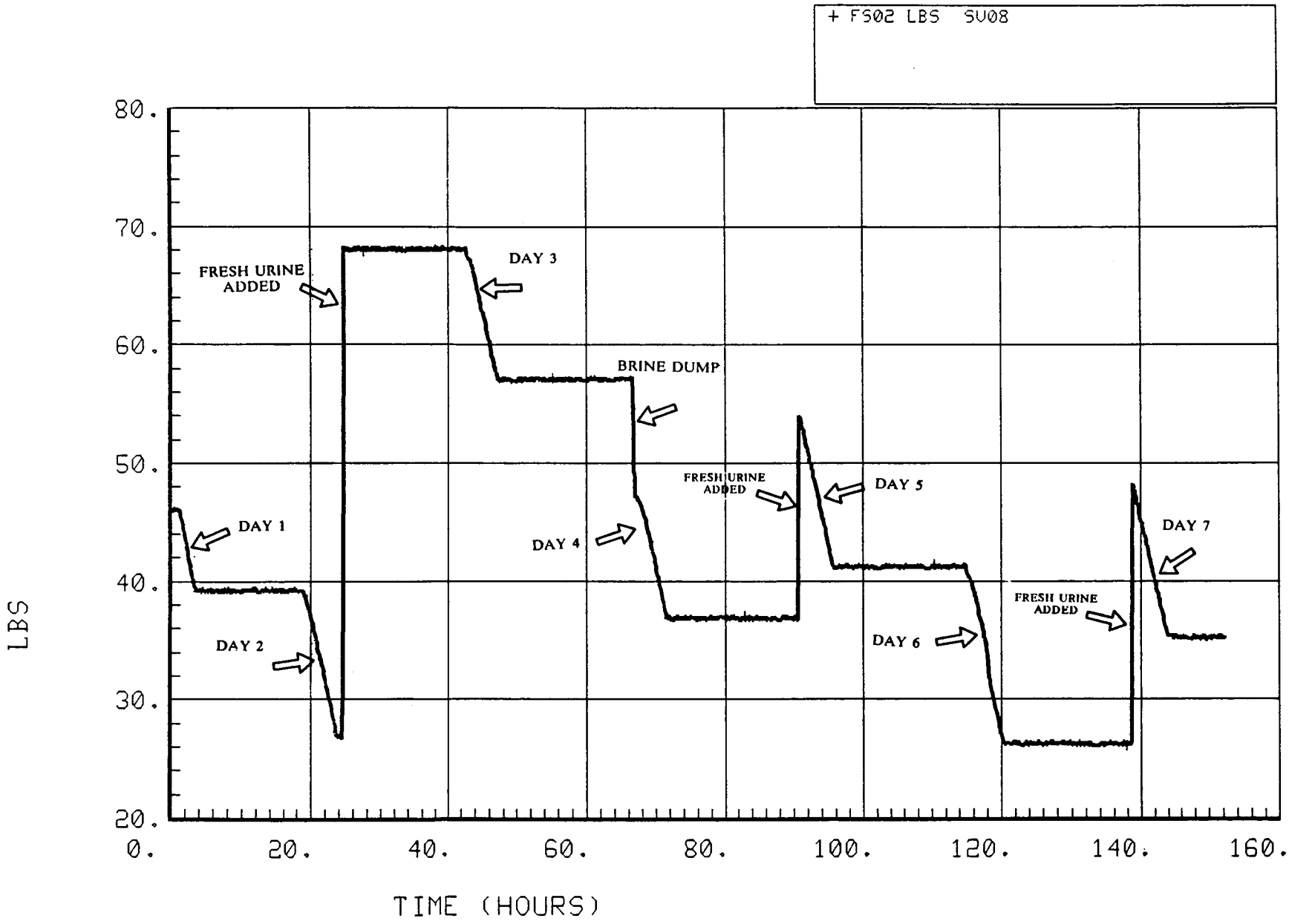

Figure 5-1.2. TIMES waste water tank scale.

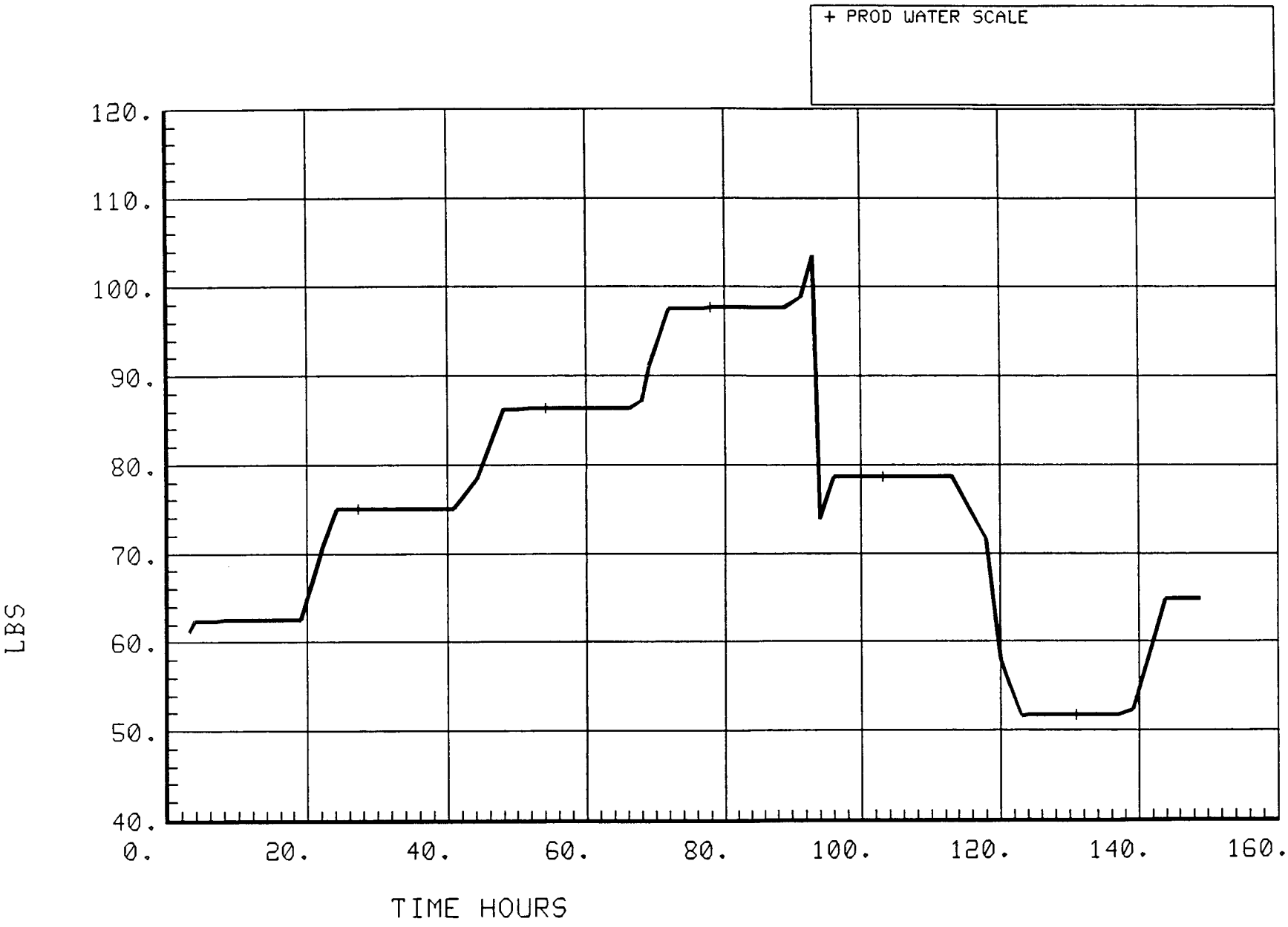

Figure 5-1.3. TIMES product water tank scale.

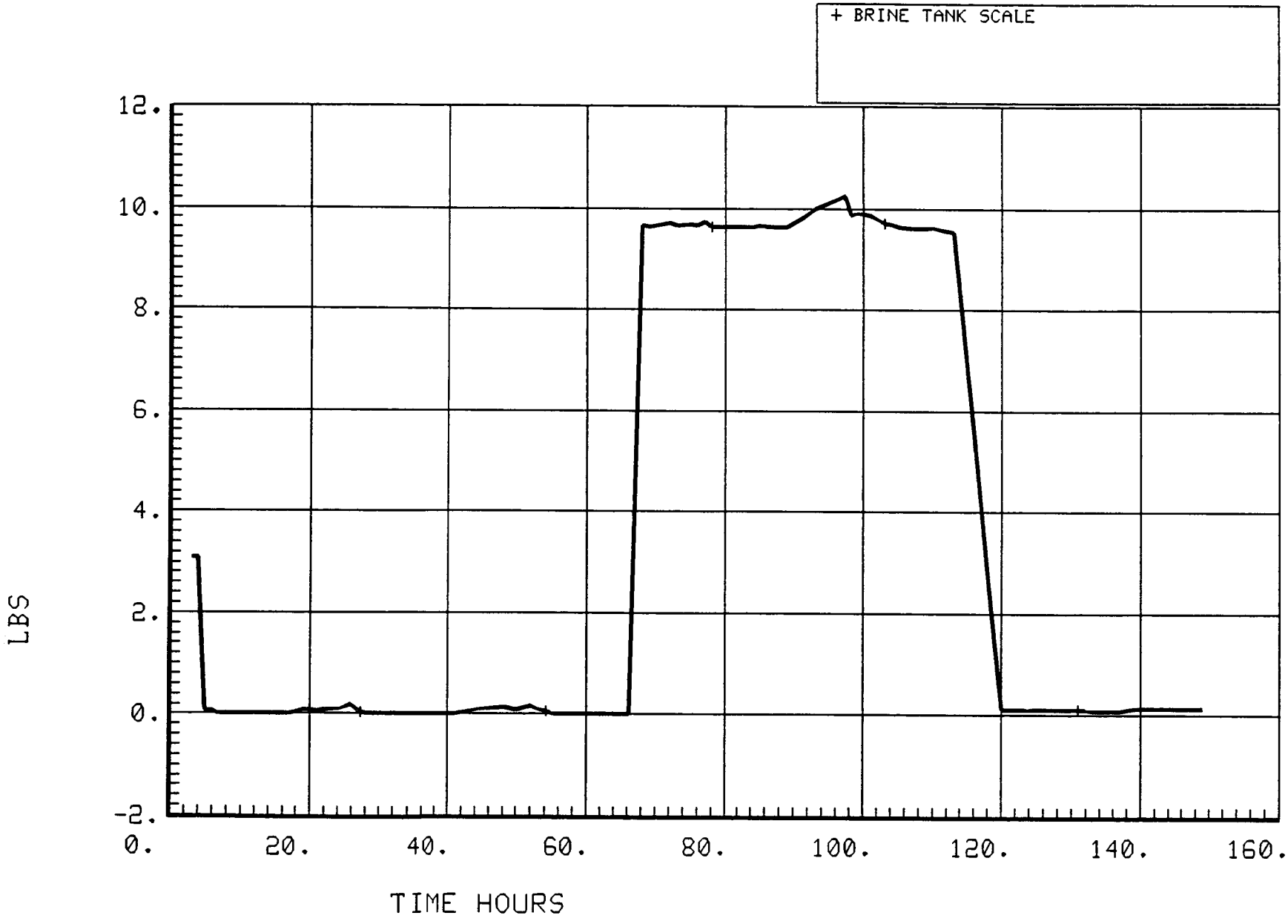

Figure 5-1.4. TIMES brine tank scale.

5.1.3.3 Product Water Quality

Routine analyses of water quality were not conducted throughout the test. Detailed water quality analyses of non-post-treated and post-treated distillate, pretreated urine, and concentrated brine were conducted near the conclusion of the test. A complete summary of these analyses is provided in Section 10. All samples, except those of post-treated distillate, were taken from the pooled sources in the respective facility tanks. Post-treated distillate samples were obtained directly from the post-treatment module effluent.

As described in Section 10, the aggregate non-post-treated distillate had a pH of approximately 3.4, a conductivity of 153 micromho/cm, a total solids concentration of 61 ppm, and a total organic carbon (TOC) concentration of 106 ppm.

Post-treated distillate generally met the water quality requirements currently defined by JSC 30000, Sec. 3, Rev. D, for space station hygiene water. A comparison of the hygiene water specification and the non-post-treated and post-treated distillate is provided in Table 5-3. Of the 52 parameters listed in the specification for hygiene water, 36 were measured analytically. Of these, the following parameters were found to be out of specification in the post-treated distillate: pH, cadmium, fluoride, iron, lead, manganese, magnesium, TOC, and residual biocide. Though the number of parameters out of specification in the post-treated distillate is high, it should be noted that the post-treatment bed used in this test was not optimized for this particular application, had processed an unaccounted quantity of distillate prior to this test, and was not actively protected from performance degradation stemming from chemical and/or microbial fouling. The data in Table 5-3 show that the concentrations of many of the indicated contaminants were not reduced significantly by the bed and, in the cases of total solids, cadmium, chloride, fluoride, iron, lead, magnesium, zinc, alcohols, and bacteria, were actually increased by the bed. This suggests that the useful life of the bed had been expended prior to the collection of the samples. It is expected that the utilization of post-treatment beds designed specifically for the polishing of urine distillate and the proper handling and monitoring of such beds would reduce the number of out-of-specification parameters considerably.

The analysis conducted for mercury did not have a lower limit of detection sufficient to verify compliance with the specification. Residual bactericide, in the form of iodine, was below the minimum required concentration due to the fact that appropriate iodine dosing equipment was not included in this test. Finally, the relatively large levels of microorganisms detected are attributable to the fact that active measures to control microbial contamination in the post-treatment beds, product water-storage tanks, and all the associated plumbing, were not included as a part of this test.

Of the TOC measured in the non-post-treated distillates, only 5 percent and 15 percent, respectively, is accounted for in the detailed analyses described in Section 10.0. Of the organic contaminants identified, the predominant one by far is ethanol at concentrations of 10.2 and 22.0 ppm in the non-post-treated and post-treated distillates, respectively.

The fact that there appears to be more ethanol in the post-treated distillate suggests that previously-removed ethanol is being displaced from the bed by other contaminants. These levels are significant in light of the fact that conventional water-treatment technologies are ineffective at removing ethanol (and related compounds). The appearance of ethanol in the distillate is most likely caused

TABLE 5-3
COMPARISON OF NON-POST TREATED AND POST TREATED DISTILLATE TO THE SPACE STATION HYGIENE WATER QUALITY SPECIFICATION

PARAMETER	SPECIFICATION LIMIT	CONCENTRATION IN NON-POST TREATED DISTILLATE	CONCENTRATION IN POST TREATED DISTILLATE
Physical			
total solids (ppm)	TBD < 500	61	90
color, true (Pt/Co)	15	3	0
taste & odor (TTN/TON)	<3	N.A. (1)	N.A. (1)
pH	5.0-8.0	**3.4**	**4.4**
particulate (max size)	40 um	N.A.	N.A.
turbidity (NTU)	11	0.58	0.37
dissolved gas	no free gas at 35 C	N.A.	N.A.
free gas	none at STP	N.A.	N.A.
Inorganic (mg/l)			
ammonia	0.5	<0.25	<0.25
arsenic	0.01	<0.005	<0.005
barium	1.0	<0.02	<0.02
cadmium	0.01	**0.02**	**0.03**
calcium	TBD	0.10	0.11
chloride	TBD	3.24	32.4
chromium	0.05	<0.025	<0.025
copper	1.0	0.05	0.05
fluoride	1.0	**9.0**	**13.9**
iodide	TBD	N.A.	N.A.
iron	0.3	**0.35**	**0.49**
lead	0.05	**0.19**	**0.20**
manganese	0.05	**0.13**	**0.12**
magnesium	0.05	**0.06**	**0.15**
mercury	0.002	<0.005	<0.005
nickel	0.05	0.06	<0.02
nitrate	TBD	<0.5	<0.5
potassium	TBD	1.27	0.10
selenium	0.01	<0.005	<0.005
silver	0.05	<0.02	<0.02
sulfide	0.05	N.A.	N.A.
sulfate	TBD	2.95	<0.5
zinc	5.0	<0.03	1.3
Organics (mg/l)			
TOC	TBD<10	**106**	**76**
TOC (less-nontoxics)	TBD<1	N.A.	N.A.
organic acids	TBD	N.A.	N.A.
cyanide	TBD	<0.02	<0.02

phenols	0.001	0.11	<0.005
halogen'd hydrocarbons	TBD	0.015 (2)	0.015 (2)
organic alcohols	TBD	10.2 (3)	22.0 (3)
specific toxicants	TBD	N.A.	N.A.
Microbial (CFU)			
total bacteria	TBD	4/ml	2000/ml
anaerobes	TBD	<1/10ml	28/ml
aerobes	TBD	N.A.	N.A.
gram positive	TBD	1/ml	2000/ml
gram negative	TBD	3/ml	N.A.
E-coli	TBD	N.A.	N.A.
enteric	TBD	N.A.	N.A.
virus	TBD	N.A.	N.A.
yeast and molds	TBD	<1/10ml	<1/10ml
Bactericide (mg/l)			
residual (min - max)	0.5-6.0	**<0.5 (4)**	**<0.5 (4)**
Radiological (pCi/l)			
alpha 90 Sr	TBD	N.A.	N.A.
alpha 226 Ra	TBD	N.A.	N.A.
beta 3H	TBD	N.A.	N.A.

(1) no analysis performed for the particular parameter
(2) chloroform, as determined by EPA 601 and 625
(3) ethanol
(4) iodine
Bold indicates out of tolerance

by chemical reactions between the oxone pretreatment and urine constituents or by the presence of ethanol in the urine feed. The detection of ethanol in urine has been previously documented in cases where the urine donor has consumed alcoholic beverages prior to donating. In any event, the presence of ethanol at these concentrations is signficant and indicates the need for the development of pretreatment and reclamation technologies which are better able to control its appearance.

5.1.3.4 Discussion of Individual Measurements

5.1.3.4.1 Evaporator Temperatures (TT01-TT04)

Figures 5-1.5 through 5-1.8 show the temperatures at the inlets (TT01 and TT03) and outlets (TT02 and TT04) of the HFMs. During each of the seven process cycles, the inlet and outlet temperatures averaged 132° to 136°F and 125° to 128°F, respectively. The drop in temperatures between inlets and outlets is typical of that associated with the heat loss through evaporation. These temperatures are approximately 6° to 7°F lower than those expected. The reason for the lower than normal operating temperatures is believed to be related to the lower than normal operating pressures maintained throughout the test (see below).

Figures 5-1.5 through 5-1.8 also show that during the periods of time when the TIMES was in the Off mode, the evaporator was maintained at temperatures between 114° to 148°F by the external evaporator heaters. Since there was no capability for automatic control of these temperatures, the variations seen were due to repeated manual adjustments of the power applied to the heaters.

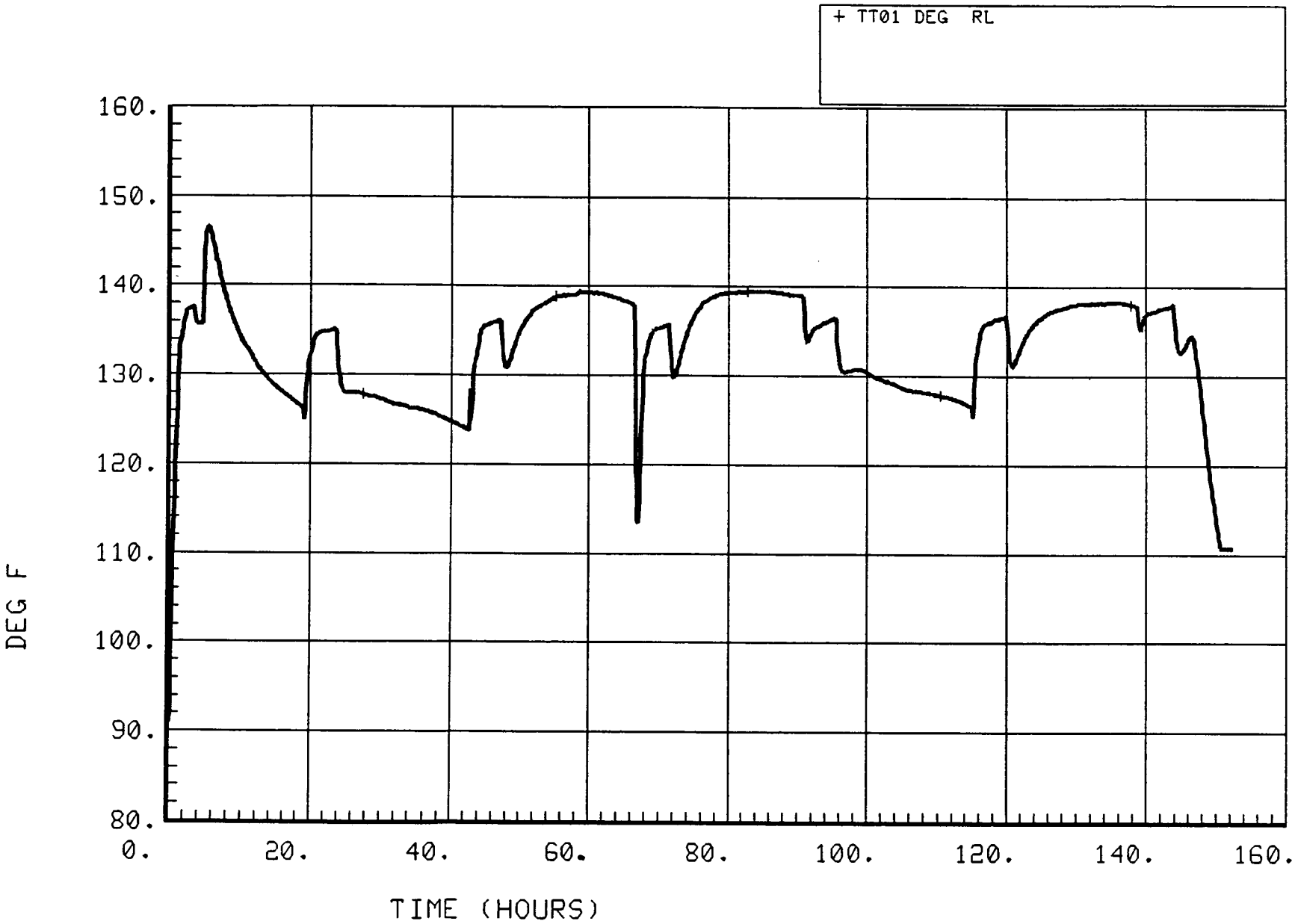

Figure 5-1.5. Evaporator inlet temperature (TT01).

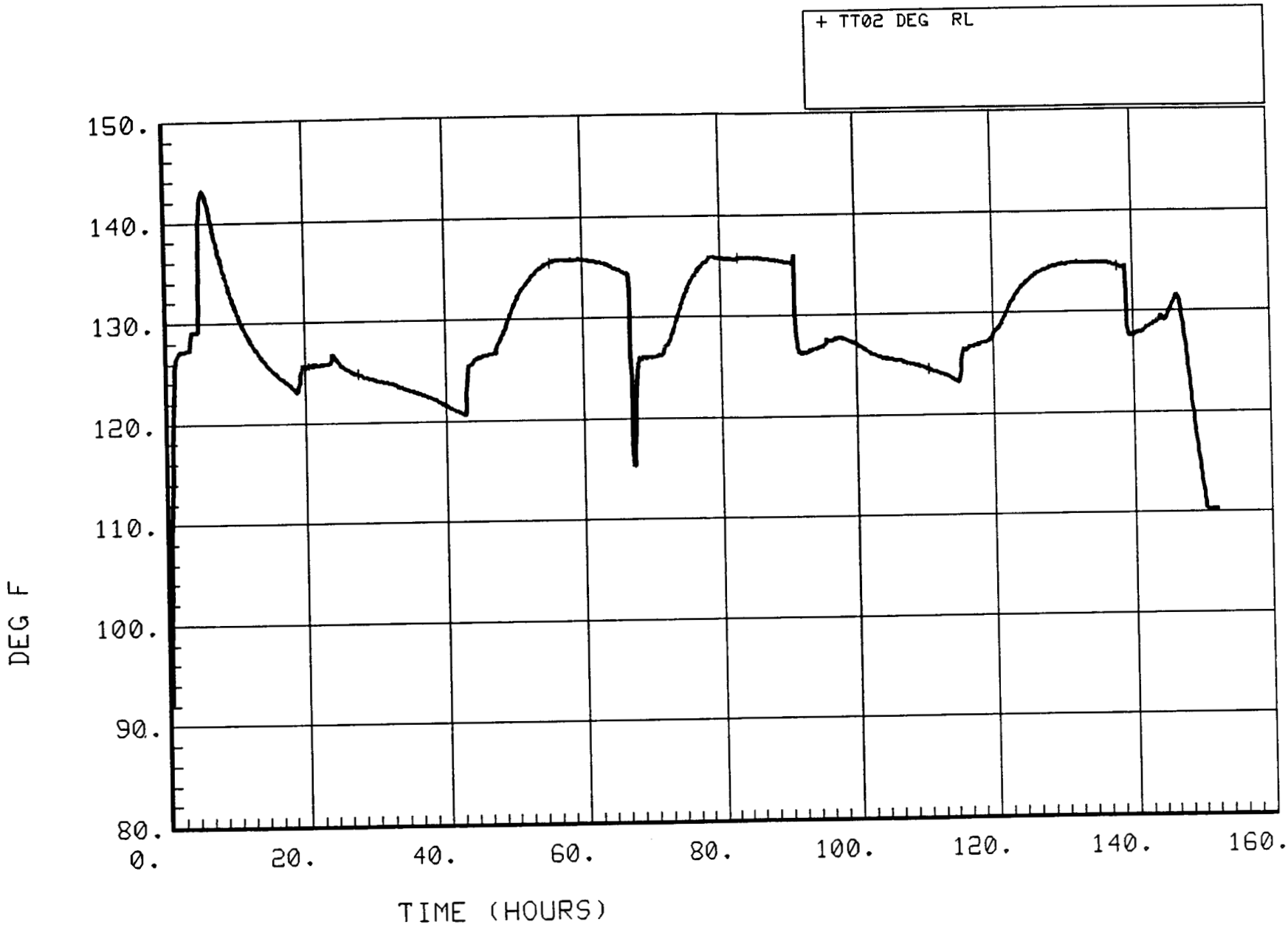

Figure 5-1.6. Evaporator inlet temperature (TT02).

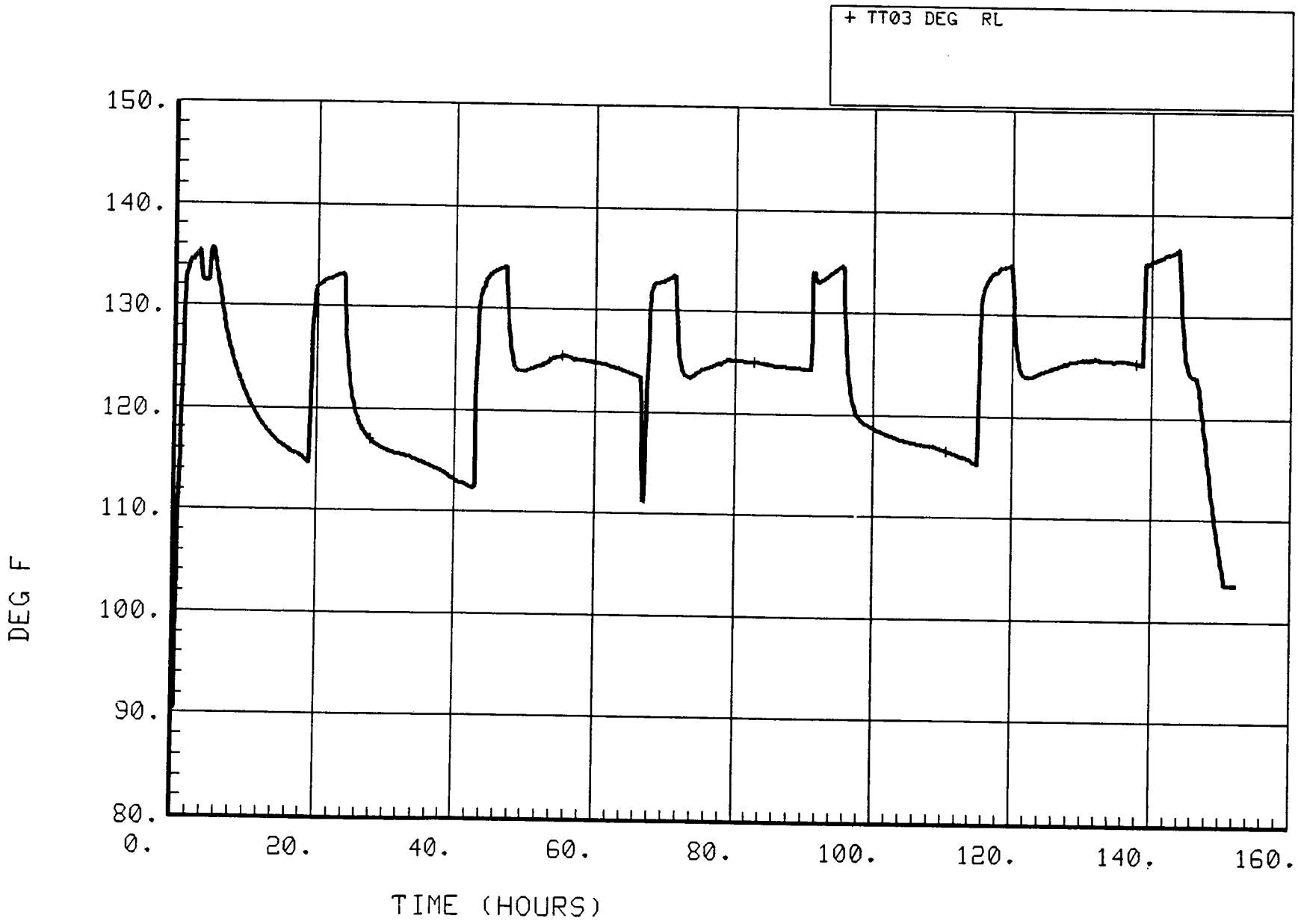

Figure 5-1.7. Evaporator inlet temperature (TT03).

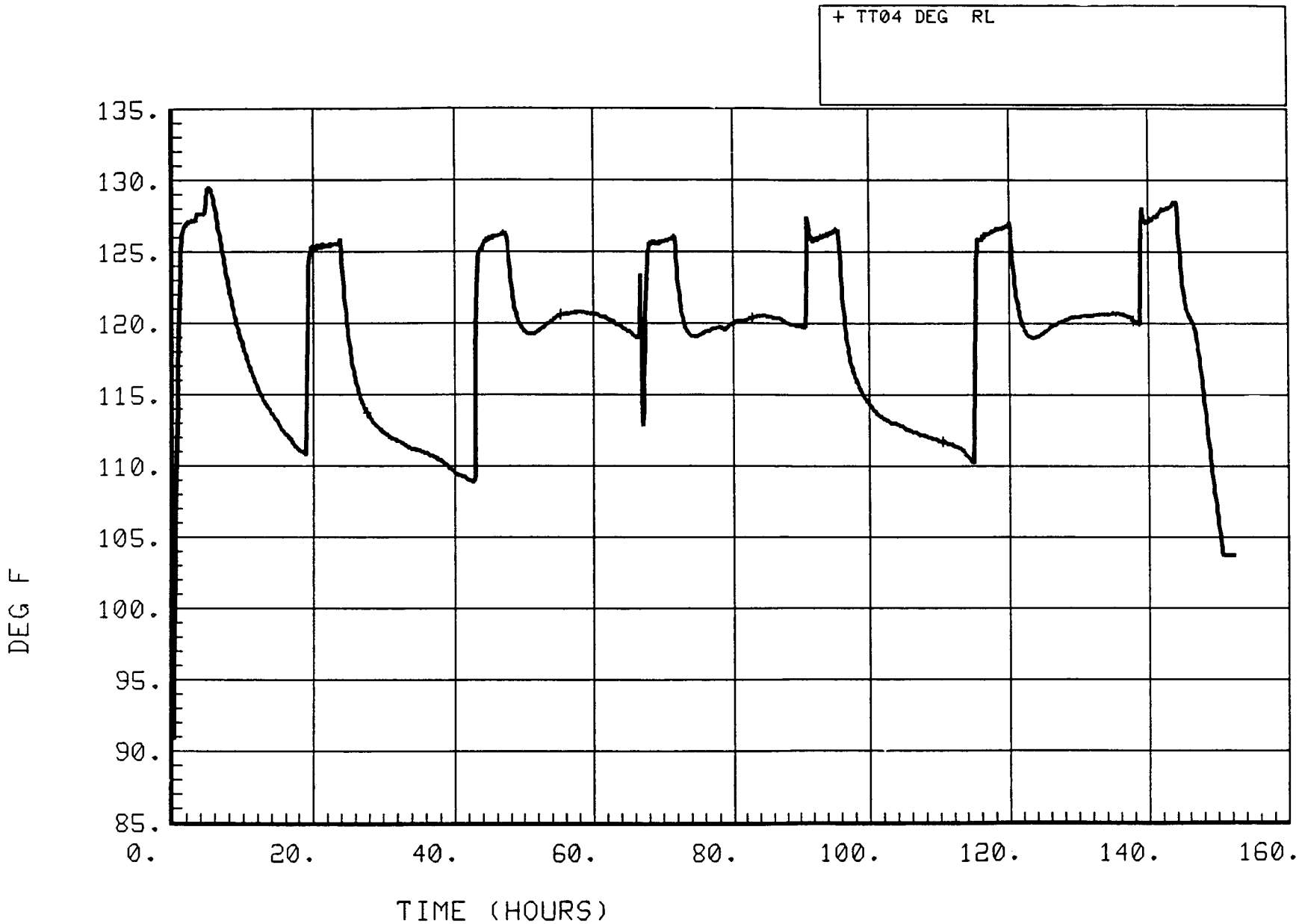

Figure 5-1.8. Evaporator inlet temperature (TT04).

The sharp drop in temperature evident on each of the figures at 67:00 hr corresponds to the displacement of hot brine by ambient urine during the brine dump.

5.1.3.4.2 Steam and Reference Pressures (TP01 and TP02)

Figures 5-1.9 and 5-1.10 show the steam pressure (TP01) measured in the evaporator and the reference pressure (TP02) measured at the purge gas accumulator. During each of the seven process cycles, the steam pressure ranged from approximately 1.6 to 2.0 psia and the reference pressure from about 1.4 to 2.0 psia. The fluctuations in both pressures during each process cycle are due to the accumulation of noncondensable gases within the evaporator and the accumulator and the periodic purging of these gases to facility vacuum.

As shown in the figures, at the end of each process cycle the steam and reference pressure gradually increased to ambient over 12 to 16 hr. This suggests that a small leak may have existed in the subsystem somewhere between the evaporator and the purge gas valve. The leak was not large enough to significantly affect the performance of the TIMES other than raising the steam and reference pressures slightly above the normal operating ranges (1.2 to 2.0 psia and 2.0 to 2.7 psia, respectively).

5.1.3.4.3 Brine Conductivity (TC01)

Figure 5-1.11 shows the conductivity of the internal brine solution measured by sensor TC01. The function of the sensor is to trigger brine dumps. However, during this test the brine dump was initiated manually. The conductivity measured by TC01 during the seven process cycles varied between 18 and 38 millimho/cm. During the periods in Off mode, the brine conductivity was erratic within the range of 1 to 27 millimho/cm. Such erratic conductivity measurements are typical of non-flowing, heterogeneous solutions like brine.

A gradual increase in conductivity would be expected as the contaminant concentration in the brine increased with time. Such an increase is evident through the four process cycles following the brine dump at 67:00 hr. A similar increase during the first three process cycles prior to the brine dump is not readily apparent, however. This type of inconsistent behavior supports the conclusion that conductivity may not be a reliable parameter on which to base process control within brine solutions.

5.1.3.4.4 Condensate Conductivity (TC02)

Figure 5-1.12 shows the conductivity of the distillate as measured by TC02 prior to delivery to the subsystem outlet. Prior to the MCT, a replacement sensor was installed and the orientation of the sensor was modified in an effort to provide a more reliable measurement than was obtainable with the original sensor. The data in Figure 5-1.12 shows that the sensor performed marginally. The conductivity measured by TC02 ranged between 100 to 200 micromho/cm during each of the process cycles. These values are consistent with the conductivity of 153 micromho/cm measured in the aggregate non-post-treated distillate near the conclusion of the test.

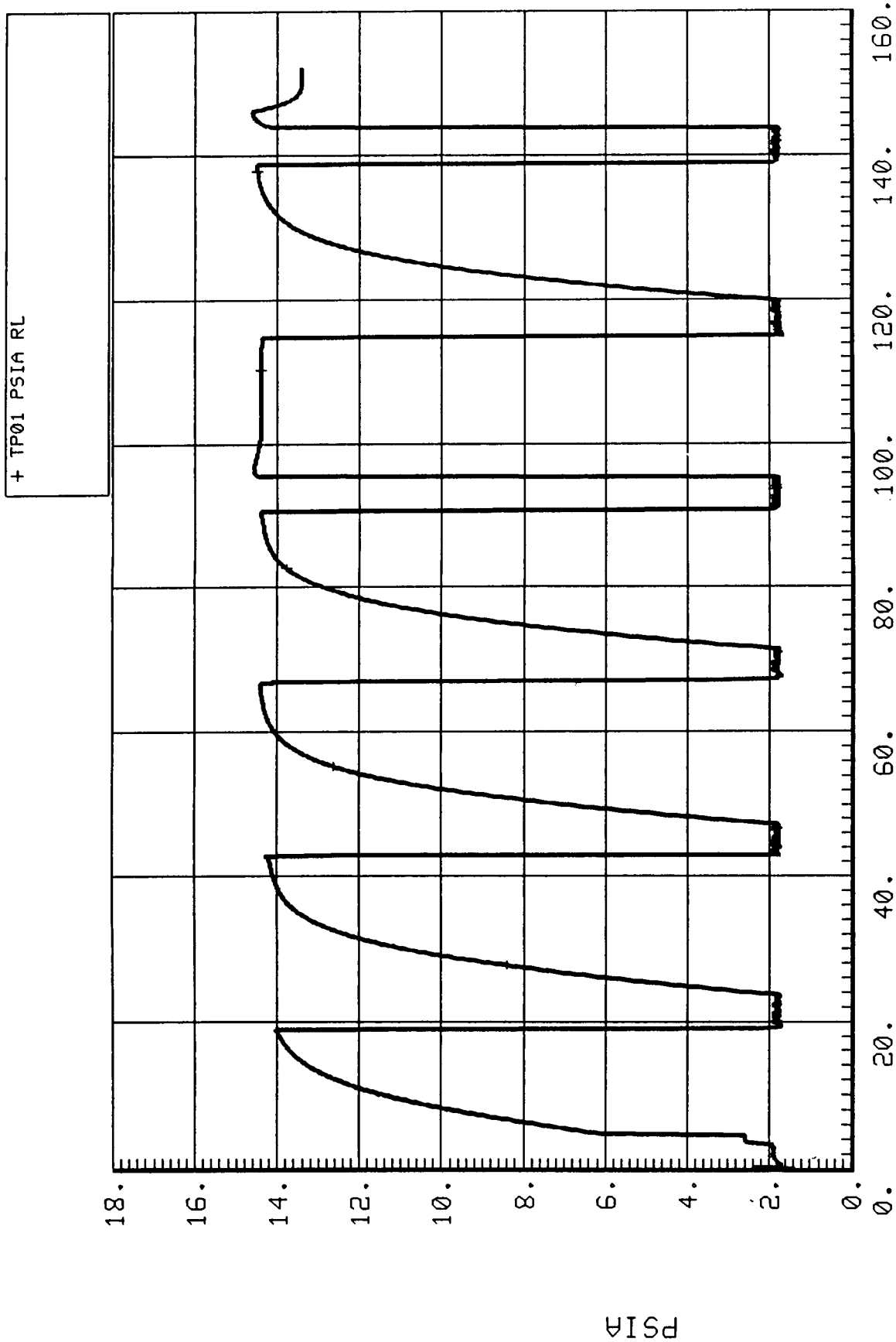

Figure 5-1.9. Steam passage pressure (TP01).

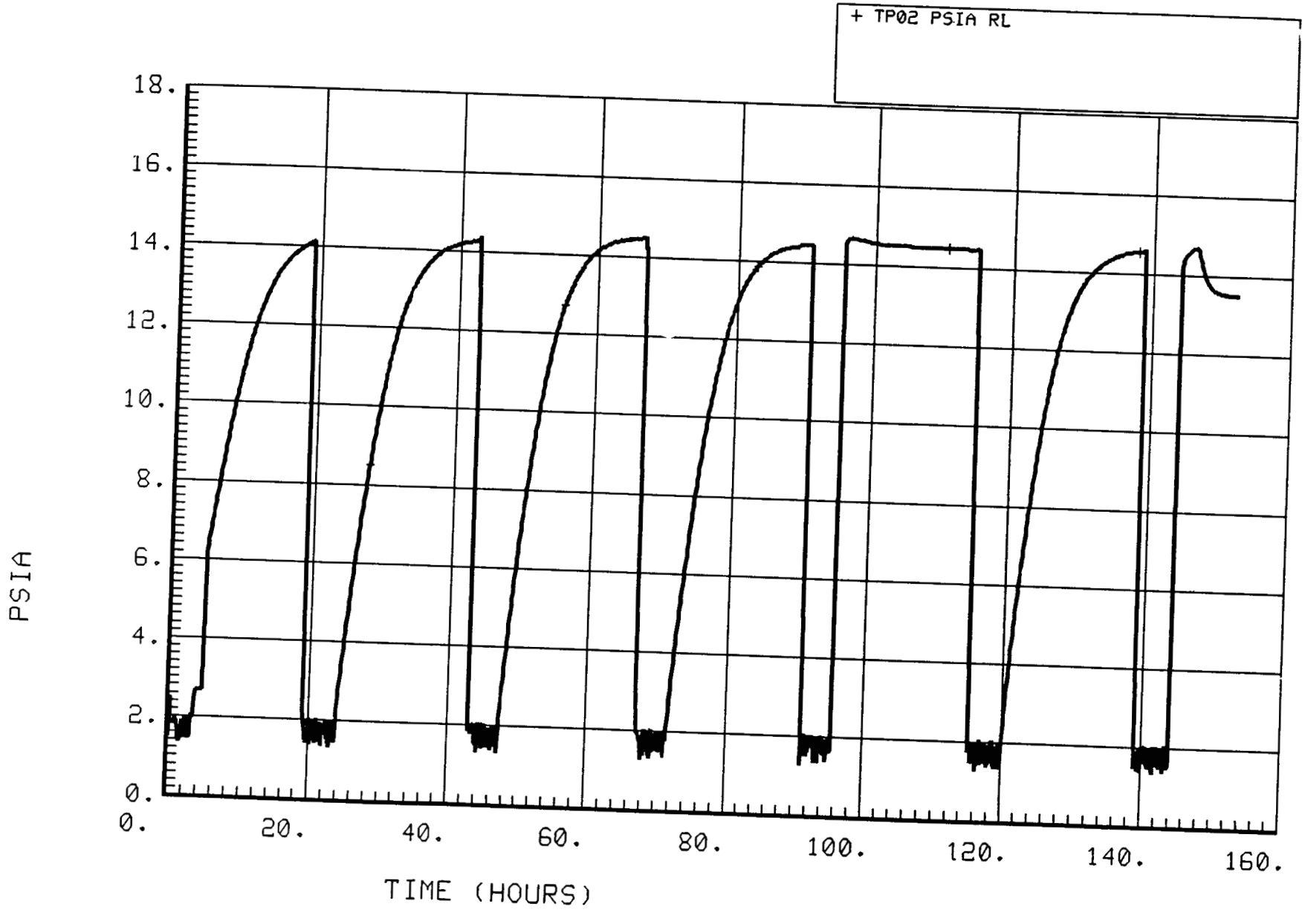

Figure 5-1.10. Condenser reference pressure (TP02).

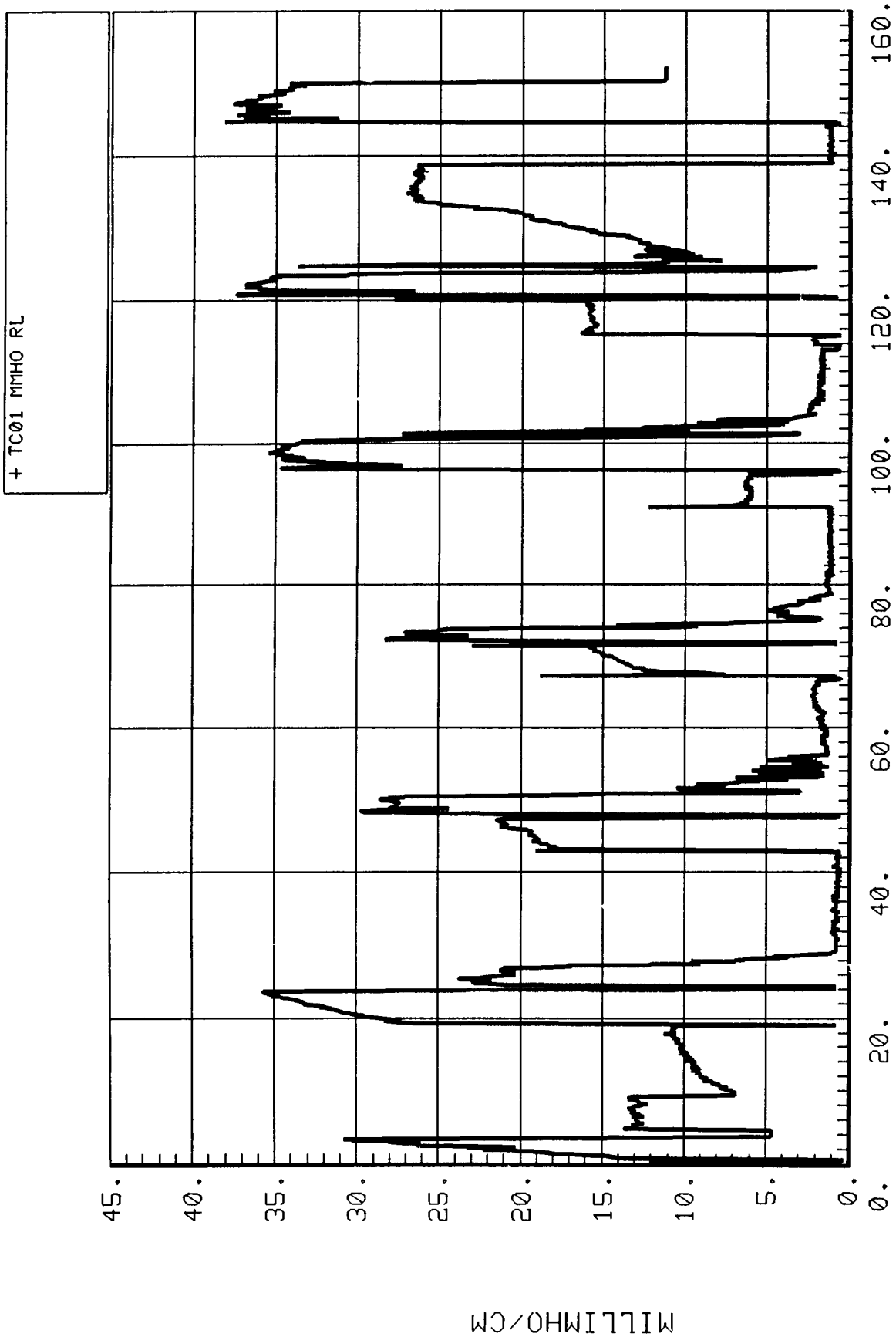

Figure 5-1.11. Brine conductivity (TC01).

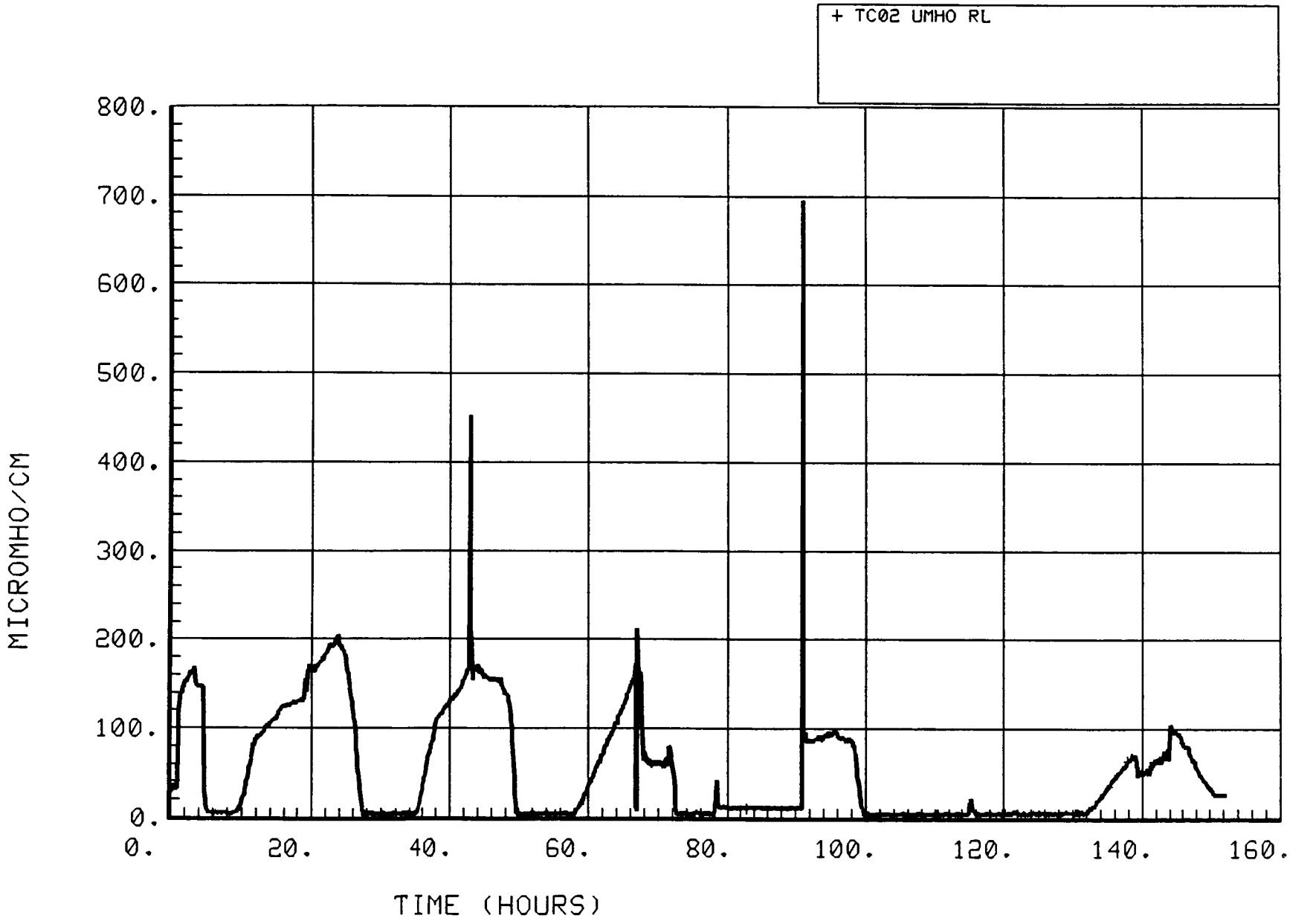

Figure 5-1.12. Condensate conductivity (TC02).

The conductivity measured during the Day 6 process cycle was significantly below that measured during all other process cycles and only slightly above that registered by the sensor during Off modes. Since there was nothing during Day 6 that would suggest that significantly cleaner distillate was being produced, it is expected that the indicated behavior is attributable to some sort of sensor anomaly.

5.1.3.4.5 TER Voltage (TV02) and Current (TI01 and TI02)

Figure 5-1.13 shows that the TER operated at a nominal voltage of 27.7 V. The operating current for the two arrays of TEDs are shown in Figures 5-1.14 and 5-1.15. Each array drew currents of approximately 3.5 to 4.3 A, for a combined current draw of about 7.4 to 8.5 A. The numerous spikes in the current curves are typical of the On/Off operation of the TEDs during normal operation. The gradual declines in current draw for each array between Days 1 and 3 (before the brine dump) and between Days 4 and 7 are attributed to the reduced vapor evolution rate, and hence the reduced heat load, resulting from the accumulation of contaminants within the brine loop.

5.1.3.4.6 Pump/Separator Current (TI03)

Figure 5-1.16 shows the current draw of the motor driving the water separator and recycle pump. A nominal draw of 0.22 to 0.23 A occurred as expected.

5.1.3.4.7 Ancillary Current (TI04)

Figure 5-1.17 shows the current draw of miscellaneous components. The predominant spikes correspond with the cyclic operation of the vacuum vent valve.

5.1.4 Recommendations/Lessons Learned

During the MCT it was demonstrated that the TIMES could adequately reclaim water from pretreated urine. Integration of the TIMES with a non-optimized post-treatment bed was sufficient to meet many of the hygiene water-quality specification requirements over the short term of the test. However, the possibility that the useful life of the bed had been exceeded prior to the test reduced the quality of the final post-treated water relative to a number of parameters.

The following list of recommendations is compiled based on the experiences in the MCT.

The data communications between the SCATS and the facility tank scales must be established in order to provide sufficient data required for the determination of the overall water-production rate and water-recovery efficiency. Detailed records should be kept of all additions to, and removals from, all facility storage tanks.

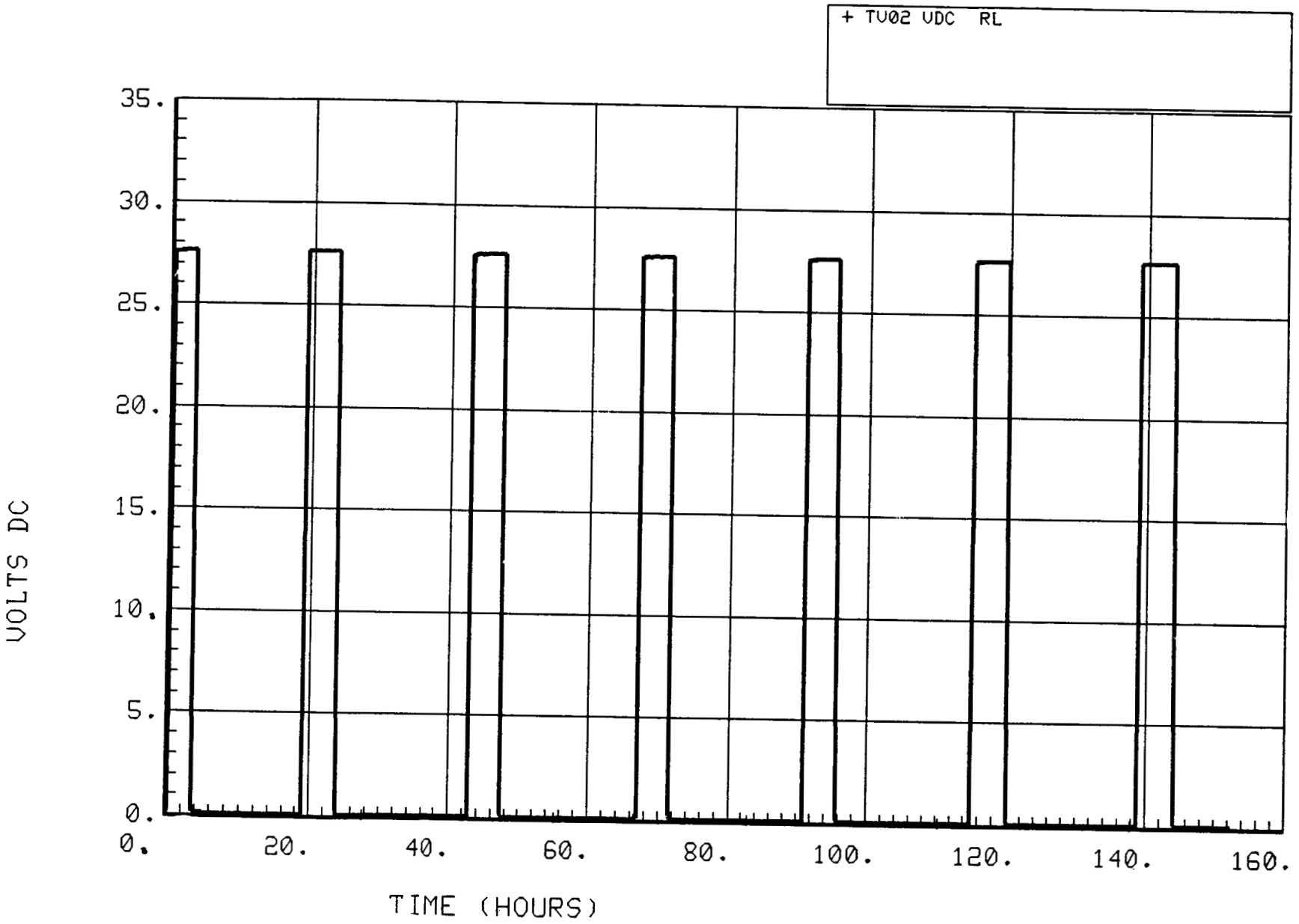

Figure 5-1.13. Thermoelectric regenerator voltage (TV02).

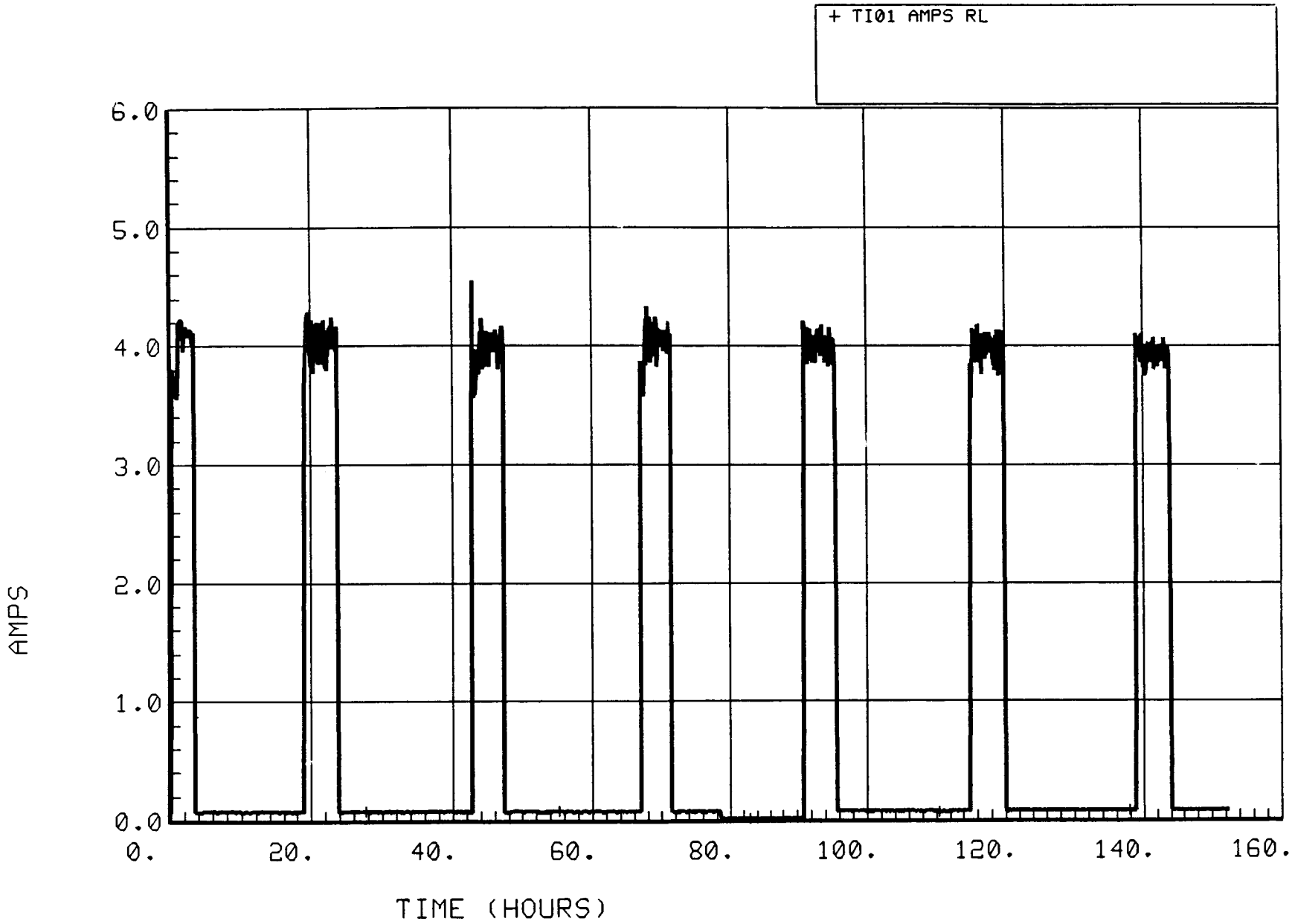

Figure 5-1.14. Thermoelectric regenerator current No. 1 (TI01).

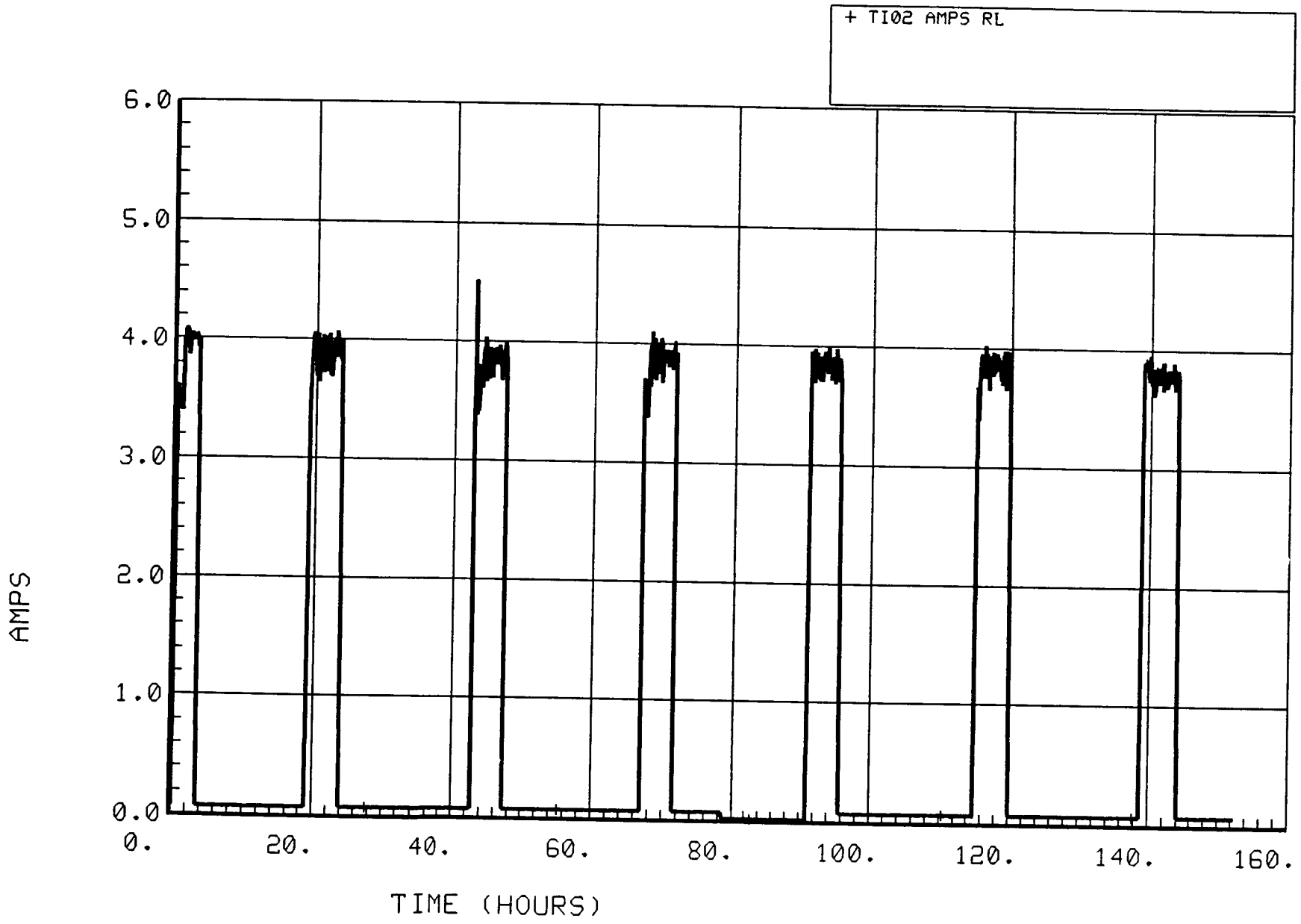

Figure 5-1.15. Thermoelectric regenerator current No. 2 (TI02).

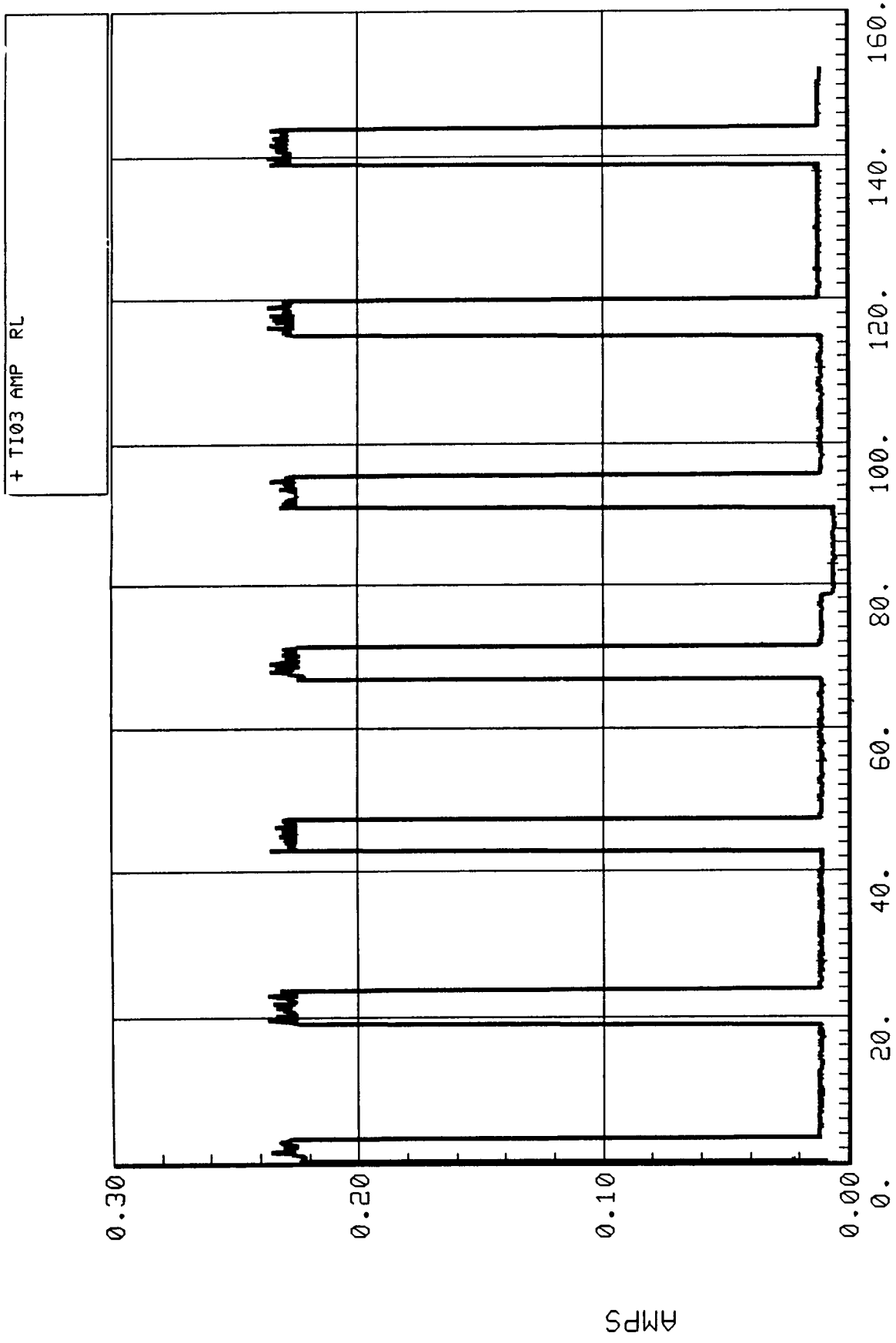

Figure 5-1.16. Pump/separator current (TI03).

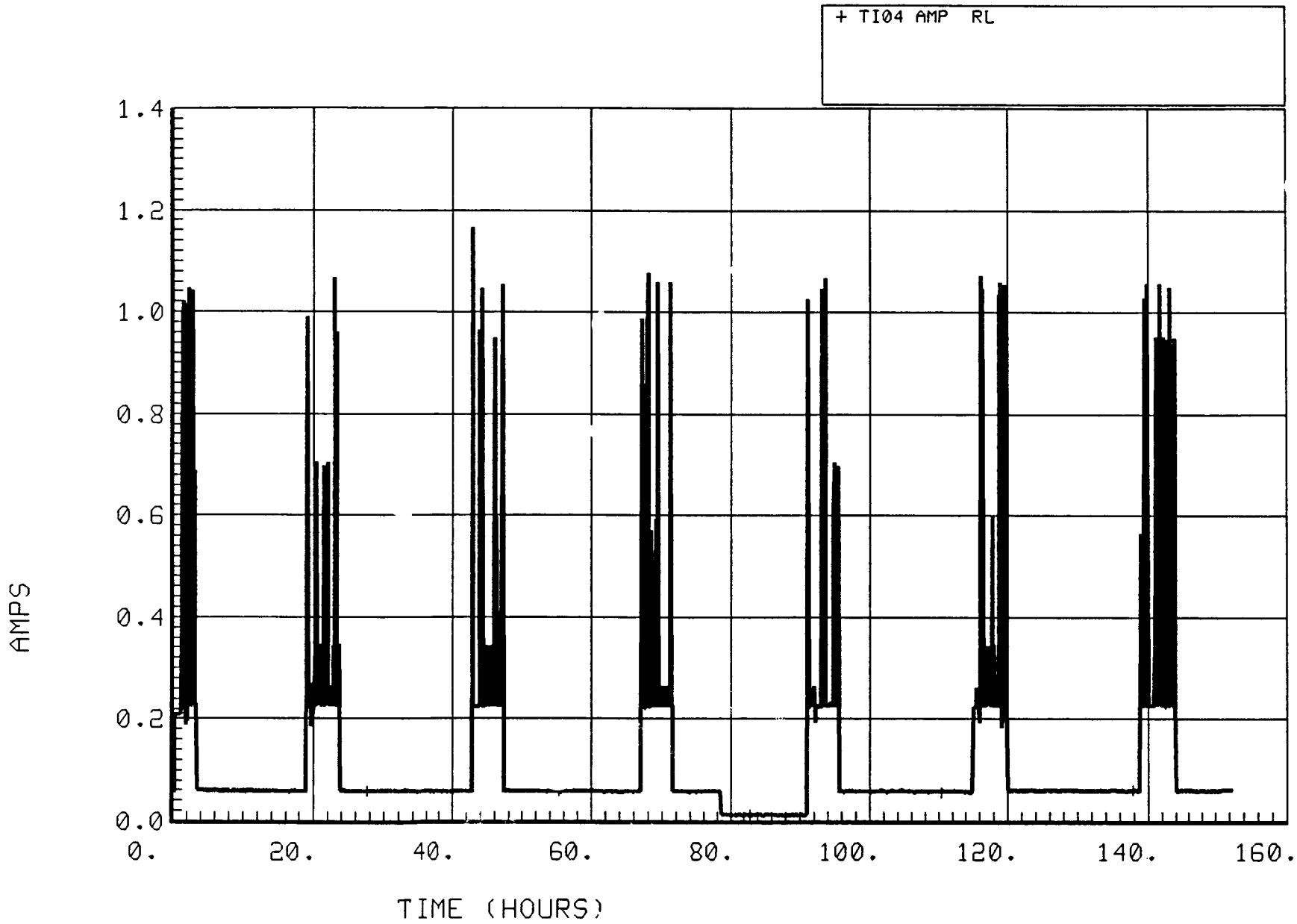

Figure 5-1.17. Ancillary current (TI04).

The integrity of the TIMES process package should be pressure-checked for leaks. Any leaks, if found, should be repaired prior to future testing.

Improved provisions should be made to collect and quantify the amount of water lost to vacuum during the normal purging of the subsystem. This data is required to complete the overall water balance around the TIMES.

An optimized post-treatment bed should be used for the polishing of TIMES distillate. Such a bed should contain known quantities of specified sorbents and resins and should have appropriate provisions for the control of microorganisms. Accurate records must be kept of the total distillate processed through the bed during its entire installed life in order to facilitate bed life calculations and to provide the highest quality of post-treated distillate at all times.

All storage tanks, especially the product water tank, should be sanitized prior to each test and should be vented to ambient in such a way as to preclude the introduction of microbial contaminants from the atmosphere. Plumbing lines should be arranged to allow sanitization and flushing prior to all tests. Without these provisions, the capacity of the TIMES and post-treatment elements to meet potential microbial specifications cannot be adequately determined.

5.2 Four Bed Molecular Sieve

5.2.1 Subsystem Description

The 4BMS was used to remove CO_2 from the module simulator air and concentrate it for processing by the Sabatier CO_2 reduction subsystem. The basic concept of the 4BMS is as follows: a mixed air stream (including CO_2) flows thorough a sorbent material and the CO_2 is selectively adsorbed while the remaining air flows through. Adsorption is the physical trapping of individual molecules in voids in the sorbent structure and does not result in a physical or chemical change of the sorbent itself (distinct from the process of absorption which involves a chemical reaction or a physical change or both in the sorbent material). In addition to the molecular size, the polarity of the molecules and the vapor pressure are important factors in selecting molecules for adsorption.

For the 4BMS, the CO_2 sorbent material used is a synthetic zeolite which was selected for its superior ability to adsorb CO_2. The designation for the CO_2 sorbent is Zeolite 5A. Due to the preference of Zeolite 5A for water vapor over CO_2, it is necessary to first dry the air. The desiccants used to do this are silica gel and another type of zeolite, designated Zeolite 13X. The sorbents are in the form of pellets approximately 1/8-in. long by 1/16-in. diameter. During operation, the sorbents alternately adsorb and desorb the water vapor and CO_2, which requires two beds each of desiccant and CO_2 sorbent to perform CO_2 removal in an essentially continuous manner. The cycling is controlled by a timer which causes valve positions to reconfigure at each mode change.

A schematic of the 4BMS is shown in Figure 5-2.1. The flowpath of the air through the 4BMS takes it first through a two-layer desiccant bed. The first layer is silica gel which can adsorb water vapor readily at higher relative humidities but its capacity falls off at relative humidities less than 50 percent. The second layer is Zeolite 13X which has a higher capacity than silica gel at relative humidities less than 35 percent. By having a two-layer bed of the desiccants, essentially all of

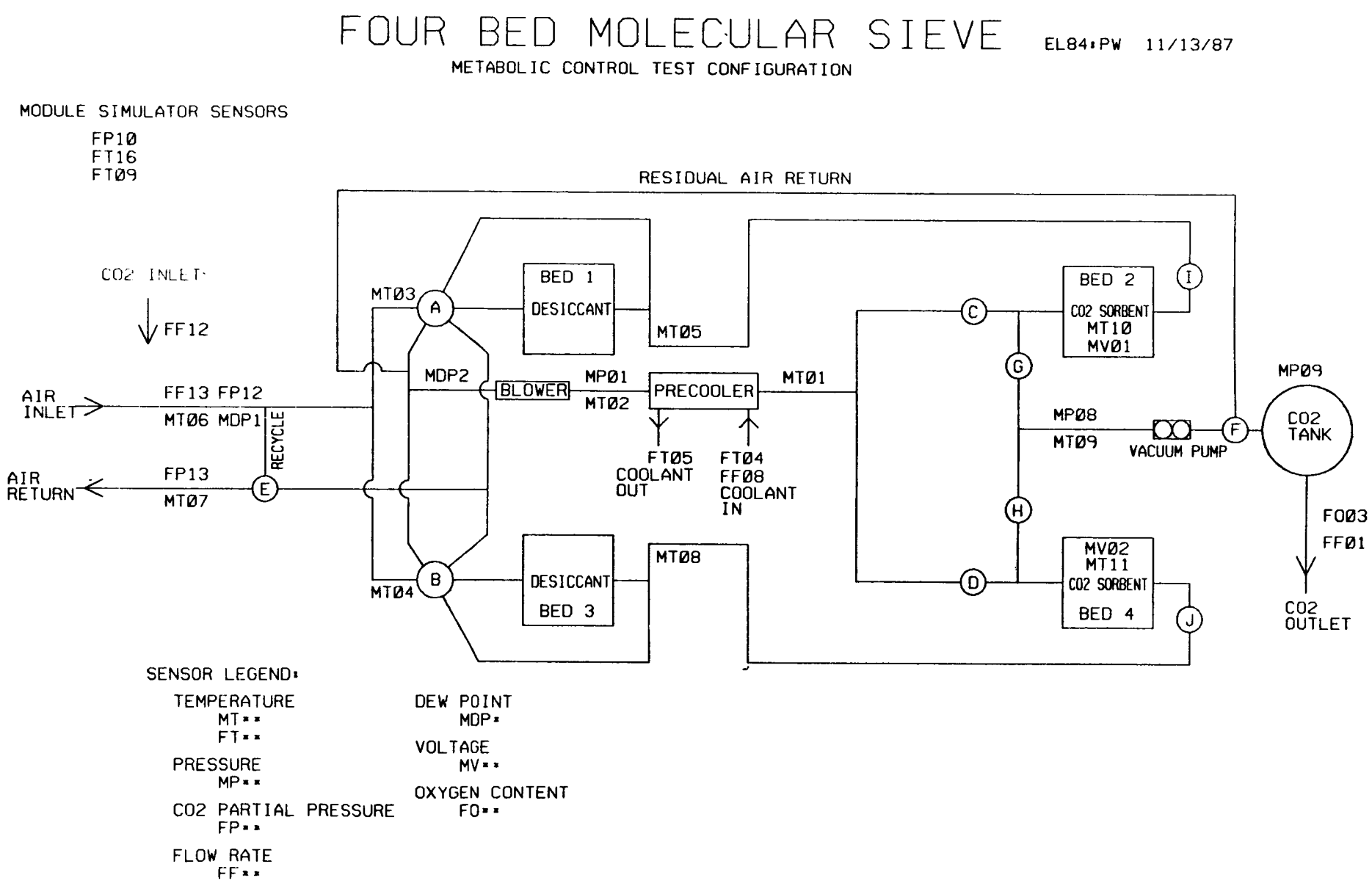

Figure 5-2.1. 4BMS schematic.

the water vapor can be removed. The adsorption process results in a temperature rise in the air stream. There is also a temperature rise across the blower. The blower is located downstream of the desiccant bed so that the temperature rise does not cause a drop in the relative humidity of the incoming air. Downstream of the blower, the precooler reduced the temperature of the air stream to temperatures more conducive to CO_2 adsorption (from about 190° to 70°F). The dry, cool air then flows through a CO_2 sorbent bed, cooling the bed (heated during the previous desorb half-cycle) to a temperature where much of the CO_2 is removed from the air stream. The air is next directed through the second desiccant bed to desorb the water from the desiccant that was adsorbed during the previous half-cycle. To improve performance, at the beginning of each adsorb half-cycle the outlet air is recycled to the inlet. After 11 min the desorbing desiccant bed has heated (due to residual heat in the now adsorbing CO_2 sorbent bed) enough to begin desorbing water vapor so that recycle valve switches to end recycle. The outlet air has the same average moisture content as the inlet air.

While one CO_2 sorbent bed is adsorbing CO_2, the other is desorbing CO_2 for storage in the accumulator tank prior to delivery to the Sabatier. During desorption, the residual air in the canister is pumped back to the duct upstream of the blower. This is done for 2 min. Then the heater activates to raise the bed temperature to about 400°F which, in combination with the vacuum pump reducing the pressure to about 0.5 psia, releases the CO_2 from the zeolite. After about 55 min the desorption is complete and the next half-cycle begins. (See Figure 5-2.2 for the operating modes.)

The subsystem was constructed on an accelerated schedule from Skylab hardware (canisters and heaters, the five-way sorbent valves were replaced after the SIT) and commercially available components (blower, vacuum pumps, CO_2 holding tank, controller). As a result, the subsystem was not completely optimized with regard to weight, volume, or power usage.

The 4BMS was installed so that it could be operated independently (vent CO_2) or integrated with the Sabatier for CO_2 reduction. The subsystem as installed included a CO_2 liquefaction capability, which was not used for this test program. During operation, air from the THC heat exchanger was ducted directly to the inlet of the 4BMS. This duct contained a flow meter, a port for injection of CO_2, and a connection to a CO_2 partial pressure sensor. The CO_2 supply line contained a flow meter and a metering valve for regulating the CO_2 flow. As the air flowed through the subsystem, temperature measurements were made at various locations (e.g., inlet, upstream and downstream of the precooler, downstream of the sorbent beds) and, at the air exit, the CO_2 partial pressure was again measured. The air exited into the volume of the simulator.

The desorbed CO_2 was pumped to a storage tank (part of the CO_2 liquefaction unit) from where the CO_2 could be regulated to the Sabatier or vented. An O_2 sensor in the CO_2 outlet line was used to measure the percentage of O_2 (an indication of the amount of air present in the CO_2).

The five-way valves, recycle valve, and CO_2 outlet flow control valve are pneumatic type and pressurized nitrogen was supplied to actuate them.

Several changes were made to the 4BMS after analyzing the results of the SIT data. These changes are shown in Figure 5-2.1 and include:

(1) Replacement of the two Skylab five-way valves on the CO_2 sorbent beds with a combination of six two-way valves, to eliminate leak sources and to avoid having hot and cold gases flowing through a valve simultaneously.

FOUR BED MOLECULAR SIEVE

MINUTES		0	7	11	55	62	66	110
CYCLE MODE		1A	1B	2	3A	3B	4	
DESICCANT	BED 1	← ADSORB →			← DESORB →			
	BED 3	← DESORB →			← ADSORB →			
CO2 SORBENT	BED 2	△	← DESORB →		← ADSORB →			
	HEATER	ON	ON RECYCLE	ON	OFF	OFF	OFF	
	BED 4	← ADSORB →			△	← DESORB →		
	HEATER	OFF	OFF	OFF	ON	ON RECYCLE	ON	
COMPONENT DESCRIPTION		POSITION						
VALVE A		2	2	2	1	1	1	
VALVE B		1	1	1	2	2	2	
VALVE C		4	4	4	3	3	3	
VALVE D		3	3	3	4	4	4	
VALVE E		6	6	5	6	6	5	
VALVE F		7	8	8	7	8	8	
VALVE G		3	3	3	4	4	4	
VALVE H		4	4	4	3	3	3	
VALVE I		4	4	4	3	3	3	
VALVE J		3	3	3	4	4	4	
CO2 COMPRESSOR		ON	ON	ON	ON	ON	ON	
CO2 TANK		-	CHARGING TANK		-	CHARGING TANK		

EL84-PW 11/13/87

VALVE	POSITION	DESCRIPTION
A,B	1	DESICCANT BED TO AIR RETURN
A,B	2	INLET AIR TO DESICCANT BED THEN BLOWER
C,D,G,H,I,J	3	OPEN
C,D,G,H,I,J	4	CLOSED
E	5	OUTLET TO CABIN
E	6	RECYCLE OUTLET TO INLET
F	7	RESIDUAL AIR REMOVAL
F	8	CO2 TO HOLDING TANK

△ - RESIDUAL AIR REMOVAL MODE

Figure 5-2.2. 4BMS operating modes.

(2) Relocation of MT06 and MT07 to measure inlet and outlet air temperatures. (MT01 performs the function of measuring the temperature of the air entering the CO_2 sorbent beds and is in a location to get a more accurate reading.)

(3) Increasing the duration of modes 1A and 3A from 2 to 7 min to ensure that all of the residual air is removed from the CO_2 sorbent beds.

5.2.2 Discussion of Results

5.2.2.1 General

The 4BMS operated for over 150 hr, during which time measurements from 27 subsystem sensors were recorded. Plots of these measurements (plus measurements from three module simulator sensors) were made (Figs. 5-2.3 through 5-2.43) and are discussed below. The average CO_2 removal efficiency was 43.9 percent at an average pCO_2 of about 3.6 mmHg and a rate of 6.36 lb/day (2.89-person load). (The CO_2 removal efficiency calculations are discussed below in more detail.) Analysis results of samples of the outlet CO_2 are given in Table 9-1 and show that the composition was 92.7% CO_2, 4.2% N_2, 1.4% O_2 and less than 0.5 percent of other compounds (with an error of ± 10 percent). A surprising, and as yet unexplained, difference from the SIT analysis results is that an excess of O_2 is indicated (rather than N_2) compared with the proportions in air. This may be due to analysis uncertainties or a small amount of adsorption of O_2 by the sorbent.

5.2.2.2 Discussion of Individual Measurements

5.2.2.2.1 CO_2 Injection Rate Into the Module Simulator (FF12)

The rate of CO_2 injection into the module simulator was constant at 6.36 lb/day for most of the test (as shown in Fig. 5-2.3). This corresponds to a 2.89-person metabolic load. It was initially set slightly higher, but was reduced after about 19 hr to lower the CO_2 partial pressure level.

5.2.2.2.2 4BMS Inlet Airflow Rate (FF13)

The inlet air flow rate stayed mainly between 76 and 82 lb/hr (as shown in Fig. 5-2.4 and 5-2.5). The sharp, cyclic spikes dropping to near zero correspond to the recycle mode where airflow from the module HX essentially ceases while the internal air recirculates, bypassing the flow meter.

At about 37 hr into the test, a malfunction occurred which activated the Hold command. This stopped the timer, but the heaters, the compressor, and air blower continued to operate. The malfunction was not immediately noticed and it took some time to determine an appropriate workaround. The controller could not be accessed to determine if it had failed since it was inside the closed module simulator. The manual advance on the control panel outside was found to be effective and was used to advance the timer for the remainder of the test (with one exception noted below). The 4BMS operated in mode 2 for about 2.5 hr (instead of the desired 44 min) before manual control was initiated.

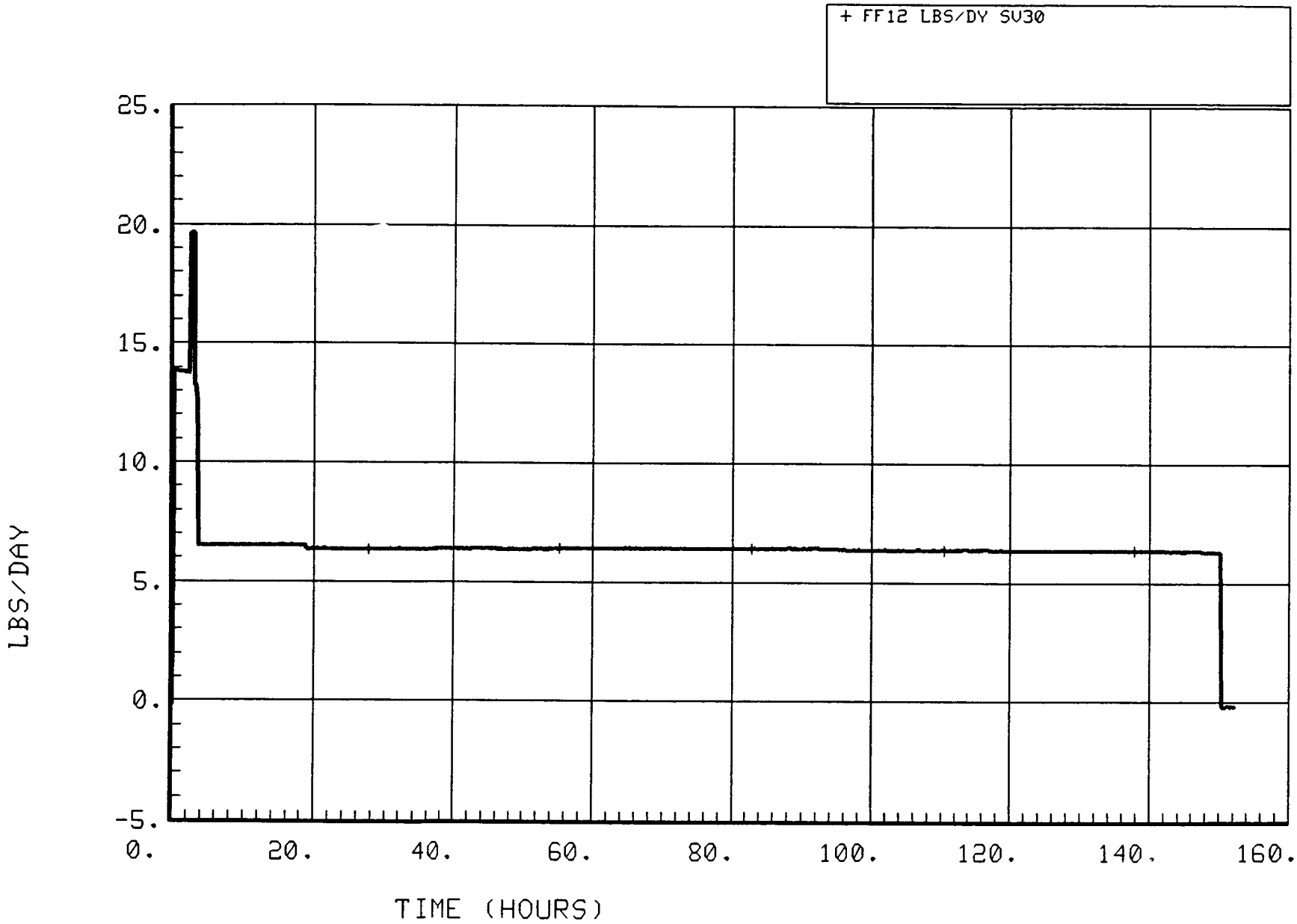

Figure 5-2.3. CO_2 simulator inject rate (FF12).

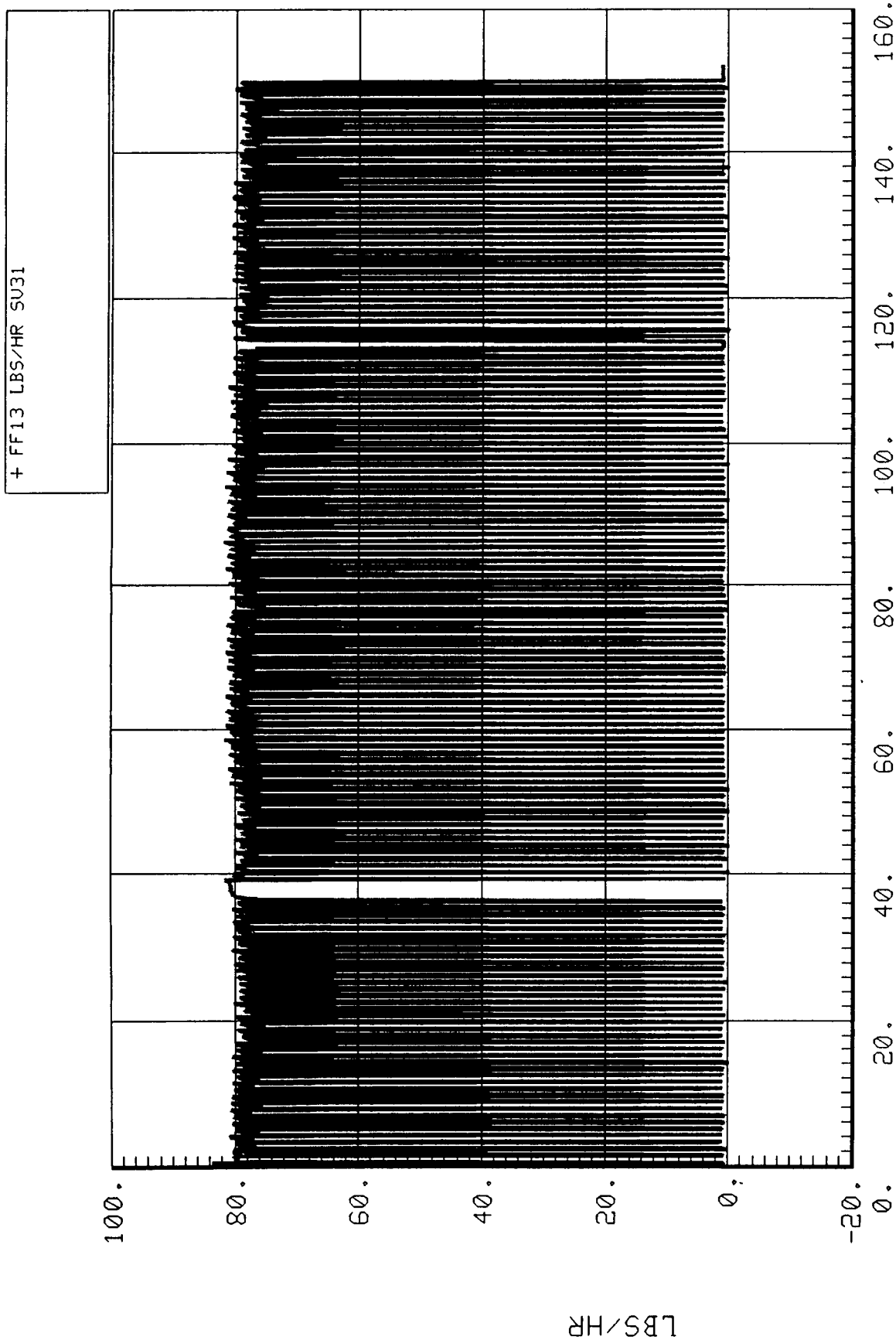

Figure 5-2.4. 4BMS inlet airflow rate (FF13).

At about 114 hr into the test, a brief power failure to the 4BMS heaters occurred and the subsystem was turned off and restarted. Upon restart, the cycle advanced properly until Mode 2 when, again, manual advancing became necessary. Another, smaller, aberration occurred in the data at this time. Aberrations occur at these two times on almost all of the 4BMS measurement plots.

5.2.2.2.3 4BMS Inlet Air CO_2 Partial Pressure (FP12)

The inlet air CO_2 partial pressure started at about 2.0 mmHg and gradually increased for the first 20 hr before leveling off at about 3.4 mmHg. The controller malfunction at 37 hr is readily apparent (in Fig. 5-2.6) by a rapid increase in pCO_2 to about 4.4 mmHg prior to initiation of manual advancing of the timer. The decrease in the pCO_2 level was fairly rapid at first, then slowed to a shallow slope. The second aberration at 114 hr repeated the pattern of the first before the pCO_2 level could return to the level prior to the first aberration. The cycle mode changes produce the sawtooth pattern and the cyclic spikes correspond to modes 1 and 3. The expanded plot (Fig. 5-2.7) shows that the sawtooth pattern is due to pCO_2 decreases of 0.1 to 0.2 mmHg as the adsorb mode (2 or 4) proceeds. During recycle the pCO_2 level in the module simulator increases until the next adsorb mode begins. This effect is also shown in the plot of FP10 (the module pCO_2 level). Spikes are evident in the plot of FP12 (but not FP10, which indicates that they are due to an internal 4BMS phenomenon) which occur during recycle of the residual air (shown on the expanded plot). As the residual air is pumped out, the heaters are beginning to raise the temperature and the most easily desorbed CO_2 is removed, mixed with the residual air, and results in a spike. The spikes during Mode 1 are larger than those of Mode 3. This is an effect related to the CO_2 sorbent beds not having identical sorbent compositions. Bed 2 contains 8 lb of Zeolite 5A, while Bed 4 contains 2.4 lb of Zeolite 13X and 5.4 lb of Zeolite 5A. This was done in order to determine any advantages of using a mixed bed. The results indicate that the CO_2 is being desorbed from the 5A since the Mode 1 spikes are larger (Bed 2 desorbing). Except for the cyclic spikes, the plot of FP12 is very similar to that of FP10 as expected.

During the SIT, downward spikes occurred during Mode 3 which were not evident during the EMCT. The spikes decline to roughly ambient pCO_2 levels which would indicate that ambient air without the injected CO_2 was reaching the sensor during Mode 3, possibly due to leakage. This spike would not be evident during the EMCT (even with leakage) since the module simulator was sealed and had an elevated CO_2 level.

5.2.2.2.4 4BMS Inlet Air Temperature (MT06)

The inlet air temperature (air from the module simulator HX) varied between 60° and 65°F for most of the test (as shown in Fig. 5-2.8). The cyclic spikes reaching up to 89°F correspond to the recycle mode where internal air was returned to the inlet duct. The mild undulations correspond to the day/night cycle. The expanded plot (Fig. 5-2.9) shows the effects of recycle more clearly.

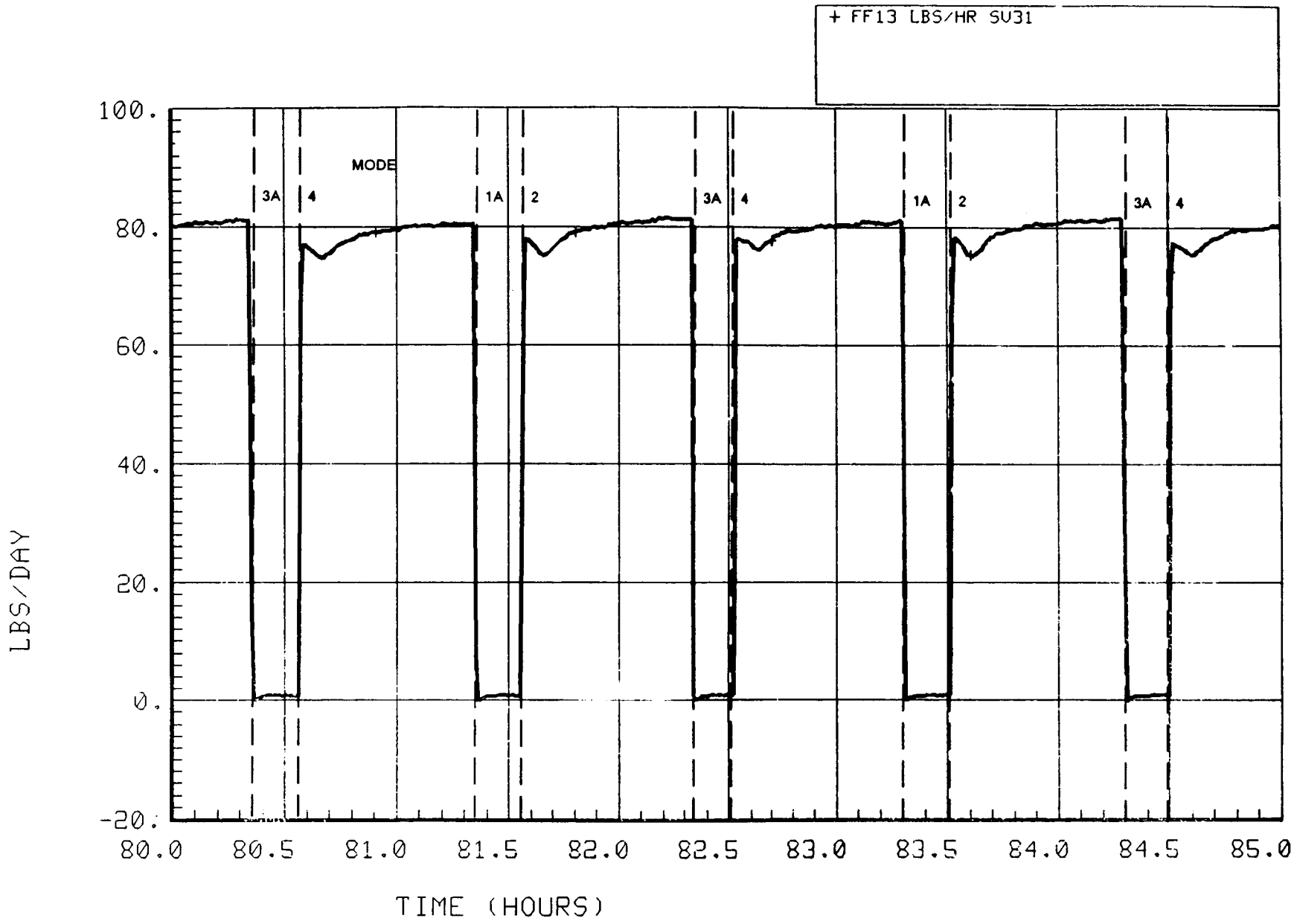

Figure 5-2.5. Expanded 4BMS inlet airflow rate (FF13).

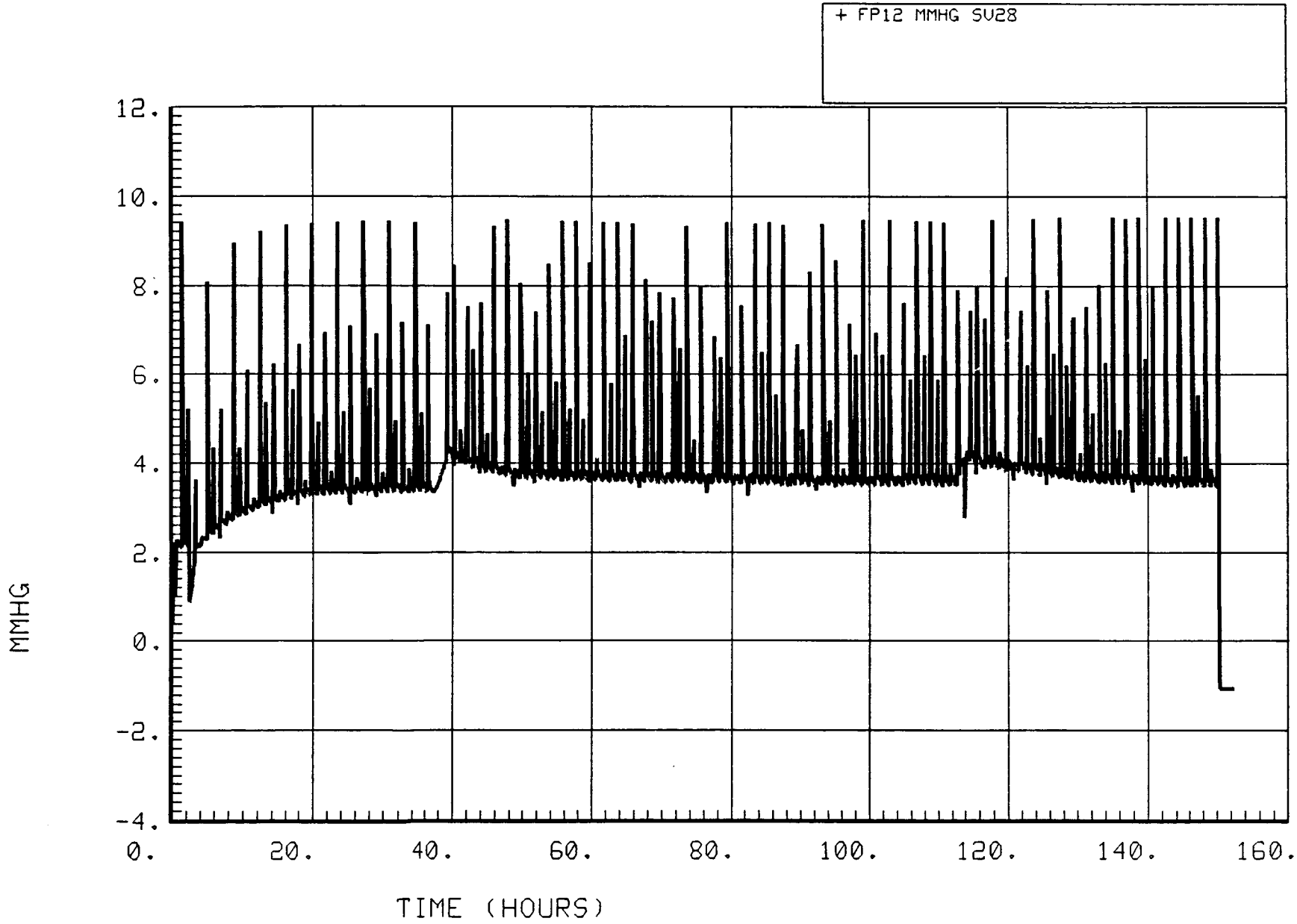

Figure 5-2.6. 4BMS air CO_2 partial pressure (FP12).

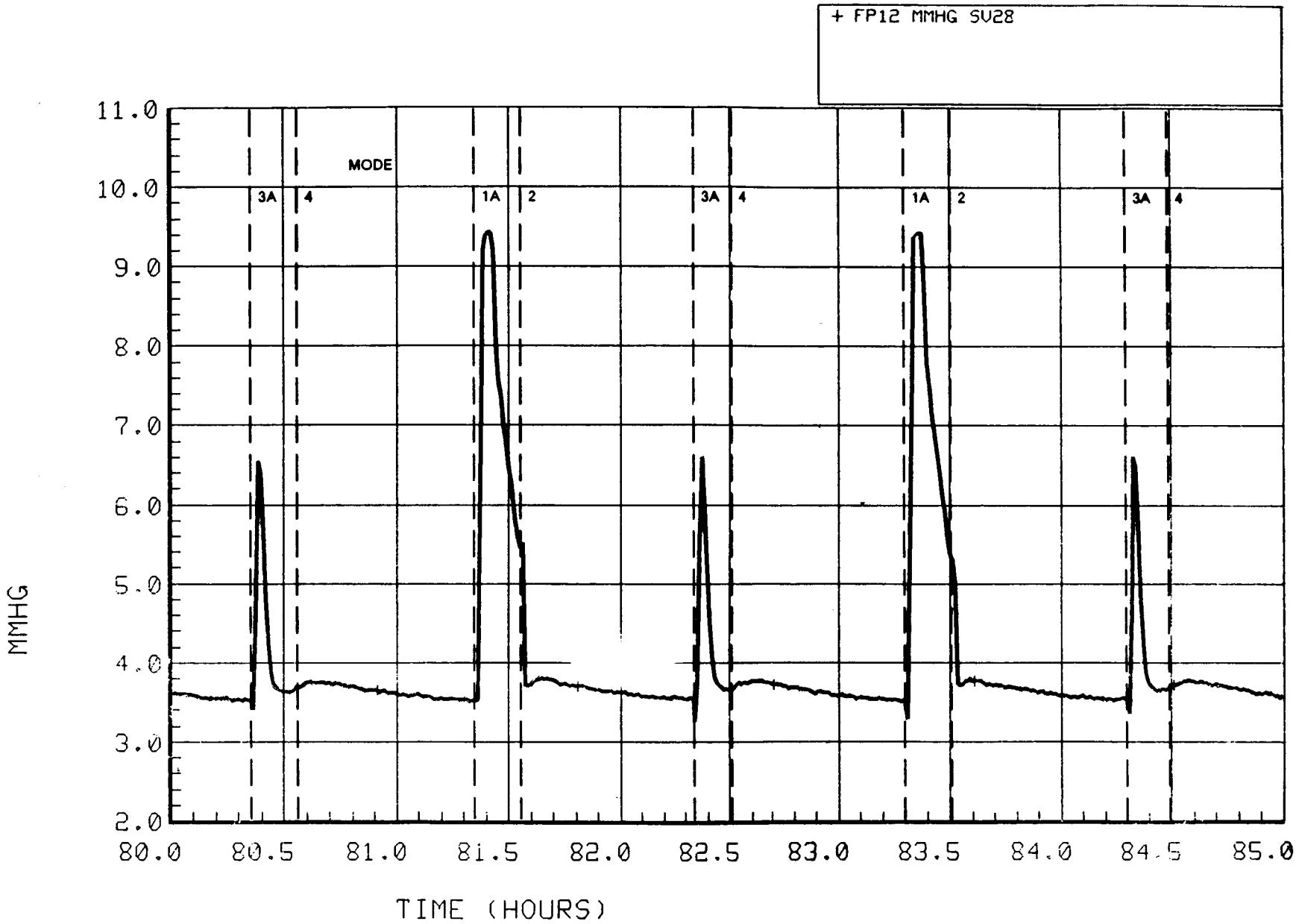

Figure 5-2.7. Expanded 4BMS air CO_2 partial pressure (FP12).

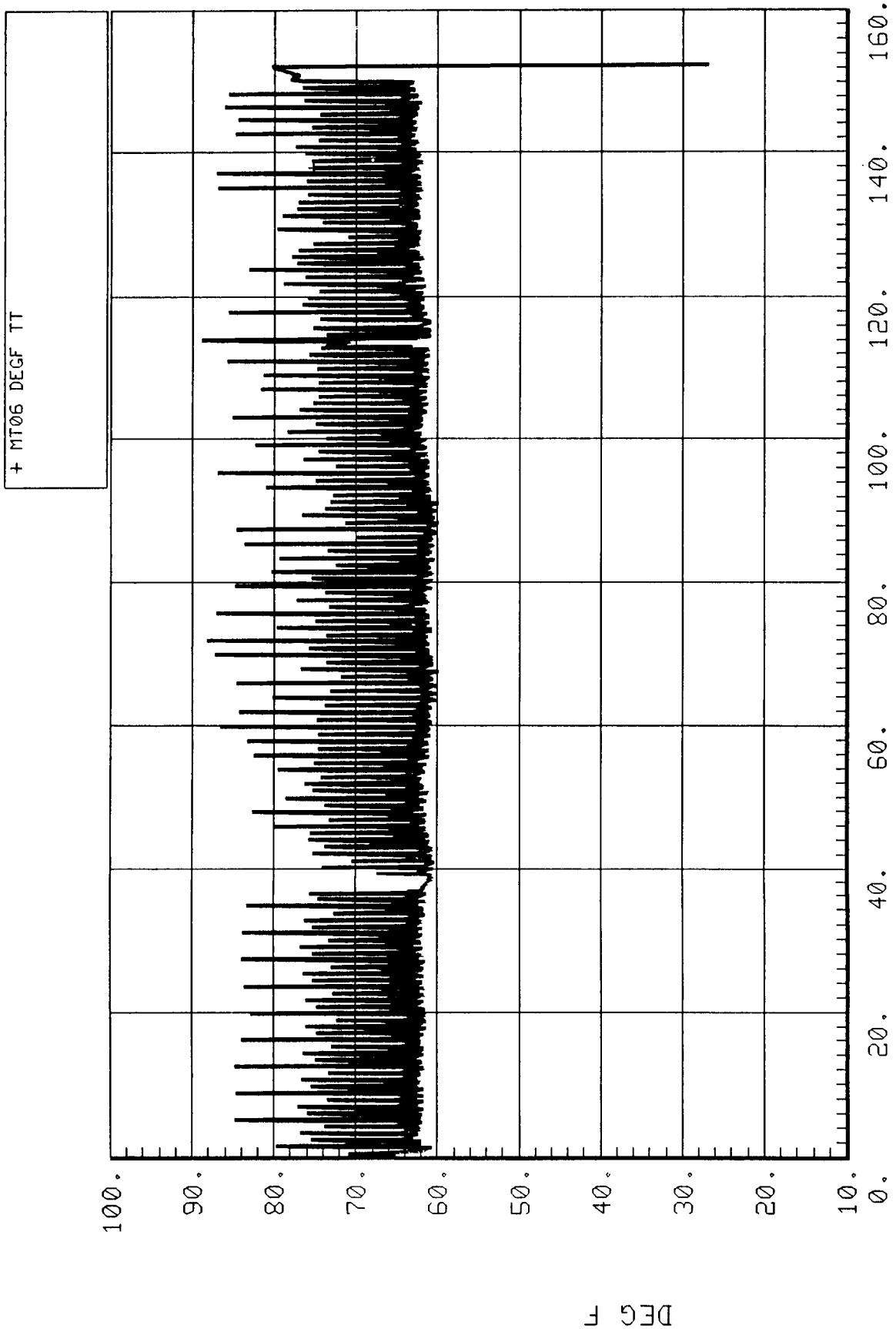

Figure 5-2.8. 4BMS inlet air temperature (MT06).

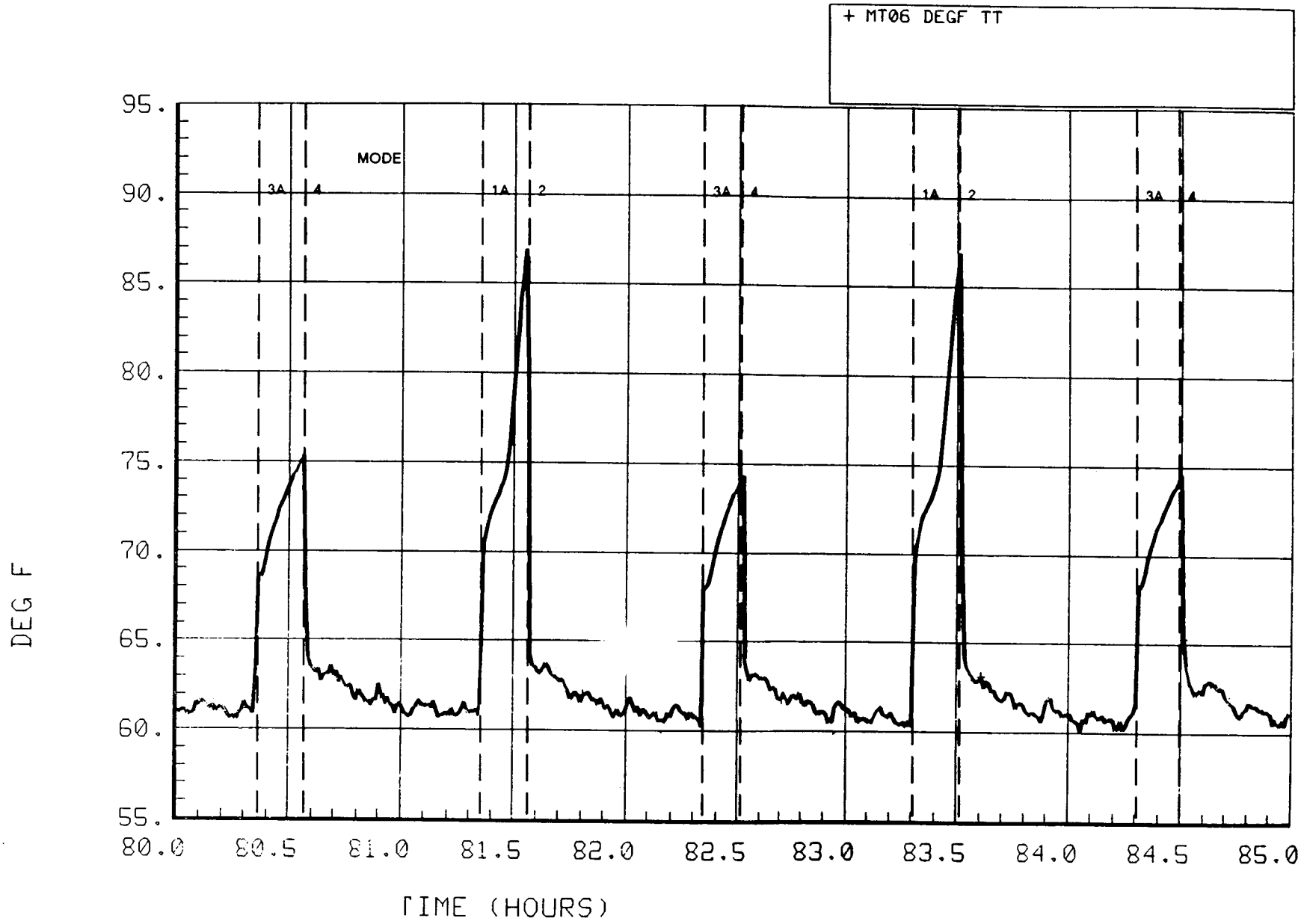

Figure 5-2.9. Expanded 4BMS inlet air temperature (MT06).

5.2.2.2.5 4BMS Inlet Air Dewpoint (MDP1)

The inlet air dewpoint (Fig. 5-2.10) usually ranged from 38° to 45°F which, when compared with the module simulator dewpoint (Fig. 6-7), shows that the HX is reducing the dewpoint by about 3°F. The cyclic spikes to about 62°F correspond with the recycle modes where the desiccant beds are starting to desorb.

5.2.2.6 4BMS Desiccant Bed 1 Inlet Air Temperature (MT03)

The Bed 1 inlet air temperature (Fig. 5-2.11) ranged from about 63° to 99°F over the course of the test. The expanded plot (Fig. 5-2.12) shows details that are correlated with the cycle mode changes. At the beginning of Mode 1, the valves reconfigure Bed 1 from desorb (with warm air flowing through the bed) to adsorb and a sharp temperature drop occurs. This does not continue, however, as the internally recycled air warms due to heat from the recently desorbed and still hot Bed 4 beginning to reach Bed 1 via Bed 3. The temperature peaks at about 93°F by the end of Mode 1B, then quickly drops as Mode 2 begins and tracks MT06 (inlet air temperature) at about 2°F higher, which may be a real temperature rise, a calibration error, or a combination thereof. As Mode 3 begins, the temperature increases sharply as heat from the just-desorbed Bed 2 is transferred by forced convection. The temperature then peaks and drops as Bed 2 cools, until the cycle repeats. The day/night cycle is also apparent. After the first aberration the temperature drops by several degrees and gradually climbs as the test progresses, reaching the highest level near the conclusion of the test.

5.2.2.2.7 4BMS Desiccant Bed 3 Inlet Air Temperature (MT04)

The plots of MT04 (Figs. 5-2.13 and 5-2.14) are very similar to those of MT03, except that they are for the alternate half-cycle. The differences are due to the different location of the sensor and the slight differences in the temperatures reached by the CO_2 sorbent beds (discussed below, MT10 and MT11).

5.2.2.2.8 4BMS Dewpoint of the Air Downstream of the Desiccant Beds (MDP2)

The dewpoint of the air downstream of the desiccant beds (Fig. 5-2.15) ranges from -42° to -90°F (by the end of the test) indicating that leakage which had occurred during the SIT (when the dewpoint ranged from -10° to -42°F) was sealed. The higher readings at the beginning probably reflect excessive moisture loading resulting from previous short-term operation periods. The drop in dewpoint shows the recovery capability of the desiccant beds. The expanded plot (Fig. 5-2.16) shows that the spikes occur every half-cycle, during Modes 2 and 4. The reason for the spikes is not presently understood, but may be related to temperature variations in the desiccant beds as Mode 2 or 4 proceeds. (Sensor MT02, which failed early in the test, would have provided useful information on temperature changes in the desiccant beds.)

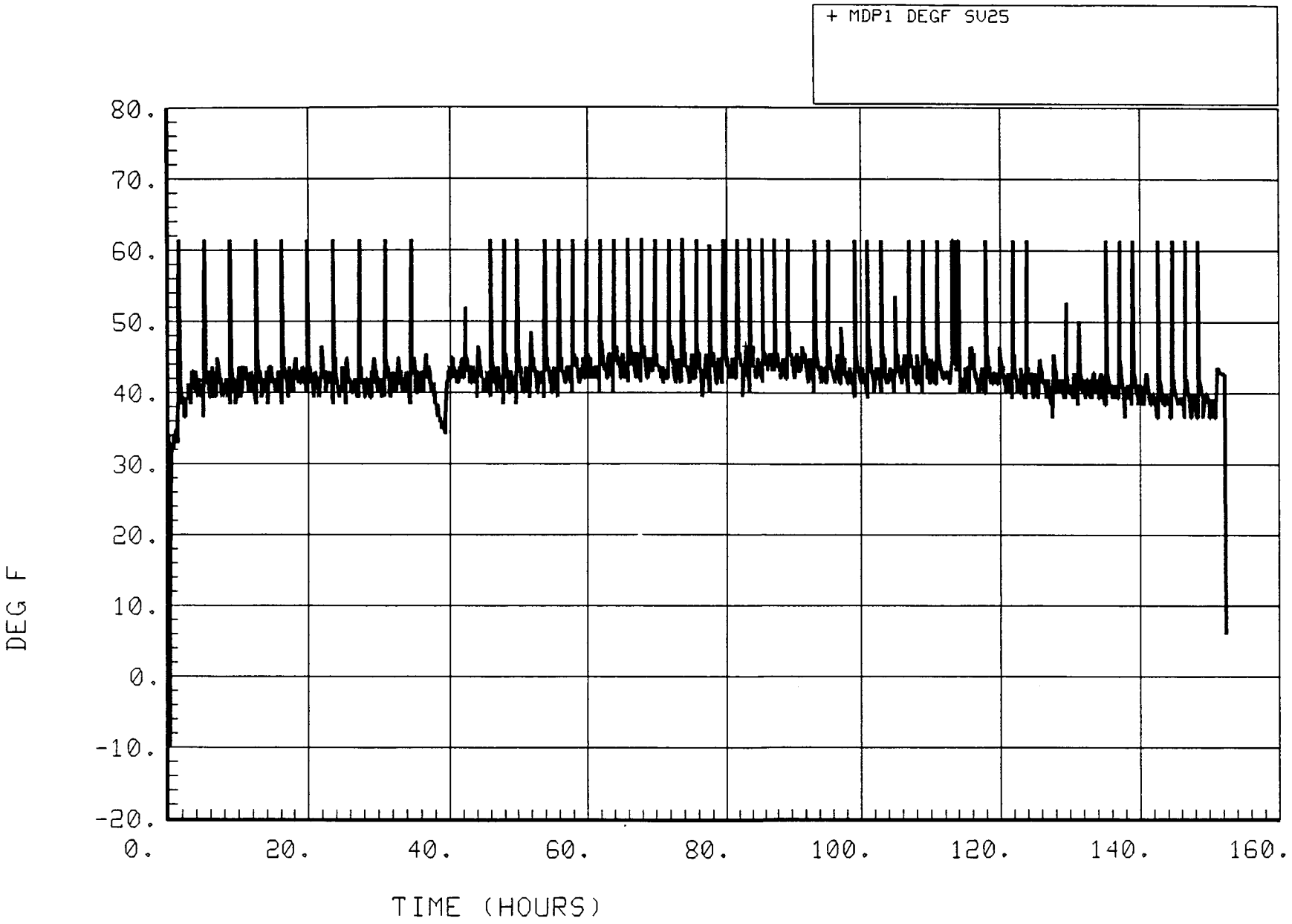

Figure 5-2.10. 4BMS inlet air dewpoint (MDP1).

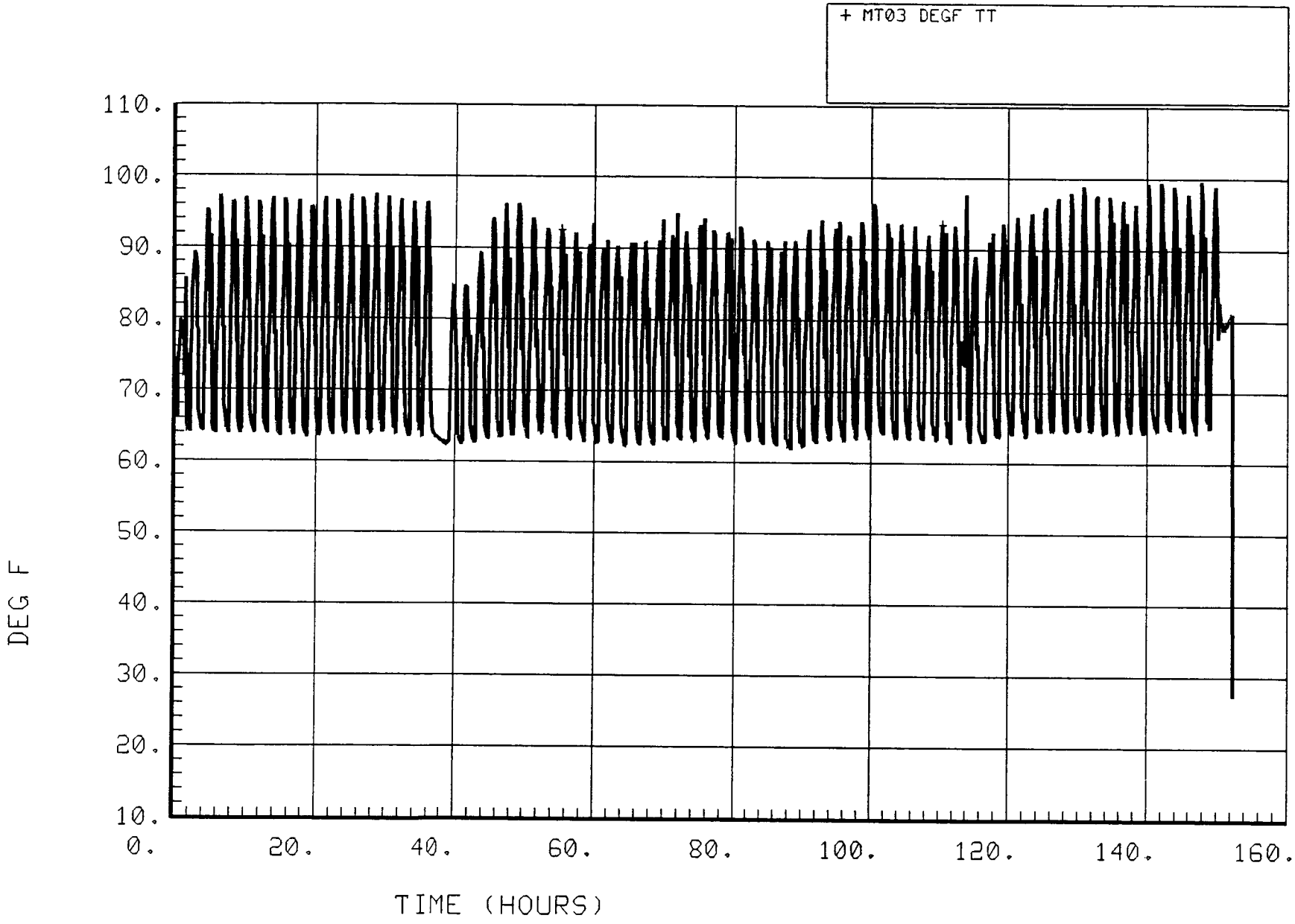

Figure 5-2.11. 4BMS desiccant bed No. 1 inlet air temperature (MT03).

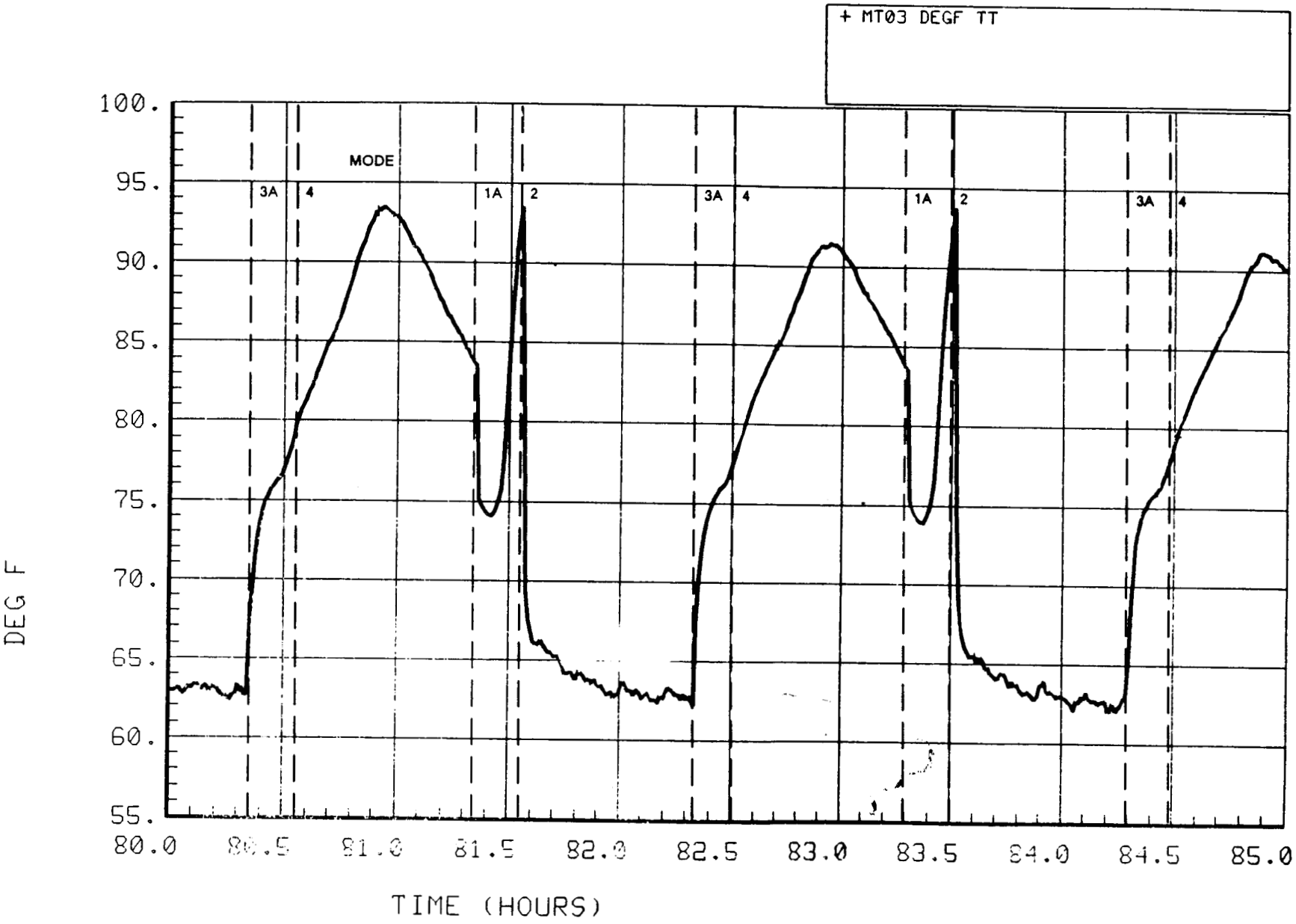

Figure 5-2.12. Expanded 4BMS desiccant bed No. 1 inlet air temperature (MT03).

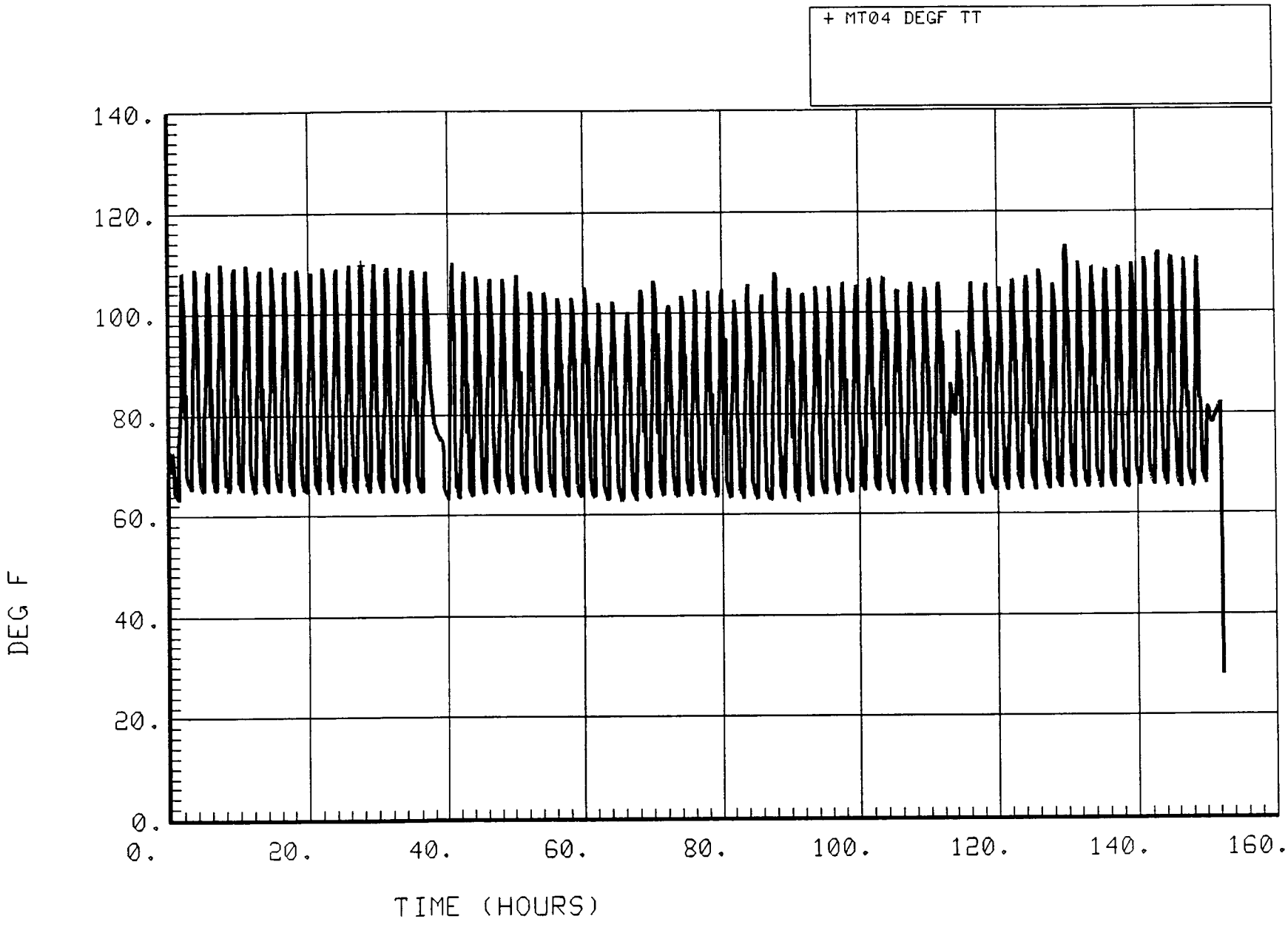

Figure 5-2.13. 4BMS desiccant bed No. 3 inlet air temperature (MT04).

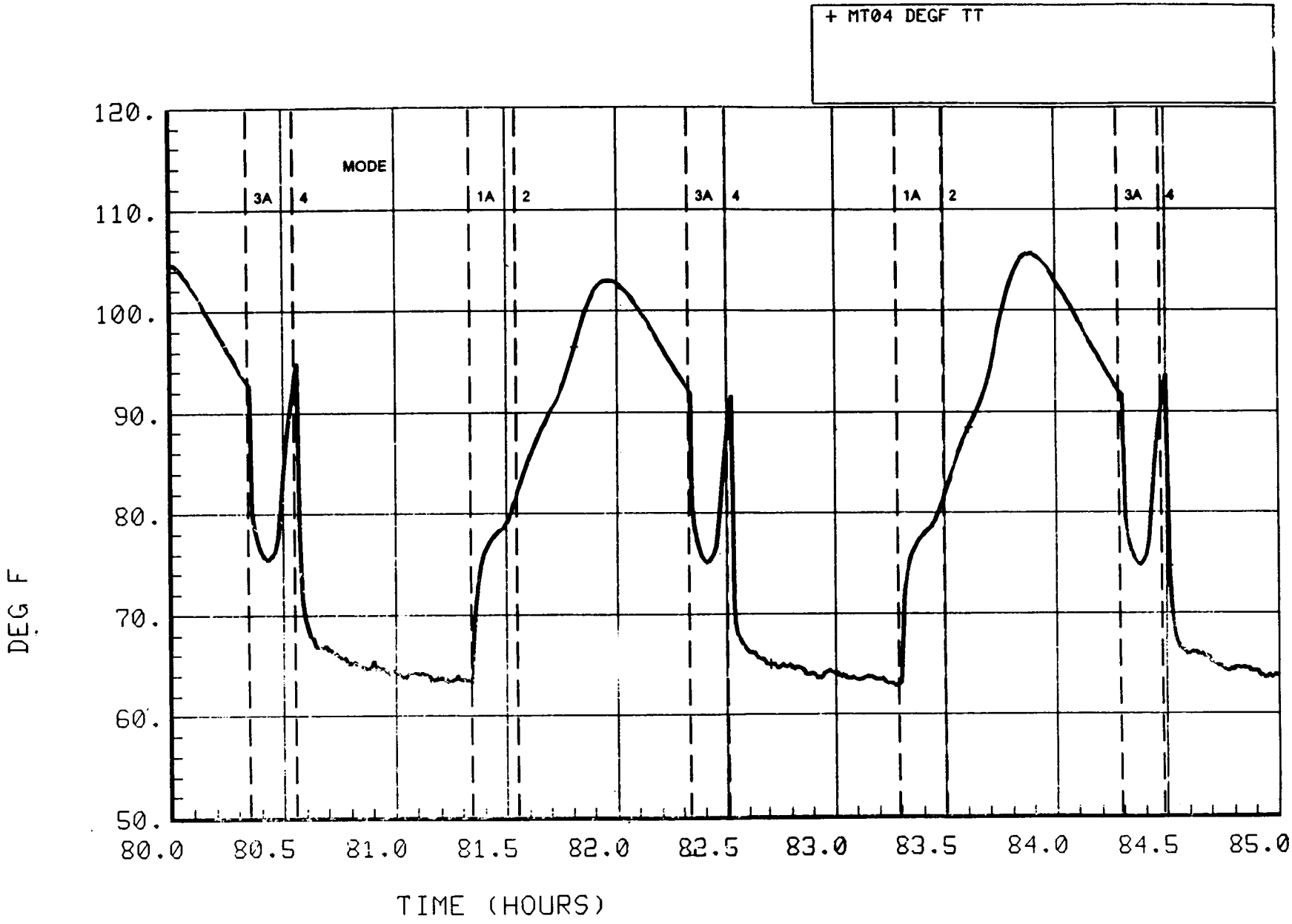

Figure 5-2.14. Expanded 4BMS desiccant bed No. 3 inlet air temperature (MT04).

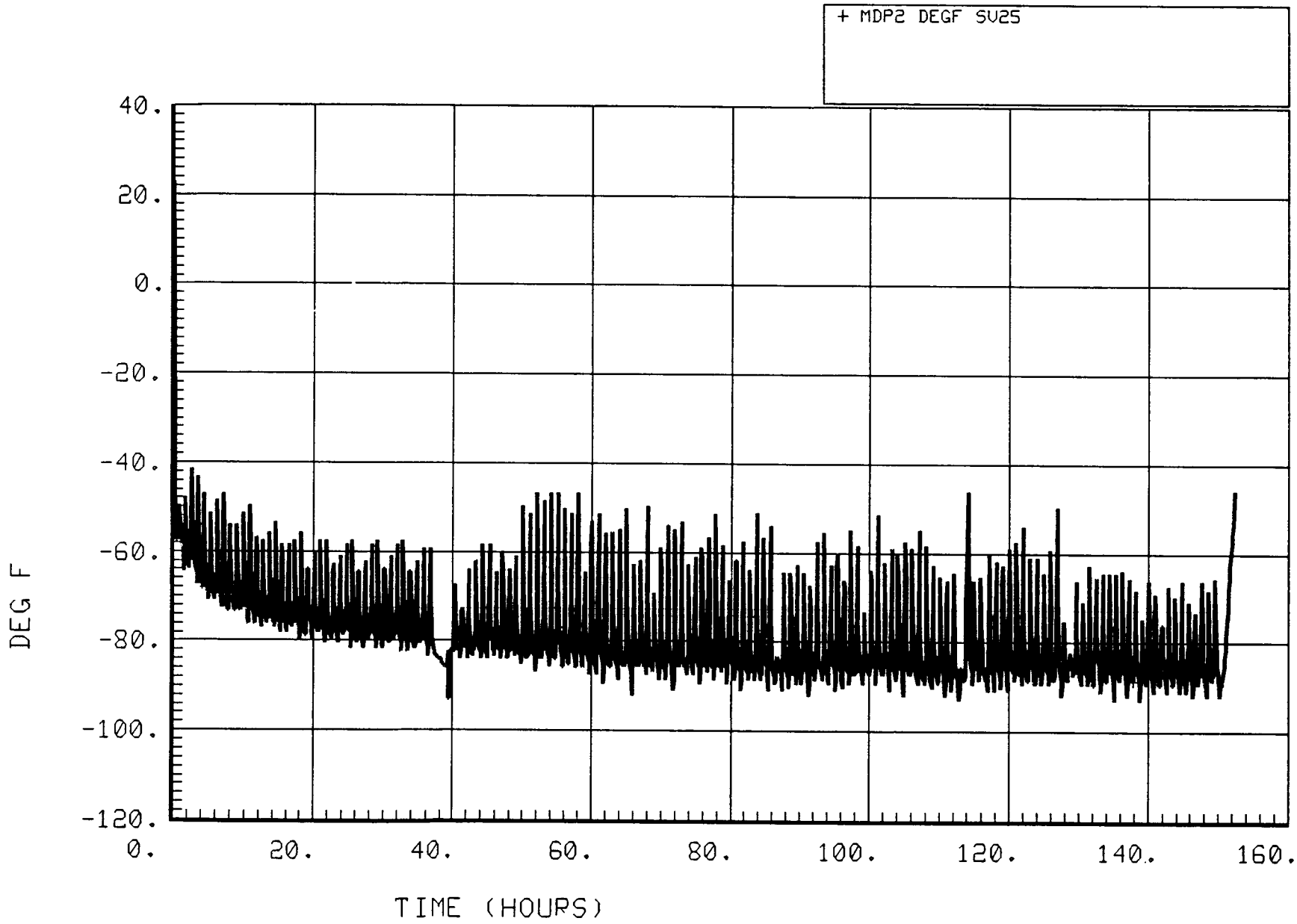

Figure 5-2.15. 4BMS dewpoint of downstream desiccant bed (MDP2).

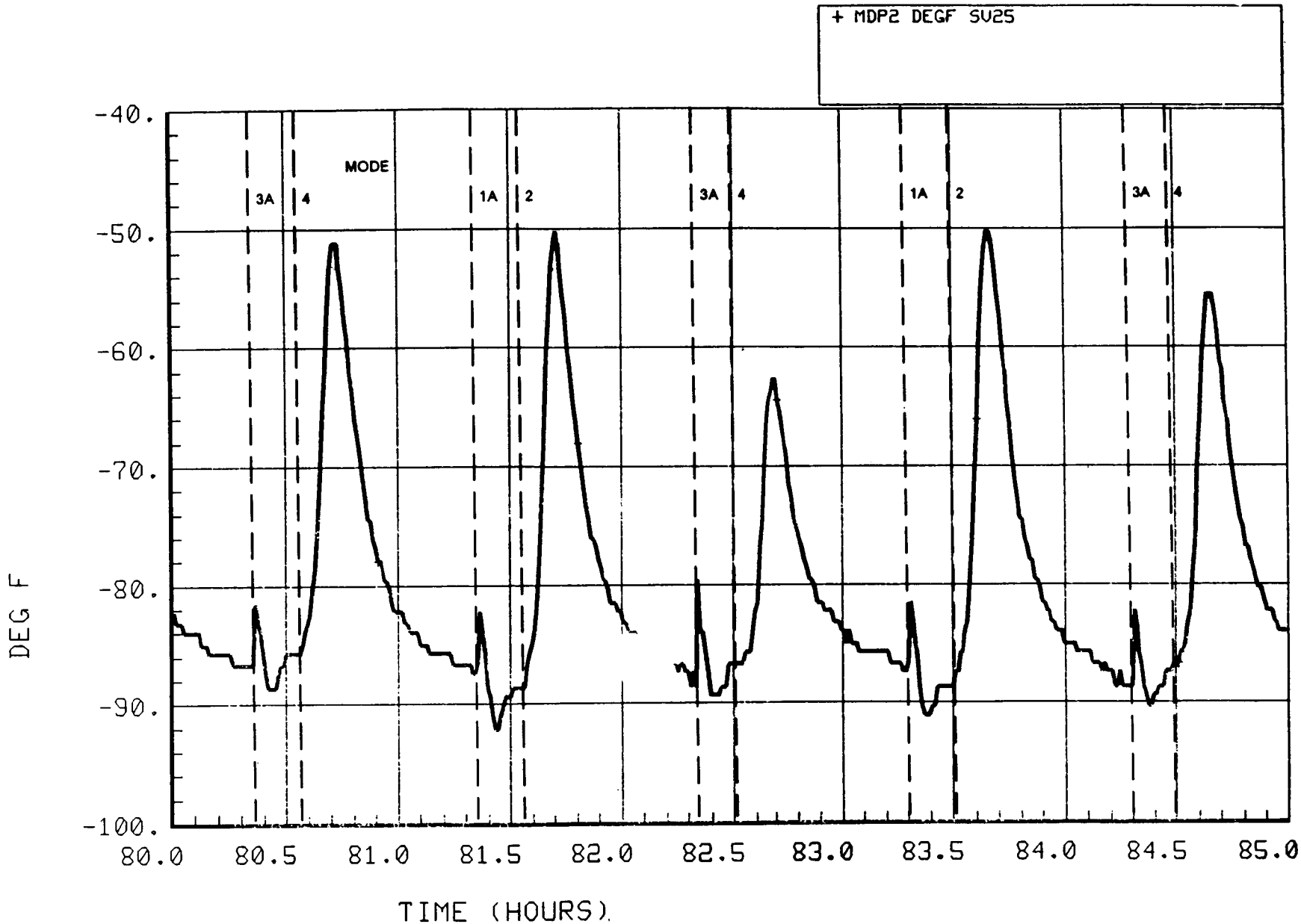

Figure 5-2.16. Expanded 4BMS dewpoint of downstream desiccant bed (MDP2).

5.2.2.2.9 4BMS Blower Outlet Pressure (MP01)

The blower outlet pressure (Fig. 5-2.17) varied from about 1.8 to 2.1 psig. The variations correspond with cycle mode changes and indicate different pressure losses during different modes. The expanded plot (Fig. 5-2.18) shows that during most of Modes 2 and 4 the pressure was essentially constant [slightly lower pressure (~0.05 psi) during Mode 4 than Mode 2, which may be due to the different sorbents used (Zeolite 5A and 13X in Bed 4, only Zeolite 5A in Bed 2)]. Upon entering Modes 1 and 3, the pressure sharply increased by 0.2 to 0.3 psi and then decreased throughout recycle and into Modes 2 and 4, dipping below 1.8 psig before returning to a more constant level of about 0.25 into Modes 2 and 4. When compared with measurements from the SIT (which ranged between 2.0 and 2.5 psig) the EMCT measurements show a significant decrease. This resulted from the modifications to the ducting and the valve replacements, which reduced the overall length of the ducting and removed constrictions at the valves. [After the SIT, the five-way valves (which have a 5/8 in. flow path on one pathway) on the CO_2 sorbent beds were replaced with 1-in. two-way valves. Also, the path length from the sorbent beds to the desiccant beds was shortened considerably. This result is reduced pressure drop and increased air flow through the 4BMS.]

5.2.2.2.10 4BMS Blower Outlet Temperature (MT02)

This sensor failed early in the test and a plot is not included. Prior to failure this sensor was reading about 180°F.

5.2.2.2.11 4BMS Precooler Outlet/Sorbent Bed Inlet Temperature (MT01)

The temperature of the precooler outlet air (Fig. 5-2.19) ranged from 70° to 76°F and showed variations due to cycle mode changes and the day/night cycle. The lower temperatures are higher than those experienced during the SIT due to elimination of leakage through valve A, which had been replaced with one of the five-way valves previously used on a CO_2 sorbent bed. The expanded plot (Fig. 5-2.20) shows an offset of about 1°F between Modes 3 and 4 and Modes 1 and 2. This same effect also occurred during the SIT but with an offset of about 5°F. This may be due to leakage of cooler air into the duct during Modes 1 and 2 or different thermal transfer characteristics associated with the different modes.

5.2.2.2.12 4BMS Coolant Flow Rate (FF08)

The coolant flow rate through the 4BMS stayed near 0.68 gpm for most of the test (as shown in Fig. 5-2.21). At about 96 hr into the test, the plot shows a sharp increase to about 0.73 gpm with a gradual reduction to 0.71 by the end of the test. Presently, the causes of the increase and of various fluctuations and spikes are not understood, although the spikes coincide with the heater failure at about 114 hr into the test.

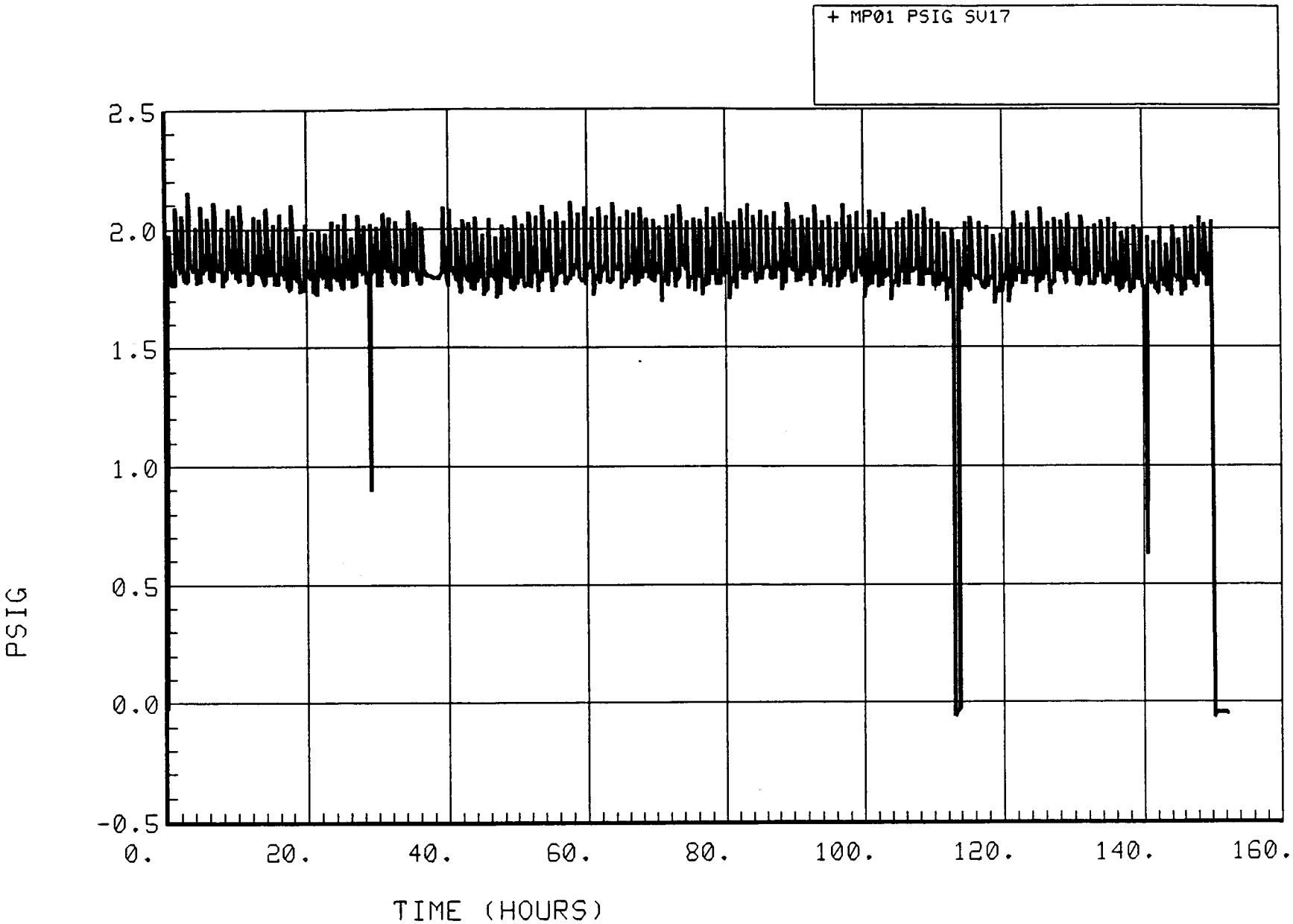

Figure 5-2.17. 4BMS blower outlet pressure (MP01).

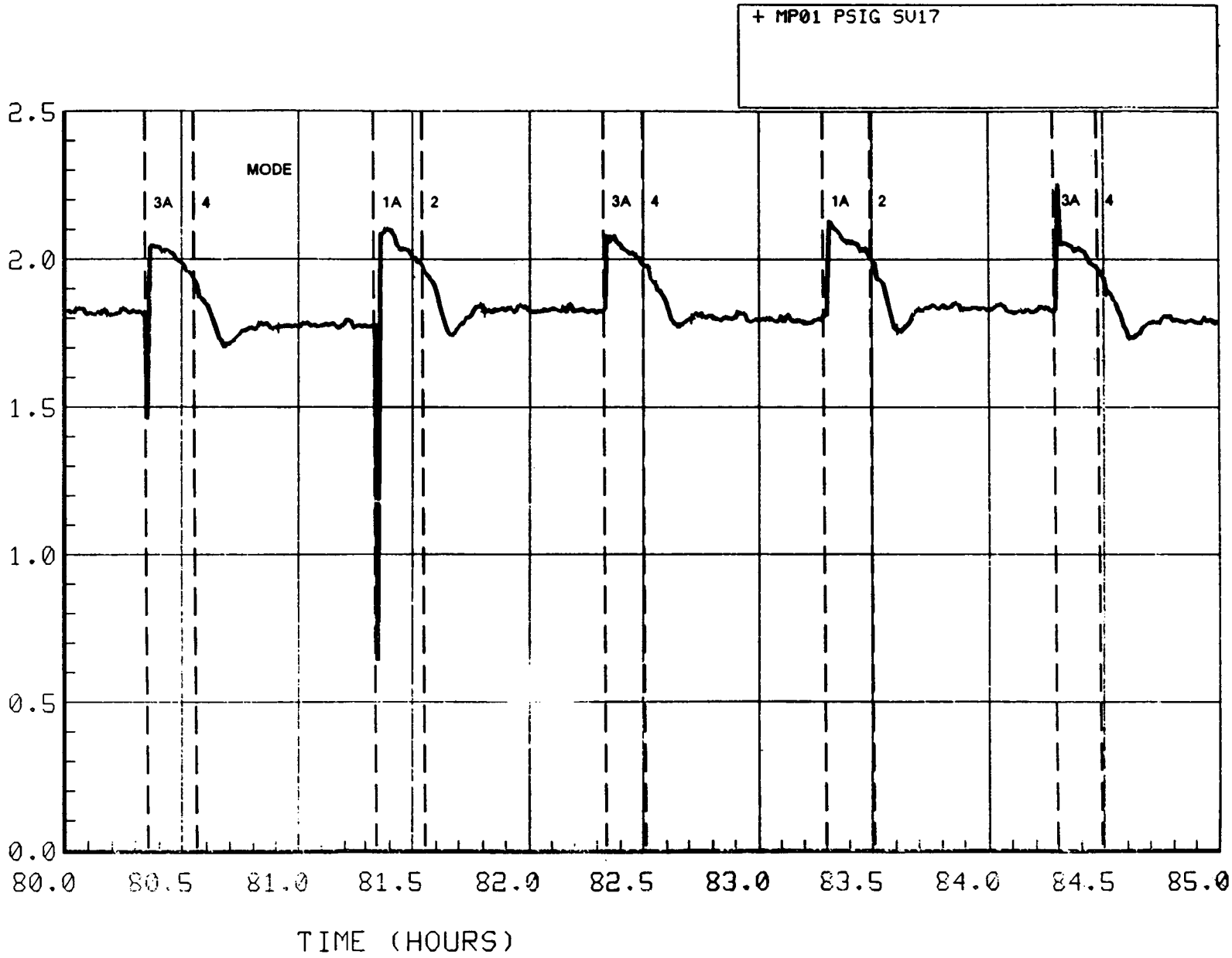

Figure 5-2.18. Expanded 4BMS blower outlet pressure (MP01).

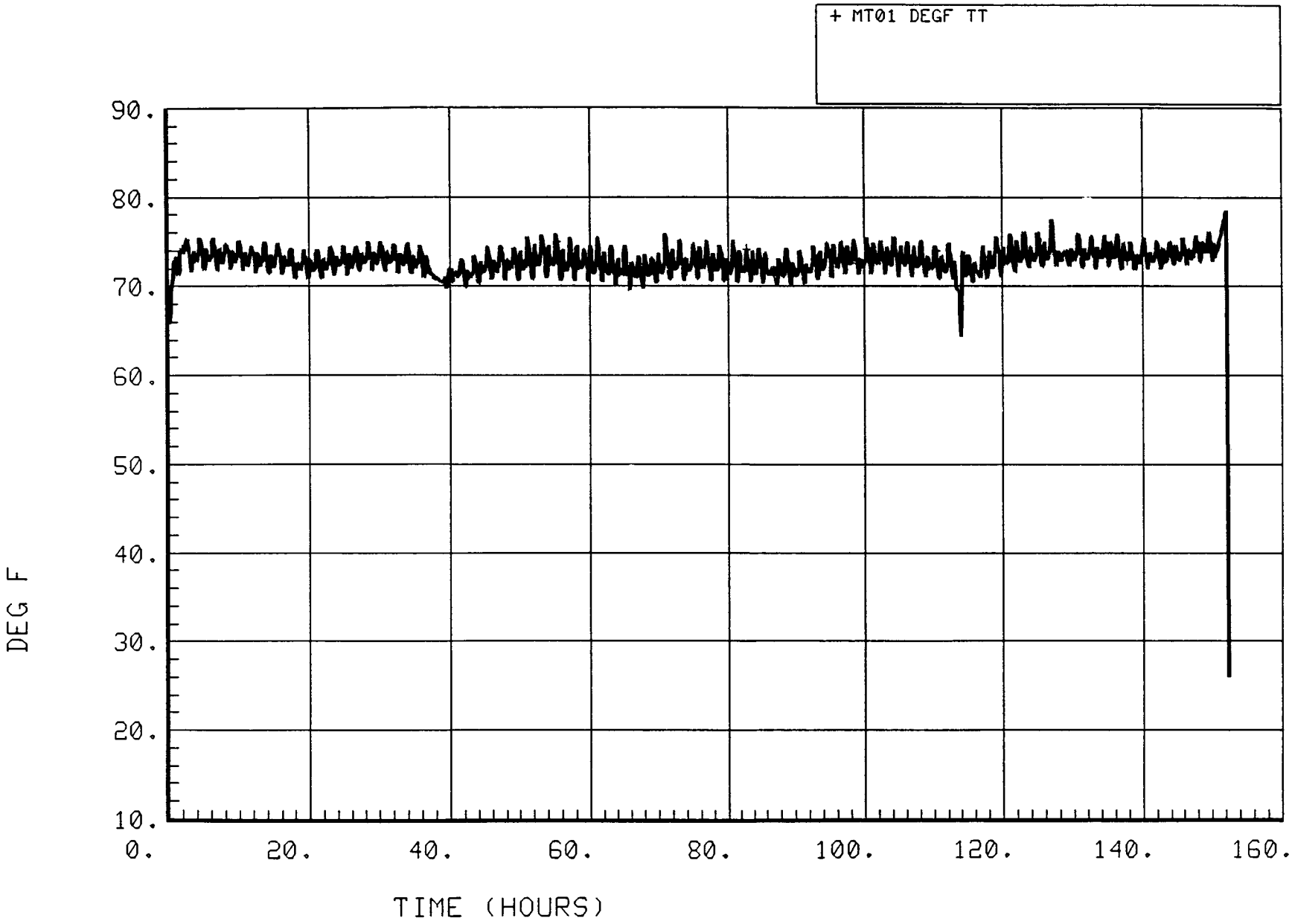

Figure 5-2.19. 4BMS precooler outlet/sorbent bed inlet temperature (MT01).

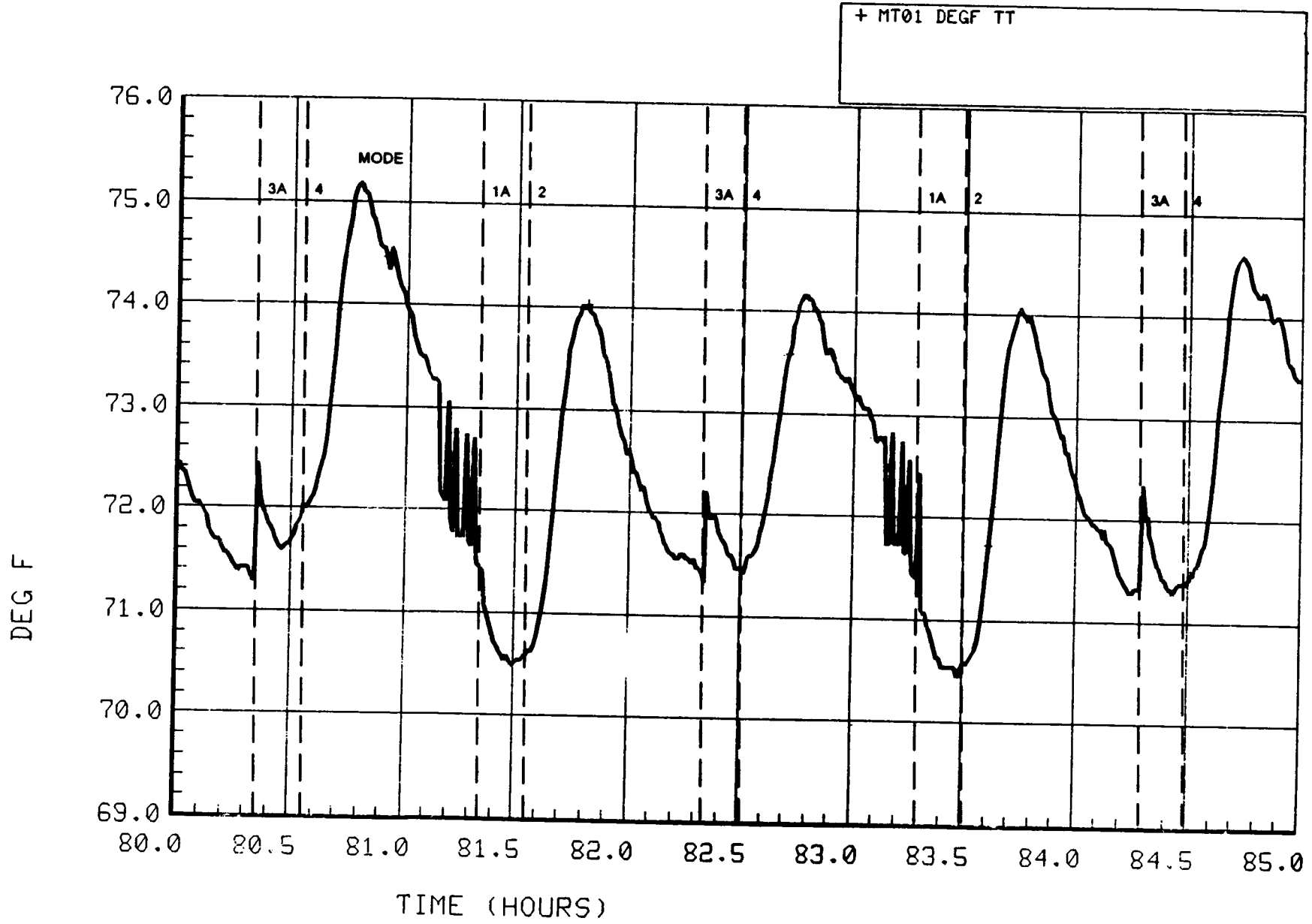

Figure 5-2.20. Expanded precooler outlet/sorbent bed inlet temperature (MT01).

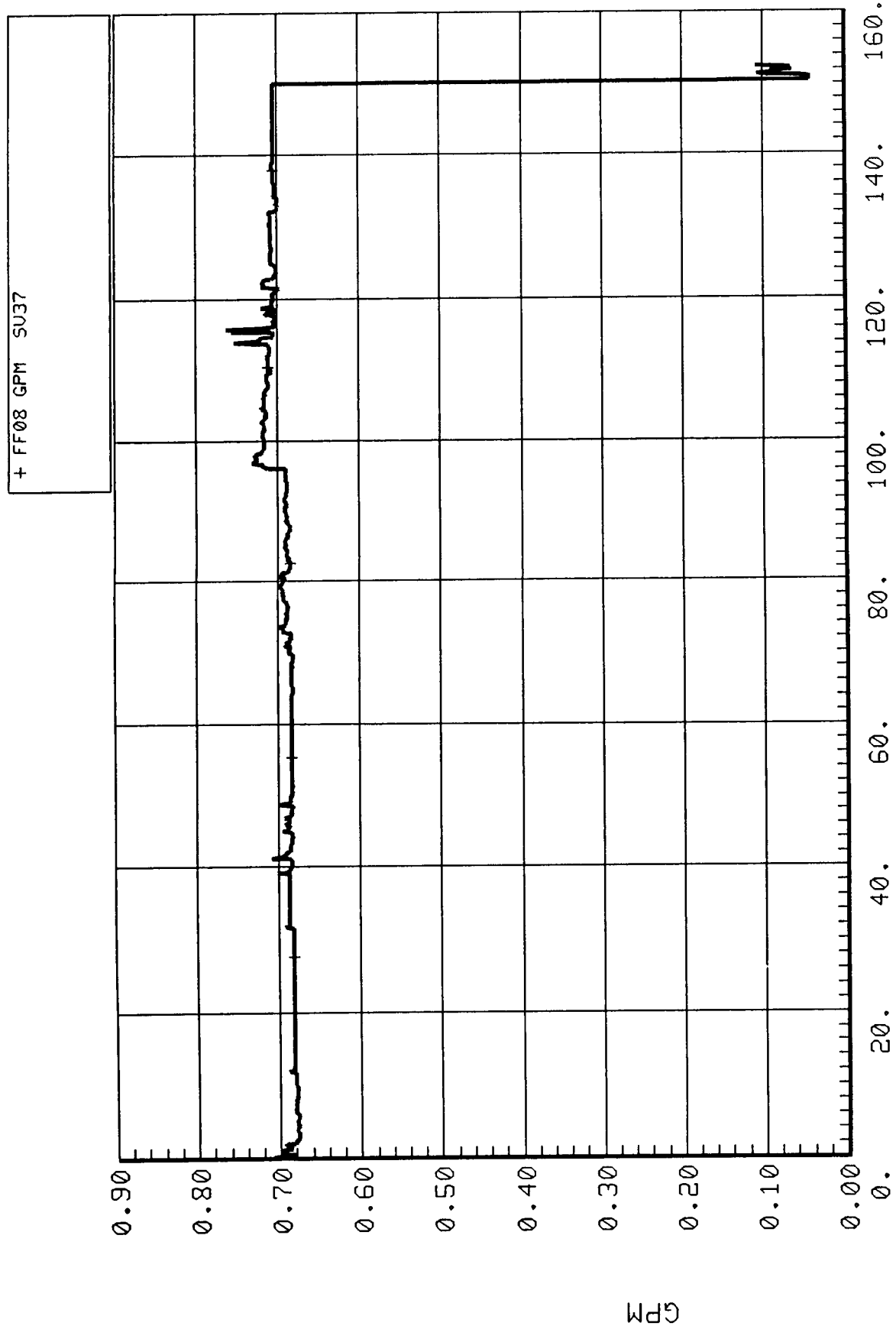

Figure 5-2.21. 4BMS coolant flowrate (FF08).

5.2.2.2.13 4BMS Coolant Inlet and Outlet Temperatures (FT04 and FT05)

Both the inlet and outlet coolant temperature plots (Figs. 5-2.22 and 5-2.23) show the cyclic fluctuations of the 4BMS. The average inlet temperature was about 42°F and the outlet temperature was 45°F. The variations shown in the plot of FF08 are not echoed in the temperature plots.

5.2.2.2.14 4BMS CO_2 Sorbent Bed 2 Temperature (MT10)

The temperatures in sorbent Bed 2 varied from about 65° to 390°F (shown in Fig. 5-2.24), as the bed cycled through CO_2 adsorption and desorption. The heaters were on during Modes 1 and 2 and, upon reaching 390°F, maintained that temperature until the end of Mode 2, as intended.

5.2.2.2.15 4BMS CO_2 Sorbent Bed 4 Temperature (MT11)

The temperatures in sorbent Bed 4 varied from about 65° to 400°F (shown in Fig. 5-2.25), as the bed cycled. The heaters were on during Modes 3 and 4 and, upon reaching 400°F, maintained that temperature until the end of Mode 4, as intended.

5.2.2.2.16 4BMS CO_2 Sorbent Bed Heater Voltages (MV01 and MV02)

The heater voltage plots show that the voltages to the sorbent bed heaters were either 0 or 26 V, corresponding to the Off and On conditions (shown in Figs. 5-2.26 and 5-2.27). Comparison of the two plots shows that the heaters alternated as intended and otherwise operated properly.

5.2.2.2.17 4BMS Desiccant Bed 1 Inlet Air Temperature During Desorption (MT05)

As shown in Figure 5-2.28, at this location the air temperature varies from about 75° to 340°F. The expanded plot (Fig 5-2.29) show both large and small peaks which correspond with the cycle mode changes. The large peaks occur when the bed is being desorbed of water and has hot air from Bed 2 (which has just been desorbed of CO_2 and is being cooled for adsorption) flowing through it. The smaller peaks occur during Mode 2 when heat is added to the airflow during adsorption of water vapor and heated air reaches this sensor.

5.2.2.2.18 4BMS Desiccant Bed 3 Inlet Air Temperature During Desorption (MT08)

As shown in Figures 5-2.30 and 5-2.31, measurements from MT08 were similar to those from MT05 except that they are for the alternate half-cycle.

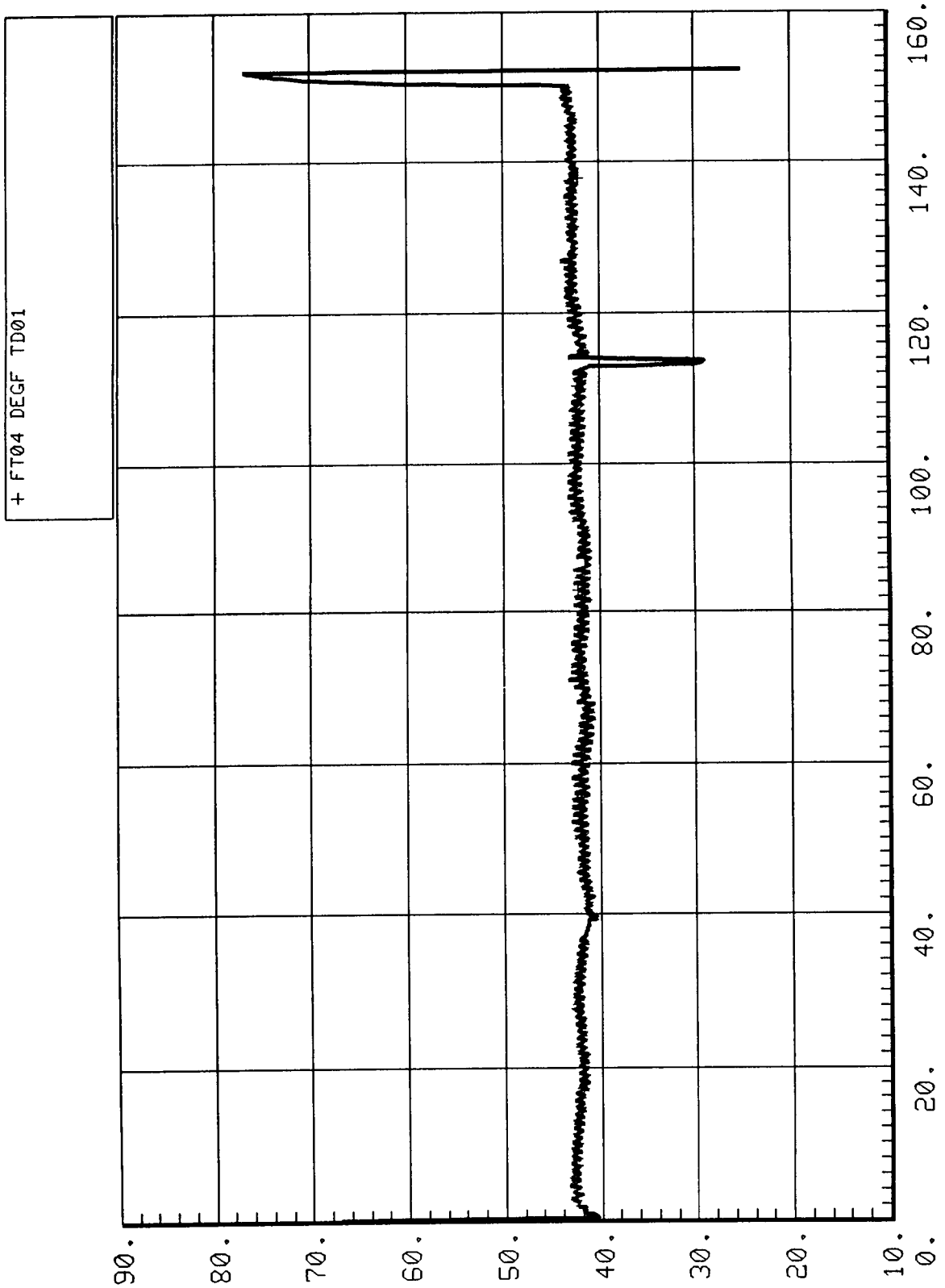

Figure 5-2.22. 4BMS coolant inlet temperature (FT04).

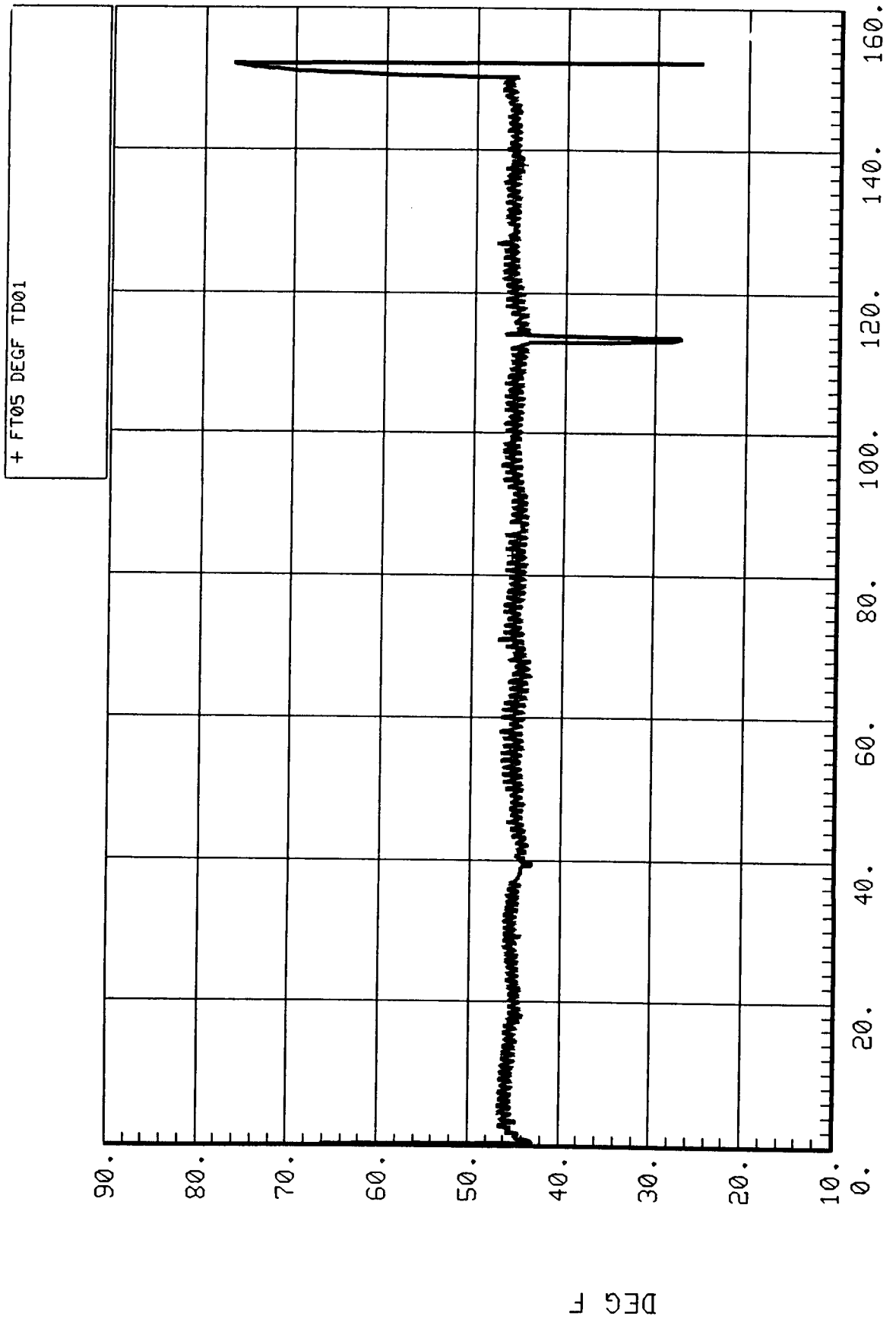

Figure 5-2.23. 4BMS coolant outlet temperature (FT05).

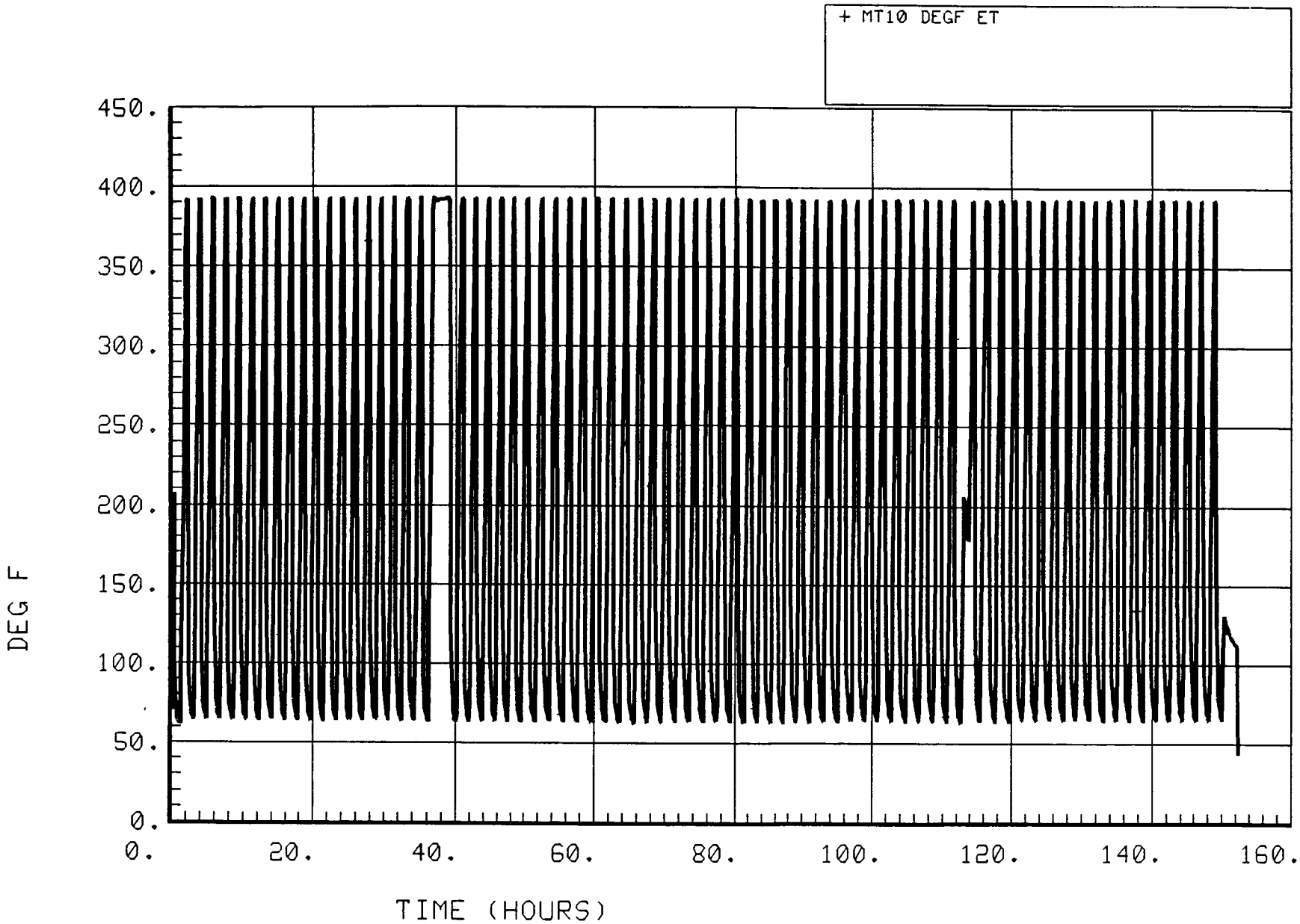

Figure 5-2.24. 4BMS CO_2 sorbent bed No. 2 temperature (MT10).

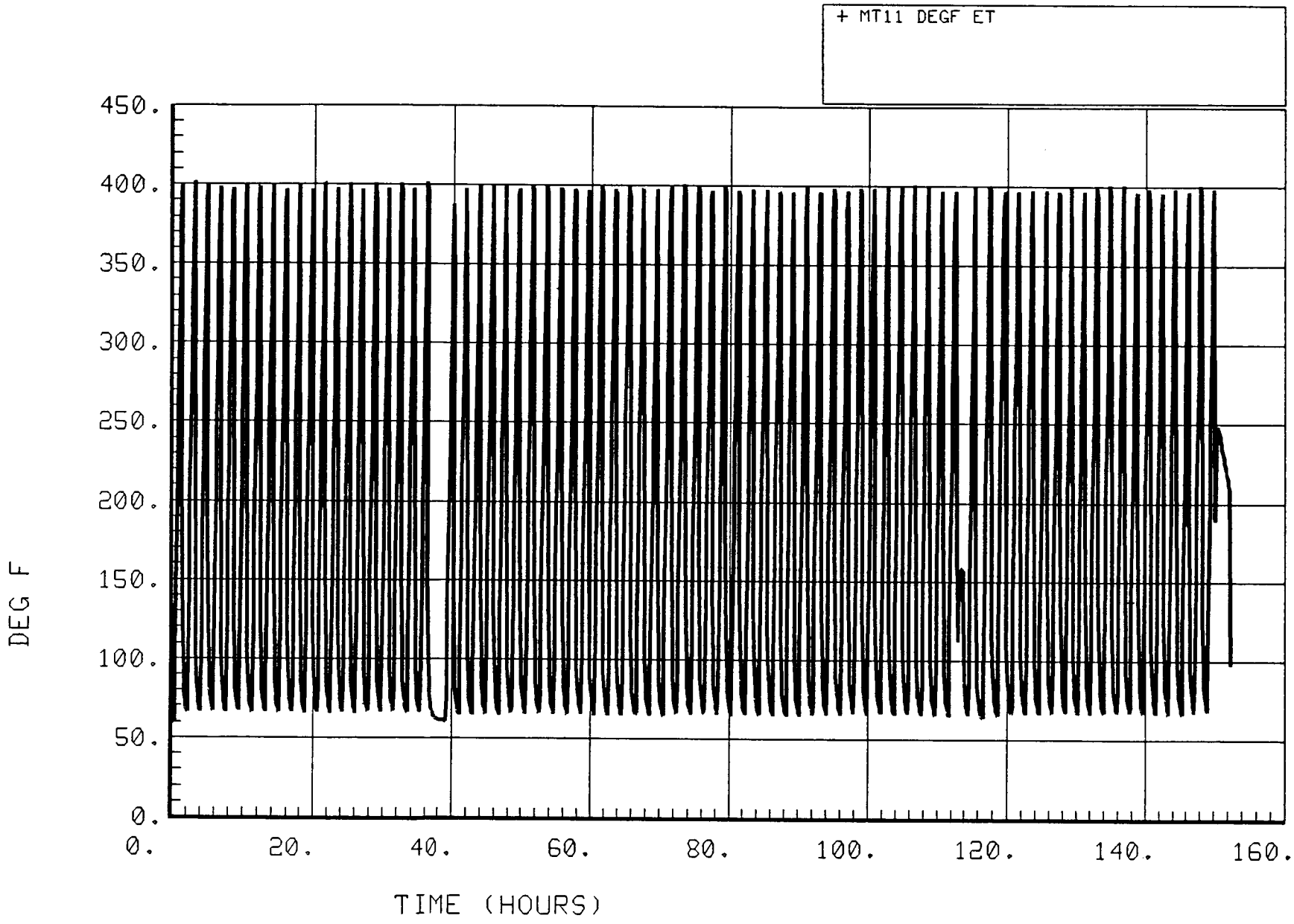

Figure 5-2.25. 4BMS CO_2 sorbent bed No. 4 temperature (MT11).

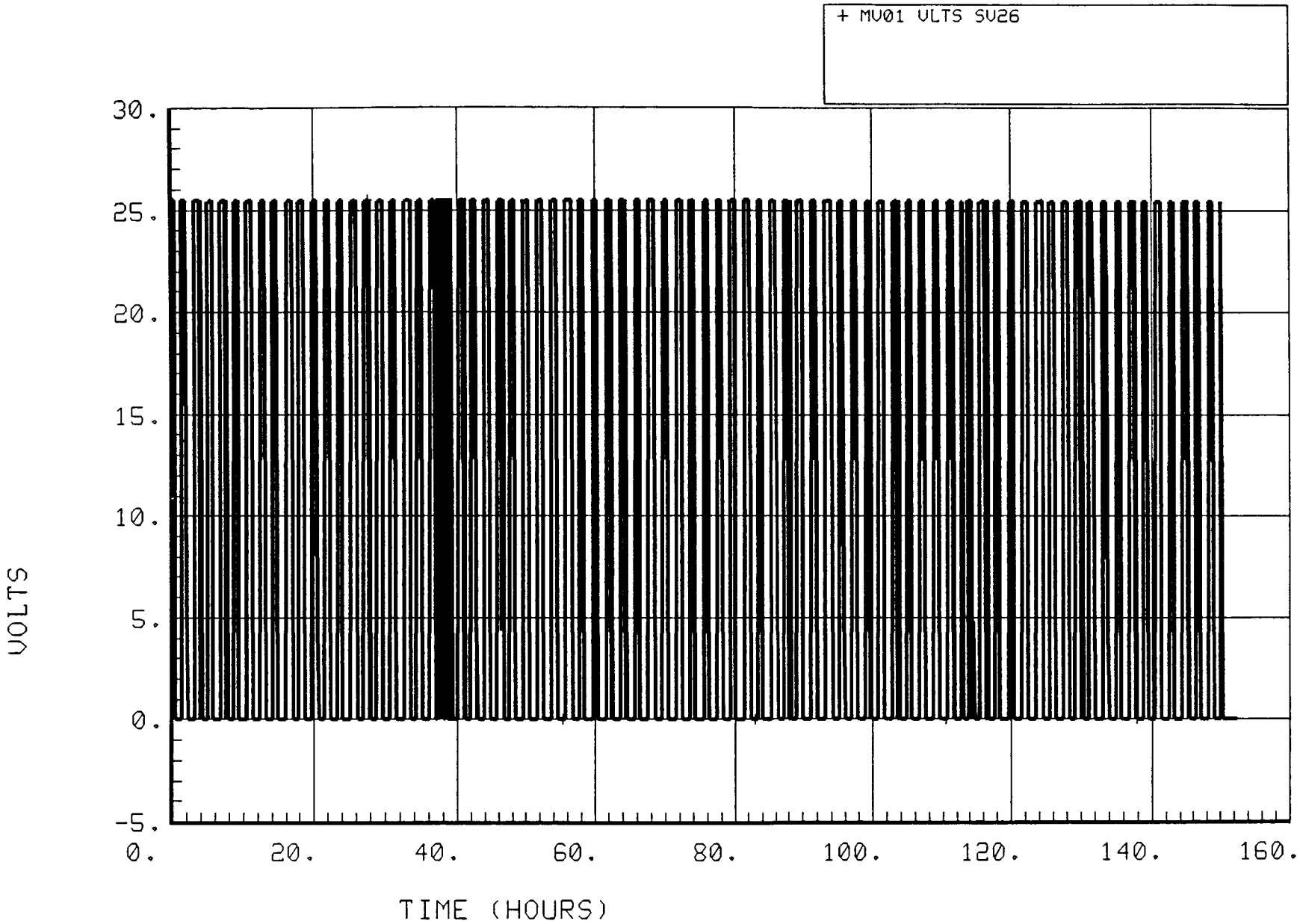

Figure 5-2.26. 4BMS CO_2 sorbent bed heater voltage (MV01).

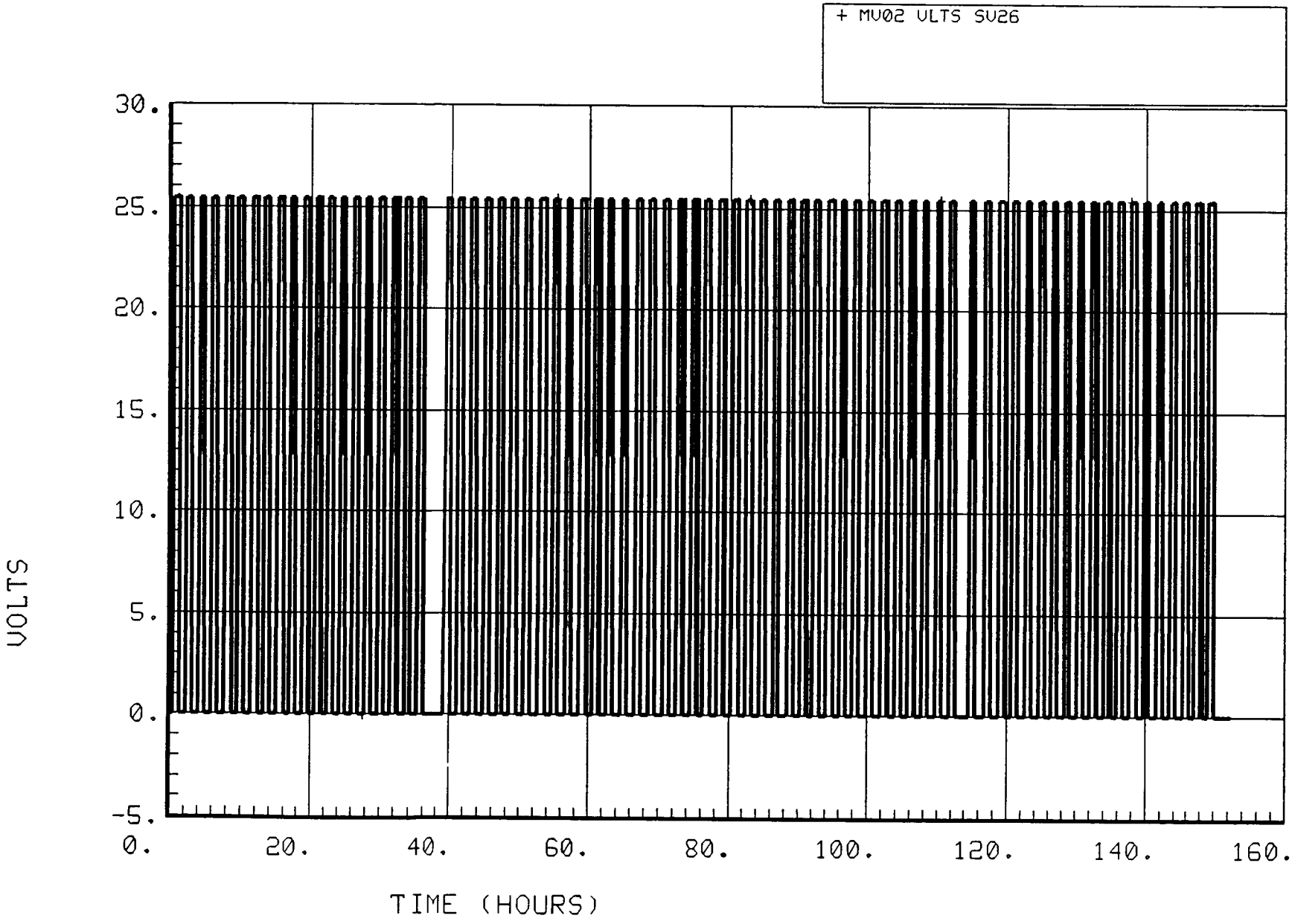

Figure 5-2.27. 4BMS CO_2 sorbent bed heater voltage (MV02).

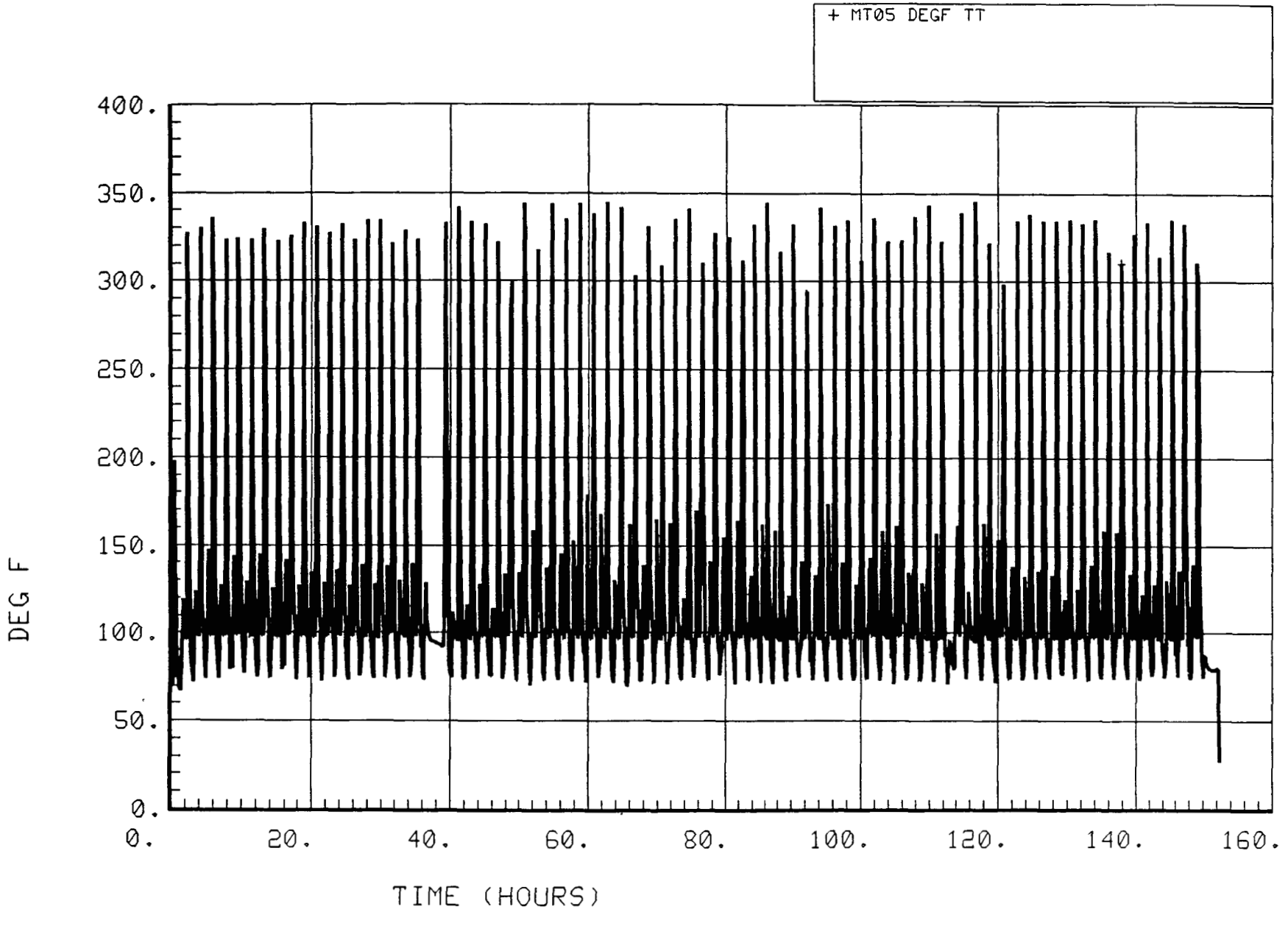

Figure 5-2.28. 4BMS desiccant bed 1 inlet air temperature during desorption (MT05).

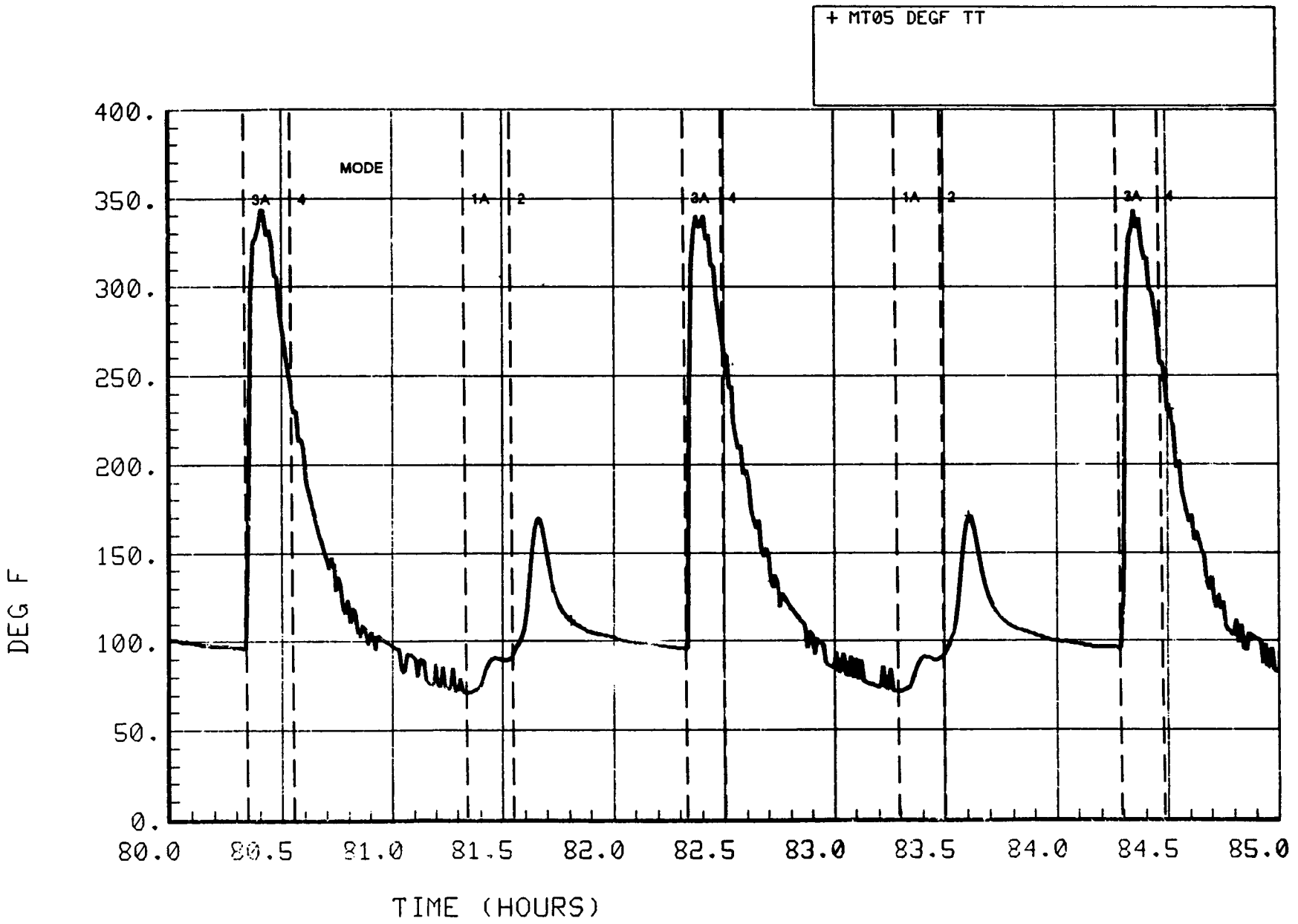

Figure 5-2.29. Expanded desiccant bed 1 inlet air temperature during desorption (MT05).

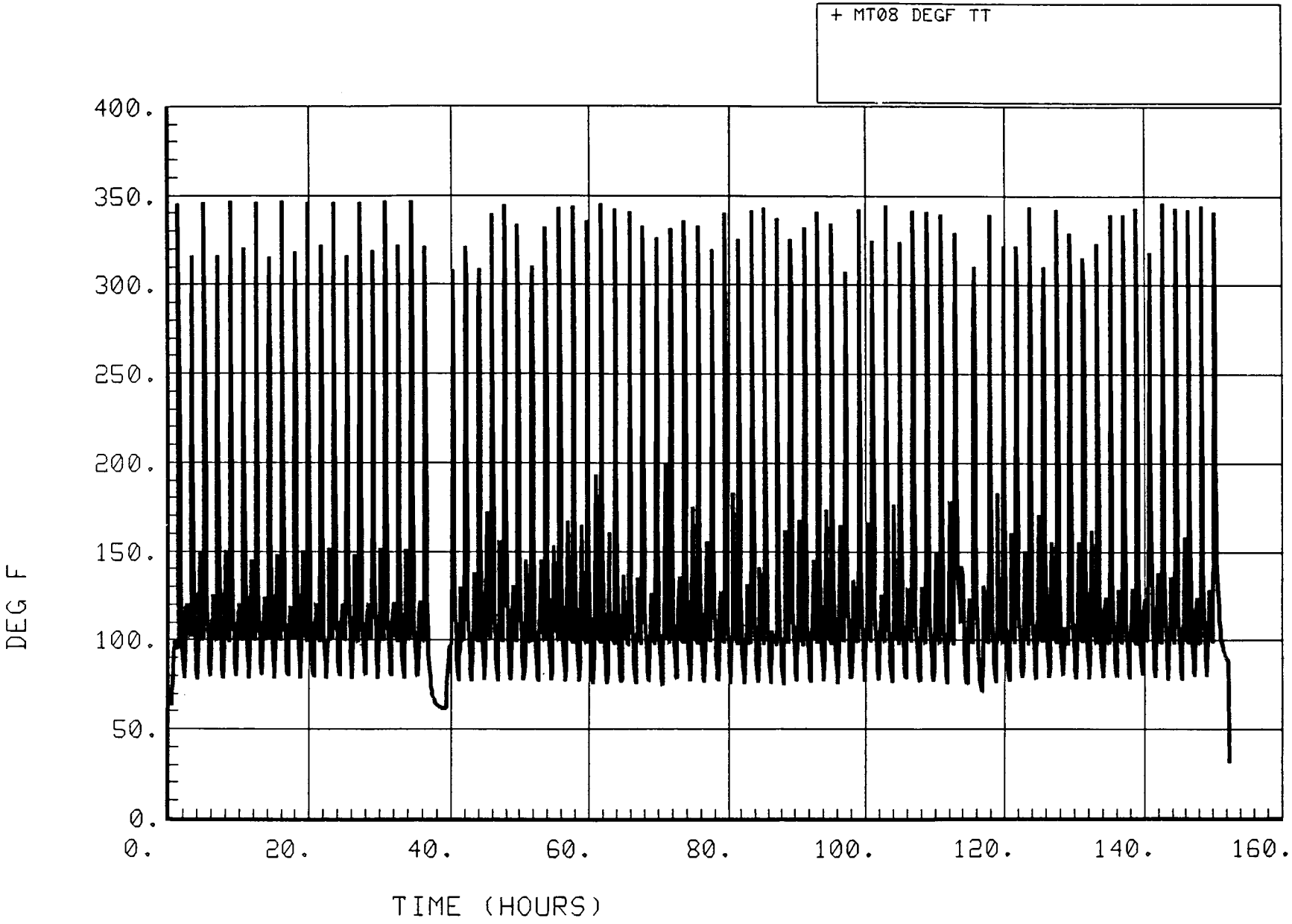

Figure 5-2.30. 4BMS desiccant bed 3 inlet air temperature during desorption (MT08).

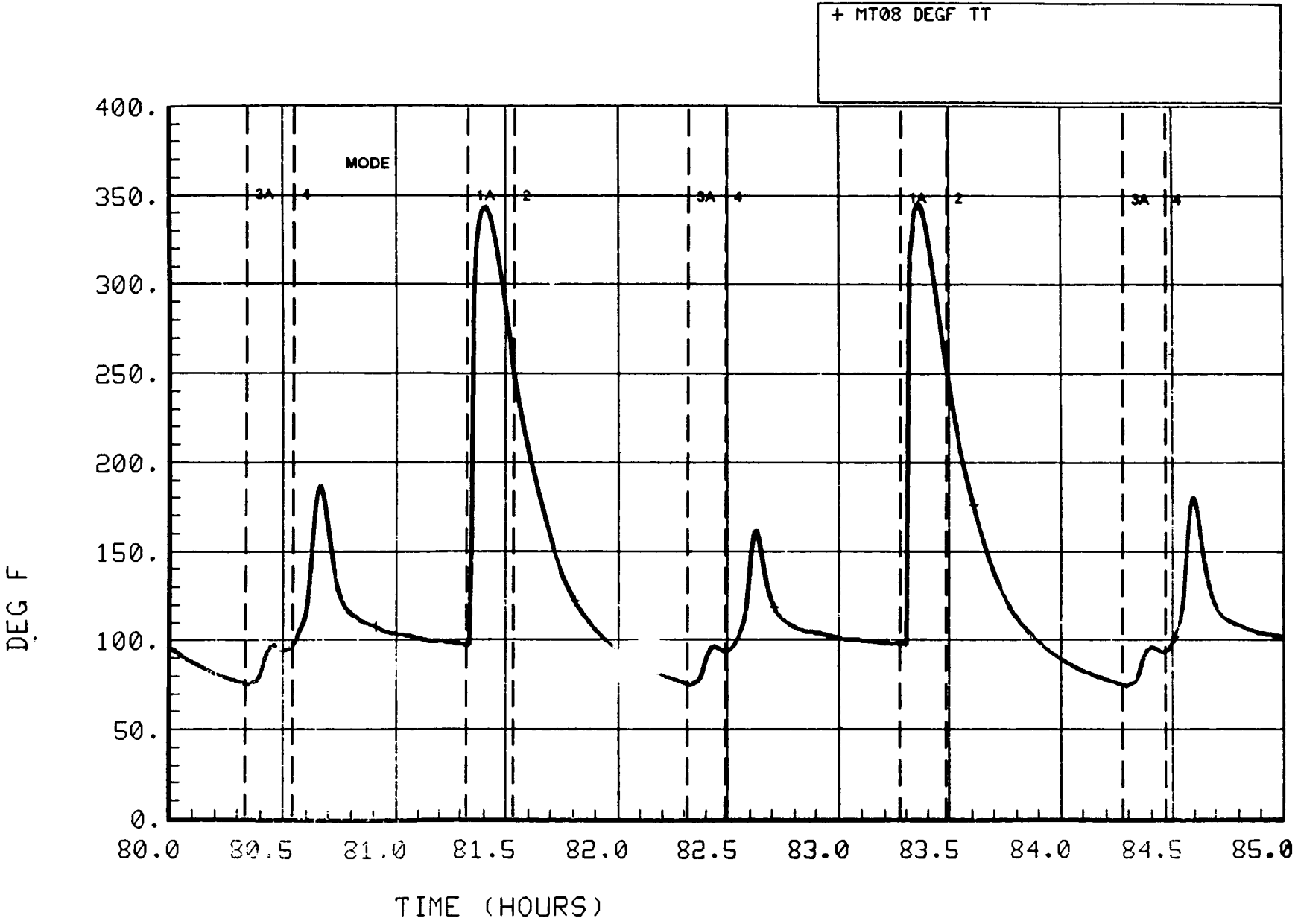

Figure 5-2.31. Expanded desiccant bed 3 inlet air temperature during desorption (MT08).

5.2.2.2.19 4BMS Return Air Temperature (MT07)

The temperature of the return air varies from about 76° to 144°F with the average about 100°F (as shown in Fig. 5-2.32). The peaks and valleys correspond to the cycle mode changes. The cycling malfunction resulted in a drop of several degrees in the temperature which persisted for most of the remainder of the test. The reason for this drop is not understood at present, but it is not thought to be significant.

5.2.2.2.20 4BMS Return Air CO_2 Partial Pressure (FP13)

As shown in Figure 5-2.33, the CO_2 partial pressure of the return air stream was as low as 0.4 mmHG near the beginning of the test but steadily rose until leveling at an average of about 2.24 mmHG. After the cycling malfunction, the level rapidly increased (by about 2 mmHg), but even more rapidly decreased to a level only slightly higher than before the malfunction. The expanded plot (Fig. 5-2.34) shows that the peaks correspond with cycle mode changes. They are due to some remaining CO_2 from Beds 2 and 4 as Modes 2 and 4, respectively, begin.

5.2.2.2.21 Module Simulator Air Temperature (FT16)

The module simulator air temperature varied from about 71° to 77.5°F over the course of the test (as shown in Fig. 5-2.35). The day/night cycles are evident in the plot as well as the 4BMS cycles. The effect of the 4BMS cycling malfunction was a reduction in the average temperature by less than 3°F. By the third day following the malfunction, the temperature was recovering until the second aberration. The temperature rise toward the end of the test is not understood presently, but is probably not related to the 4BMS.

5.2.2.2.22 4BMS Desorbing Sorbent Bed Pressure (MP08)

The pressure in the desorbing CO_2 sorbent bed usually ranged from 0.4 to 1.6 psia (as shown in Fig. 5-2.36). The pressure spikes as high as 14 psia occurred during the pumpdown portion of Modes 1 and 3. Otherwise the pressure peaked early during Modes 2 and 4 when the increasing temperature desorbed the most CO_2 (shown in the expanded plot, Fig. 5-2.37).

5.2.2.2.23 4BMS CO_2 Sorbent Bed Desorption Flow Temperature (MT09)

The temperature of the desorption flow (Fig. 5-2.38) usually ranged from about 73° to 82°F. This is significantly lower than the temperatures measured during the SIT. The reason for this difference is not presently known. The peaks and valleys correspond to cycle mode changes as shown in the expanded plot (Fig. 5-2.39). During Modes 2 and 4 (especially Mode 4) the temperature initially increases as the bed temperature rises and then decreases (slightly lagging the pressure profile). The decrease is due to the lower mass flow rate of the desorbing CO_2 and the heat loss through the uninsulated ducting and valves upstream of the temperature sensor. The differences between the peaks occurring during Mode 2 and those during Mode 4 may be due to the different sorbent materials used (as described earlier).

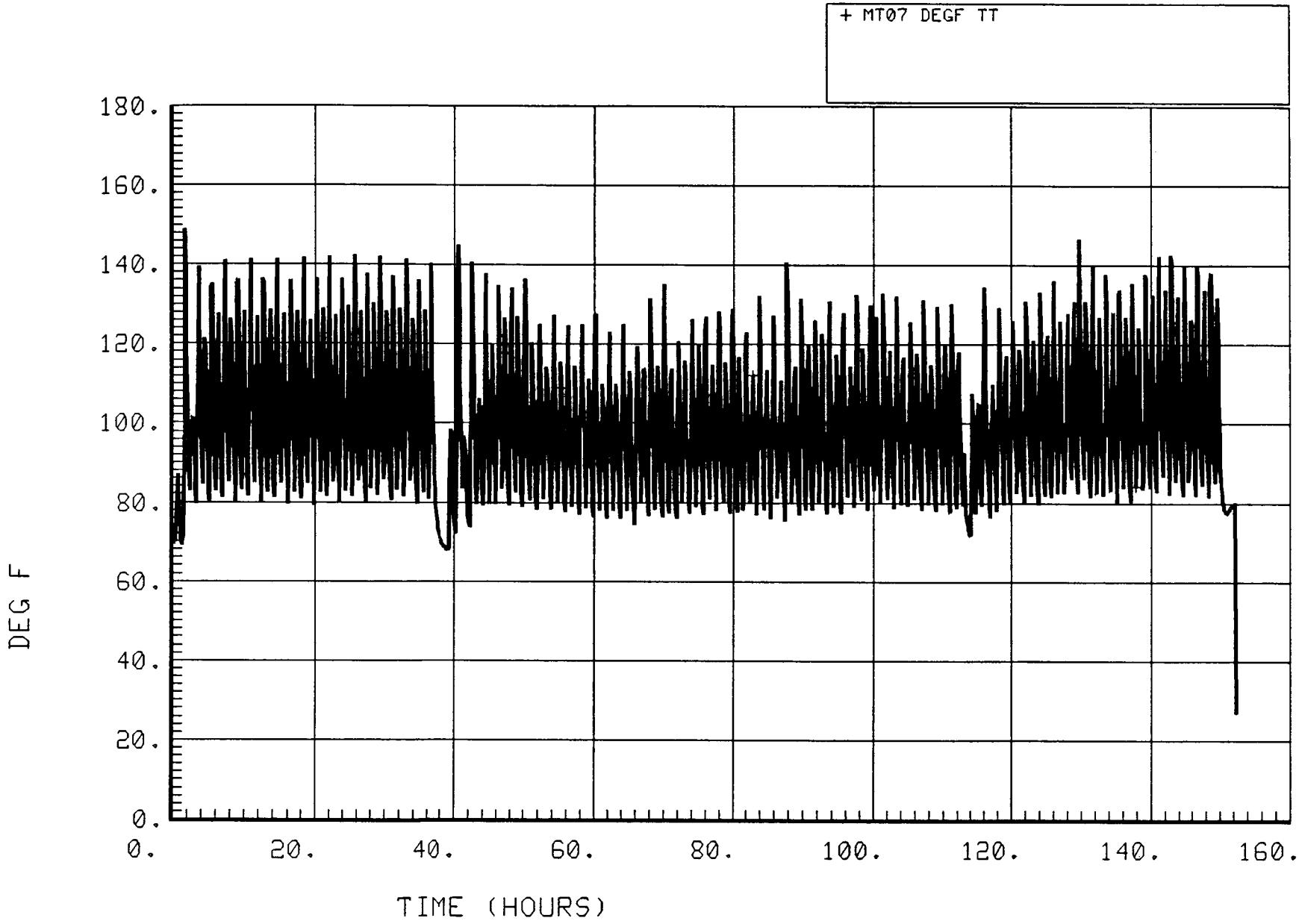

Figure 5-2.32. 4BMS return air temperature (MT07).

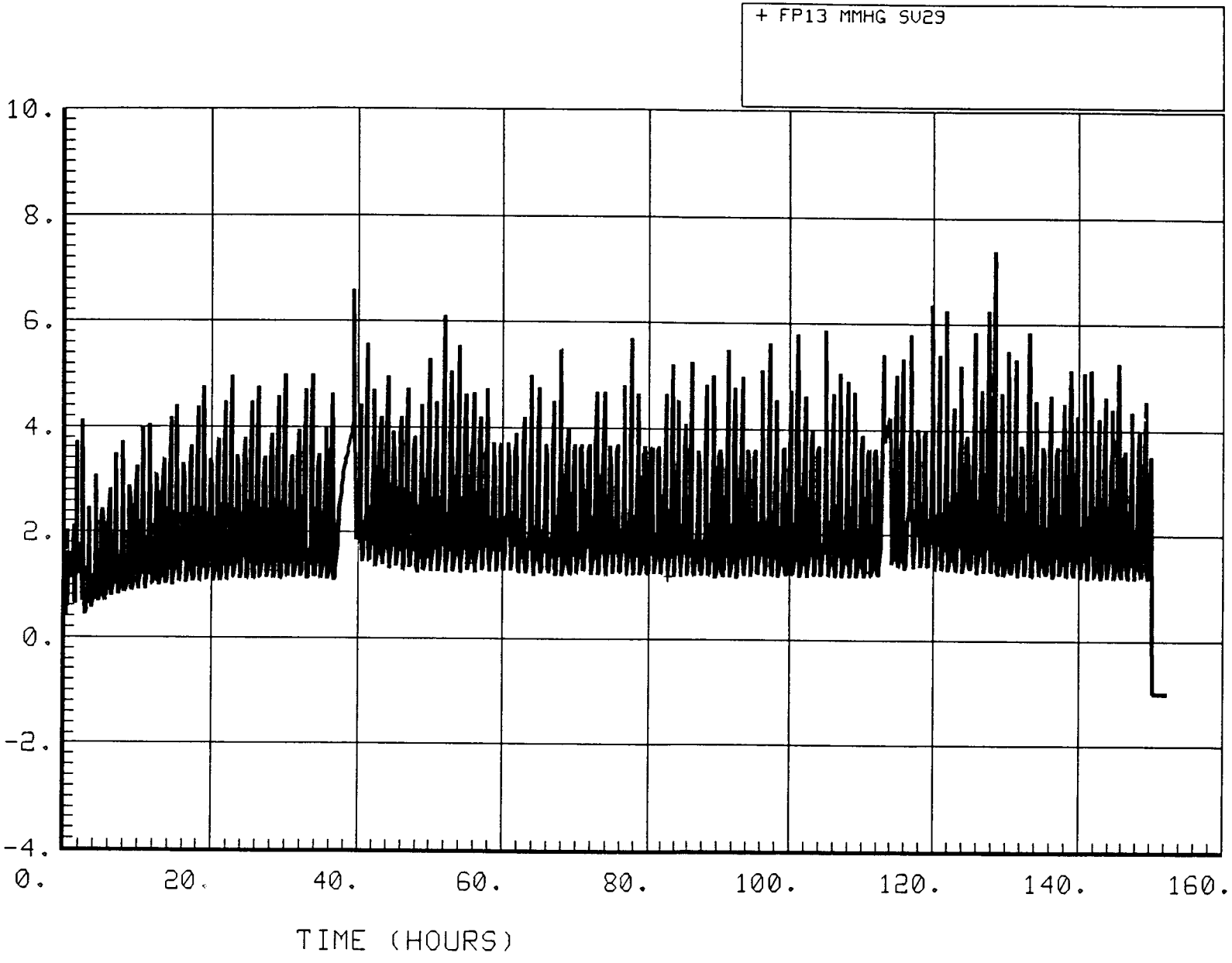

Figure 5-2.33. 4BMS return air CO_2 partial pressure (FP13).

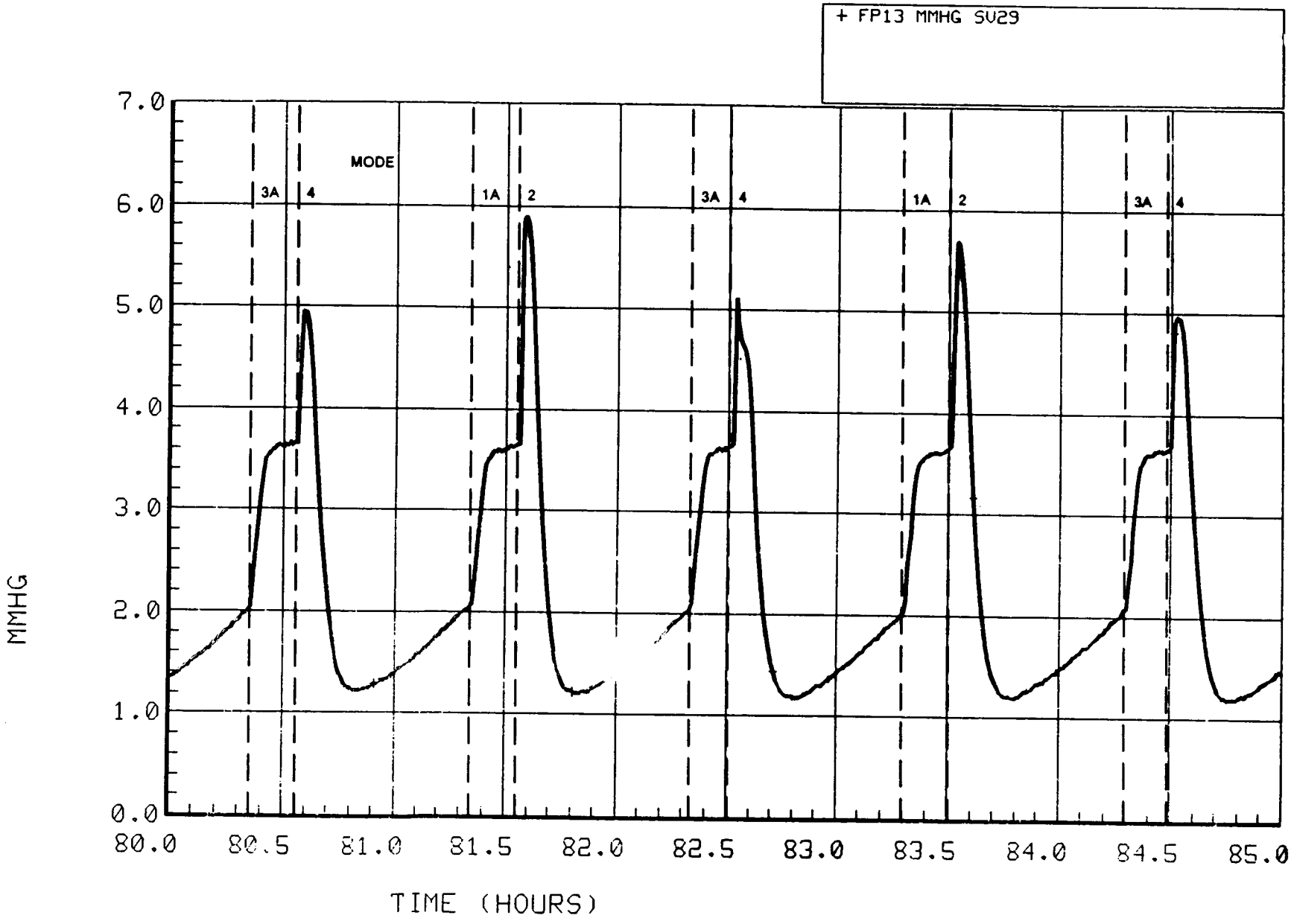

Figure 5-2.34. Expanded 4BMS return air CO_2 partial pressure (FP13).

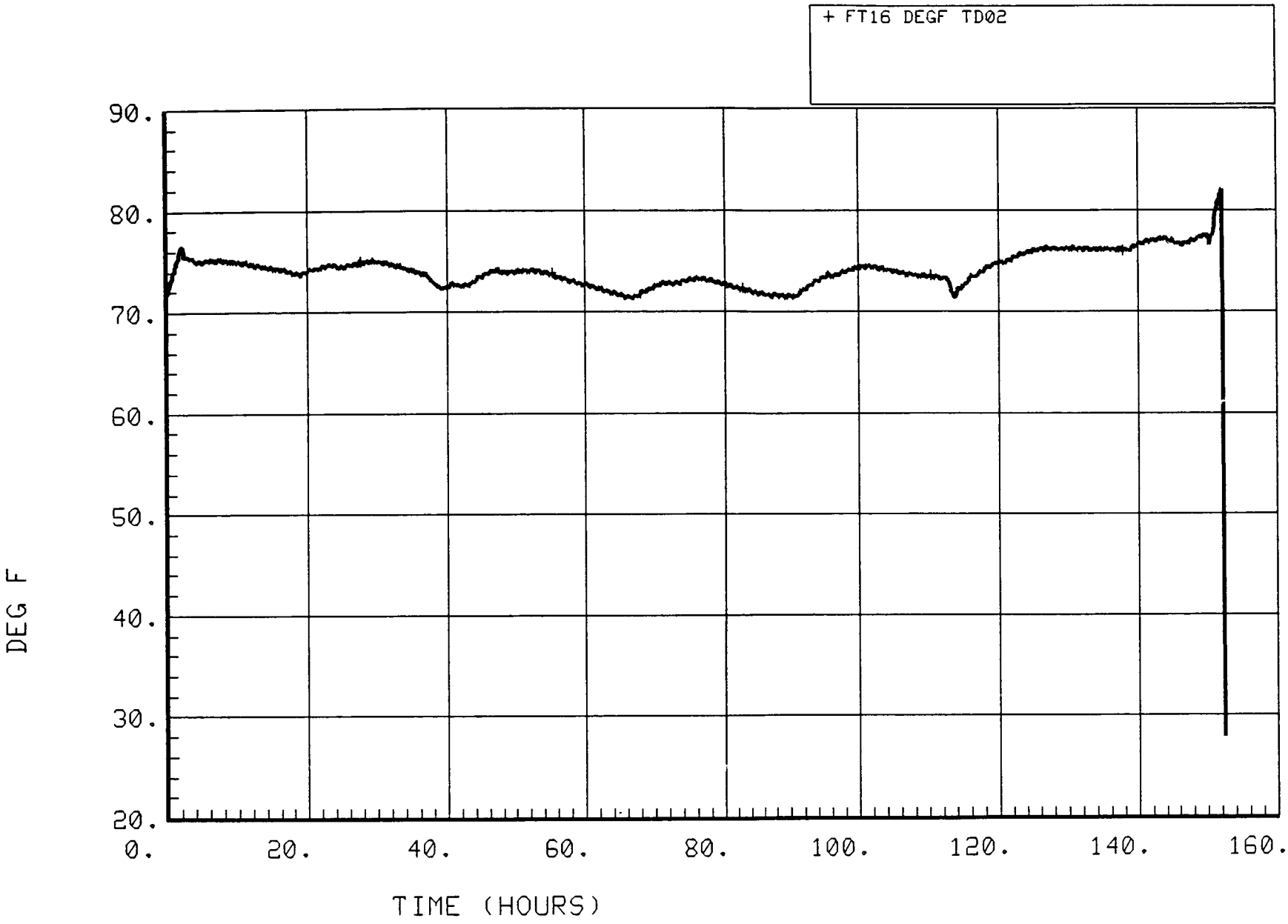

Figure 5-2.35. Module simulator air temperature (FT16).

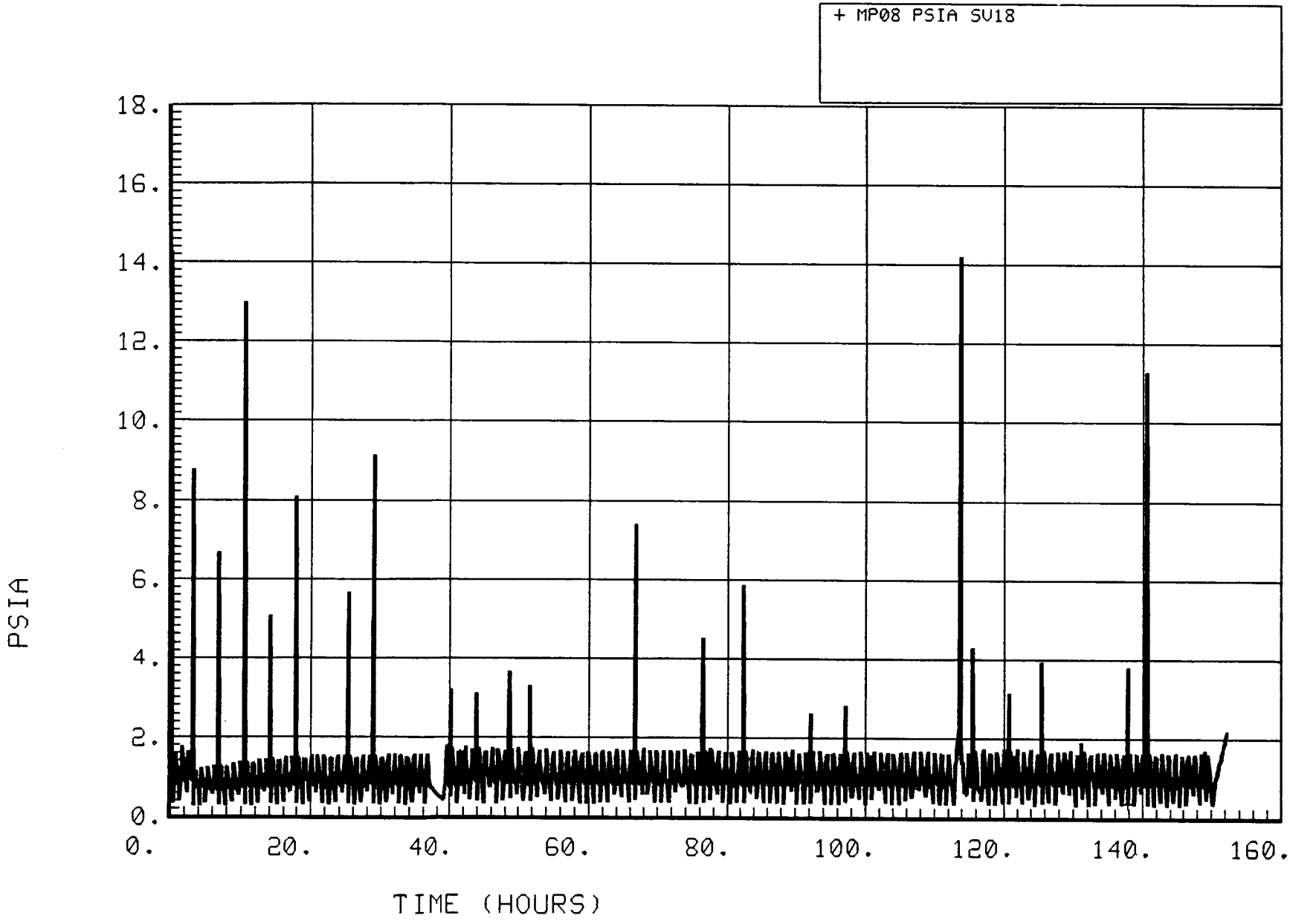

Figure 5-2.36. 4BMS desorbing sorbent bed pressure (MP08).

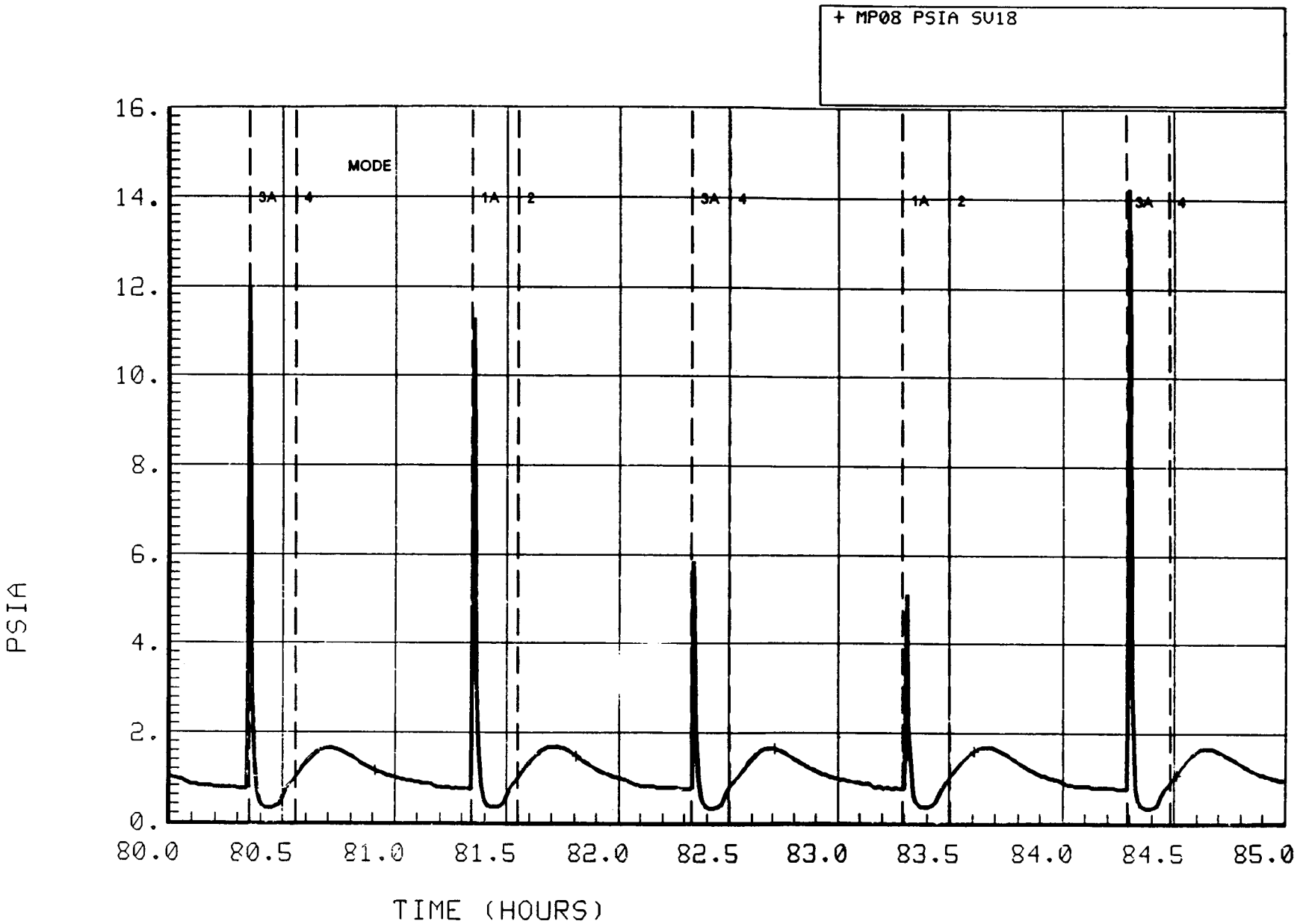

Figure 5-2.37. Expanded 4BMS desorbing sorbent bed pressure (MP08).

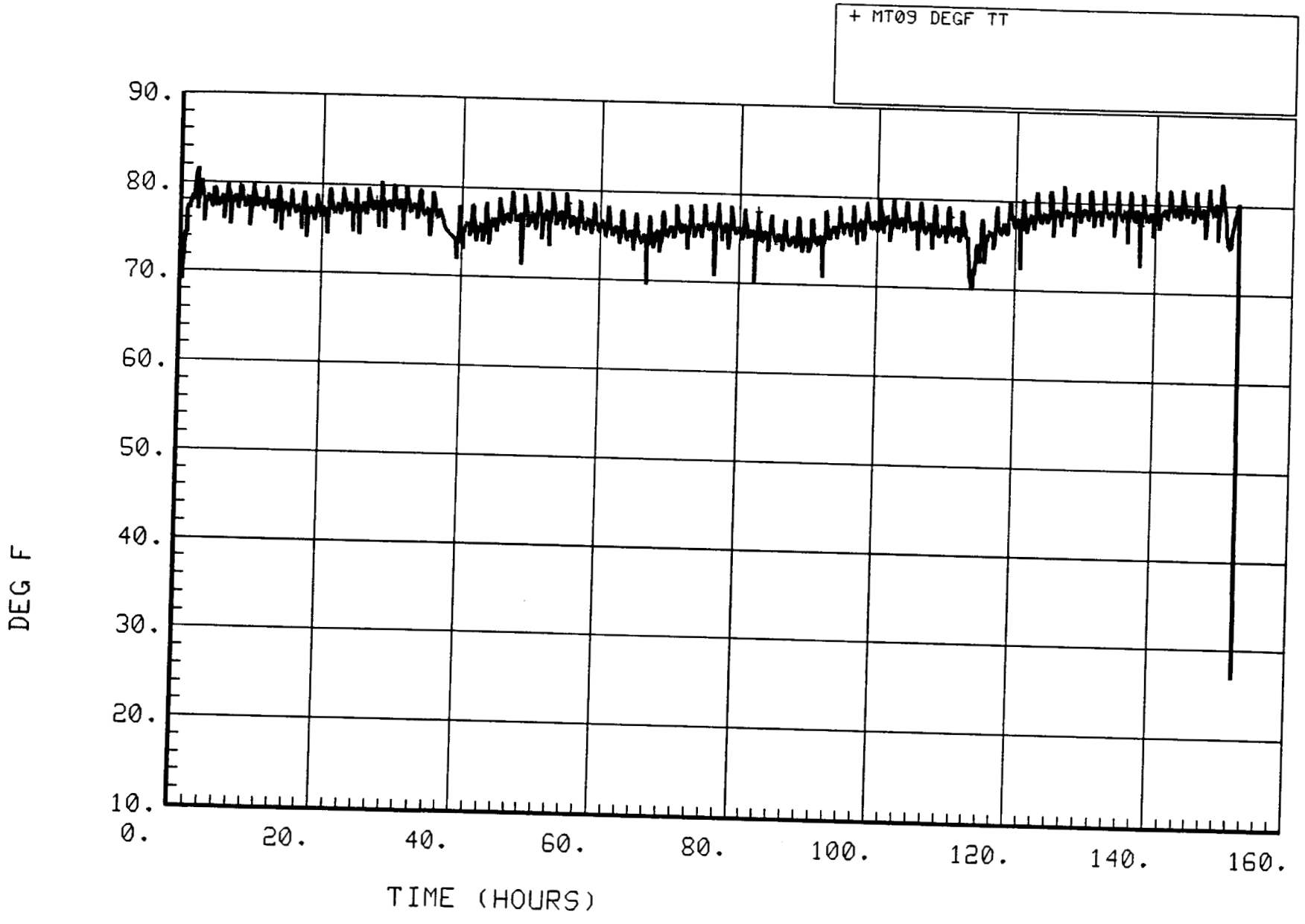

Figure 5-2.38. 4BMS CO_2 sorbent bed desorption flow temperature (MT09).

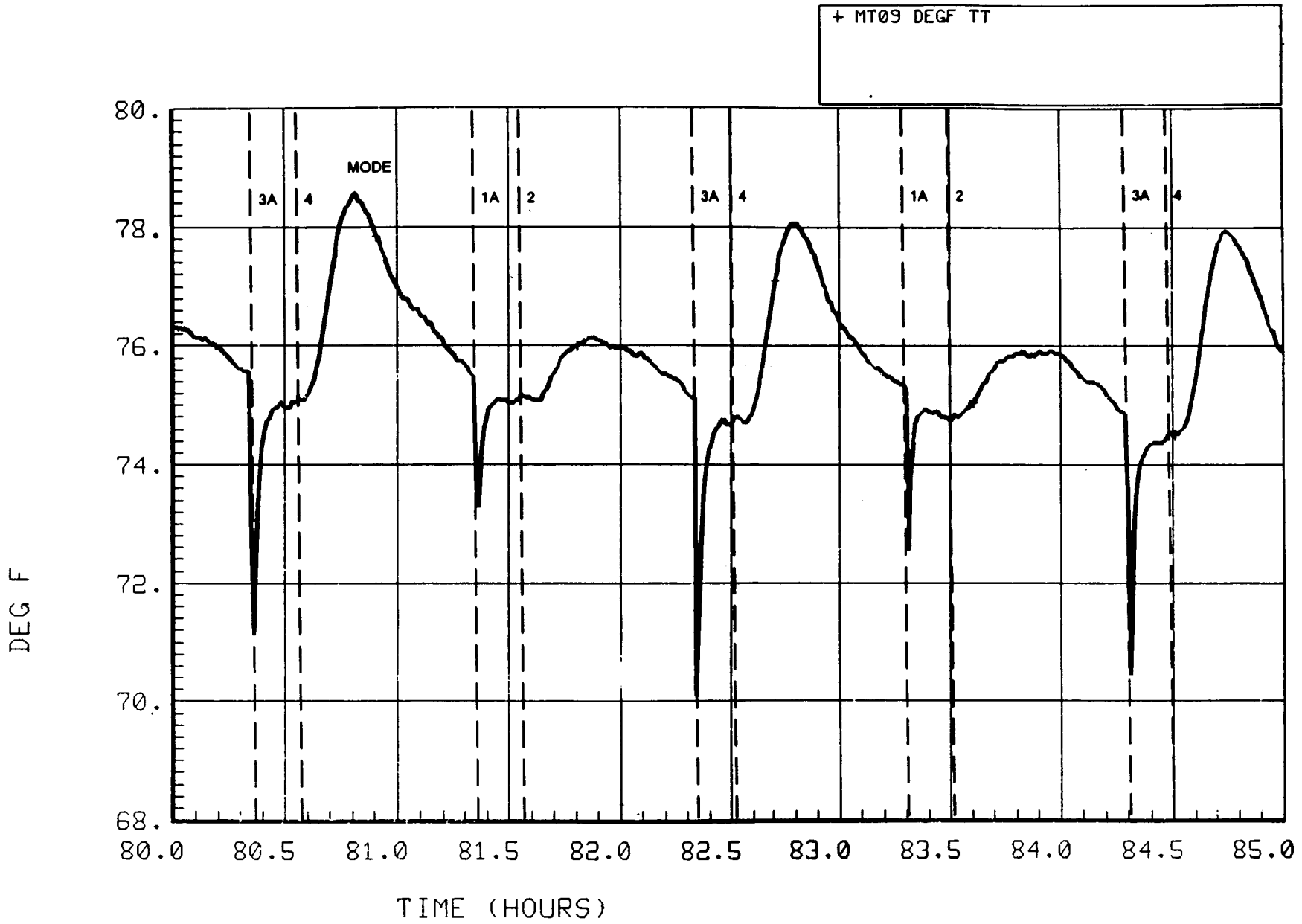

Figure 5-2.39. Expanded sorbent bed desorption flow temperature (MT09).

5.2.2.2.24 4BMS CO_2 Accumulator Pressure (MP09)

The pressure in the CO_2 accumulator ranged from about 15 to 28 psig with an average at about 22.5 psig (shown in Fig. 5-2.40). The gradual increase in average pressure was leveling off prior to the cycling malfunction. When cycling resumed, the pressure rapidly increased to a higher level and then gradually dropped to a slightly higher average than before. This corresponds closely with the plots of FP10, FP12,and FP13 (discussed above) which show a higher pCO_2 level after the malfunction. With a higher pCO_2 level, the 4BMS removes more CO_2 resulting in the higher accumulator pressures. This effect is repeated to a lesser degree after the gas samples were taken.

5.2.2.2.25 CO_2 Flow Rate to the Sabatier (FF01)

The delivery rate of CO_2 to the Sabatier usually ranged from 4.8 to 7.3 lb/day with an average of approximately 6.42 (shown in Fig. 5-2.41). The flow rate patterns closely follow the patterns of the CO_2 accumulator pressure (Fig. MP09) as expected.

5.2.2.2.26 O_2 Content in the CO_2 Flow to the Sabatier (FO03)

The plot of the oxygen content in the CO_2 flowing to the Sabatier shows that the level ranged from about 0.45 to 0.90 percent (during the cycling malfunction), well below the alarm level of 3.0 percent (shown in Fig. 5-2.42). This is much improved from the SIT during which the O_2 level reached 2.45 percent by the end of that, much shorter, test. This shows that sealing the leaks and lengthening the duration of the residual air pumpdown were effective. The plot shows a slow, but steady, increase in O_2 level after the cycling malfunction. This indicates the need for longer duration testing to determine if the O_2 content will level off. Also, it shows the need to repeat leak checks to determine if the increased operation time reopened leaks. The expanded plot (Fig. 5-2.43) shows that peaks occur early in Modes 2 and 4, indicating that a small amount of residual air is still being delivered to the CO_2 holding tank.

5.2.2.2.27 CO_2 Removal Efficiency Calculations

The CO_2 removal efficiency can be calculated by CO_2 mass balance or by CO_2 partial pressure balance. Either method should give the same results, but this was not the case. Based on the mass flows of CO_2 entering at the air inlet and exiting via the CO_2 outlet, the CO_2 removal efficiency was 51.02 percent. This was calculated from the measurements of the inlet air flow rate (FF13), the CO_2 partial pressure of the inlet air (FP12), the CO_2 outlet flow (FF01), the O_2 content of the CO_2 outlet flow (FO03), and the module pressure (FP07). Based on the inlet and outlet air pCO_2 levels (FP12 and FP13, respectively) the CO_2 removal efficiency was 43.91 percent. This discrepancy is thought to be due to inaccuracies in the air flow measurement (FF13) which may have been reading low. (During the SIT the measured air flow was about 87.3 lb/hr versus 78.8 measured for a representative period during the EMCT.) Reversing the calculations to determine the air flow rate required for a CO_2 removal efficiency of 43.91 percent results in an air flow of 92.64 lb/hr. This corresponds well with expectations of increased air flow due to the modifications made to the ducting after the SIT

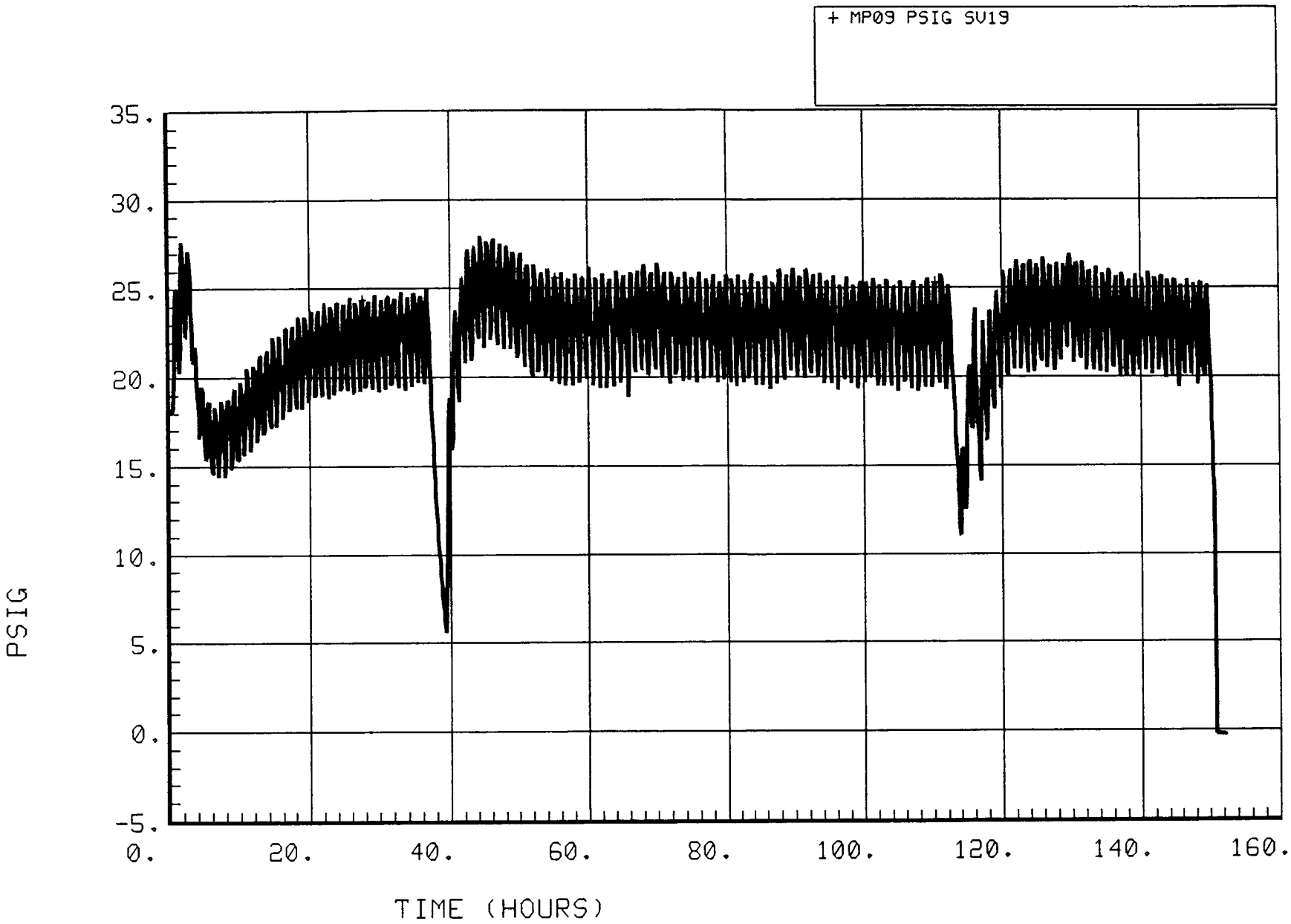

Figure 5-2.40. 4BMS CO_2 accumulator pressure (MP09).

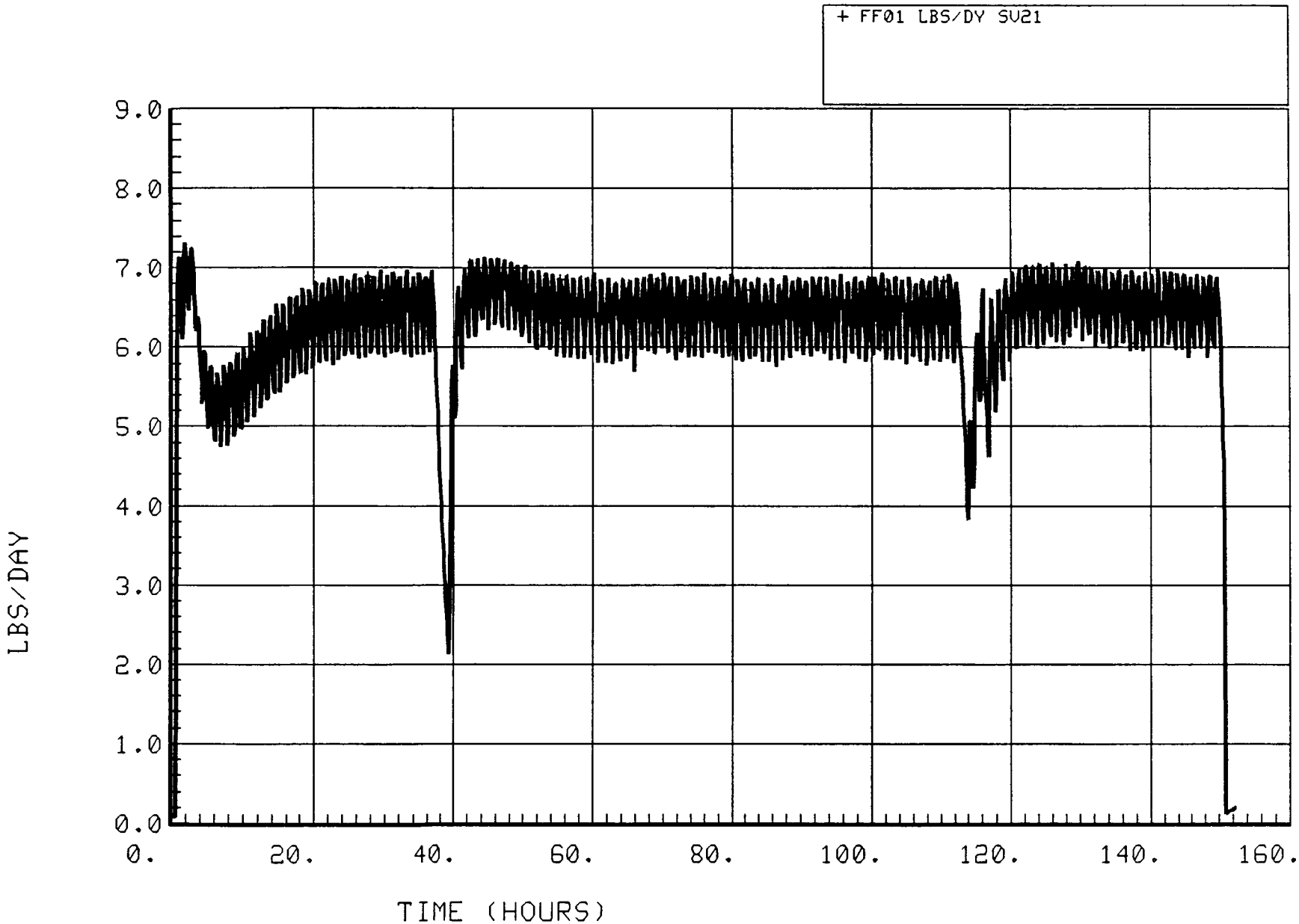

Figure 5-2.41. 4BMS CO_2 flow rate to the Sabatier (FF01).

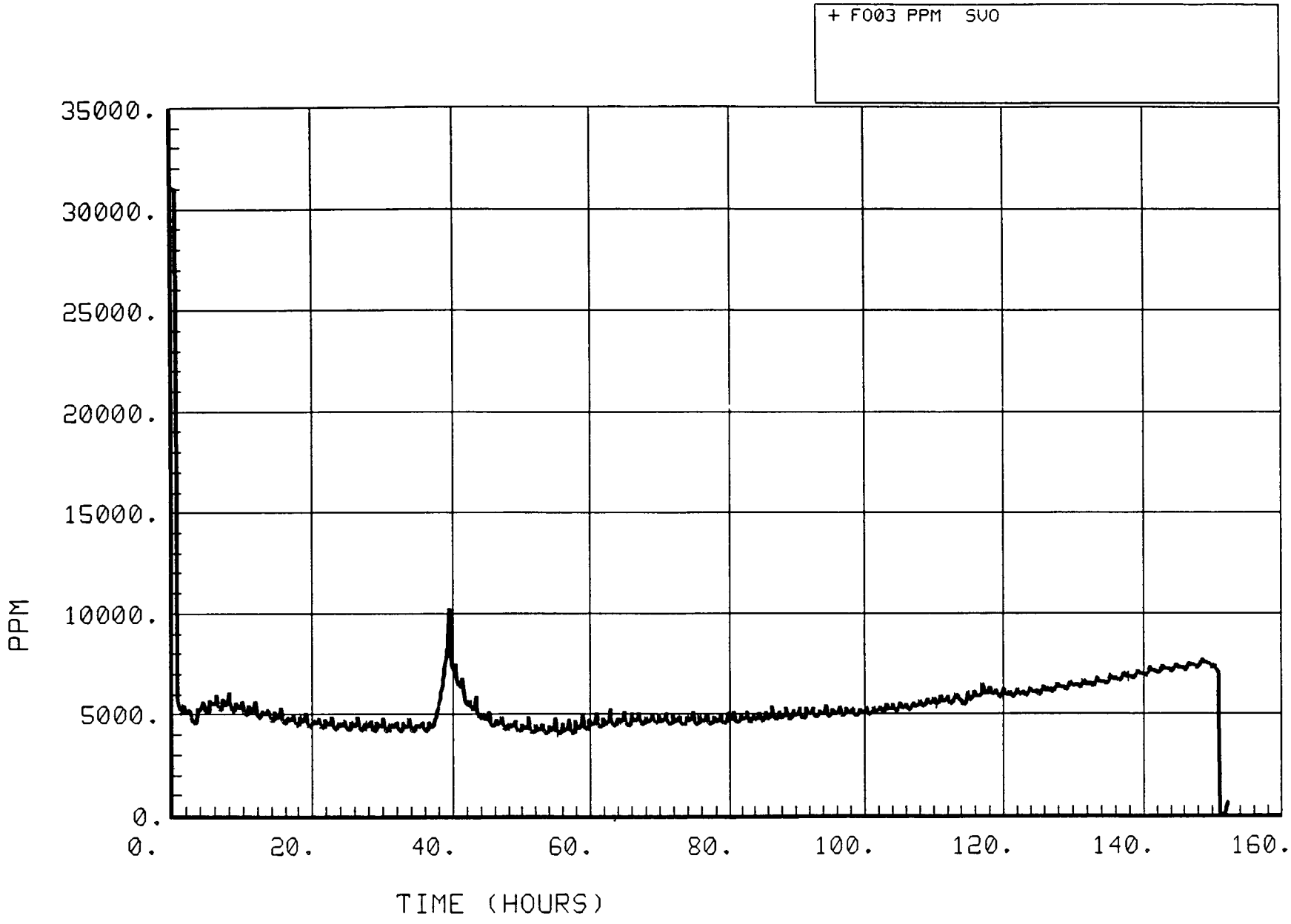

Figure 5-2.42. O_2 content in CO_2 flow to the Sabatier (FO03).

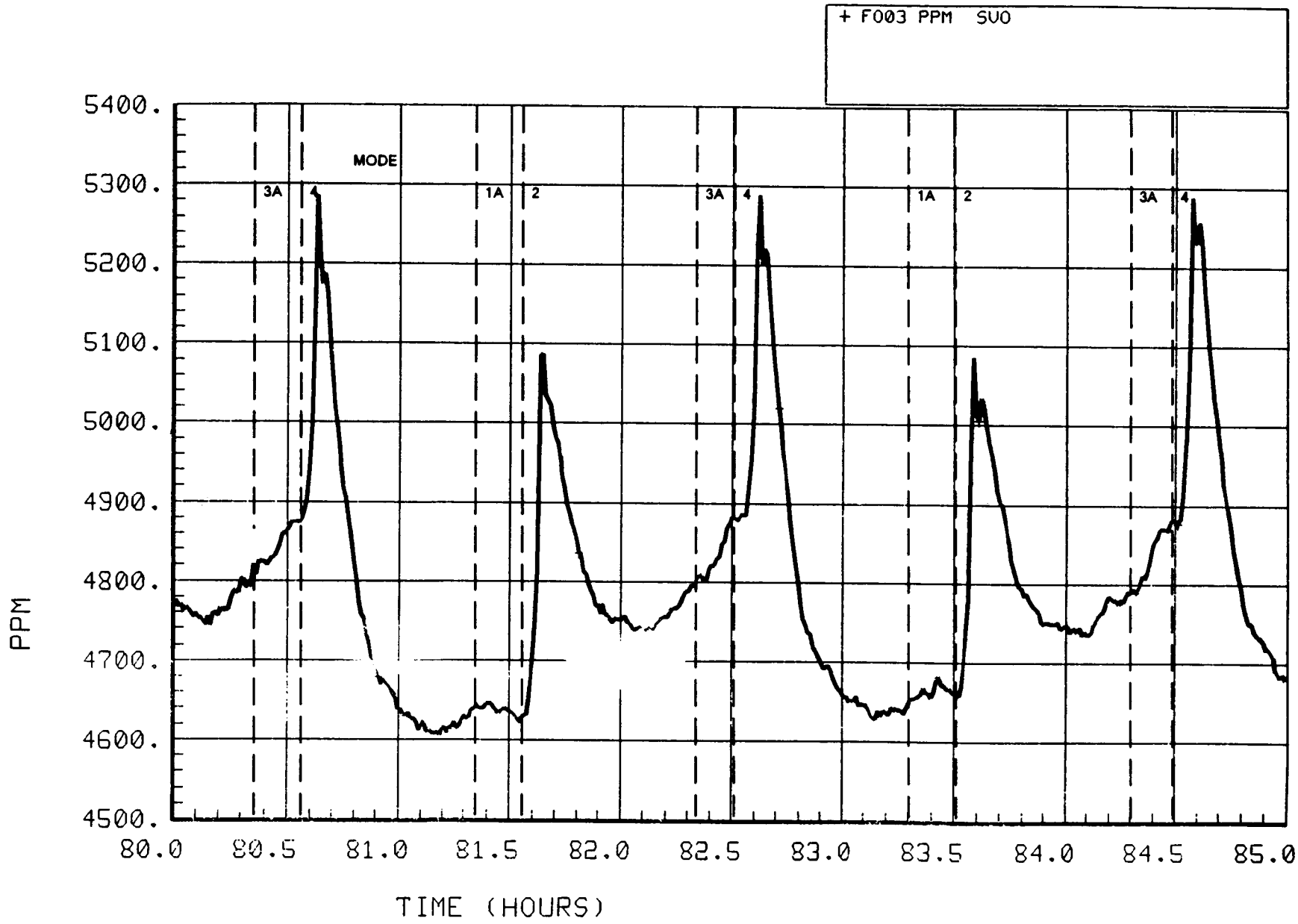

Figure 5-2.43. Expanded O_2 content in CO_2 flow to the Sabatier (FO03).

was completed. Table 5-4 below summarizes the results of the calculations. For the SIT, the reported CO_2 removal efficiency was 35.9 percent. This value was calculated from the mass flow measurements. When calculated by pCO_2 measurements the efficiency was 43.2 percent. Assuming the air flow measurement to be in error, in order to have the mass balance efficiency equal the pCO_2 balance efficiency, the air flow value becomes 70 lb/hr. Due to this discrepancy, the air flow sensor was recalibrated prior to the EMCT. But only the differential pressure transducer on the air flow sensor was recalibrated and not the entire flow sensor. This is thought to have resulted in erroneous readings that were too low during the EMCT. The CO_2 removal efficiencies by pCO_2 are essentially identical for the SIT and the EMCT, indicating that the air flow measurements are suspect. Also, it indicates that there was no change in performance capability as a result of the modifications.

TABLE 5-4 COMPARISON OF CO_2 REMOVAL EFFICIENCY CALCULATIONS

AIR INLET FLOW RATE (LB/HR)		% CO_2 REMOVED, CALCULATED BY:	
		MASS FLOW	PARTIAL PRESSURE
MEASURED	78.81	51.02	43.91
CALCULATED	92.64	43.91	43.91

5.2.2.2.28 Cycle Advance Malfunction

After the conclusion of the EMCT, it was not feasible to troubleshoot the cause of the cycle advance malfunction prior to moving the 4BMS out of the module simulator. During set up for further independent testing, several connections were checked and two diodes were replaced prior to running the 4BMS. When the subsystem was turned on, the malfunction did not recur. Apparently, during the process of moving and setting up the 4BMS, the situation that caused the malfunction to occur was corrected. Because of the work done during set up for independent testing, it is not possible to know with certainty which action(s) corrected the cause of the malfunction. However, a scenario has been developed which duplicates the significant effects noted during the EMCT. The sequence of actions and their results are as follows:

(1) Power up the subsystem – The Hold light comes on, Run light off, Bed Pressure High light comes on at startup (cannot advance until this light goes off). (Normal operation.)

(2) Press Run button – The Hold light goes off, Run light on, when the Hold button is pressed the subsystem enters the Hold mode, when the Run button is pressed the subsystem enters the Run mode. (Normal operation.)

(3) Disconnect either bed overtemperature thermocouple – The subsystem enters Hold, but can be advanced by pressing the Advance button. Pressing the Run button is ineffective. (During the EMCT, pressing the Run button would not reactivate mode cycling.) The overtemperature light comes on.

(4) Reset the overtemperature relay – The subsystem stays in Hold mode, but will enter the Run mode when the Run button is pressed. When the cycle advances to the mode where the heaters turn on in the sorbent bed with the disconnected thermocouple, the subsystem again enters Hold until the relay is reset. (The overtemperature relay could not be reset from outside the module simulator during the EMCT.)

The control panel outside the module simulator did not have a means of resetting the overtemperature relay so it was not possible to do so during the test. When the subsystem shutdown occurred at 114 hr into the test, the relay was automatically reset when the subsystem was restarted and so the automatic timer was able to function until the cycle reached Mode 2, whereupon the malfunction recurred and manual advancing resumed. A likely cause of the malfunction is, therefore, a break in a connection which resulted in tripping the overtemperature relay for Bed 2.

5.2.3 Recommendations/Lessons Learned

The results of this test show that the 4BMS does perform its intended function during closed-door integrated operation and that the modifications made to eliminate leakage were successful. Other conclusions/lessons learned are listed below.

The CO_2 removal efficiency of 43.9 percent was only slightly above the 43.2 percent calculated (by $ppCO_2$) for the SIT. Since this is dependent upon the temperature of the air flowing through the sorbent beds, which was essentially the same for the SIT and the EMCT, this was expected. Reducing the temperature should increase the percentage of CO_2 removed.

Analysis of the CO_2 outlet stream indicated a purity of 92.7 percent CO_2 which compares with 85.0 percent during the SIT. This indicates that the leaks in the ducting and fittings were effectively sealed. Additional improvements will require further optimizing the duration of the cycle modes and desorption temperature.

The modifications which increased the air flow rate had little, if any, effect on CO_2 removal efficiency. More air, and therefore more CO_2, flowed through the 4BMS, but the percentage of CO_2 removed was essentially the same.

5.3 Static Feed Electrolysis (SFE)

5.3.1 Subsystem Description

The SFE subsystem was used to generate oxygen at a three-man metabolic rate and hydrogen for use by the Sabatier subsystem. A schematic of the SFE is shown in Figure 5-3.1. The SFE consists of five major components: (1) the electrolysis module, (2) the fluids control assembly (FCA), (3) the pressure control assembly (PCA), (4) the coolant control assembly (CCA), and (5) the feed water tank.

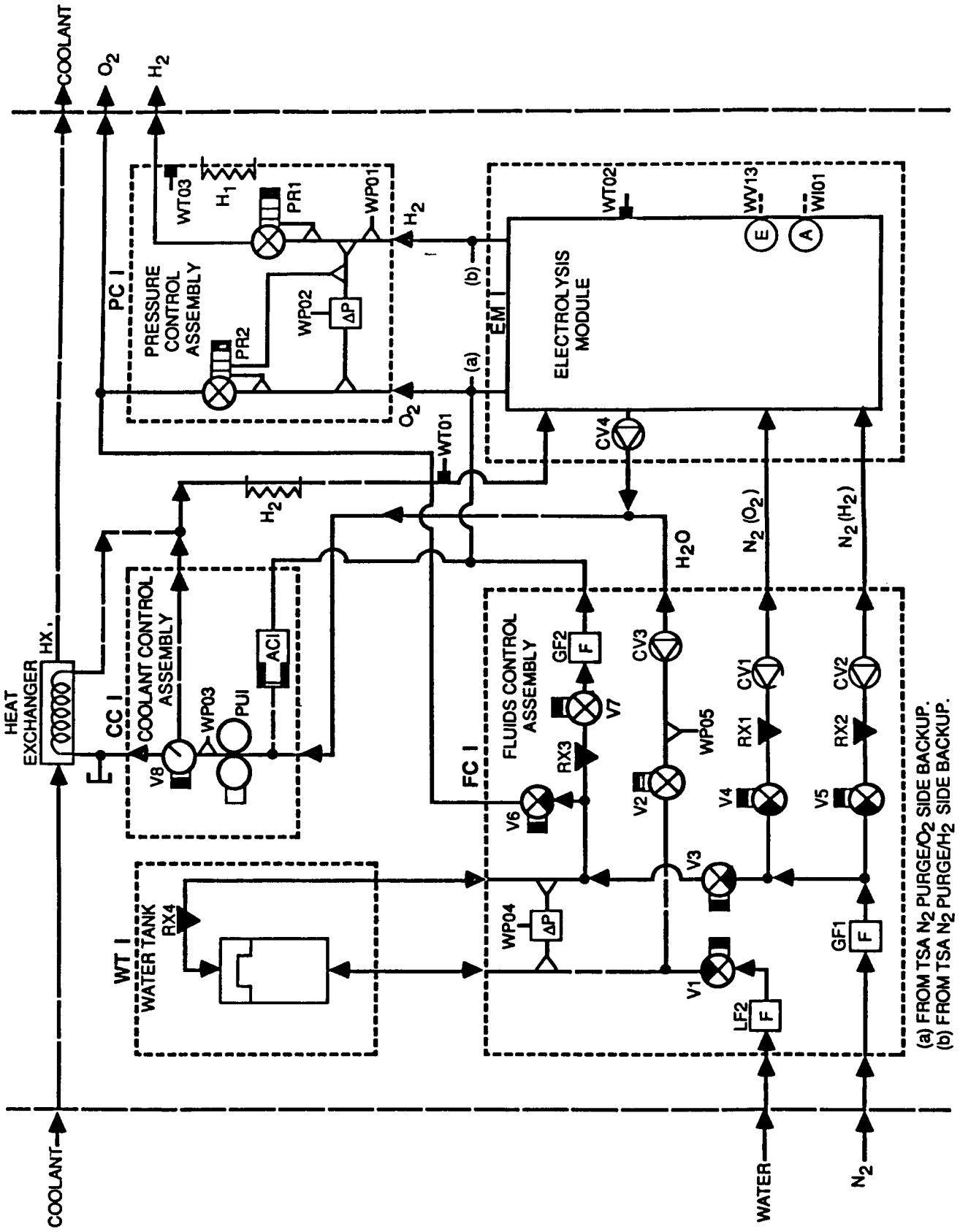

Figure 5-3.1. SFE mechanical schematic with sensors.

The electrolysis of water to oxygen and hydrogen takes place in the electrolysis module which consists of twelve cells stacked together between two insulation platces and two end plates. Each cell contains a water compartment, an oxygen compartment, and a hydrogen compartment. The water and hydrogen compartments are separated by a water feed membrane, while the two gas compartments are separated by the electrolyte matrix/electrode assembly. The electrolyte is aqueous potassium hydroxide (KOH).

The reactions which occur in the cells are:

Cathode: $2e- + 2\ H_2O = => H_2 + 2\ OH-$

Anode: $2\ OH- = => H_2O + 1/2\ O_2 + 2e-$

The resulting overall reaction is:

Electrical Energy $+ H_2O = => H_2 + 1/2\ O_2 +$ Heat

Before power is applied to the module, the water feed cavity and the electrolyte matrix contain equal concentrations of KOH electrolyte. As power is applied to the electrodes, water is electrolyzed from the electrolyte matrix resulting in a KOH concentration increase and a water vapor pressure decrease in the matrix. As the water pressure in the electrolyte matrix drops below that in the water feed cavity, water diffuses from the water feed cavity through the hydrogen cavity into the electrolyte matrix in an attempt to reestablish the initial equilibrium. As water diffuses from the water feed cavity it is statically replenished from the feed water tank. The processes of electrolysis, diffusion, and the static replenishment of feed water occur continually as long as power is applied to the cell electrodes.

The electrolysis module is equipped with the voltage, current, and temperature sensors required to monitor its performance.

The Fluids Control Assembly (FCA) consists of seven valves which are mounted on two motor-driven cams. The cams are driven to the required positions to open and close the valves which control the purge gas and feed water flows and water tank fills.

During normal mode operations, valves V2 and V7 (see Fig. 5-3.1) are open. V2 permits the flow of water from the feed water tank, WT1, while V7 allows the air side of the tank to be pressurized with product oxygen.

The water tank is refilled every three hours. During the tank fill sequence, V2 and V7 are closed. V6 opens briefly to vent the air side of the tank to ambient pressure and V1 opens to refill the tank from an external water supply. When V6 and V1 close, V3 opens and facility nitrogen flows in to repressurize the tank. Upon completion of the fill sequence, V3 closes and V2 and V7 reopen. The time required for a tank fill is approximately 2 min.

A nitrogen purge is included in the startup and shutdown sequences. During the purge, V4 and V5 open to allow nitrogen flow through the subsystem oxygen and hydrogen passages.

The FCA is instrumented with valve position indicators and pressure sensors necessary for monitoring its operation.

The PCA consists of two motor-driven regulators, an absolute pressure sensor and a differential pressure sensor. Regulator PR1 controls the hydrogen production pressure, while PR2 controls the oxygen to hydrogen differential pressure. PR1 and PR2 also control the pressurization and depressurization of the SFE during startups and shutdowns.

The PCA is equipped with feedback valve position indicators which, with the pressure and differential pressure sensors, provide for monitoring of its operation.

The CCA consists of a motor, a pump, an accumulator, and a motor-operated diverter valve. The diverter valve controls the ratio of flow through the heat exchanger HX1 to flow through the bypass in order to control the temperature of the feed water. The accumulator AC1 accommodates thermal expansion and contraction of the feed water.

The CCA is instrumented with the pressure and temperature sensors and the valve position indicator required to monitor its performance.

5.3.2.2 Discussion of Individual Measurements

5.3.2.2.1 Cell Current (WI01)

The SFE oxygen production rate is a function of the current applied to the cell stack. The required current for a three-man metabolic rate is 29.2 A. The applied current (Fig. 5-3.2) was controlled to this value during normal mode operation as shown by WI01.

5.3.2.2.2 Cell Voltage (WV13)

Cell voltage (Fig. 5-3.3) is a function of both current and temperature. The total voltage for the 12 cells, measurement WV13, ranged from 19.5 V to 20.0 V during normal mode operation. This corresponds to an average voltage range of 1.63 V to 1.67 V.

5.3.2.2.3 SFE Operating Temperature (WT01)

The SFE operating temperature (Fig. 5-3.4) is controlled within a predetermined range by the CCA. For the metabolic control test the control band was 137° to 140°F. The CCA functioned nominally as indicated by the operating temperature measurement, WT01.

5.3.2.2.4 SFE Operating and Delta Pressure (WP01 and WP02)

WP01 and WP02, shown in Figures 5-3.5 and 5-3.6, are measurements of the subsystem operating pressure and the oxygen to hydrogen differential pressure, respectively. The PCA regulators, PR1 and PR2, are driven to the positions required to control the subsystem operating pressure to

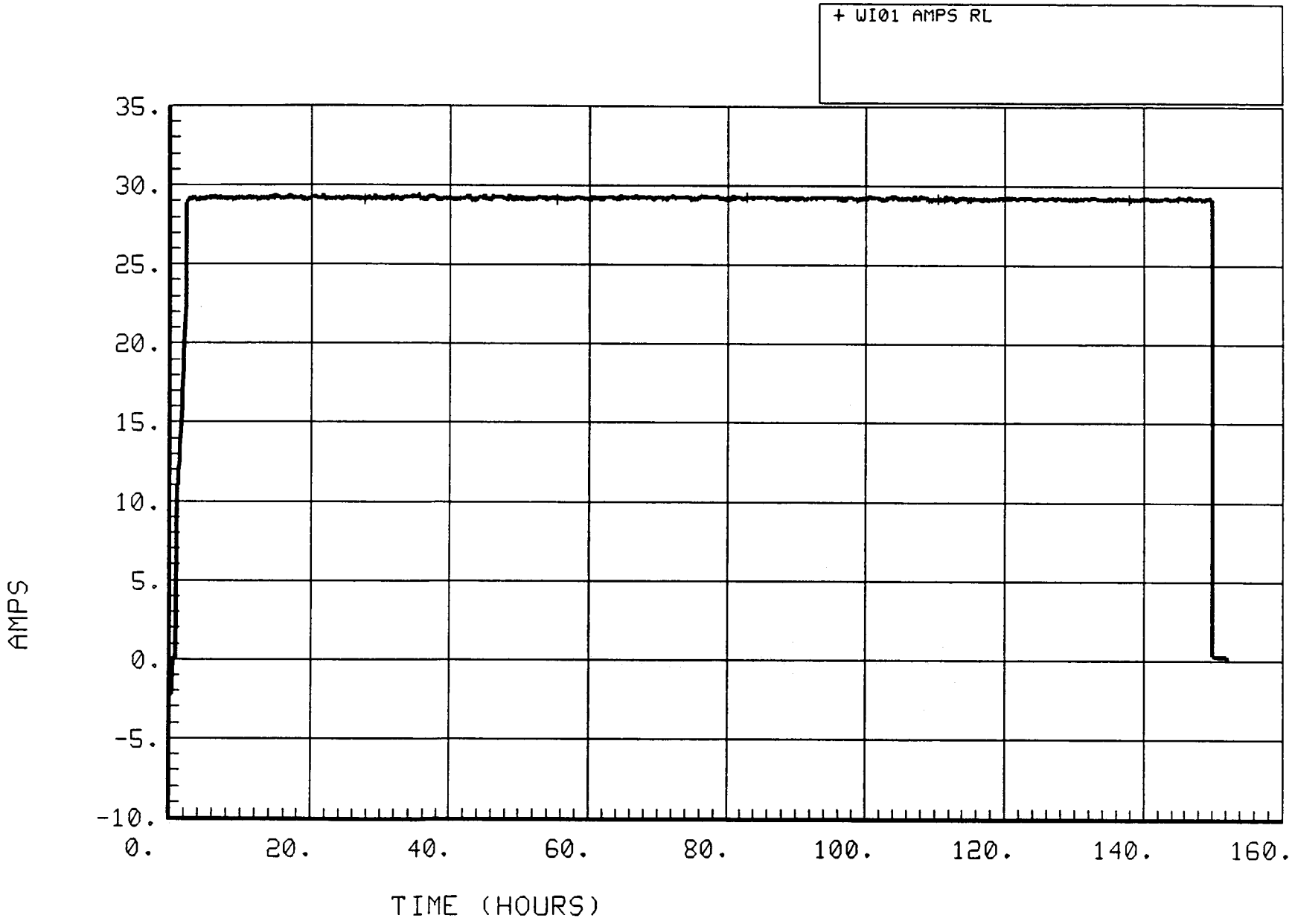

Figure 5-3.2. SFE cell current (WI01).

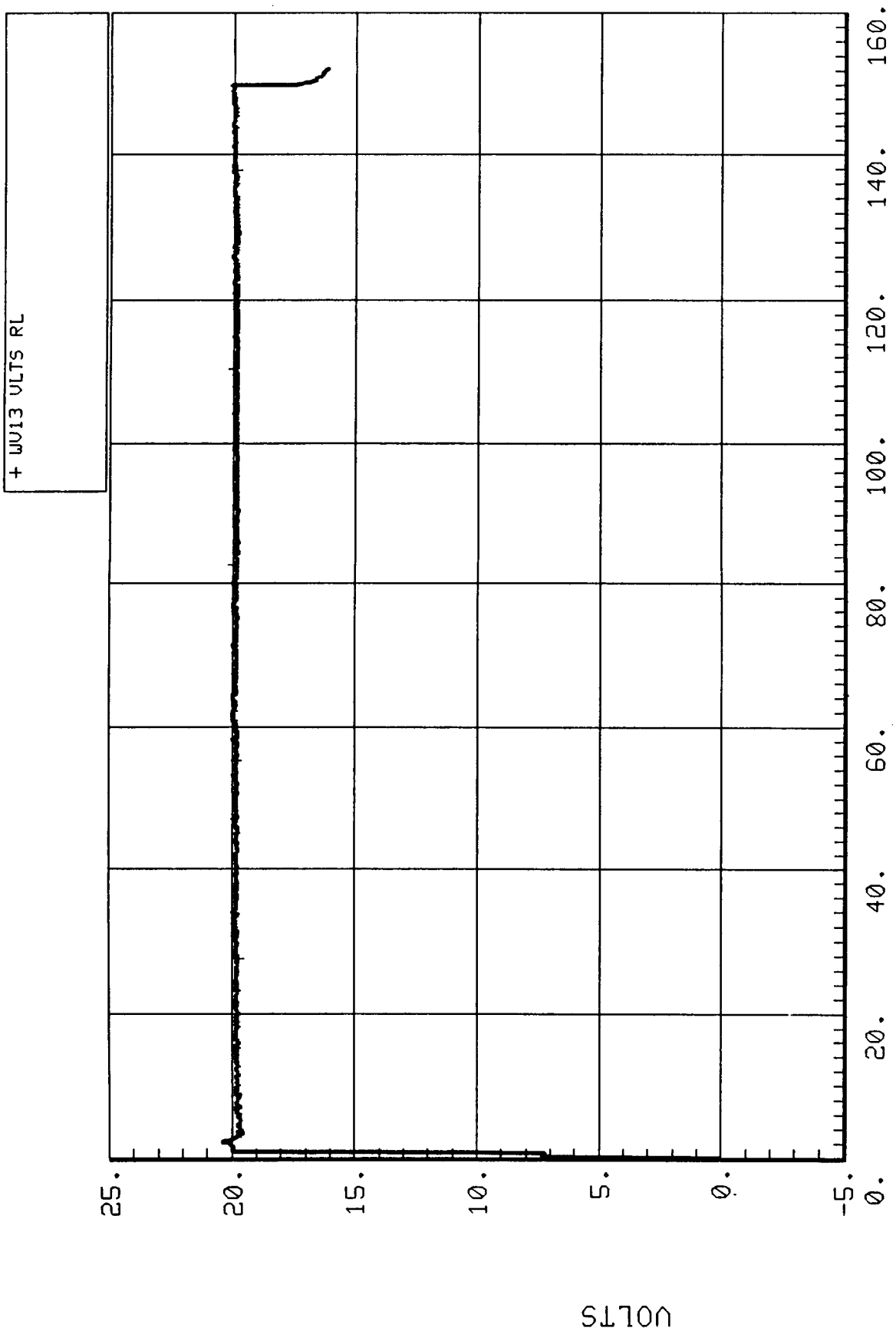

Figure 5-3.3. SFE cell voltage (WV13).

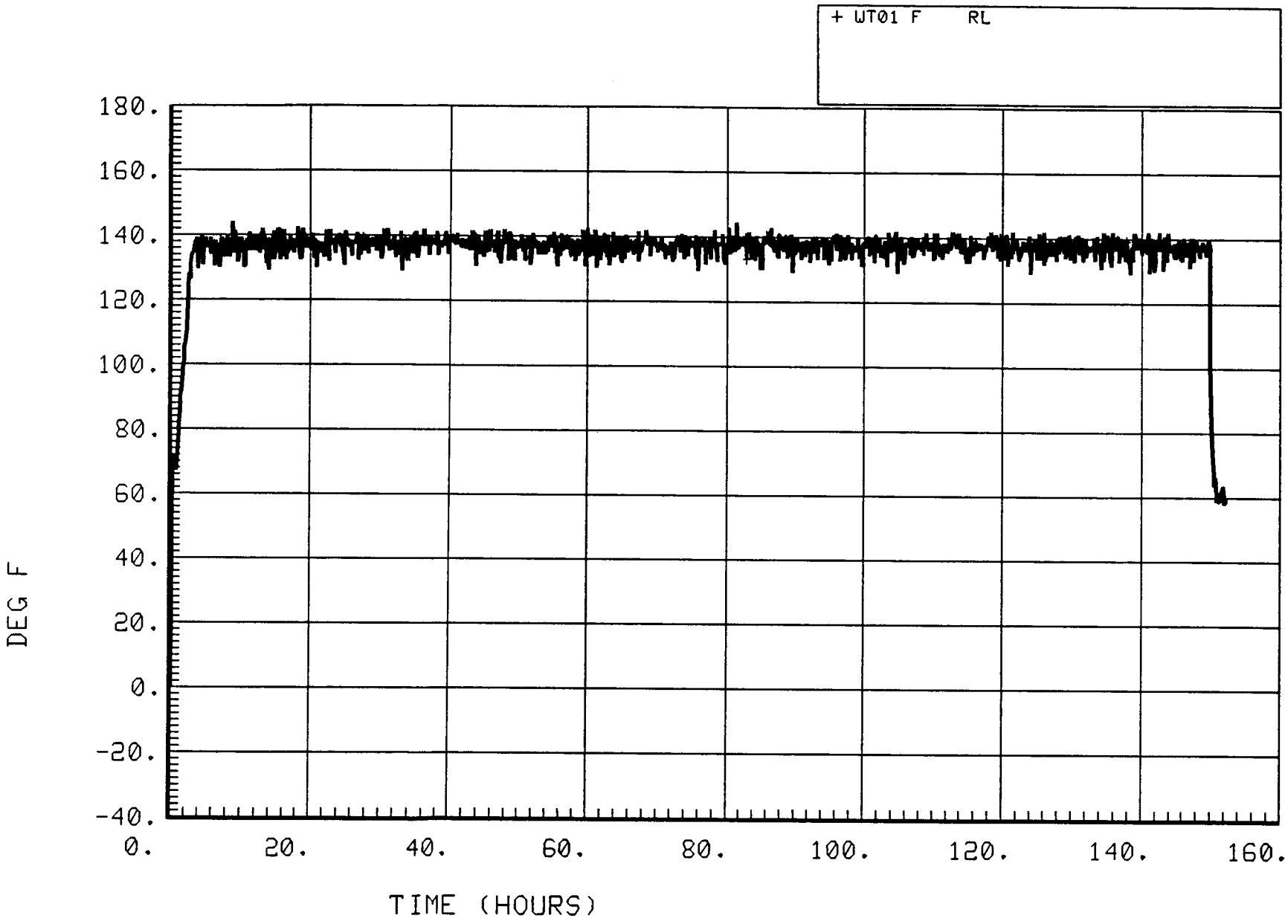

Figure 5-3.4. SFE operating temperature (WT01).

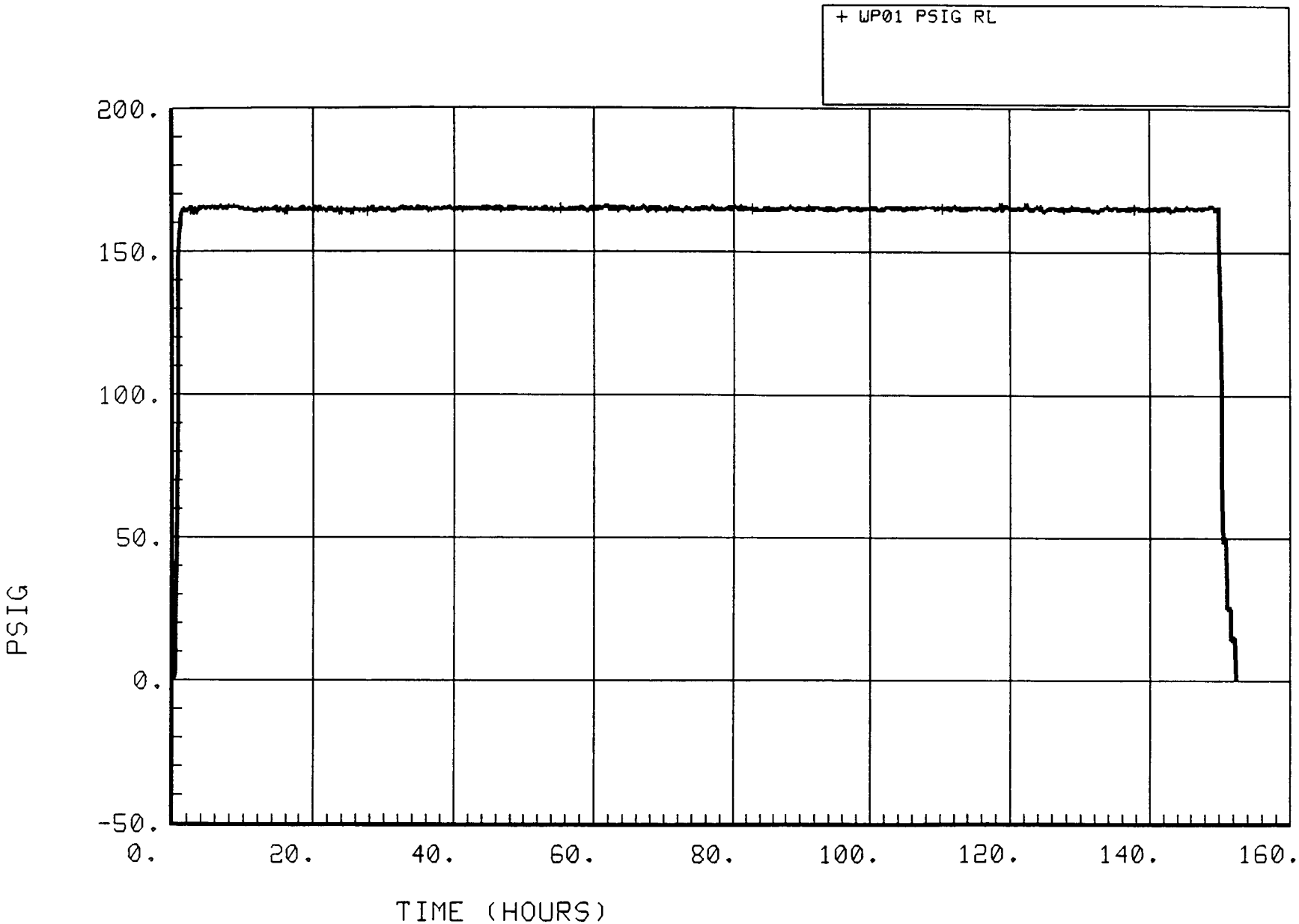

Figure 5-3.5. SFE operating pressure (WP01).

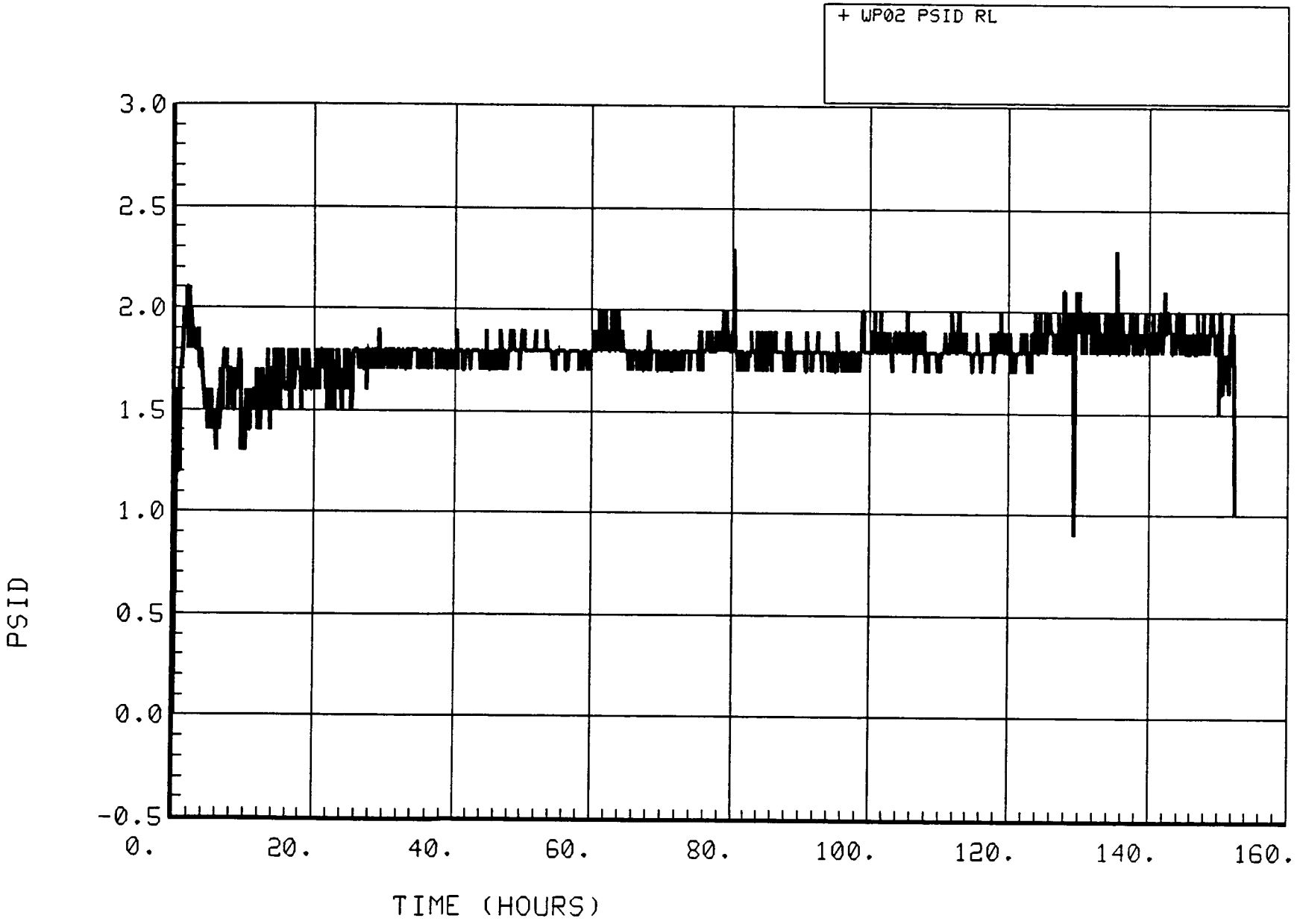

Figure 5-3.6. SFE delta pressure (WP02).

165 psig and the oxygen to hydrogen differential pressure to approximately 2 psid. The PCA performed well throughout the test as shown by plots of WP01 and WP02. Subsystem pressure was maintained at 165 psig, and the oxygen to hydrogen differential pressure was maintained between 1.5 and 2.0 psid.

5.3.2.2.5 Feed Water Tank Delta Pressure (WP04)

The feed water tank delta pressure is shown in Figure 5-3.7. The spring-loaded bellows in the feed water tank maintains the tank differential pressure at approximately 2 to 3 psid. The cyclic nature of the WP04 reading is due to the periodic tank refills.

5.3.2.2.6 Oxygen Outlet Flowrate and Pressure (FF05 and FP04)

The oxygen outlet flowrate and pressure, FF05 and FP04 (Figs. 5-3.8 and 5-3.9), were as expected except for the period from 4 to 10 hr. During that time the oxygen flow and pressure experienced sharp increases which coincide with SFE water tank fills. The cause of these peaks is not understood at this time. If this phenomenon recurs in subsequent testing, a sample of the product oxygen should be taken to determine the composition of the gas during the flow peaks. The composition will be a good indication of the source of the flow.

5.3.2.2.7 Hydrogen Outlet Flowrate and Pressure (FF04 and FP03)

The hydrogen outlet flowrate and pressure, FF04 and FP03 (Figs. 5-3.10 and 5-3.11), were as expected throughout the test. The sharp drop in flow and pressure at 116 hr coincides with hydrogen sampling. Hydrogen flow to the Sabatier was somewhat restricted by metering valve MV1 which maintained a slight back pressure on the hydrogen line.

5.3.2.2.8 Oxygen Outlet Temperature and Dewpoint (FT18 and FD02)

The oxygen outlet temperature and dewpoint, measurements FT18 and FD02 (Figs. 5-3.12 and 5-3.13), show that the dewpoints were consistently lower than outlet temperatures. Thus, there were no condensate problems in the downstream lines.

5.3.2.2.9 Hydrogen Outlet Temperature and Dewpoint (FT17 and FD03)

The hydrogen outlet temperature and dewpoint, measurements FT17 and FD03 (Figs. 5-3.14 and 5-3.15), show that the dewpoints were consistently lower than outlet temperatures. Thus, there were no condensate problems in the downstream lines.

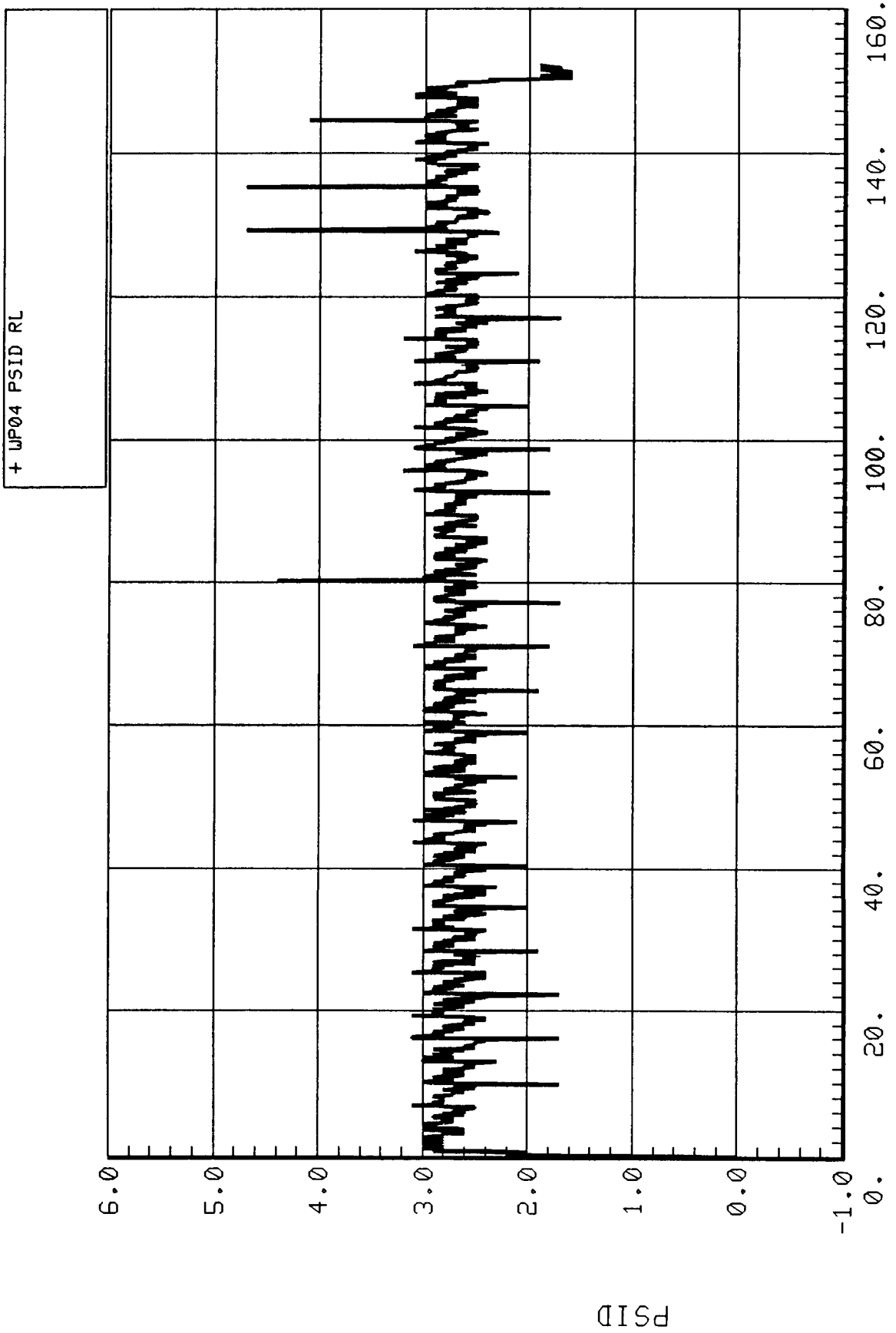

Figure 5-3.7. Feed water tank delta pressure (WP04).

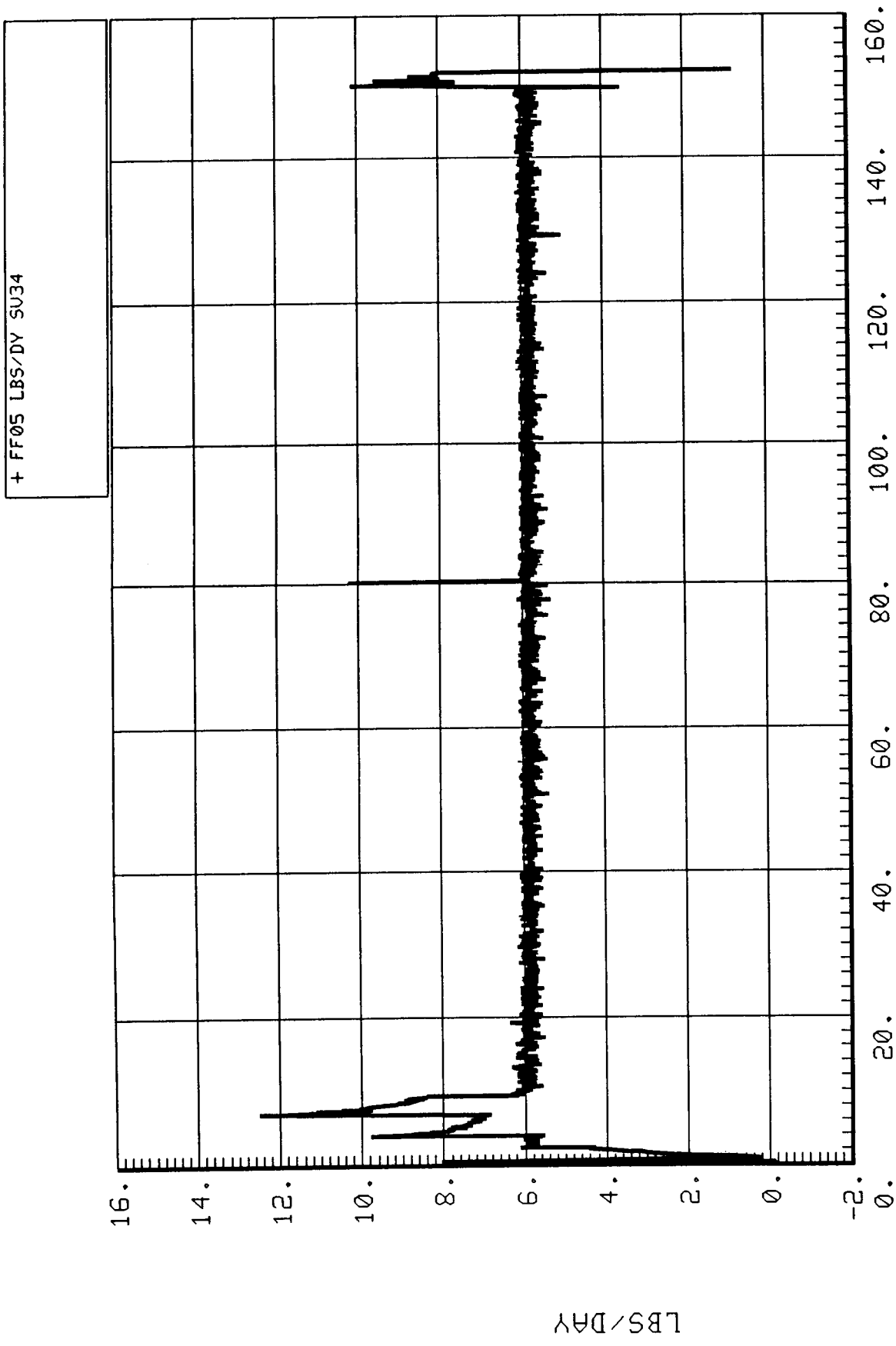

Figure 5-3.8. Oxygen outlet flowrate (FF05).

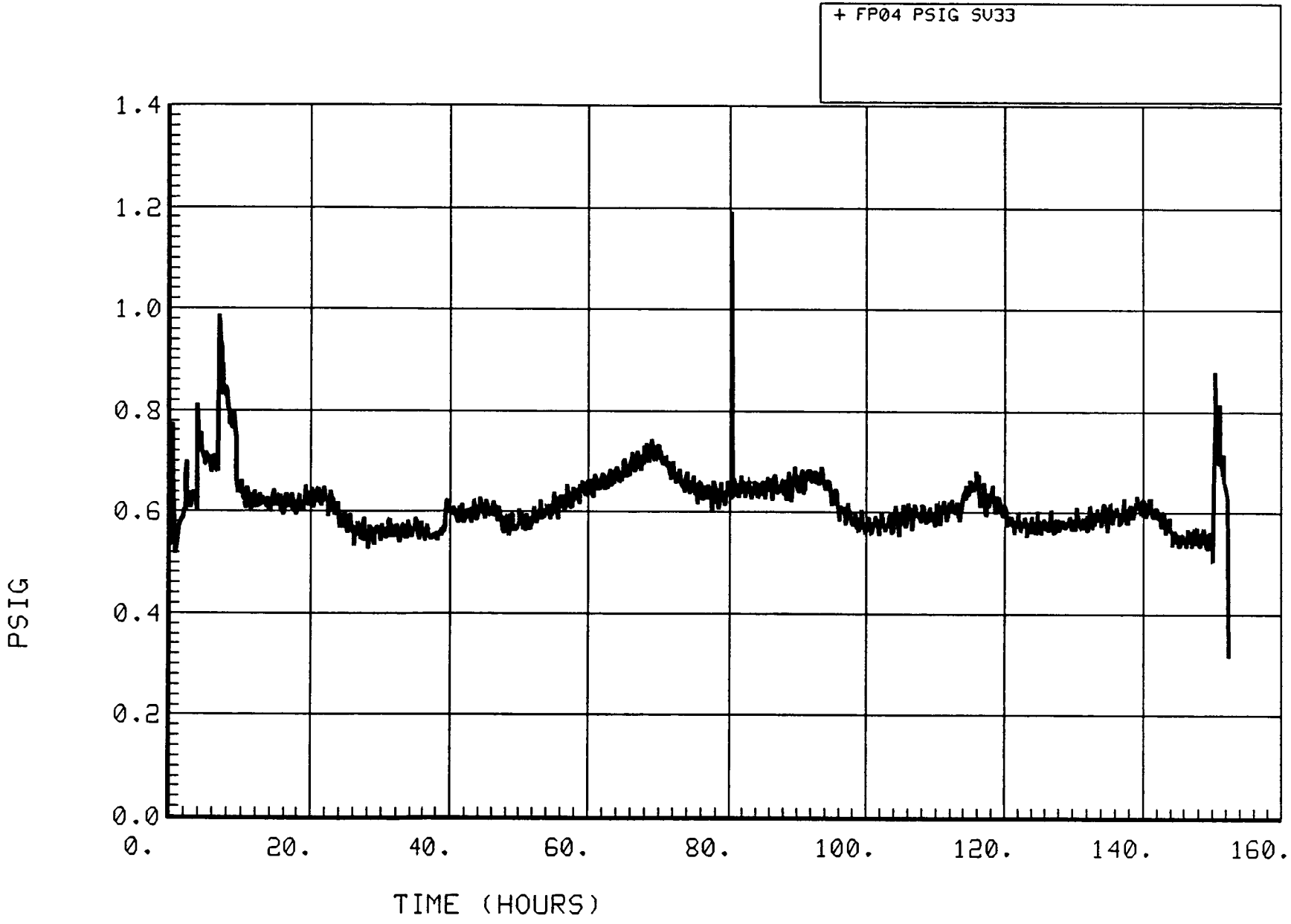

Figure 5-3.9. Oxygen outlet pressure (FP04).

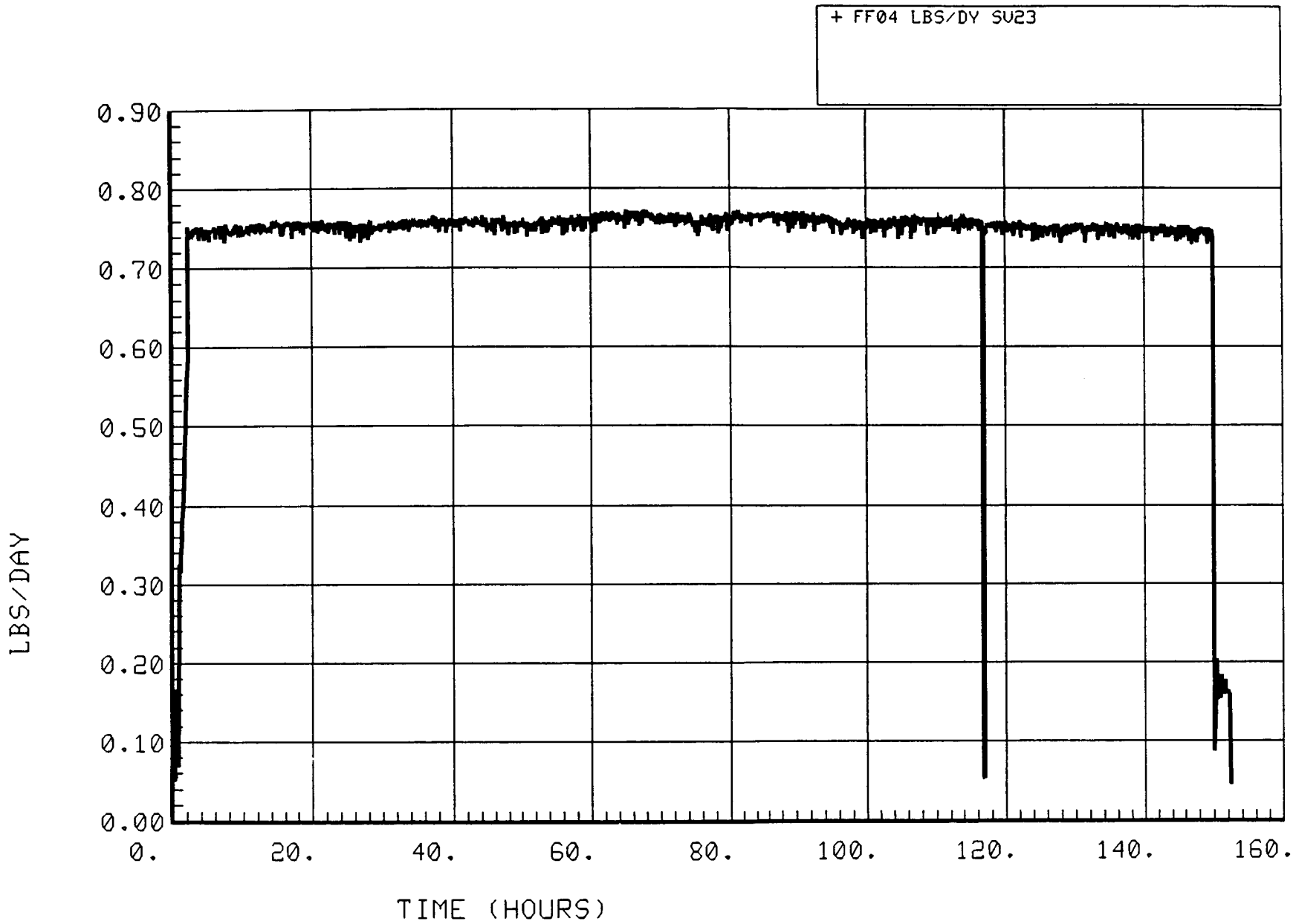

Figure 5-3.10. Hydrogen outlet flowrate (FF04).

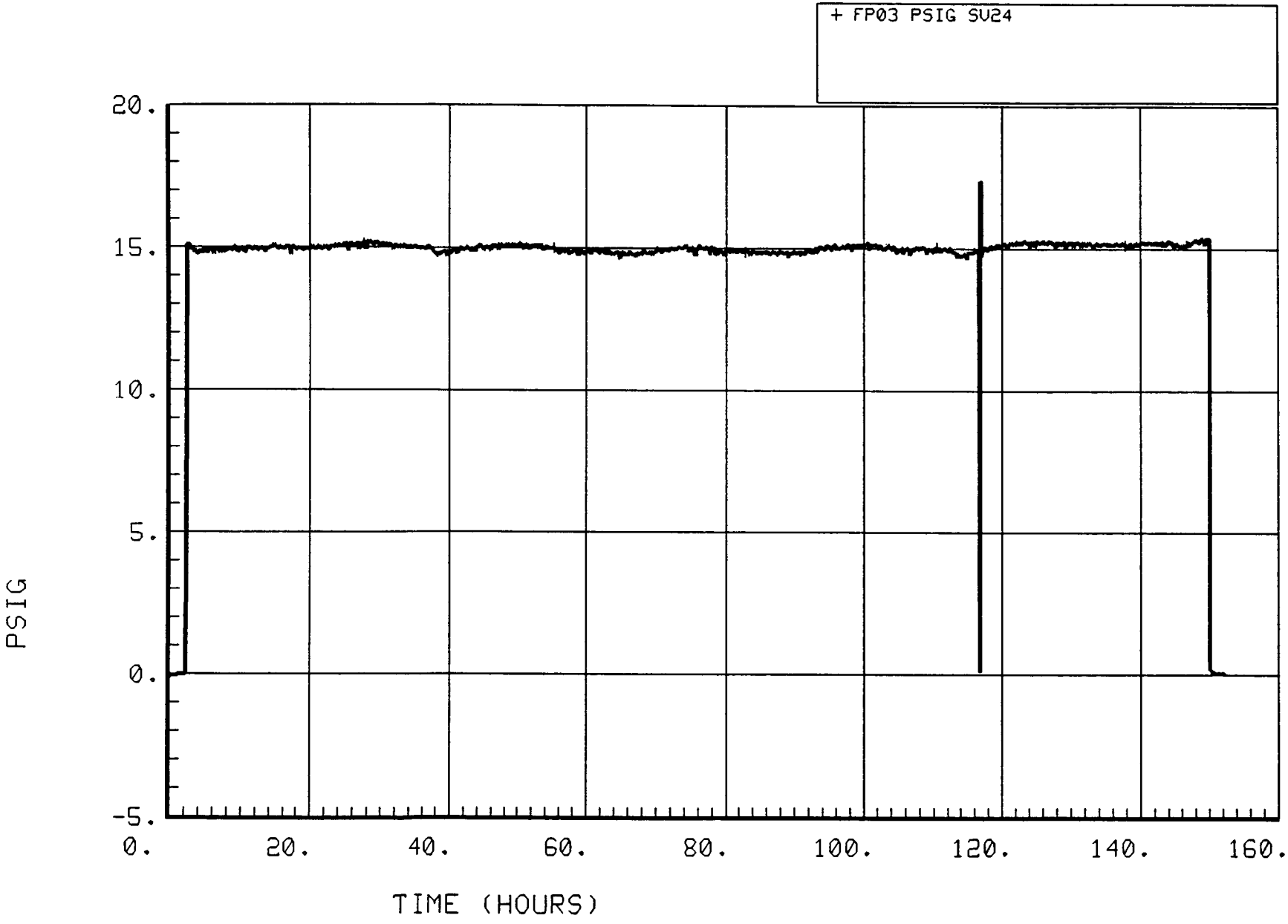

Figure 5-3.11. Hydrogen outlet pressure (FP03).

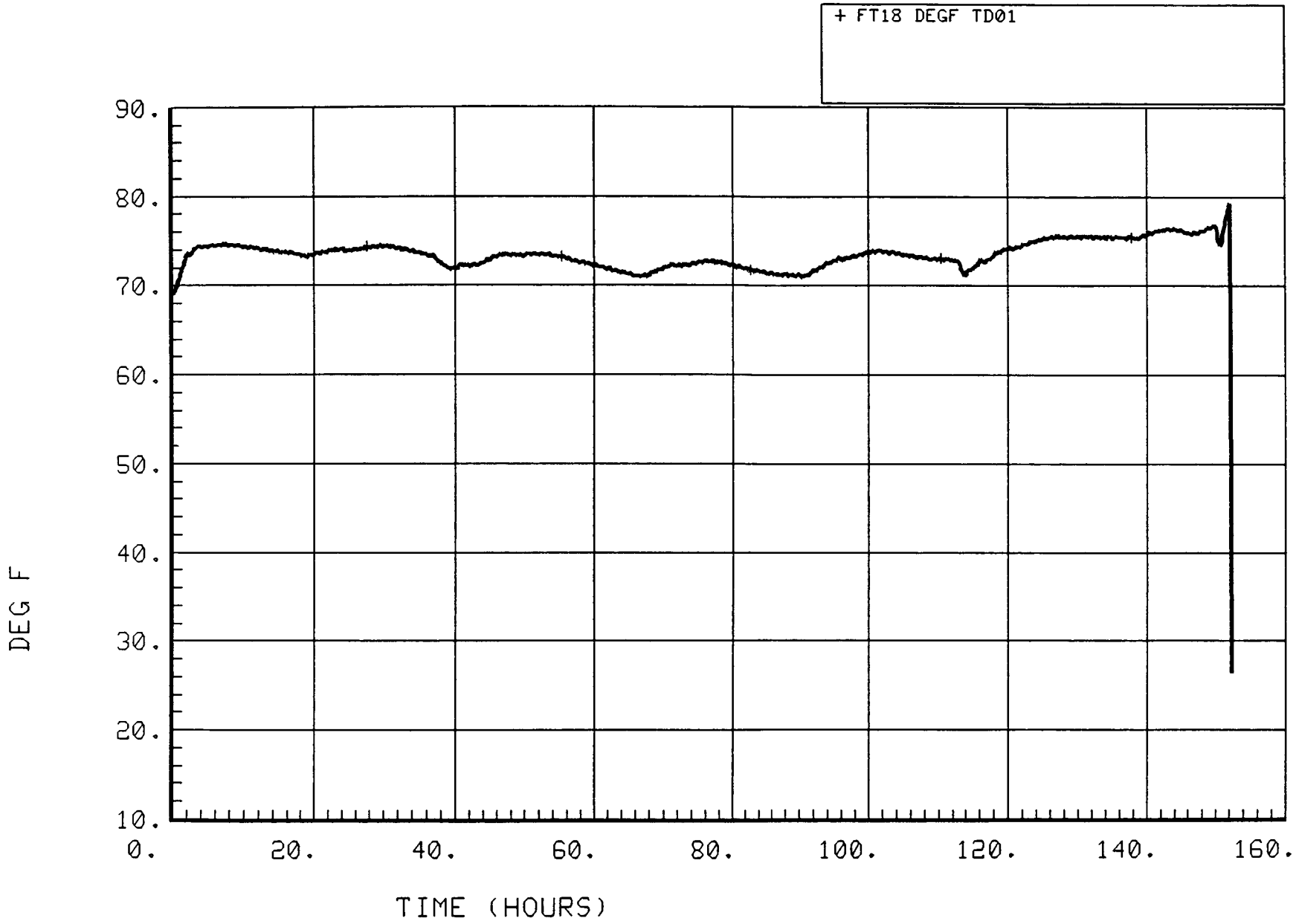

Figure 5-3.12. Oxygen outlet temperature (FT18).

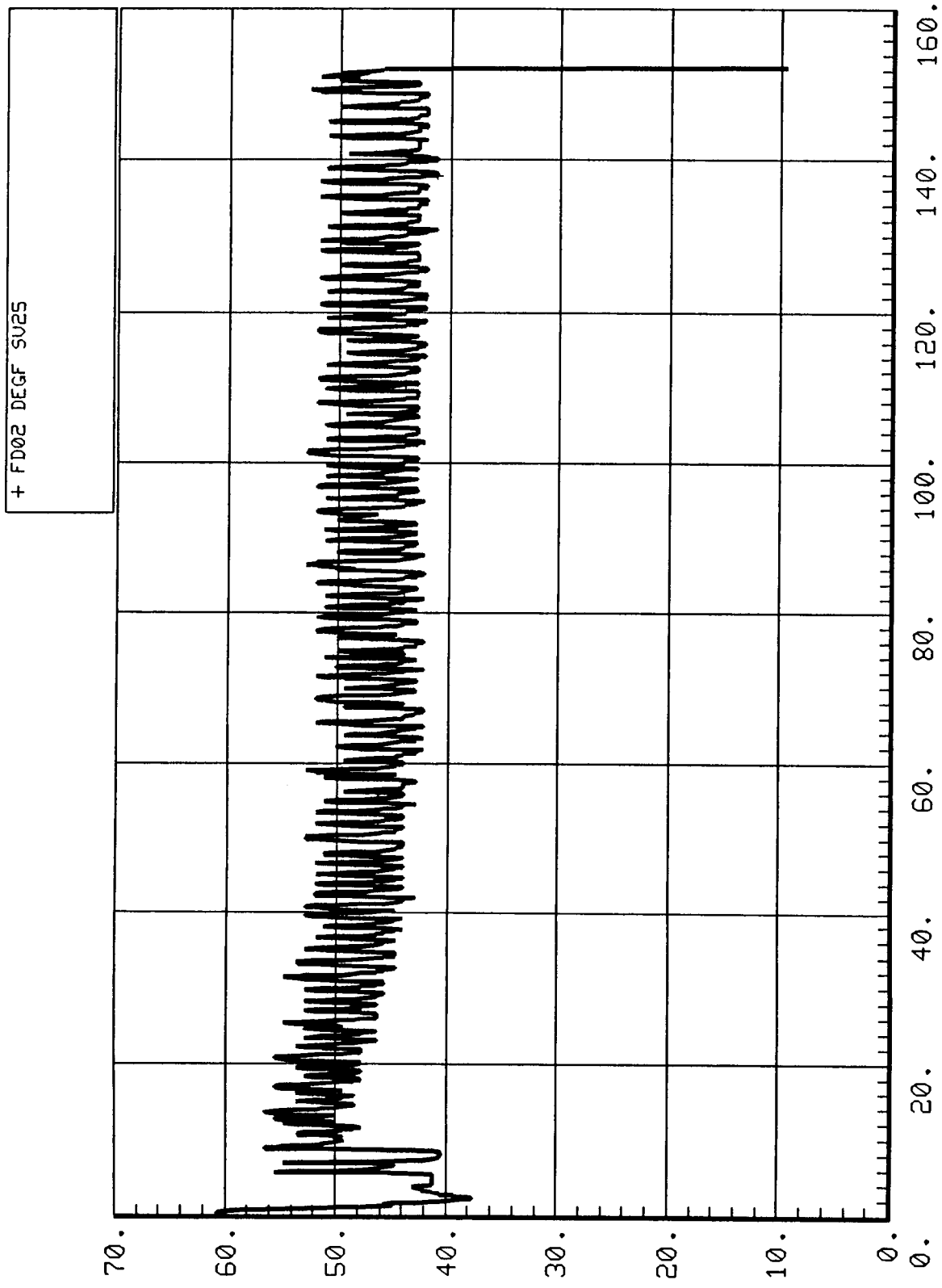

Figure 5-3.13. Oxygen outlet dewpoint (FD02).

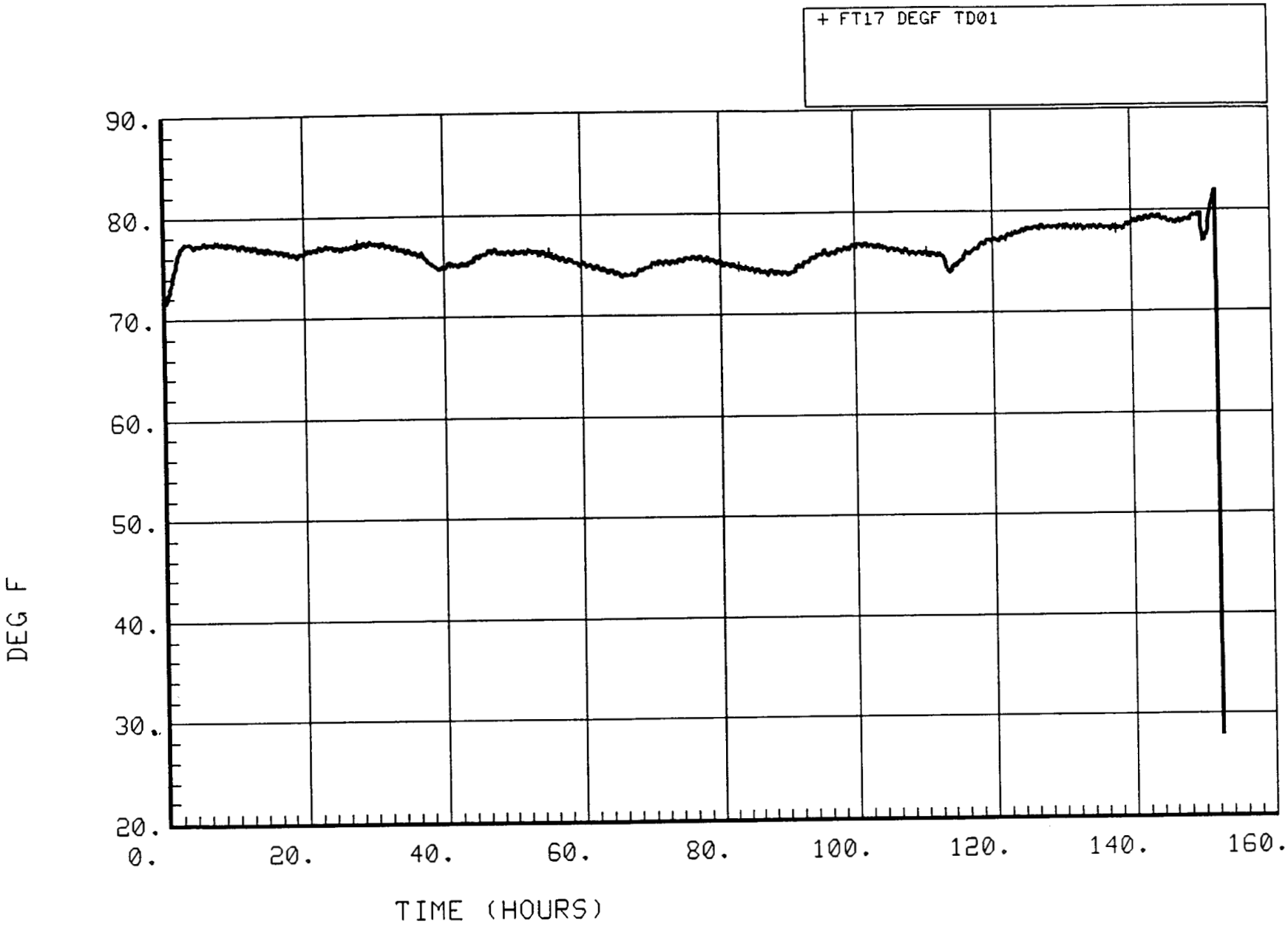

Figure 5-3.14. Hydrogen outlet temperature (FT17).

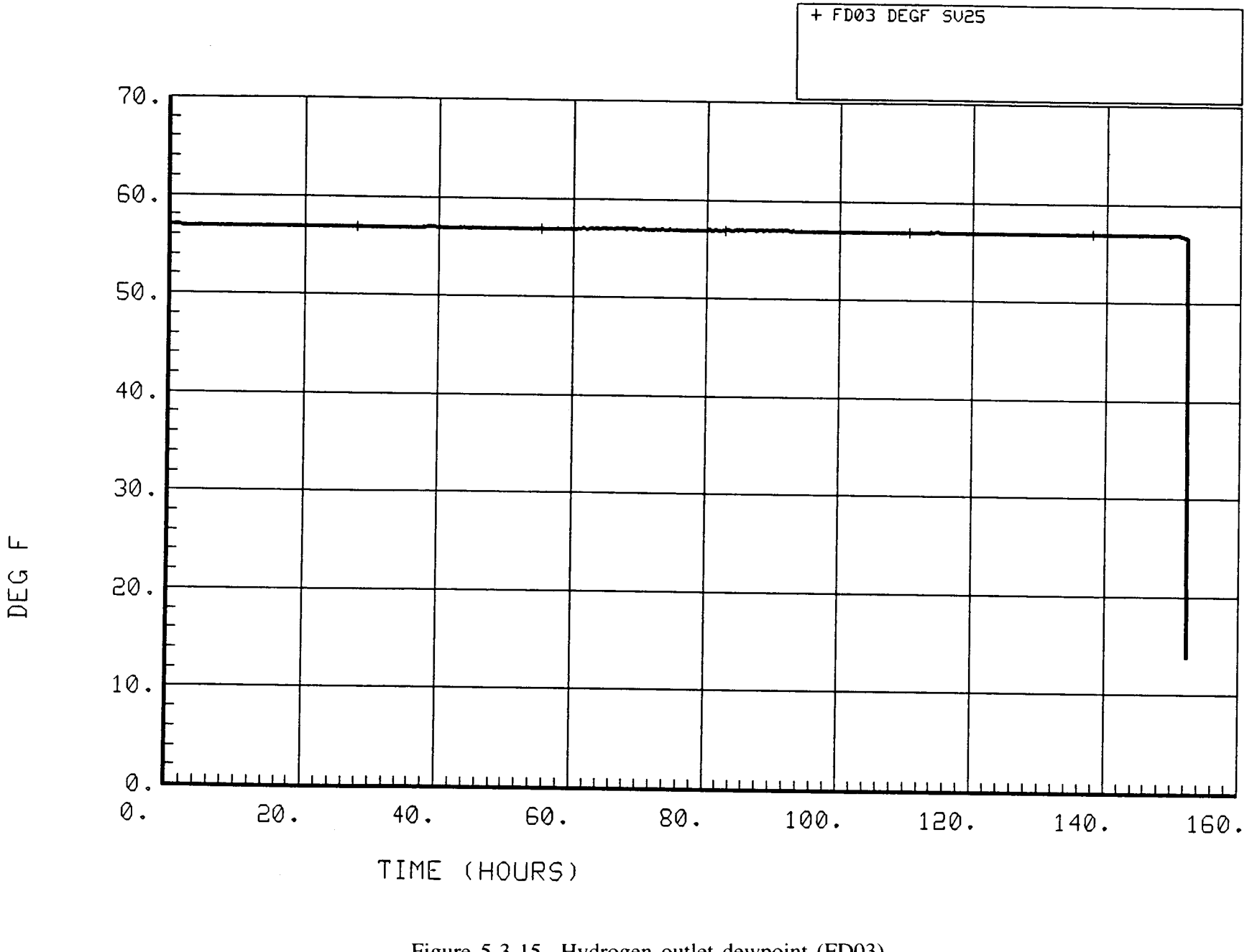

Figure 5-3.15. Hydrogen outlet dewpoint (FD03).

5.3.3 Recommendations/Lessons Learned

The SFE operated in the normal mode for 148 hr. During that time all subsystem measurements remained within their control bands. All facility measurements, with the exception of FF05 and FP04, were also within their nominal ranges for the entire test. The SFE satisfactorily demonstrated its ability to produce oxygen and hydrogen from recovered water in an integrated ECLS system.

5.4 Sabatier

5.4.1 Subsystem Description

The Sabatier CO_2 reduction subsystem was used in the EMCT to catalytically reduce carbon dioxide and hydrogen into methane gas and water. A schematic of the Sabatier subsystem, along with associated facility inputs and outputs, is shown in Figure 5-4.1. Subsystem and facility sensor designations are also noted on the schematics of individual measurements included in this section.

The input carbon dioxide and hydrogen are combined before entering the Sabatier. The CO_2/H_2 mixture passes first through an activated charcoal filter which removes any contaminants present which could poison the reactor catalyst, and enters the preheated reactor. The reaction

$$CO_2 + 4H_2 ==> CH_4 + 2H_2O$$

takes place in a packed Ruthenium on Alumina catalyst bed. The reaction is exothermic and self-sustaining up to a temperature of about 1100°F and is at least 99 percent efficient in converting the lean reactant in a single pass. The reactor heaters are used only at startup to initiate the reaction and automatically shutoff when the bed reaches 350°F. Two thermocouples located in the center and outside radius of the reactor bed monitor the reaction temperature. After passing through the catalyzed portion of the reactor, the reaction products (methane, water vapor, and either excess carbon dioxide or hydrogen) flow through two successive air-cooled heat exchange zones in the reactor and exit to the air-cooled condensing heat exchanger. A 25-cfm blower provides the cooling air for the reactor and condensing heat exchanger. The water vapor is condensed from the gas stream and is then separated by a rotary motor-driven water separator. A relief valve in the water outlet line provides back pressure to the water separator to prevent gas from exiting with the water. The product water may be, depending on the configuration of the three-way valve, pressurized out to facility storage or measured by an internal water quantity sensor before exiting to facility storage. The gas exiting the water separator is vented outside the building. There is a sample port in the gas outlet line for taking grab samples for analysis.

The subsystem is purged with nitrogen gas at subsystem startup and cooldown. A nitrogen accumulator tank inside the Sabatier ensures that enough nitrogen is always present to purge the reactor in case of loss of power or N_2 pressure.

5.4.2 Discussion of Results

5.4.2.1 General

The Sabatier CO_2 Reduction subsystem ran for the entire test without a shutdown. The subsystem was fed CO_2 from the Molecular Sieve at approximately 6.2 lb/day, the equivalent of a 2.8-man level. The reactant hydrogen flow from the SFE was a steady 0.74 lb/day, resulting in an H_2 to CO_2 mixture ratio of 2.6:1. The CO_2 flow is based on the actual flowmeter reading corrected for the percentage of air (2.5 percent based on O_2) present as output by the Molecular Sieve.

Since the reaction mixture was hydrogen-lean, the Sabatier outlet gas should have been a mixture of methane and carbon dioxide with some uncondensed water vapor and unreacted air. Results of the gas sample of the Sabatier vent showed 61.5% CH_4, 29.9% CO_2, 4.1% H_2, 3.6% N_2, 0.9% O_2, and 34 ppm water vapor (see Table 9-1). The actual reaction efficiency based on the percentage of unreacted hydrogen and measured flows was 98.3 percent. The theoretical products calculated using this efficiency would have been 1.46 lb/day CH_4, 2.16 lb/day CO_2, 0.012 lb/day H_2, 0.08 lb/day N_2, 0.02 lb/day O_2, and 3.26 lb/day water. The actual vent products based on sample results and measured vent flowrate were 1.55 lb/day CH_4, 2.08 lb/day CO_2, 0.013 lb/day H_2, 0.16 lb/day N_2, and 0.04 lb/day O_2. There is good agreement between theoretical and actual results for the gas products; however, it appears that, since there was twice as much air in the sample results than predicted, some air may have contaminated the sample either during collection or analysis.

Sabatier water production based on the 98.3 percent reaction efficiency and measured inlet flowrates of reactants should have been 3.26 lb/day. Steady state measurement of water collected at the product water tank showed 2.76 lb/day, or 84.7 percent of theoretical. In addition, water collected in the coalescent filter in the outlet vent line was periodically emptied and measured an average of 0.15 lb/day, or 4.7 percent of the theoretical water production. This leaves about 10 percent of the product water unaccounted for. A good assumption is that typically about 5 percent of the water leaves the subsystem uncondensed in the saturated product gases which, when factored in, would result in 95 percent of the theoretical product water being accounted for as either condensed and separated, condensed but not separated (collected in the coalescent filter), or uncondensed.

5.4.2.2 Discussion of Individual Measurements

This section discusses each of the subsystem and Sabatier-related facility measurement plots that follow. Refer to Figure 5-4.1, Sabatier subsystem schematic, for sensor locations.

5.4.2.2.1 Inlet CO_2 Flowrate (FF01)

The CO_2 inlet flowrate (Fig. 5-4.2) from the Molecular Sieve cycled around an average of 6.4 lb/day, except for three events: the Molecular Sieve failure at 38 hr when CO_2 production decreased until manual cycling was initiated, the Molecular Sieve heater current failure at 114 hr, and gas sampling of the product CO_2 at approximately 116 hr. After correcting the measured flowrate for air content, the actual CO_2 flowrate would have been 6.2 lb/day.

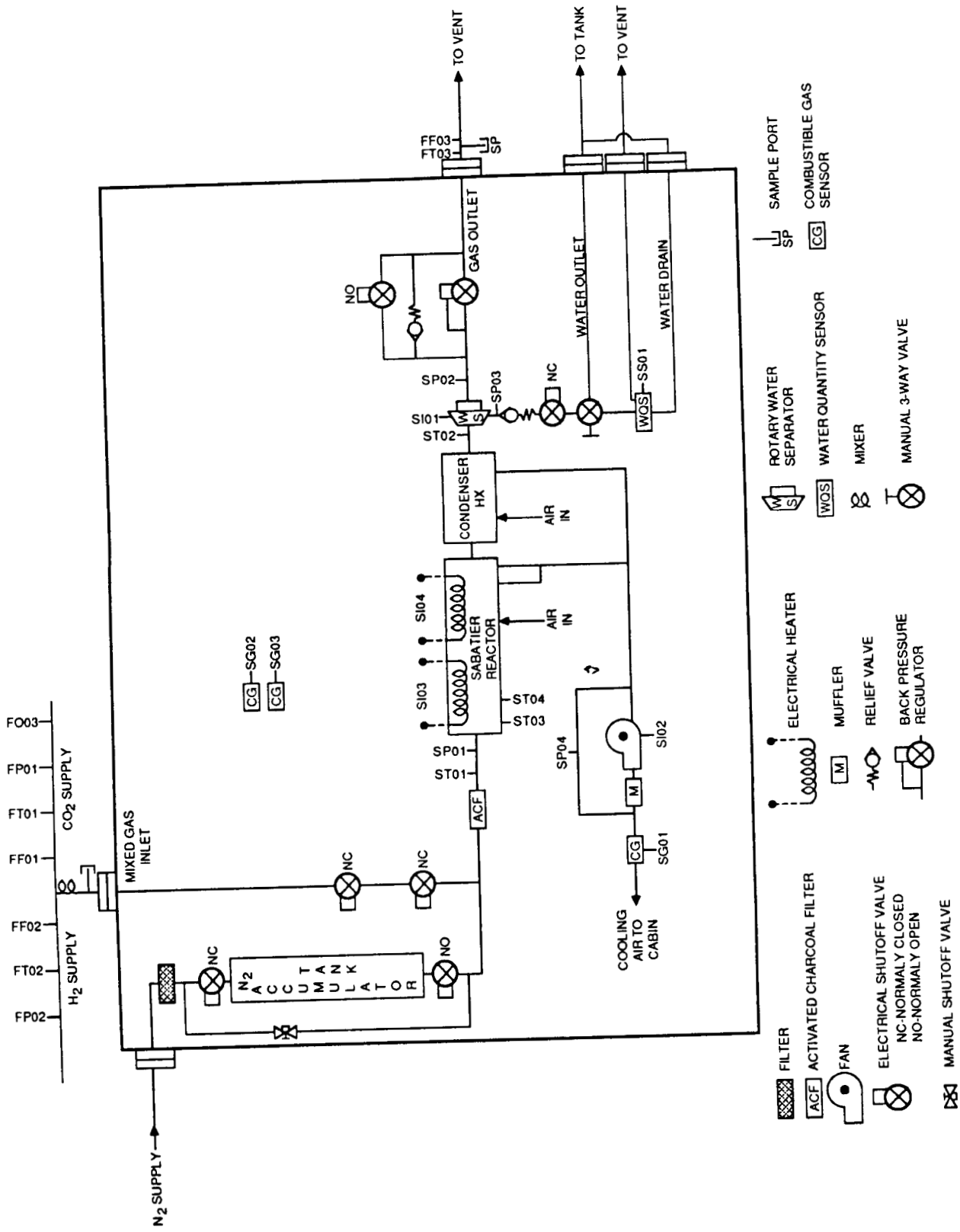

Figure 5-4.1. Sabatier CO_2 reduction subsystem schematic.

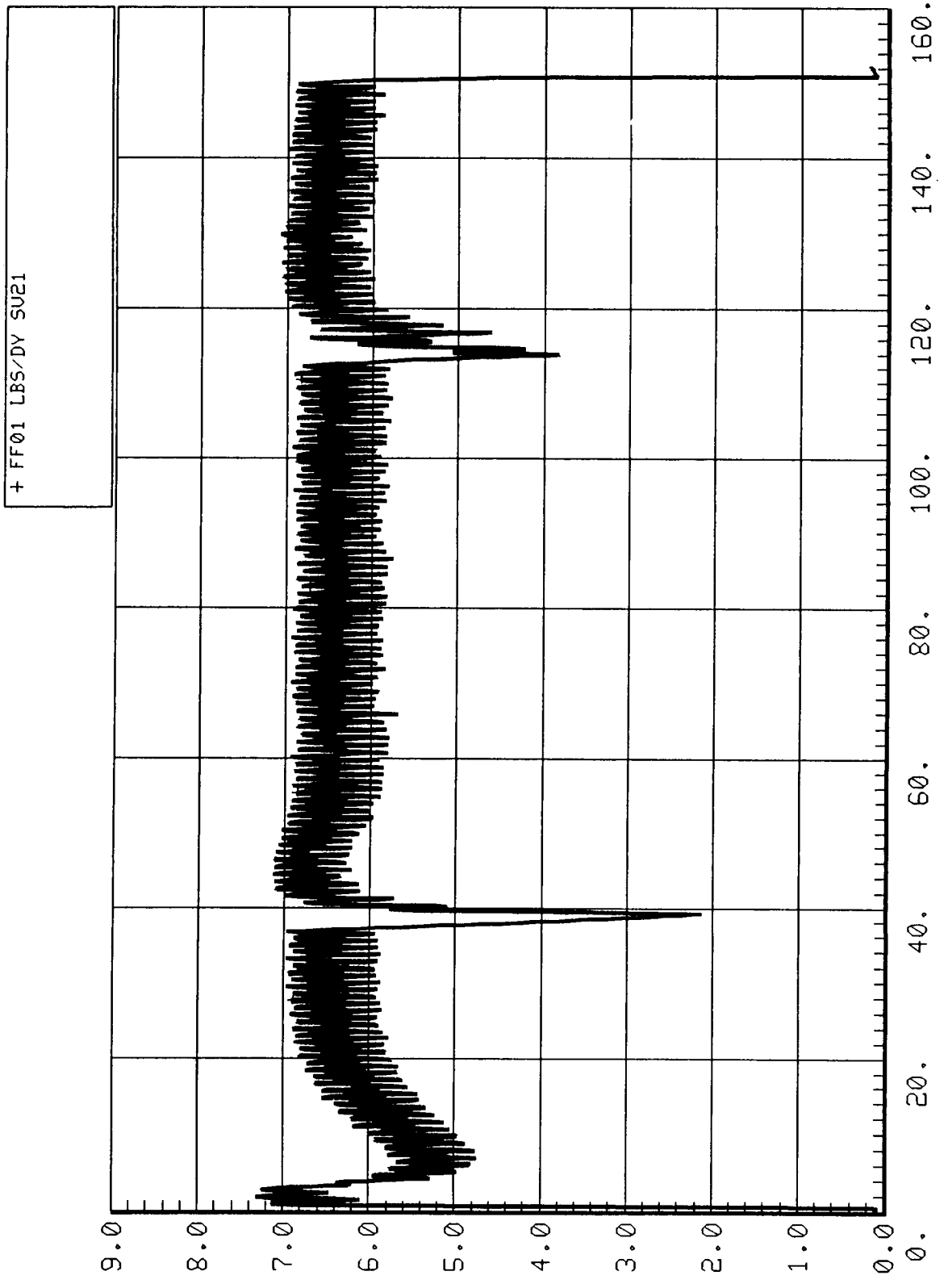

Figure 5-4.2. Inlet CO_2 flowrate (FF01).

5.4.2.2.2 Inlet CO_2 Pressure (FP01)

The CO_2 inlet pressure to the Sabatier (Fig. 5-4.3) cycled around an average of 2.4 psig, with the exception of the events mentioned above where corresponding pressure drops can be seen.

5.4.2.2.3 Inlet CO_2 Temperature (FT01)

The temperature of the CO_2 inlet stream (Fig. 5-4.4) fluctuated in 24-hr major cycles with smaller 1-hr Molecular Sieve cycles. The measurements ranged from about 75° to 81°F normally. It appears that flowrate and pressure affect the measurement somewhat as the two fluctuations in the flow and pressure also show in the temperature plot.

5.4.2.2.4 Inlet H_2 Flowrate (FF02)

The flowrate of hydrogen from the SFE to the Sabatier (Fig. 5-4.5) was steady at about 2.83 slpm, or 0.74 lb/day. Because sampling of the SFE hydrogen during the Simplified Integrated Test resulted in a Sabatier shutdown, it was decided for this test to switch the Sabatier to facility hydrogen feed during SFE H_2 sampling. The flowrate to the subsystem was uninterrupted during this transition (around 116.5 hr into the test).

5.4.2.2.5 Inlet H_2 Pressure (FP02)

The inlet H_2 pressure is shown in Figure 5-4.6. Hydrogen feed pressure cycled as the module simulator temperature varied during the day, averaging about 2.6 psig for the test. Slight drops in pressure at the time of the Molecular Sieve failures at 38 and 114 hr can be explained by the probable back pressure decrease from the Sabatier to its hydrogen feed when the CO_2 inlet pressure dropped off. Also, the normal 1-hr pressure cycles of the Molecular Sieve affected the hydrogen feed pressure slightly. Another slight pressure drop can be seen at 116.5 hr when the subsystem was switched to facility hydrogen while the SFE hydrogen was being sampled.

5.4.2.2.6 Inlet H_2 Temperature (FT02)

Hydrogen feed temperature from the SFE (Fig. 5-4.7) ranged from 77° to 88°F throughout the test. A 24-hr cycle can be seen as the module simulator temperature varied during the day.

5.4.2.2.7 Reactor Inlet Temperature (ST01)

The Sabatier reactant inlet temperature (Fig. 5-4.8) ranged from about 84° to 90°F during the length of the test, cycling with the module simulator temperature and the Molecular Sieve. The decrease in pressure and flowrate from the Molecular Sieve during the failures and sample times (at 38, 114 and 116 hr, respectively) affected the temperature measurement somewhat.

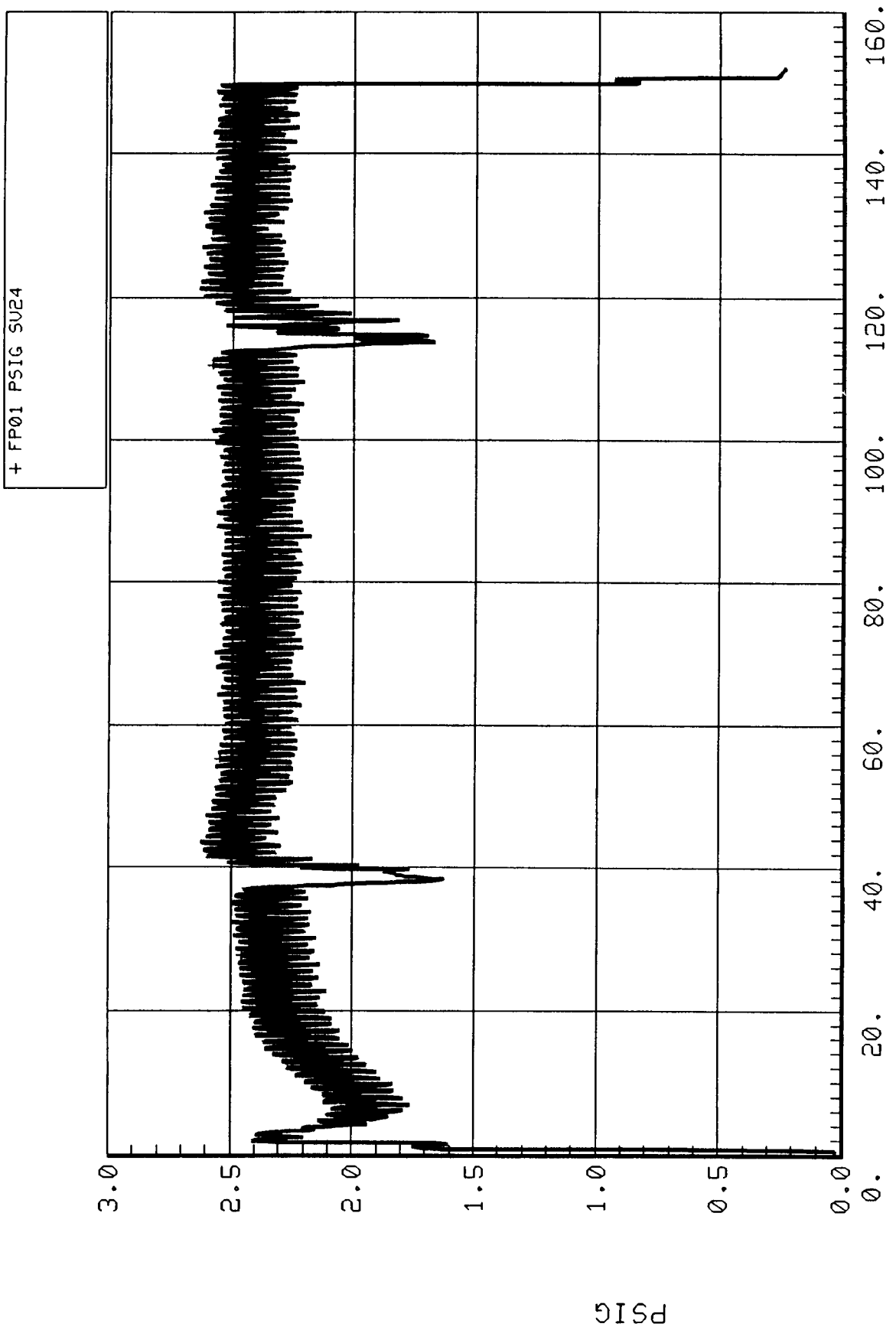

Figure 5-4.3. Inlet CO_2 pressure (FP01).

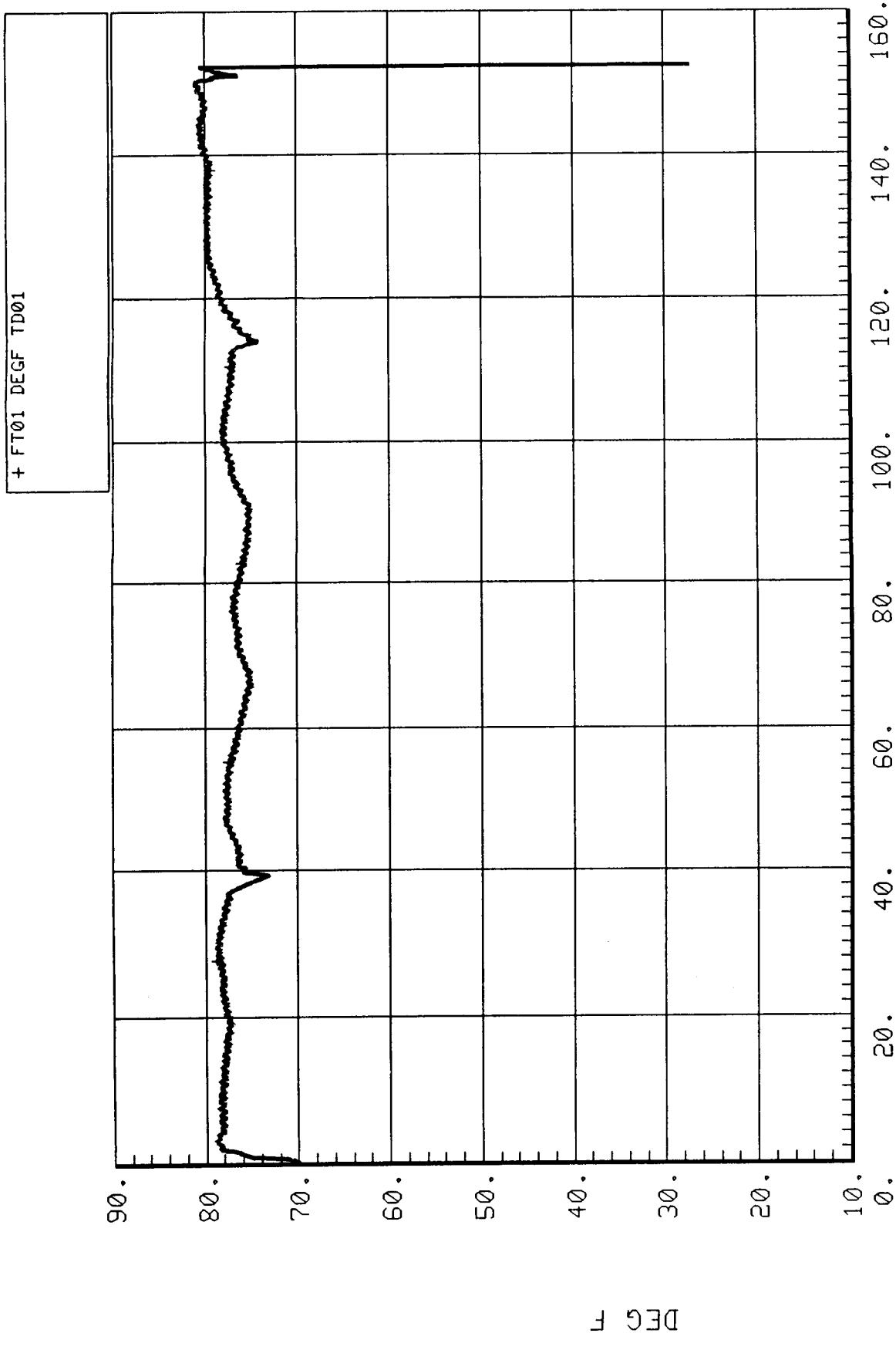

Figure 5-4.4. Inlet CO_2 temperature (FT01).

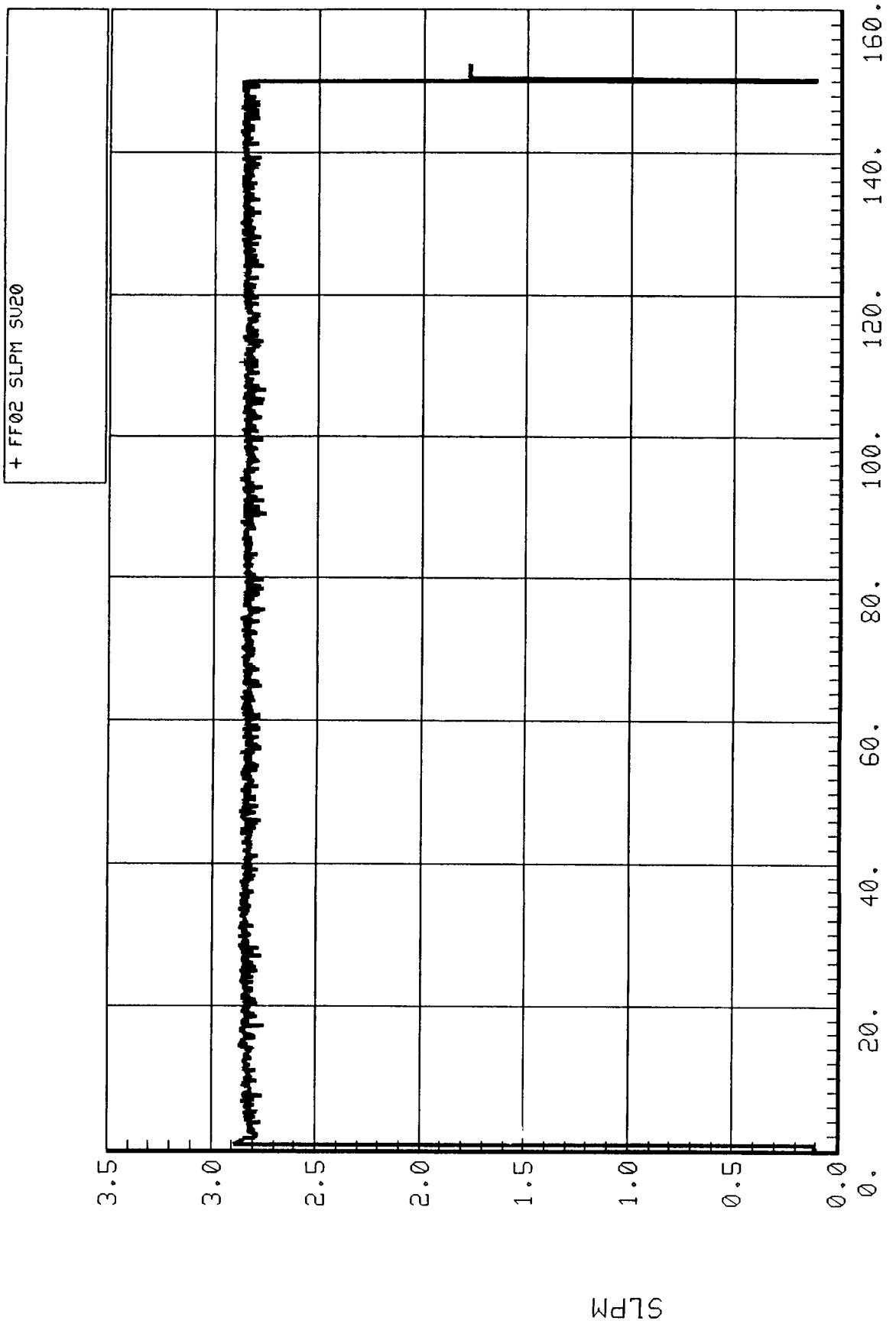

Figure 5-4.5. Inlet H_2 flowrate (FF02).

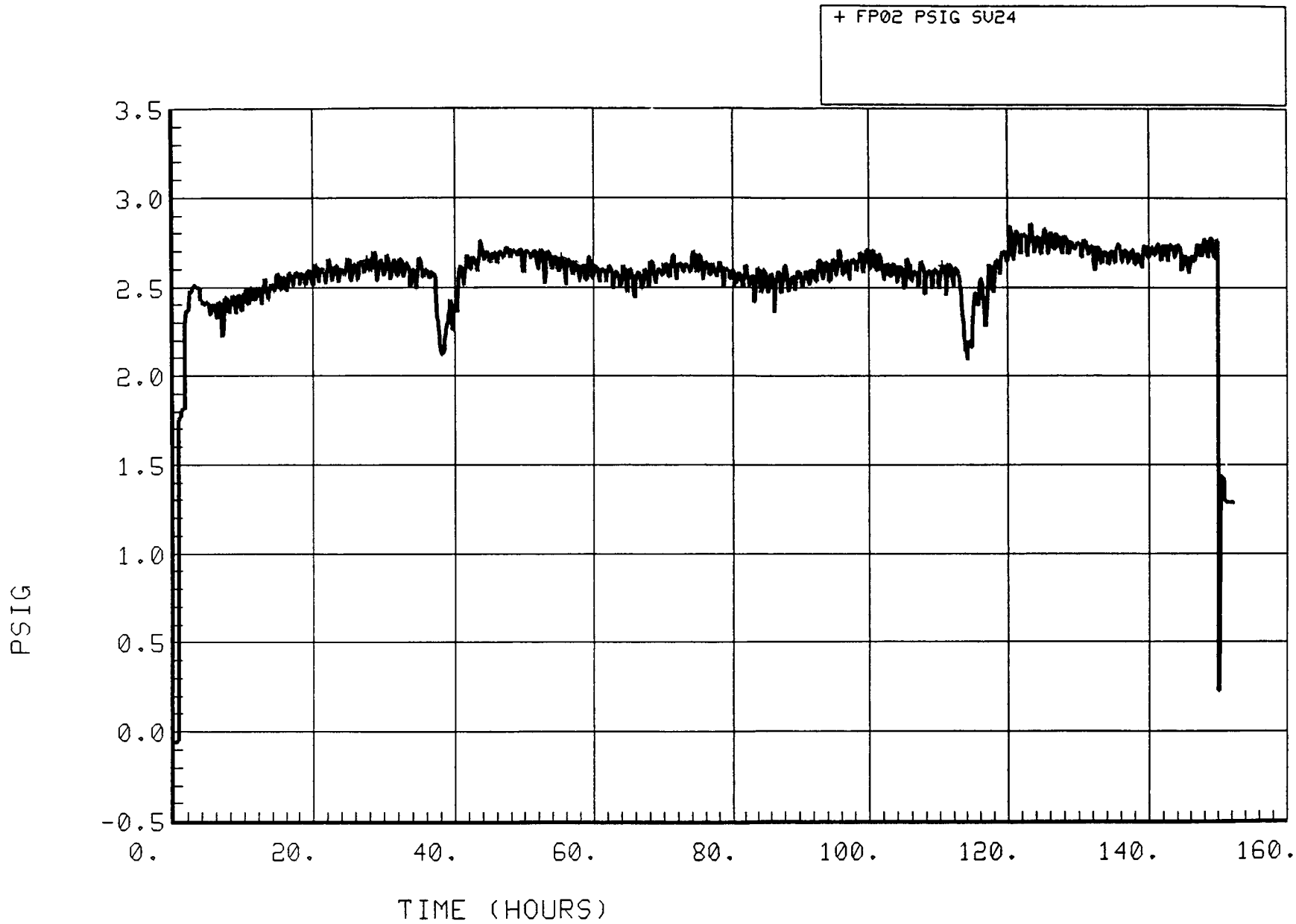

Figure 5-4.6. Inlet H_2 pressure (FP02).

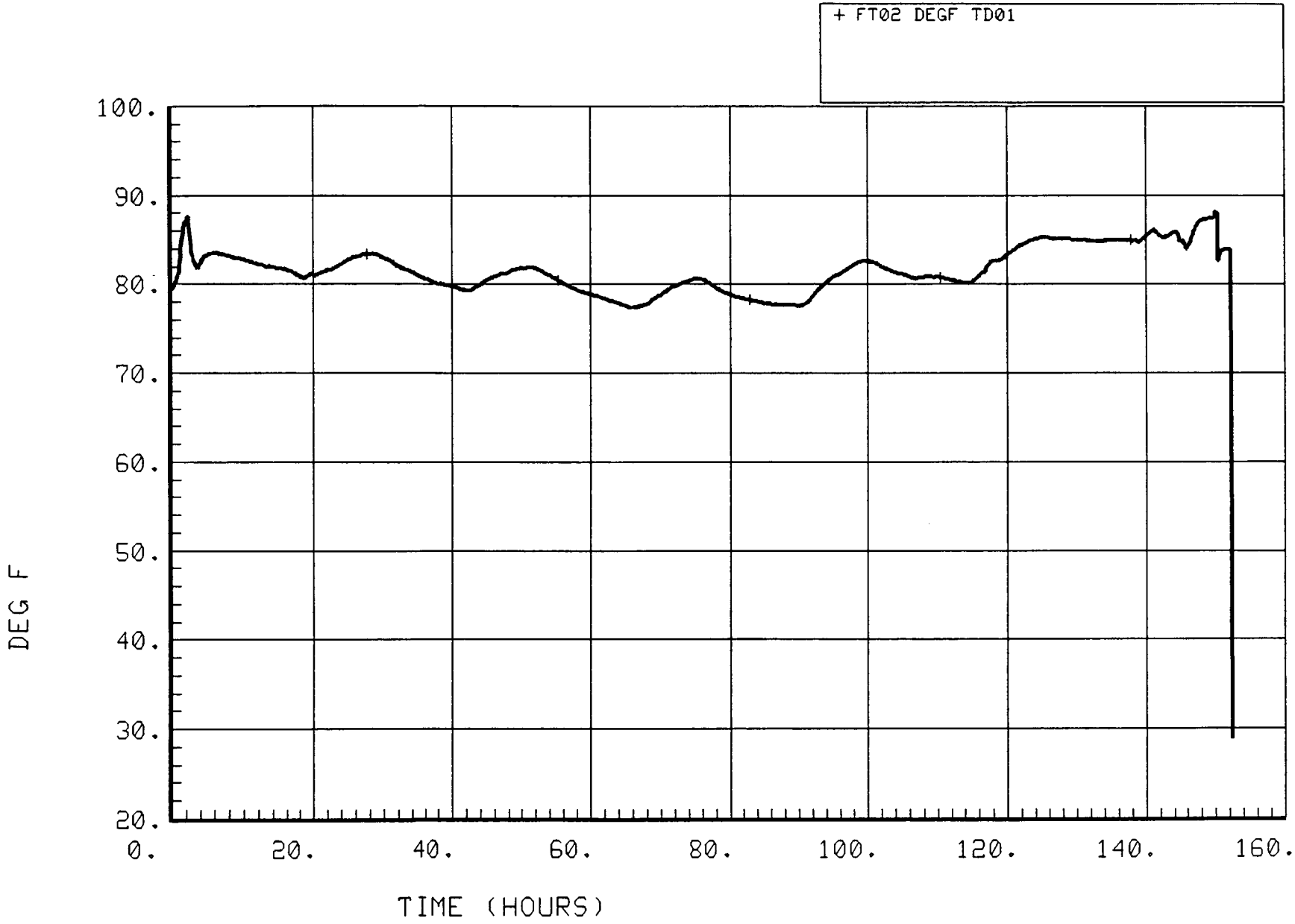

Figure 5-4.7. Inlet H_2 temperature (FT02).

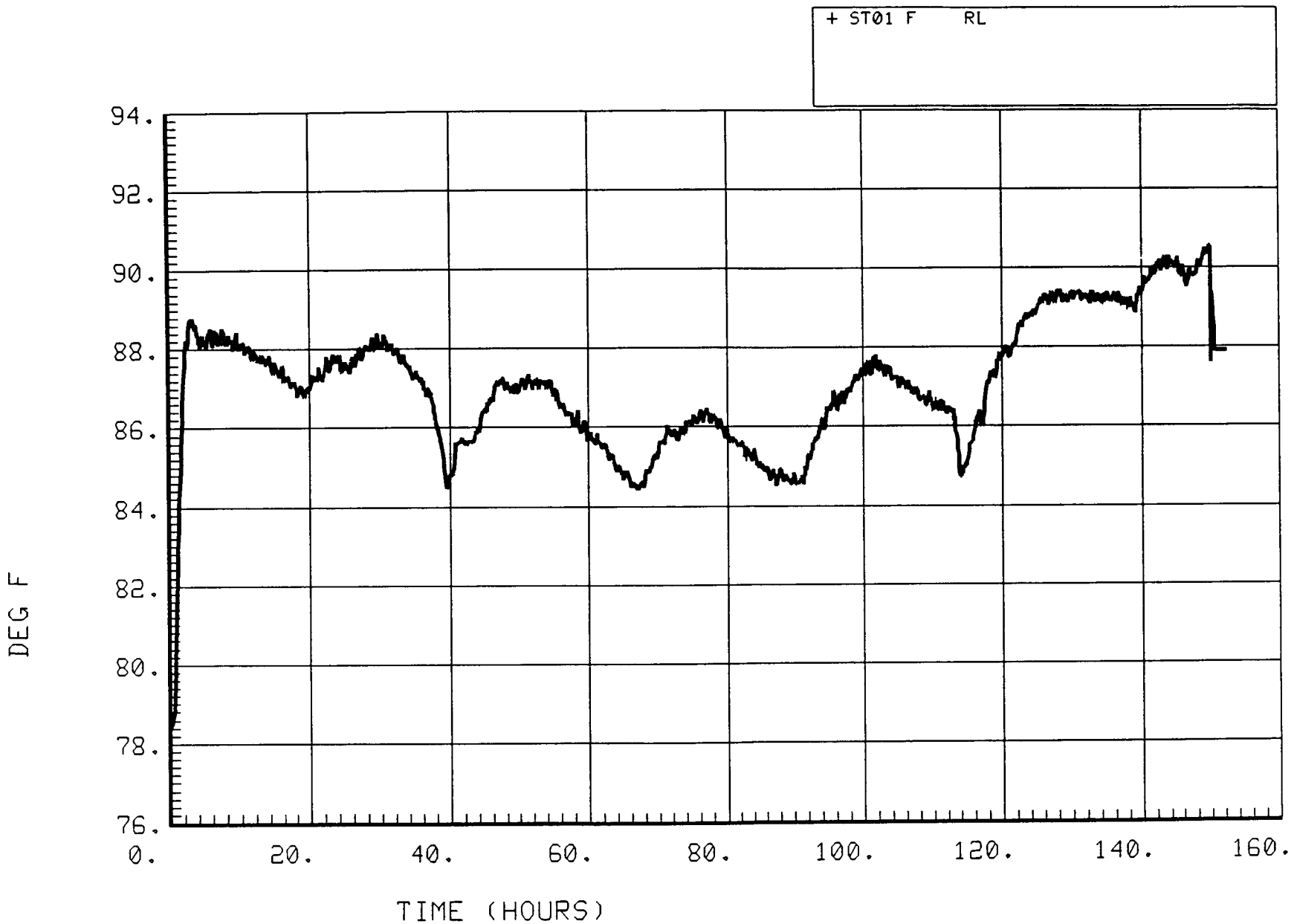

Figure 5-4.8. Reactor inlet temperature (ST01).

5.4.2.2.8 Reactor Inlet Pressure (SP01)

The Sabatier reactant inlet pressure (Fig. 5-4.9) averaged about 16.2 psia over the test. Peaks to 24 psia at the beginning and end of the plot represent normal startup and shutdown purges with higher pressure nitrogen gas. Slight drops in pressure corresponding to the Molecular Sieve failure and inlet reactant sampling can be seen at 38, 114, and 116 hr.

5.4.2.2.9 Reactor Bed Temperature 1 (ST03)

The thermocouple that measures the Sabatier center bed temperature, shown in Figure 5-4.10, began reading erratically shortly after the Molecular Sieve failure, which can be seen on the plot at 38 hr as a drop in reactor temperature due to decreased CO_2 flow. Normal three-man steady-state bed temperature ranges from 850° to 900°F with little change. It was feared that if the sensor failed, it would either fail high and cause an automatic shutdown, or low, possibly causing the reactor heaters to come on unnecessarily. Fortunately, neither happened; in fact, the sensor actually steadied out toward the end of the test. This sensor is presently undergoing checkout and will probably require replacement.

5.4.2.2.10 Reactor Bed Temperature 2 (ST04)

The temperature at the outside radius of the reactor bed (Fig. 5-4.11) was a constant 650°F throughout the test with the exception of the cool down during the Molecular Sieve failure. The steady reading of ST04 provided reassurance that the erratic readings of ST03 were not actual but the result of a bad sensor.

5.4.2.2.11 Condenser Exit Temperature (ST02)

The temperature of the reaction products exiting the condensing heat exchanger is shown in Figure 5-4.12. This temperature ranged from 95° to 101°F during the test. One-hr and 24-hr cycles can be seen due to Molecular Sieve and room temperature effects, respectively, as well as slight drops corresponding to the Molecular Sieve failure and gas sampling.

5.4.2.2.12 Gas Outlet Pressure (SP02)

Product gas outlet pressure from the water separator (Fig. 5-4.13) averaged 15.2 psia with only very slight dips at 38, 114, and 116 hr from the three events mentioned previously. As with SP01, purge pressure peaks are evident at startup and shutdown.

5.4.2.2.13 Water Outlet Pressure (SP03)

The Sabatier water outlet pressure is shown in Figure 5-4.14. Water production from the Sabatier began at about 2 hr as denoted by the outlet pressure increase to 38 to 40 psia. Cycling of

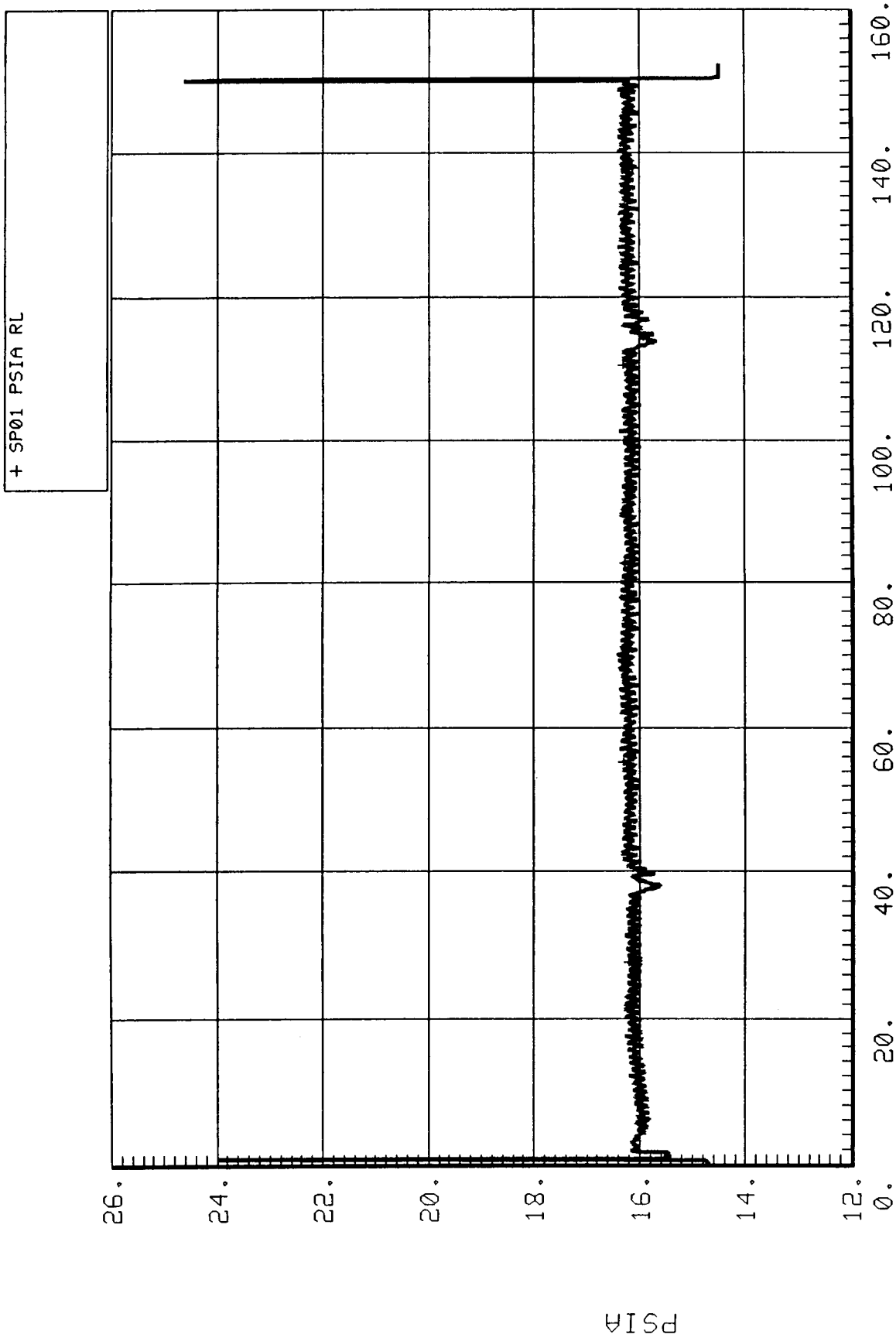

Figure 5-4.9. Reactor inlet pressure (SP01).

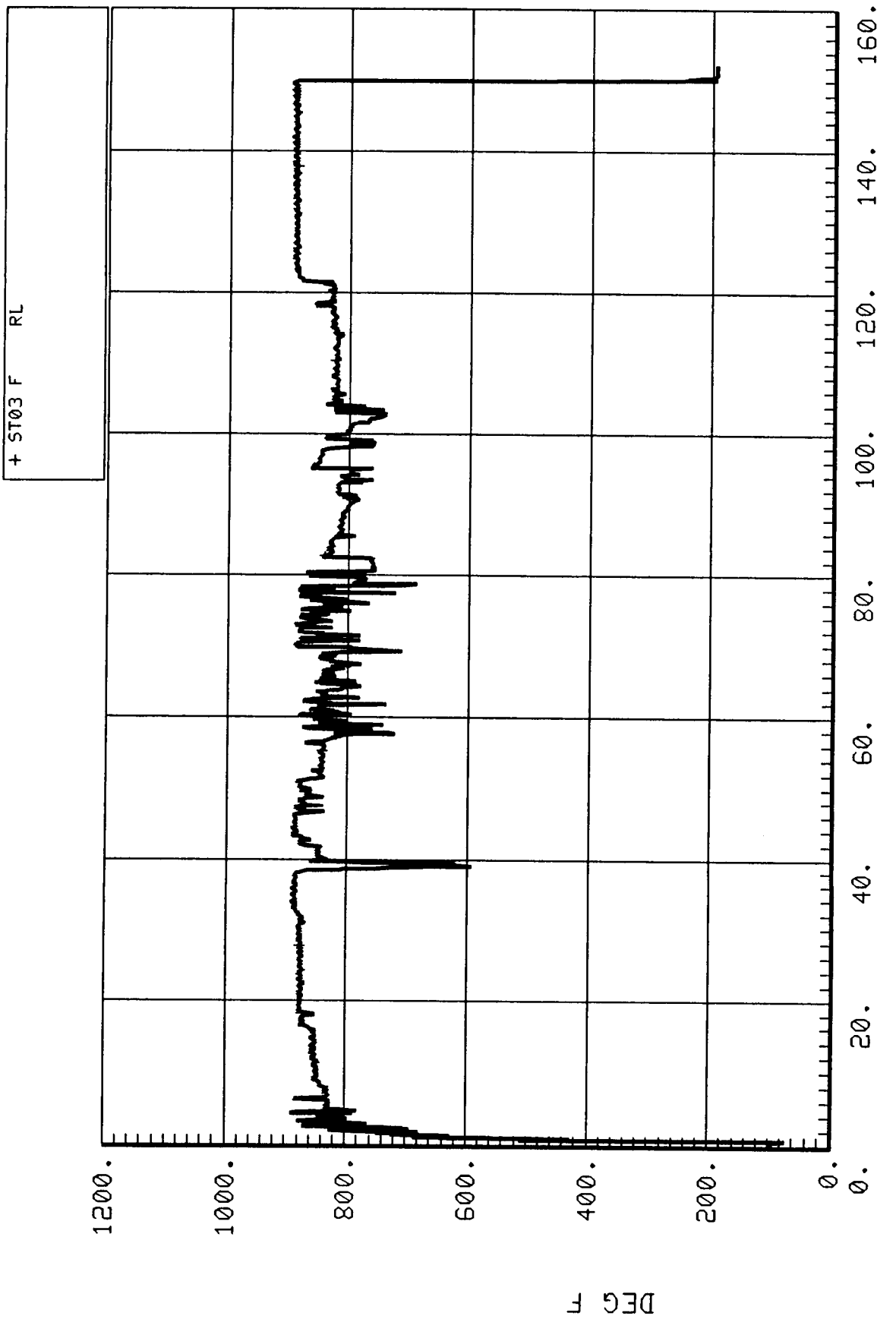

Figure 5-4.10. Reactor bed temperature No. 1 (ST03).

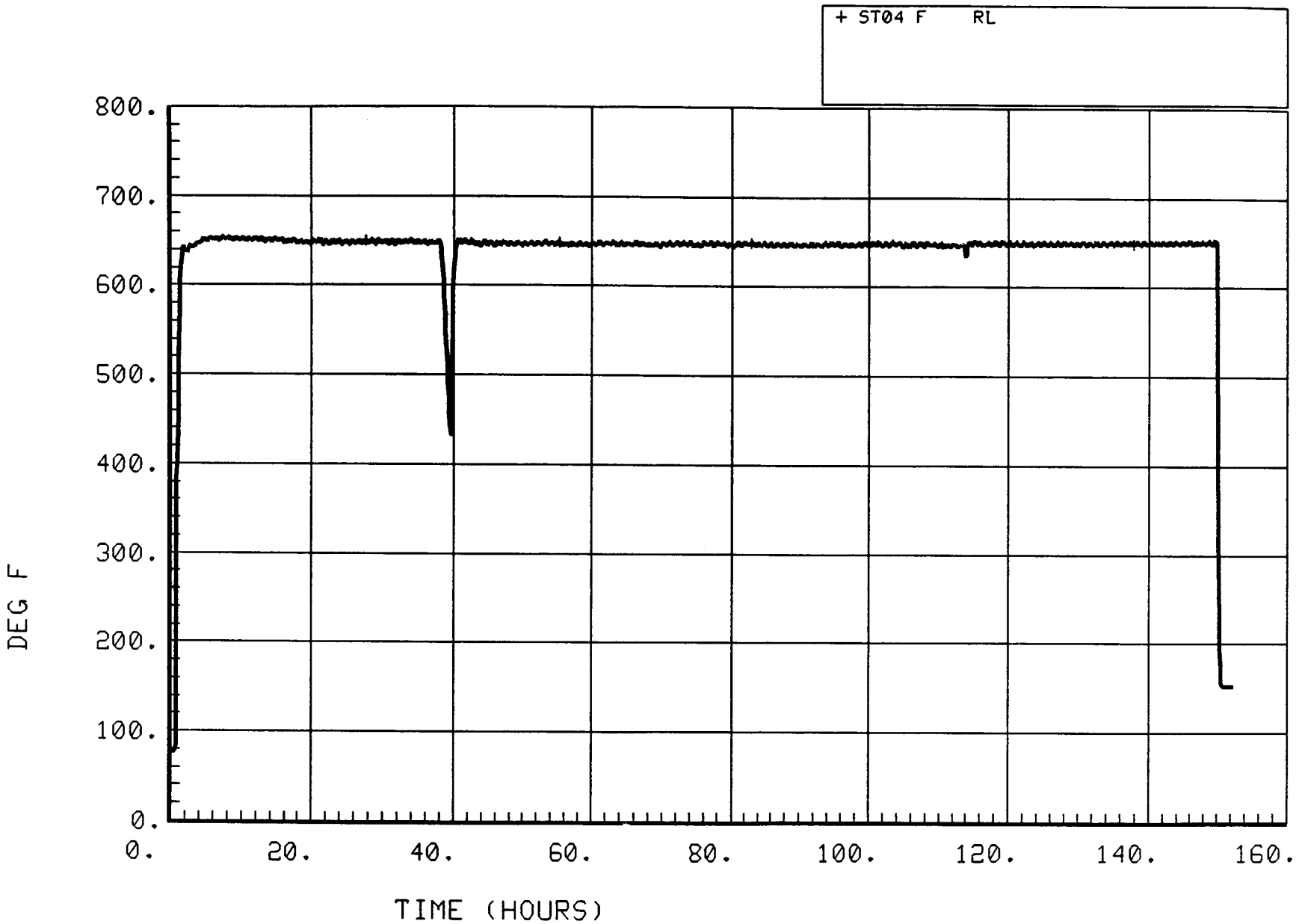

Figure 5-4.11. Reactor bed temperature No. 2 (ST04).

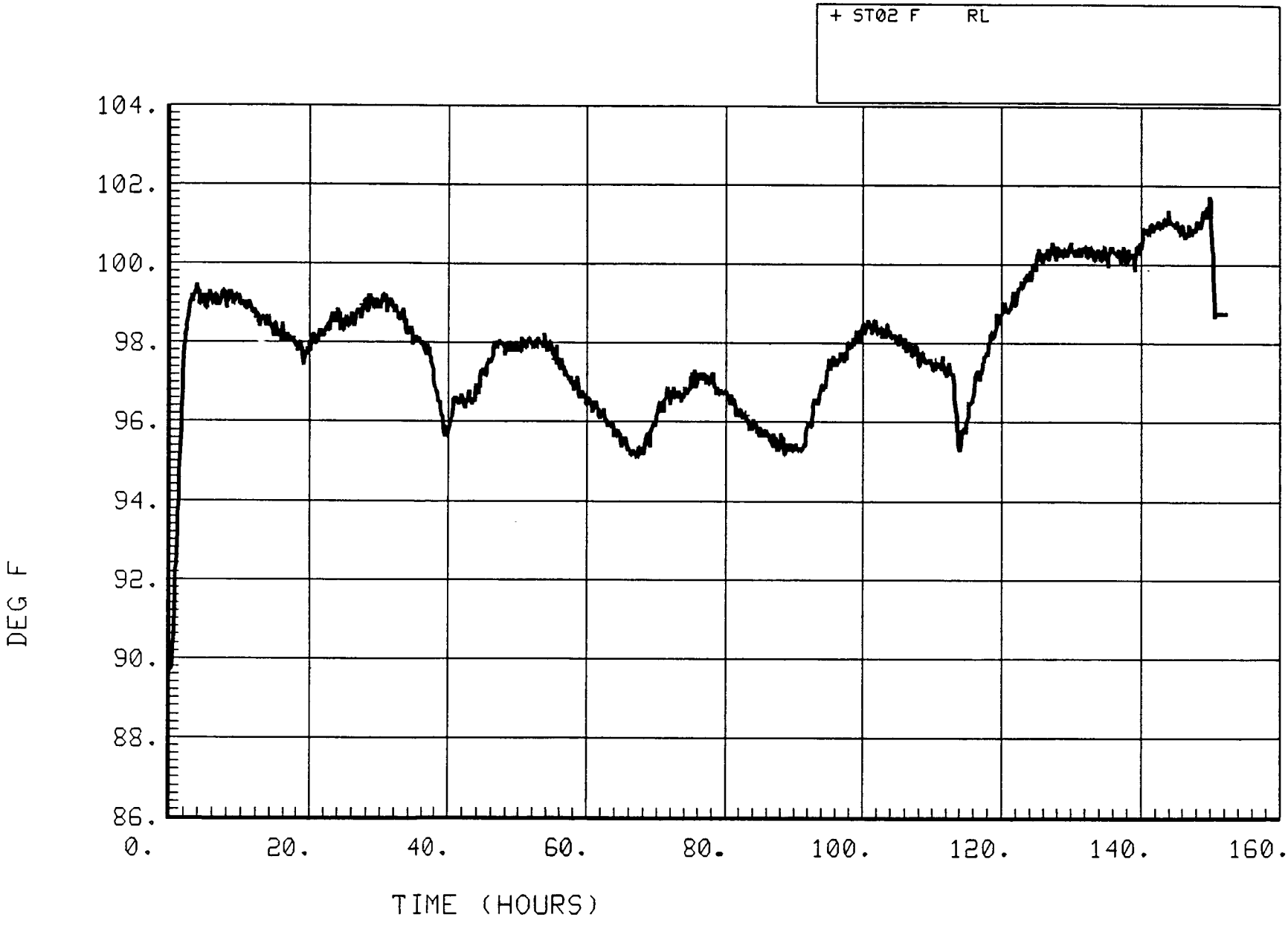

Figure 5-4.12. Condenser exit temperature (ST02).

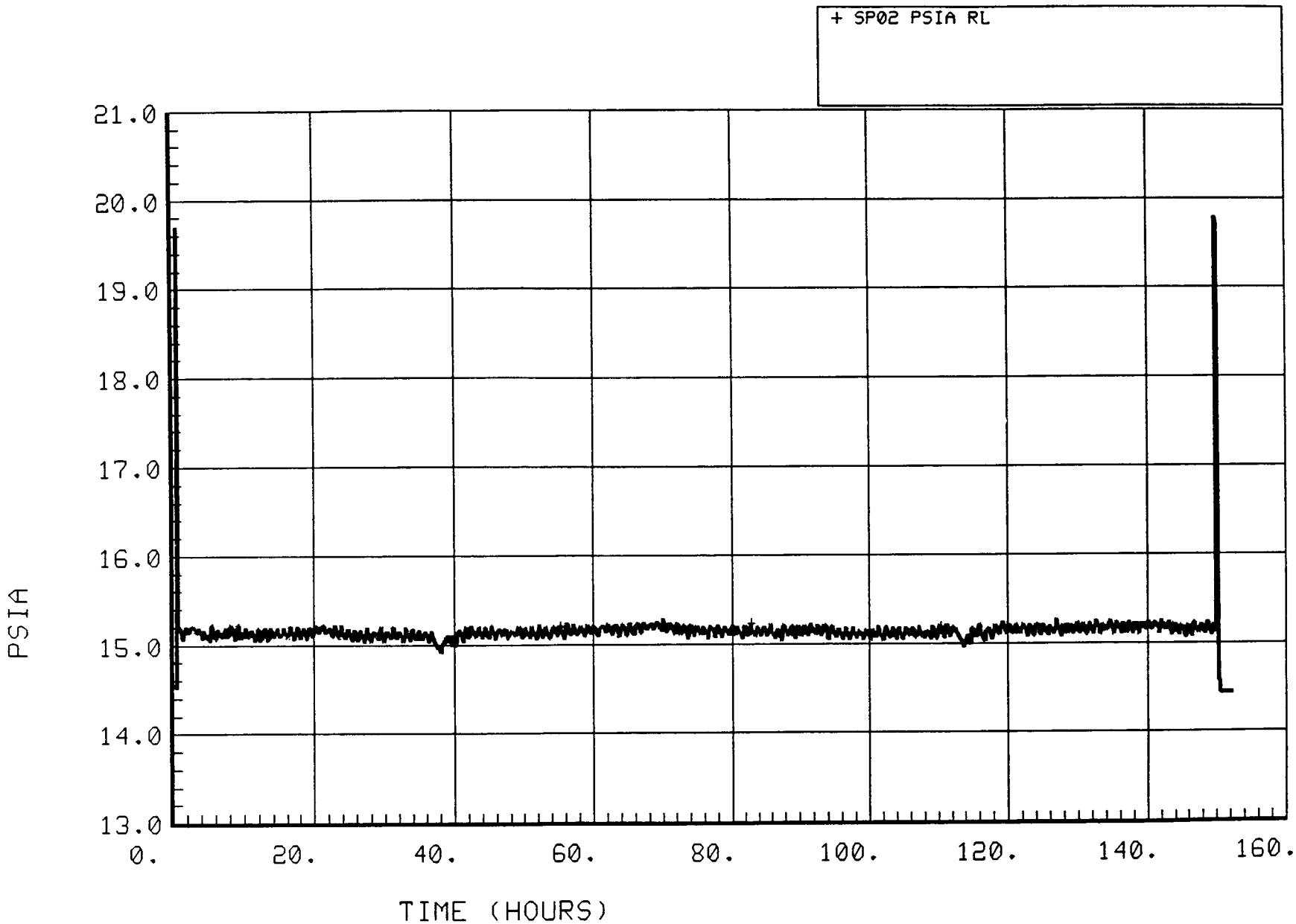

Figure 5-4.13. Gas outlet pressure (SP02).

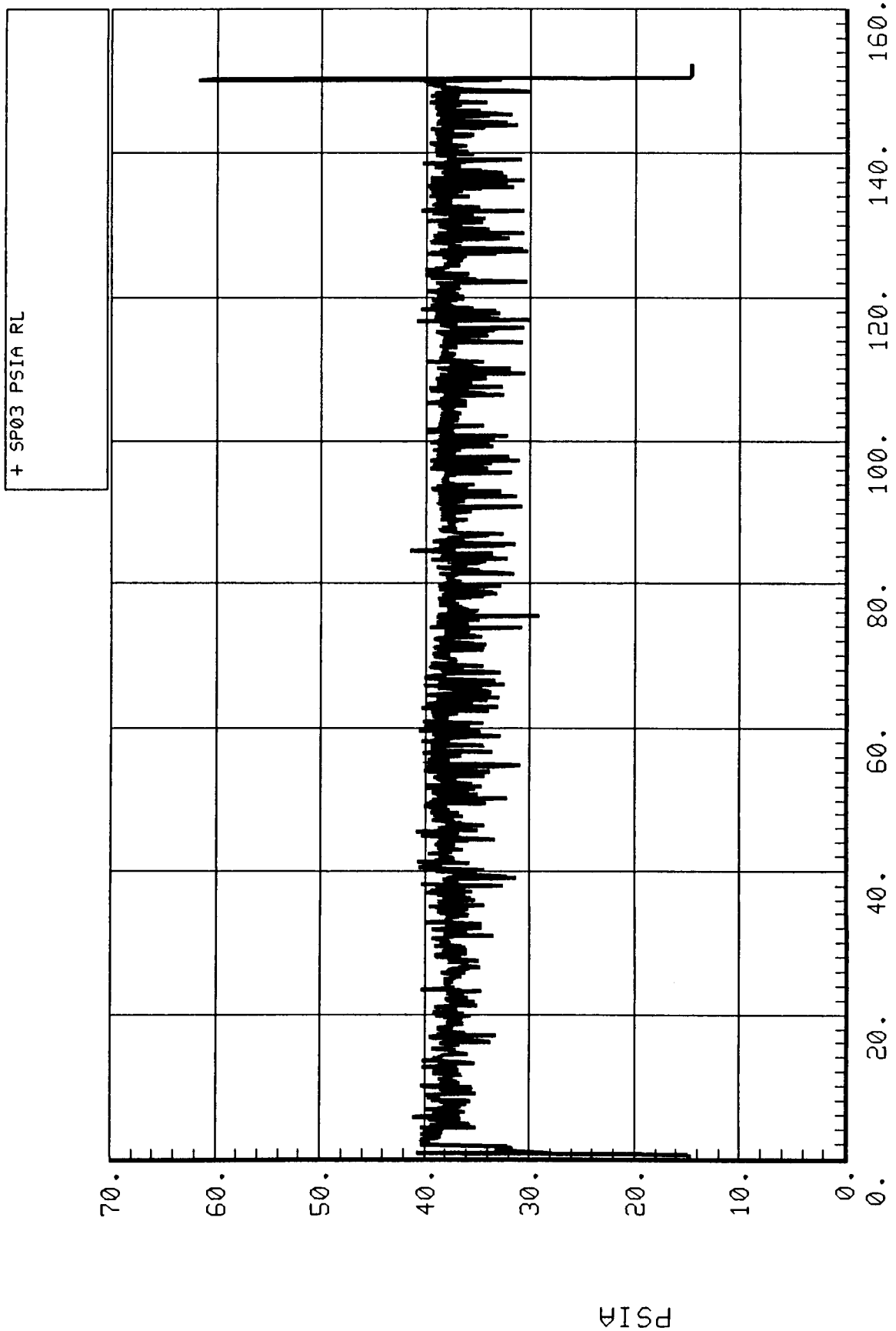

Figure 5-4.14. Water outlet pressure (SP03).

the relief valve at the water outlet which keeps the pressure at 38 psia and prevents any gas from exiting with the water can be seen throughout the test.

5.4.2.2.14 Fan Differential Pressure (SP04)

The differential pressure across the fan (Fig. 5-4.15) which pulls cooling air through the reactor and condensing heat exchanger was approximately 0.82 in. H_2O. The fan provides about 25 cfm of air flow.

5.4.2.2.15 Water Separator and Fan Currents (SI01 and SI02)

Plots of water separator and fan current (Figs. 5-4.16 and 5-4.17) show that these components operated continuously through the test.

5.4.2.2.16 Reactor Bed Heater Currents (SI03 and SI04)

The reactor bed heater currents are shown in Figures 5-4.18 and 5-4.19. These plots represent the two heater currents and have been expanded to show only the first 10 hr of the test. The reactor heaters were on approximately 10 min at startup to heat the bed to initiate the reaction, then remained off for the rest of the test as the normal heat of reaction was enough to sustain itself.

5.4.2.2.17 Combustible Gas Sensors (SG01 to SG03)

The three Sabatier combustible gas sensors are shown in Figures 5-4.20 through 5-4.22. These sensors monitor the level of combustible gas detected around the subsystem. It appears that SG02 is out of calibration as it reported negative values. None of the levels detected neared the shutdown value of 50 percent of the lower explosion limit.

5.4.2.2.18 Outlet Vent Flowrate (FF03)

The Sabatier outlet vent flowrate is shown in Figure 5-4.23. The installation of the coalescent filter upstream of the exit gas flowmeter served to correct the problem discovered in the Simplified Integrated Test in which carryover water in the gas stream condensed in the flowmeter and caused erroneous readings. The flowmeter read approximately 1.2 slpm throughout the test with the exception of three small disturbances corresponding to the Molecular Sieve shutdown at 38 hr, the Molecular Sieve heater failure at 114 hr, and gas sampling at 116.5 hr.

5.4.2.2.19 Exit Gas Temperature (FT03)

The temperature of the exit gas from the Sabatier (Fig. 5-4.24) to facility vent ranged from about 72° to 83°F with cycling due to ambient air temperature changes throughout the day.

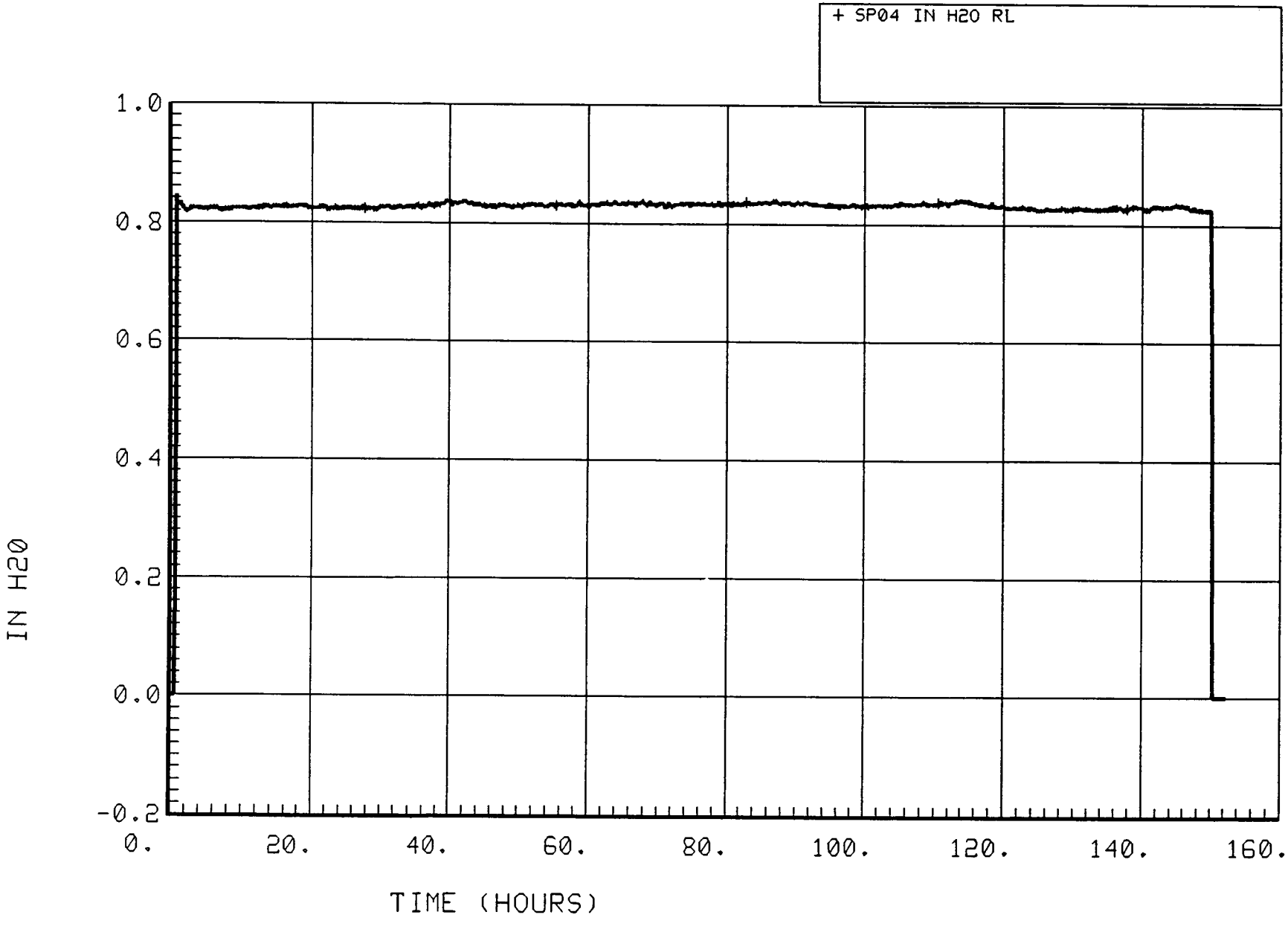

Figure 5-4.15. Fan differential pressure (SP04).

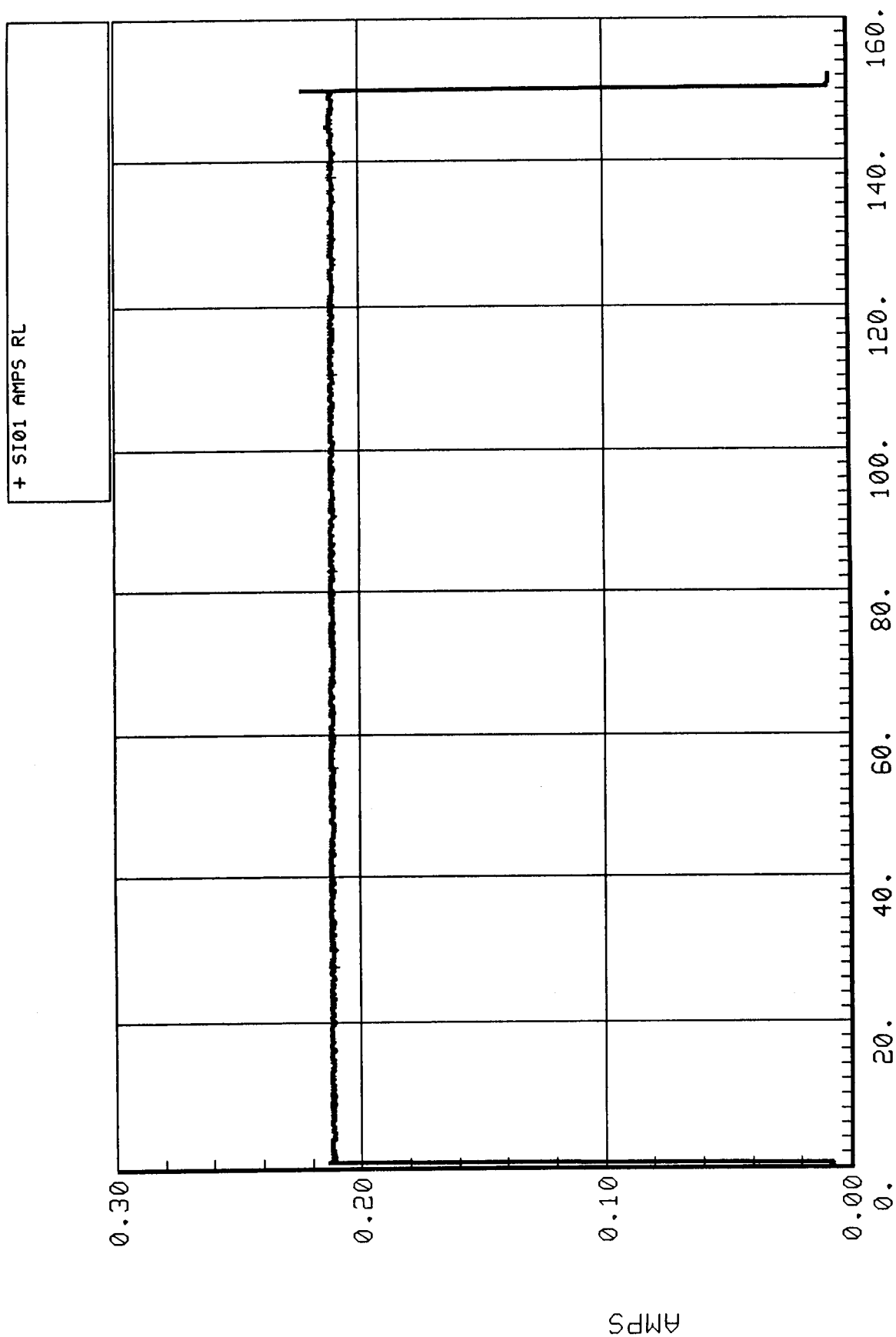

Figure 5-4.16. Water separator current (SI01).

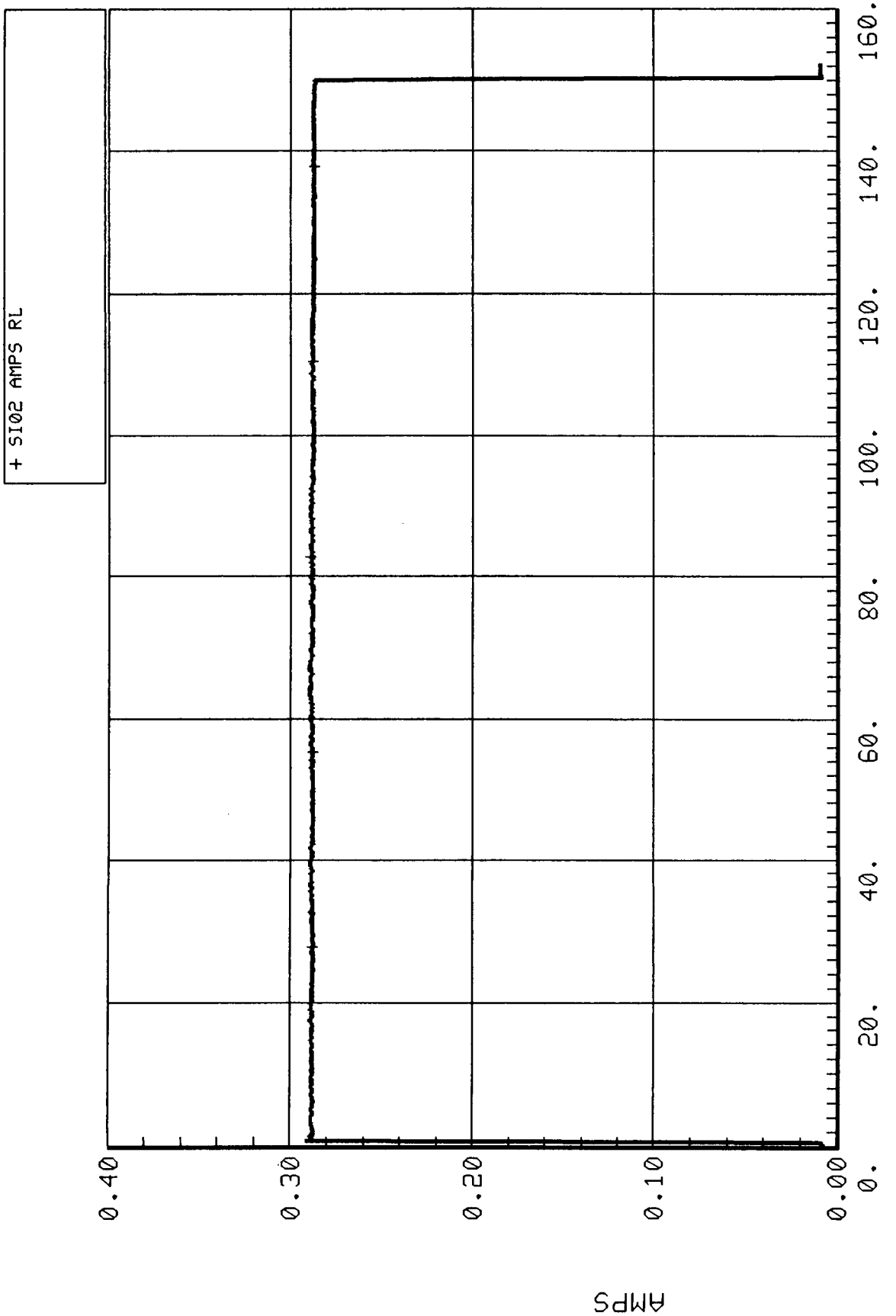

Figure 5-4.17. Fan current (SI02).

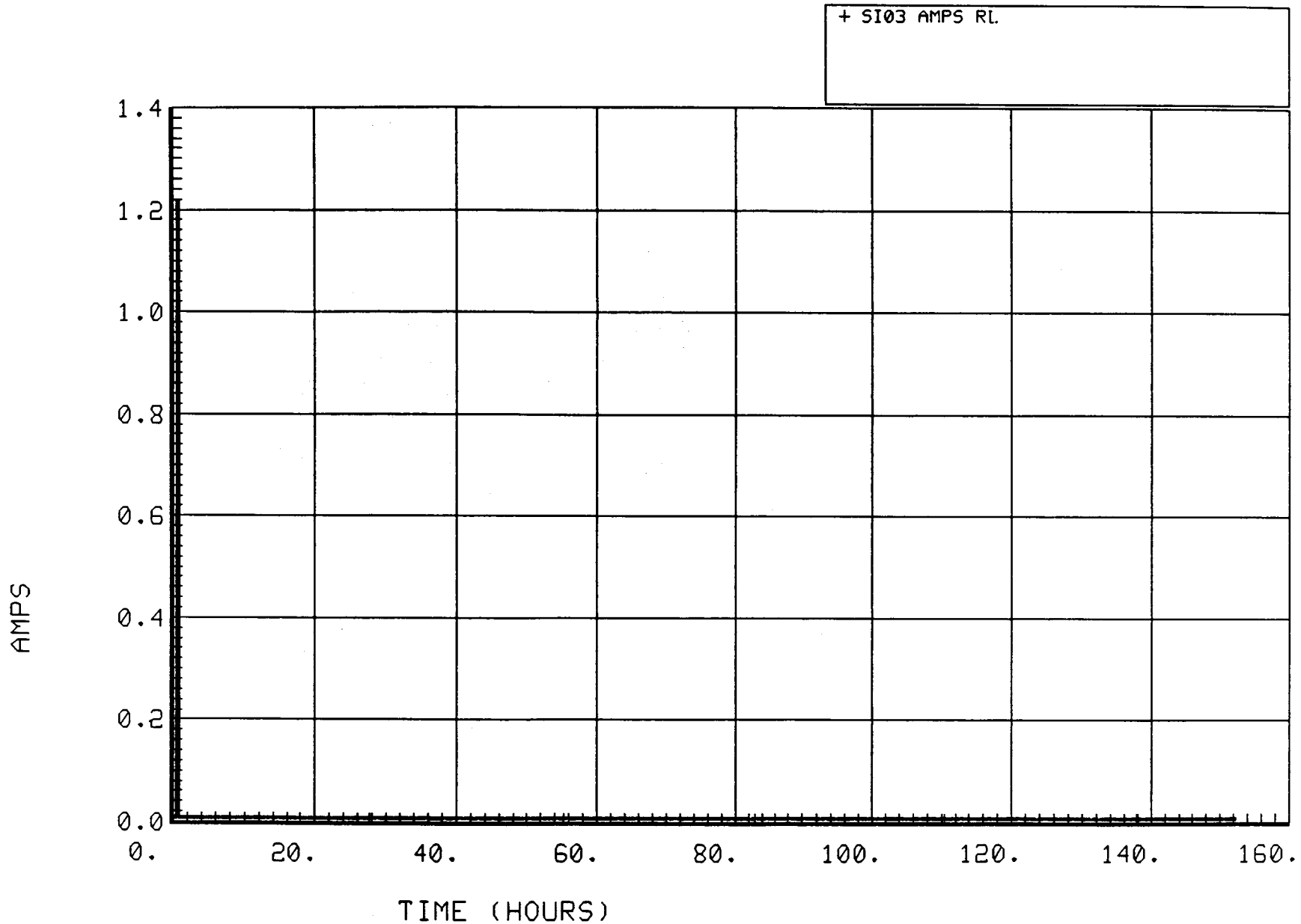

Figure 5-4.18. Reactor heater bed current (SI03).

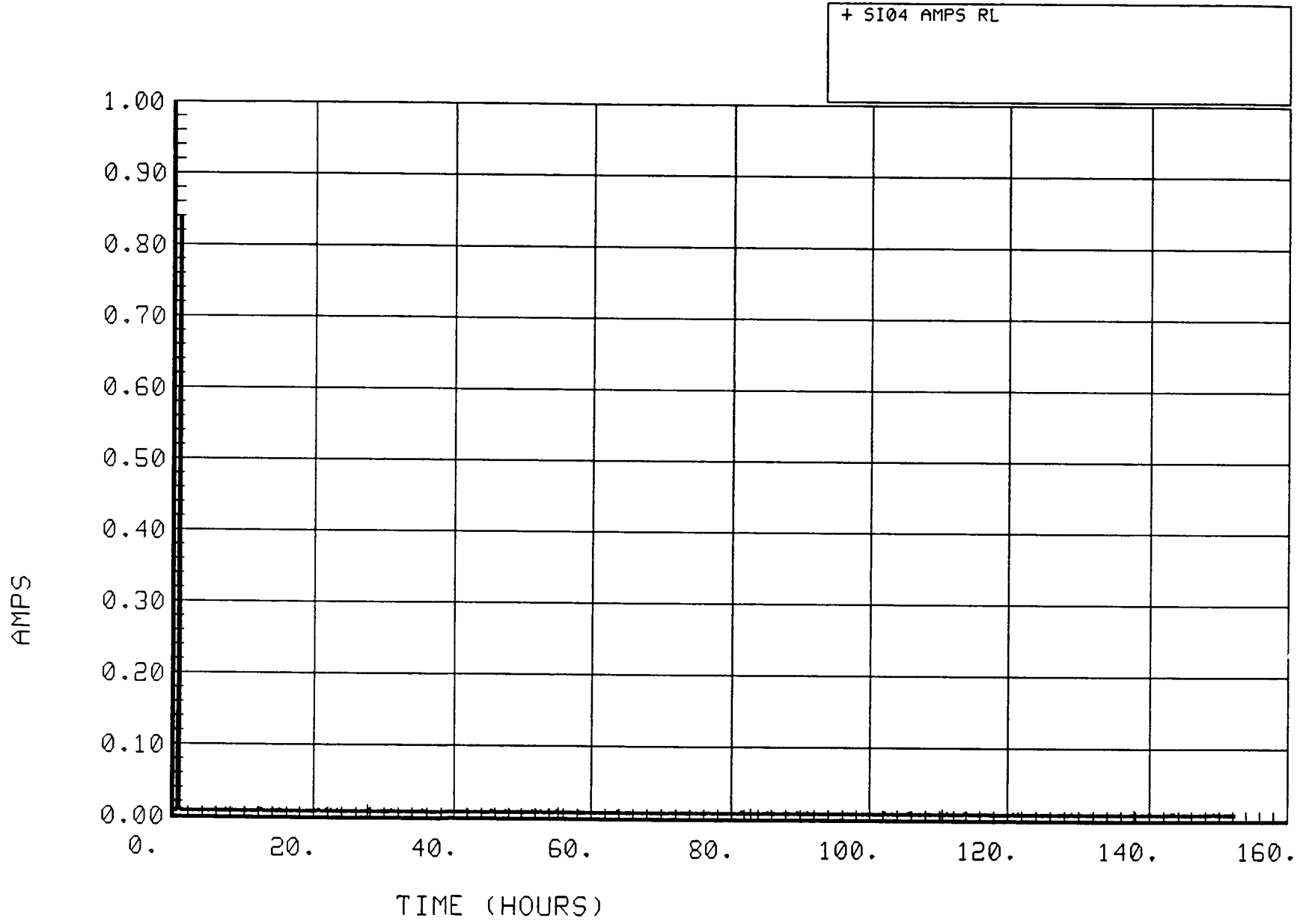

Figure 5-4.19. Reactor heater bed current (SI04).

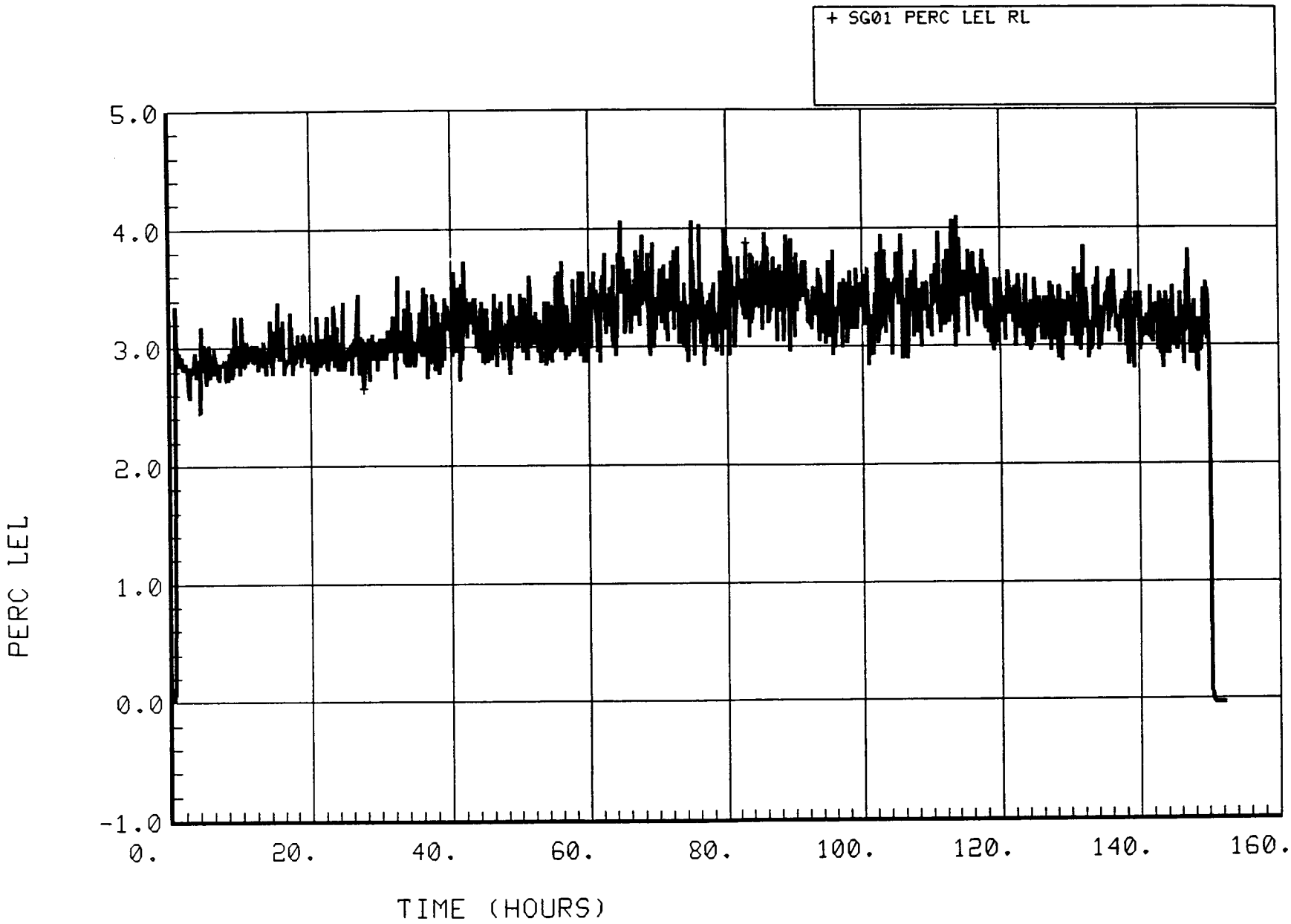

Figure 5-4.20. Combustible gas sensor No. 1 (SG01).

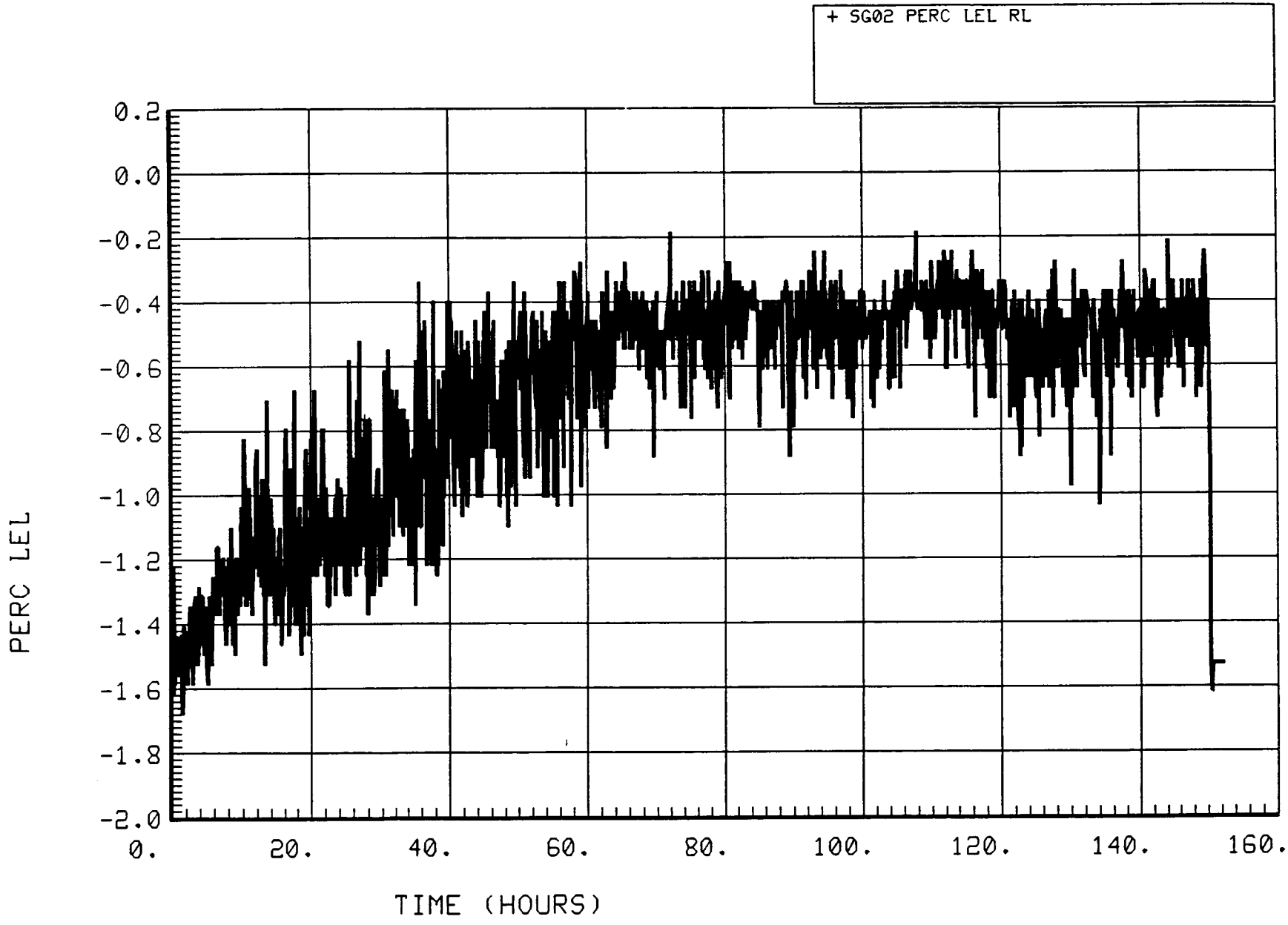

Figure 5-4.21. Combustible gas sensor No. 2 (SG02).

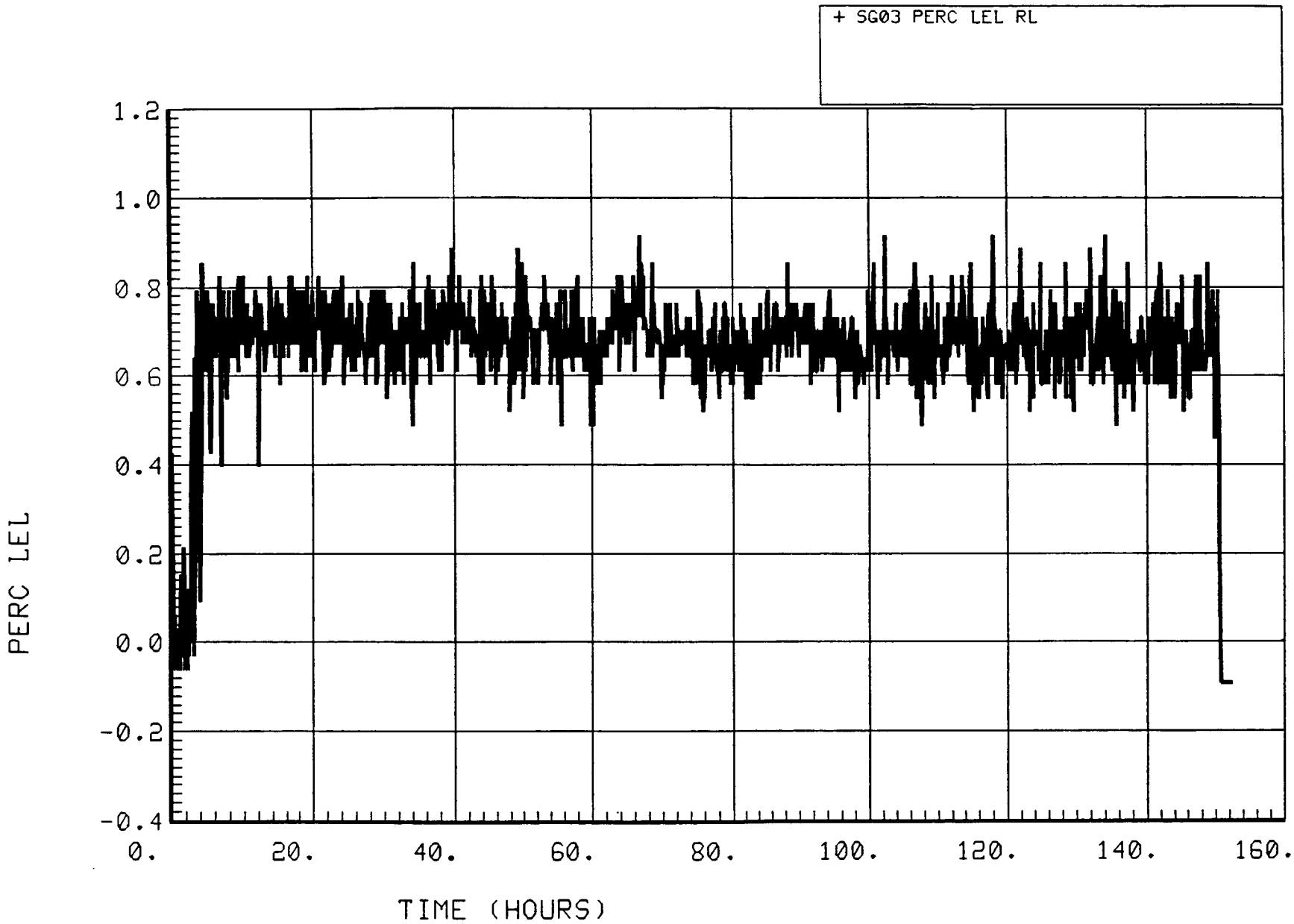

Figure 5-4.22. Combustible gas sensor No. 3 (SG03).

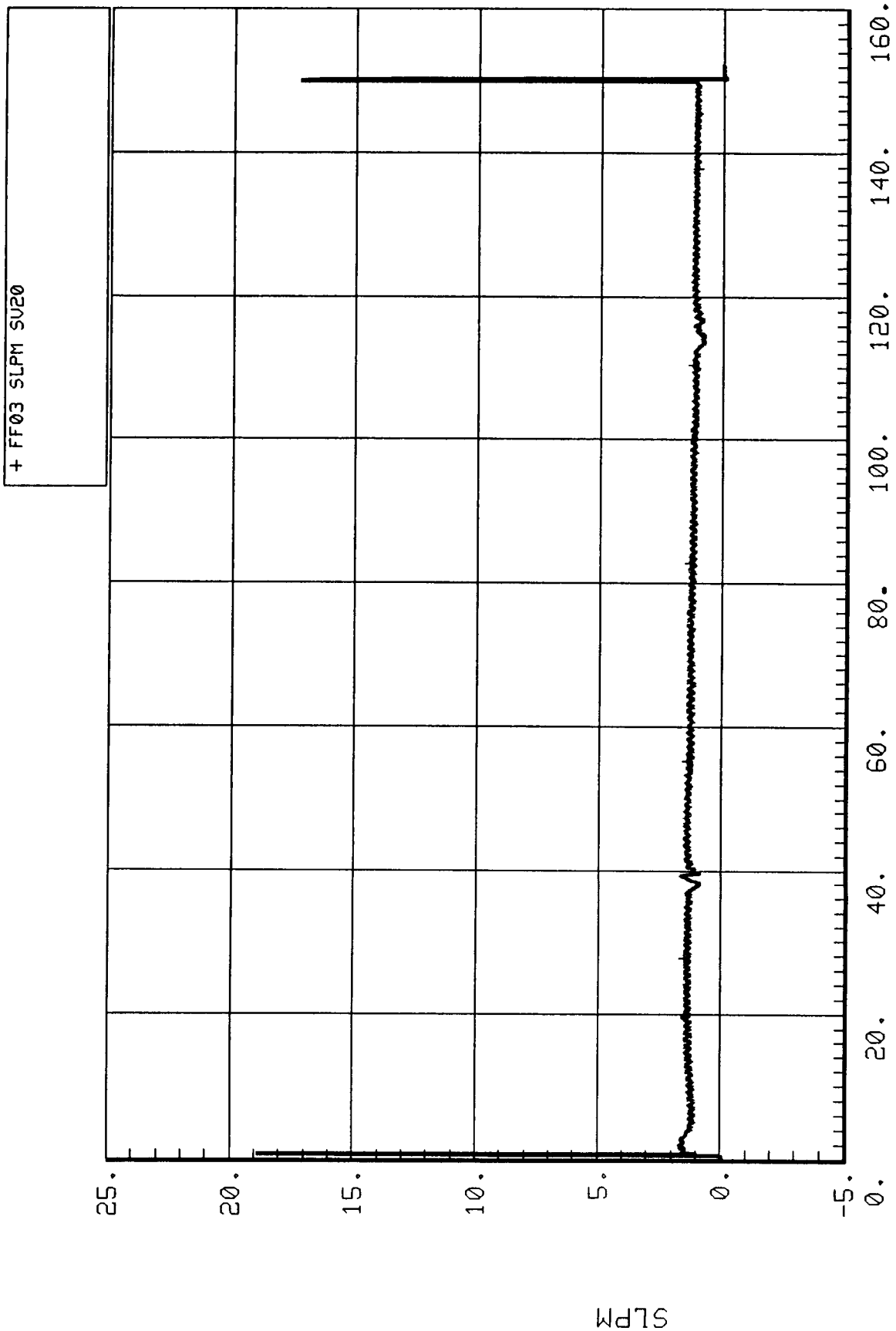

Figure 5-4.23. Sabatier outlet vent flowrate (FF03).

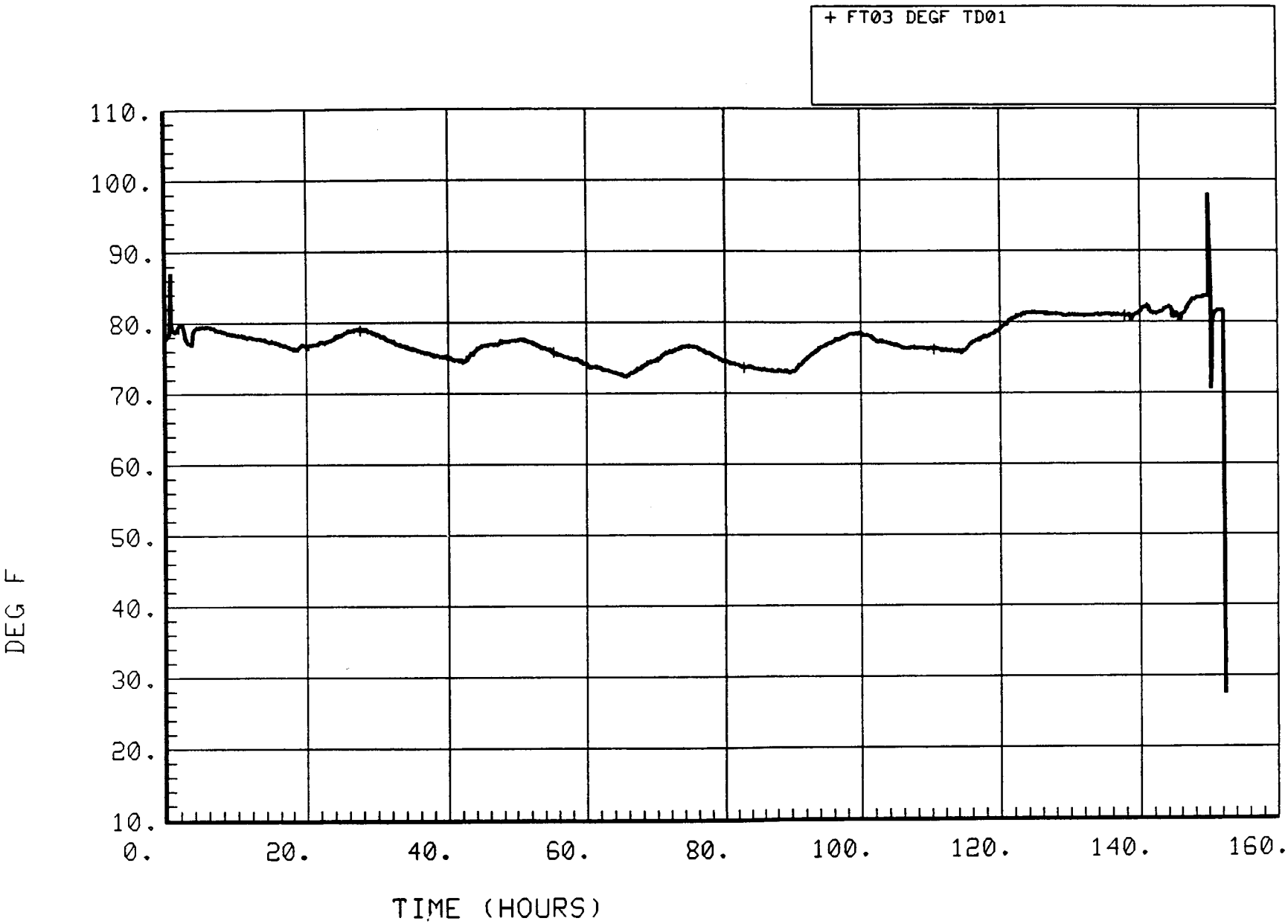

Figure 5-4.24. Exit gas temperature (FT03).

5.4.3 Recommendations/Lessons Learned

The Sabatier operated normally throughout the direction of the test and all measurements were within normal operating ranges with the exception of reactor bed temperature sensor ST03. This sensor is currently undergoing checkout and may require replacement. A more accurate water balance was attained during this test as well as a measurement of reaction conversion efficiency through sampling.

6.0 SIMULATOR BULK AIR MEASUREMENTS

A number of measurements were utilized to track bulk simulator parameters such as temperature, total pressure, and partial pressure of oxygen. Discussions for each of these measurements are included below.

6.1 Simulator Bulk Air Temperature (FT16)

The simulator bulk air temperature (shown in Fig 6-1) was maintained between 70° and 78°F during the EMCT. The five large variations are due to the day/night temperature variation of coolant water from the chiller. The secondary variations which appear to occur on hourly intervals are due to the cyclic behavior of the Molecular Sieve subsystem.

6.2 Simulator Total Pressure (FP07)

The simulator total pressure (shown in Fig. 6-2) varied between 14.38 and 14.52 psia during the EMCT. No active pressure control was used during the EMCT other than to add nitrogen at a constant rate for leakage makeup and a relief valve to vent the simulator for internal to ambient delta pressures greater than 3 mmHg. The large variations in pressure are due to variations in the external barometric pressure and to a lesser extent the cyclical nature of the simulator internal temperature. The small hourly variations are also temperature dependent.

6.3 Simulator to Ambient Differential Pressure (FP08)

The simulator to ambient differential pressure is shown in Figure 6-3. One of the goals of the EMCT was to maintain a positive differential pressure so that leakage would always be out of the simulator and not input. It was projected that a constant nitrogen addition rate of 3 lb/day or less would be enough to maintain the simulator total pressure above ambient. The simulator also had a relief valve set at approximately 3 mmHg above ambient in case of an over-pressure situation. The maximum measured delta pressure was 3.50 mmHg and delta pressures in excess of 3 mmHg were recorded three times during the test indicating that the relief valve vented three times.

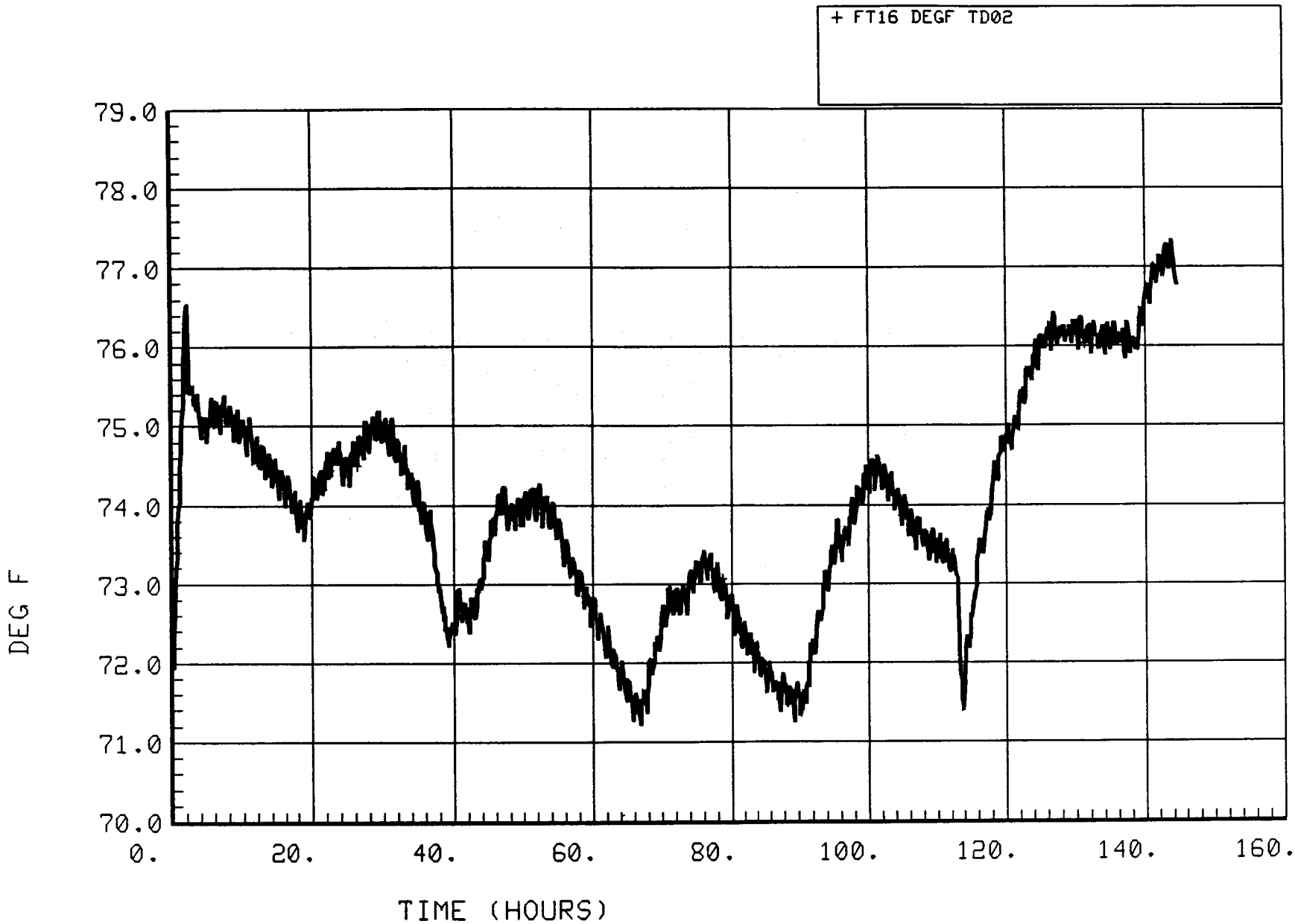

Figure 6-1. Simulator bulk air temperature (FT16).

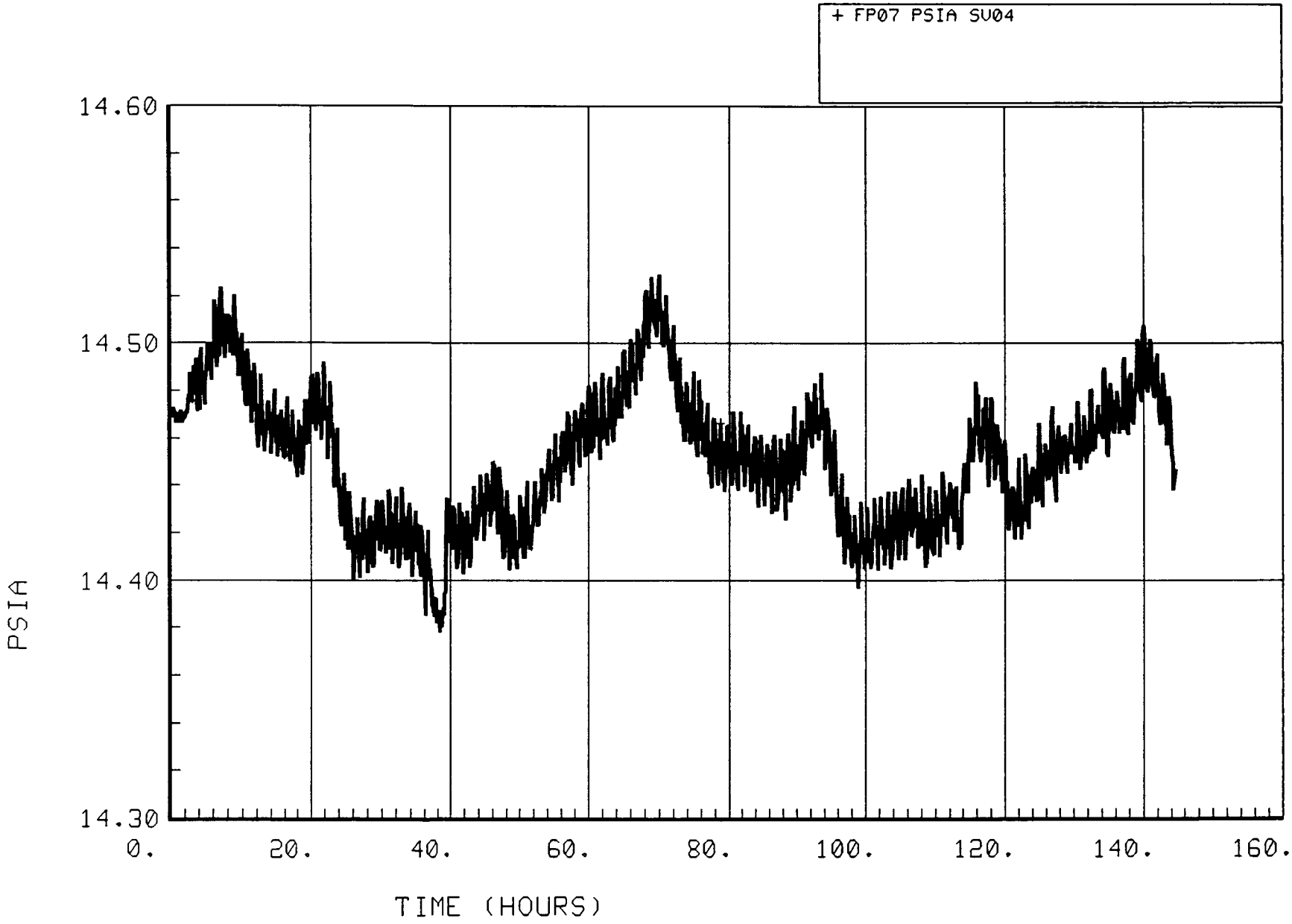

Figure 6-2. Simulator total pressure (FP07).

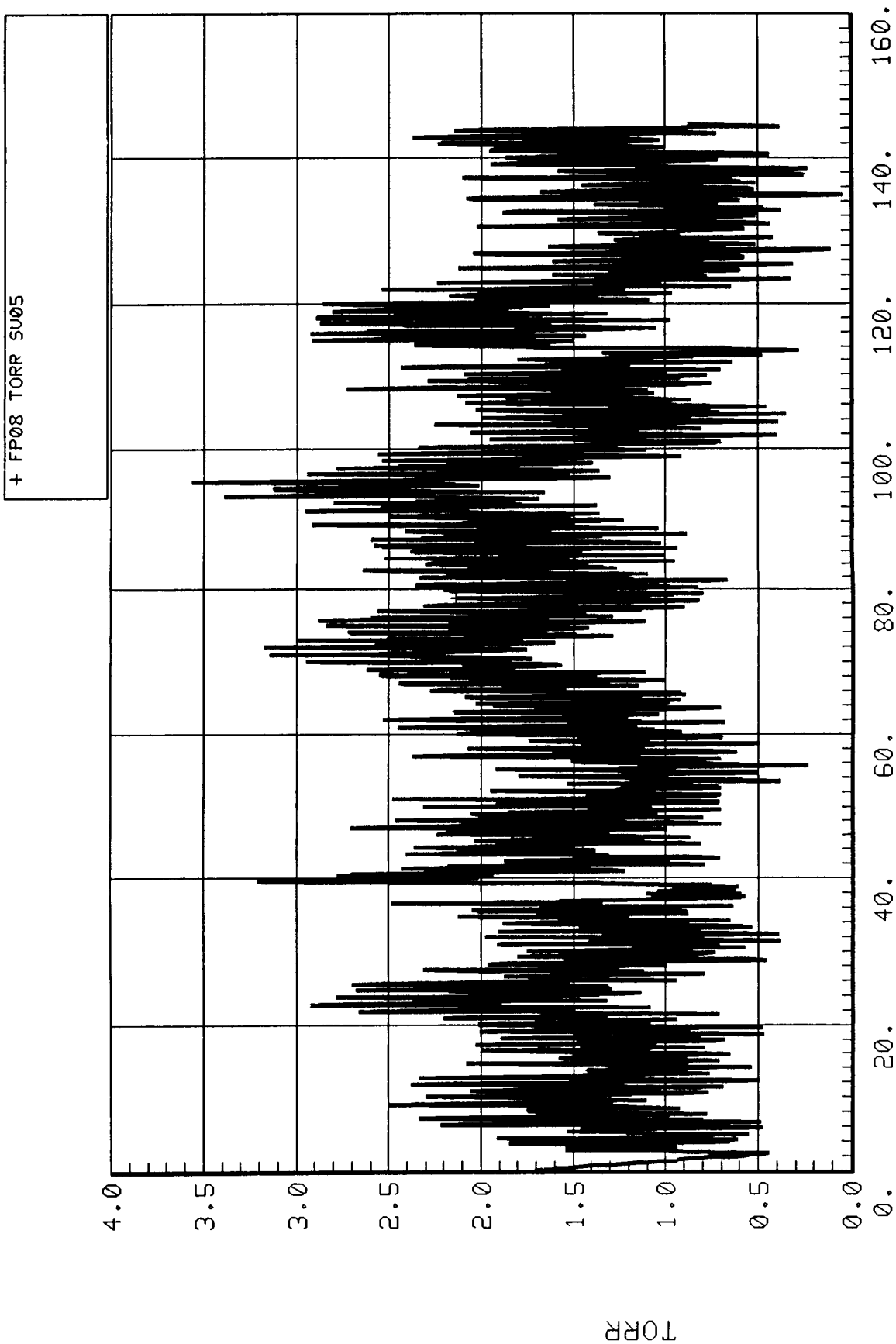

Figure 6-3. Simulator to ambient differential pressure (FP08).

6.4 External Barometric Pressure

No actual barometric pressure measurement was recorded during the EMCT, but a plot of barometric pressure computed from the simulator total and differential pressures is provided in Figure 6-4. Several steep increases and declines are evident in the plot. Although no weather records were kept during the EMCT, these transitions may indicate the passage of a weather front.

6.5 Simulator Bulk O_2 Percentage (FP09)

A plot of the simulator bulk oxygen pecentage is shown in Figure 6-5. The bulk air O_2 percentage was 22.8 percent at the beginning of the test and declined steadily to 20.9 percent by the conclusion of the test. At the beginning of the test, the O_2 concentrator was set to remove oxygen at a three-crew-person level. After several hours of steep decline in oxygen partial pressure, it was decided to try to adjust the O_2 consumption rate for a constant oxygen partial pressure. This was not successful, although the oxygen decline did decrease for the remainder of the test. The oxygen deficit could be explained in any of the following ways: (1) the SFE was producing oxygen at somewhere below a three-crew-person level, (2) simulator leakage, or (3) atmosphere lost during TGA sampling.

6.6 Simulator Bulk CO_2 Partial Pressure (FP10)

The simulator bulk carbon dioxide partial pressure is shown in Figure 6-6. The two Molecular Sieve failures at 39:19 hr and 113:50 hr are evident in the plot of carbon dioxide partial pressure. During these times, the Molecular Sieve's capability to remove carbon dioxide was diminished resulting in an upward spike of carbon dioxide partial pressure. Once Molecular Sieve operation was restored, the carbon dioxide partial pressure would decrease and eventually reach a steady state value. After the first anomaly at 39:19 hr, it is evident that the partial pressure did not fully return to the initial steady state value. This is probably due to the decreased efficiency of the Molecular Sieve due to manual mode cycling as a result of the first anomaly.

6.7 Simulator Dew Point (FD01)

The simulator bulk dew point is shown in Figure 6-7. Aside from a downward decrease in dewpoint at approximately 39 hr, the simulator dewpoint was maintained between 44.0° and 47.0°F during the test. The downward spike corresponds with the first Molecular Sieve failure. During this failure the Molecular Sieve remained in a mode which did not allow the adsorbing desiccant bed to switch over to the desorb mode. The bed continued to trap moisture forcing the simulator dewpoint down. Once the Molecular Sieve was manally advanced between modes, the simulator dewpoint returned to normal, indicating that the saturated desiccant bed readily desorbed the trapped moisture.

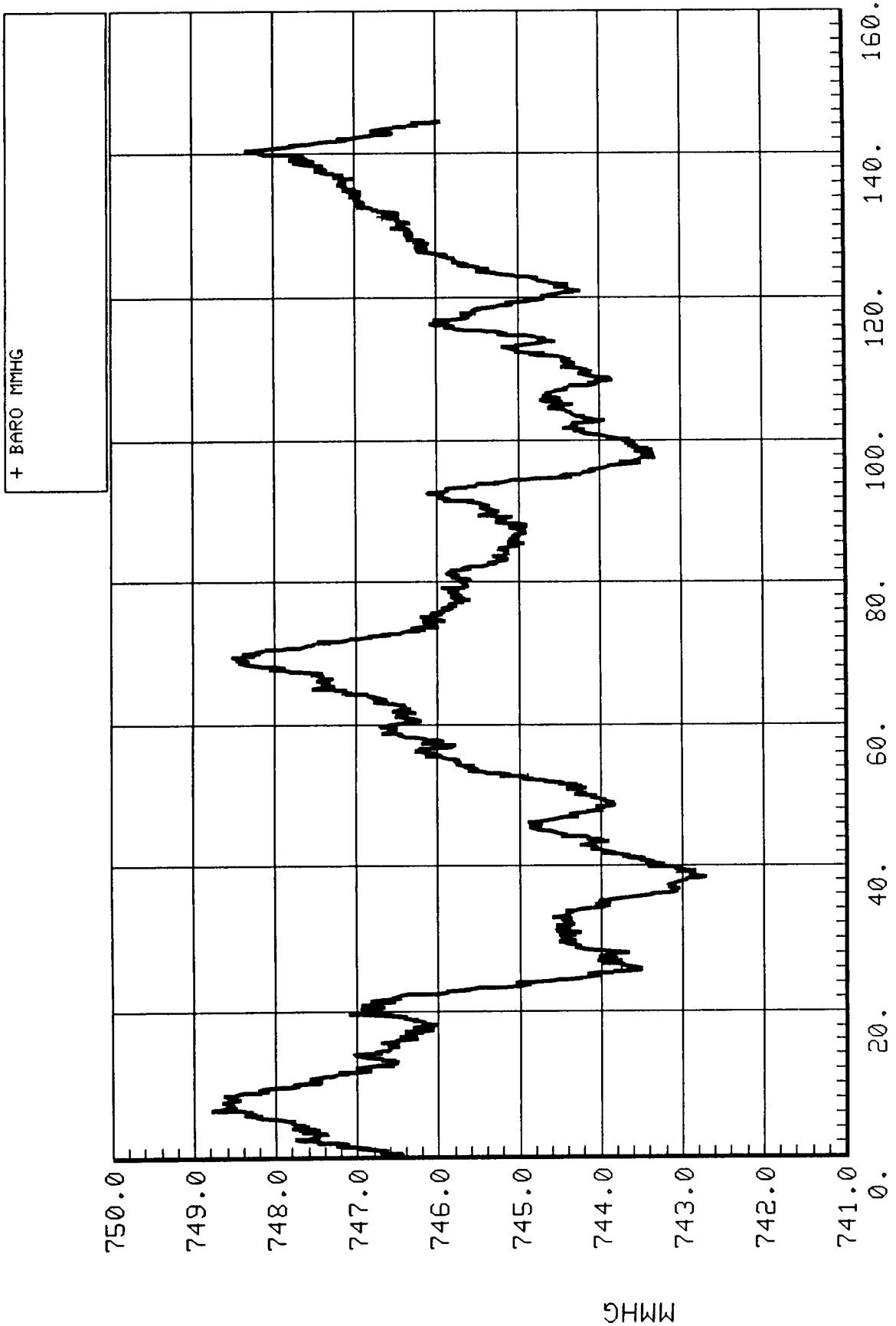

Figure 6-4. External barometric pressure (computed).

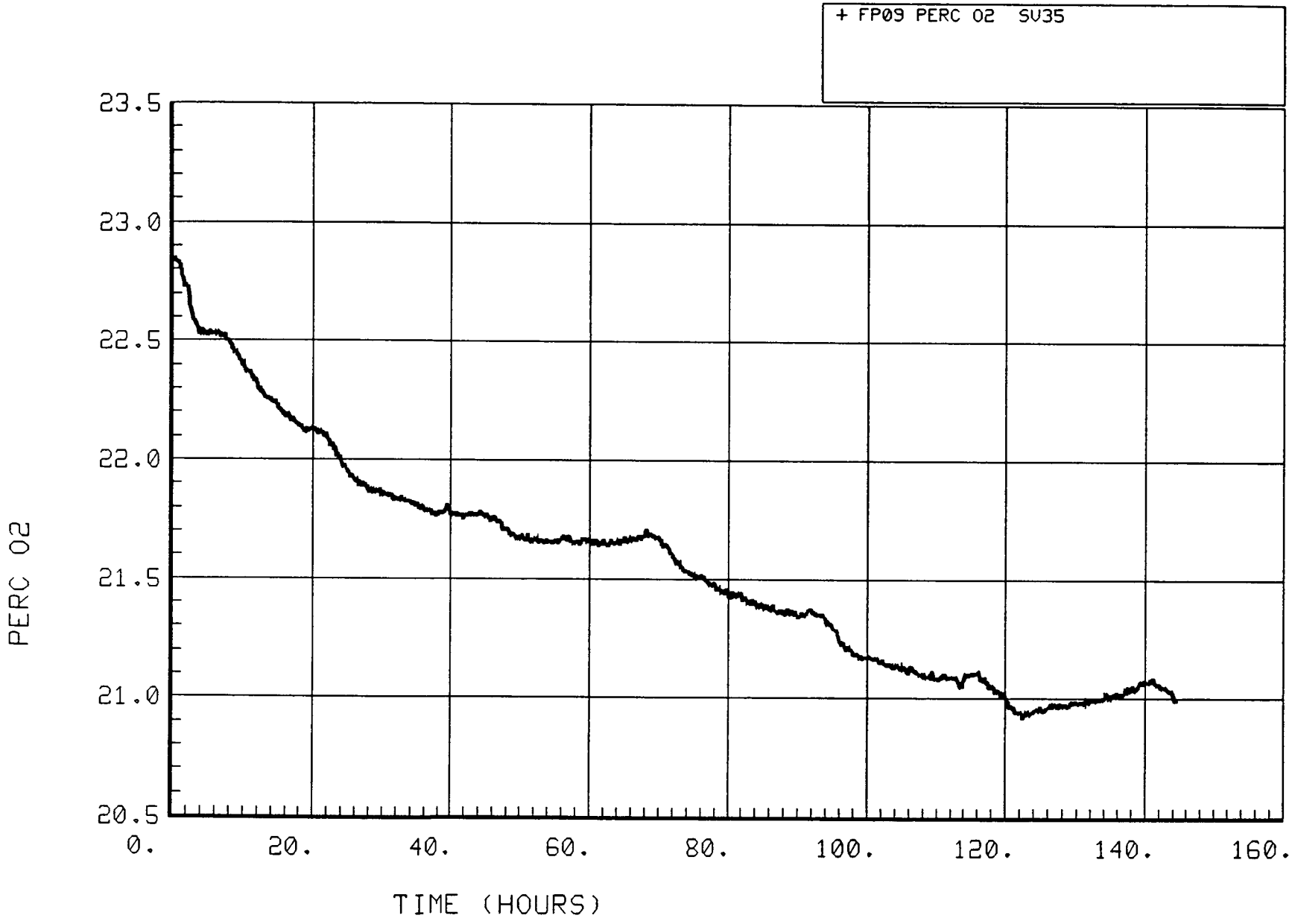

Figure 6-5. Simulator oxygen percentage (FP09).

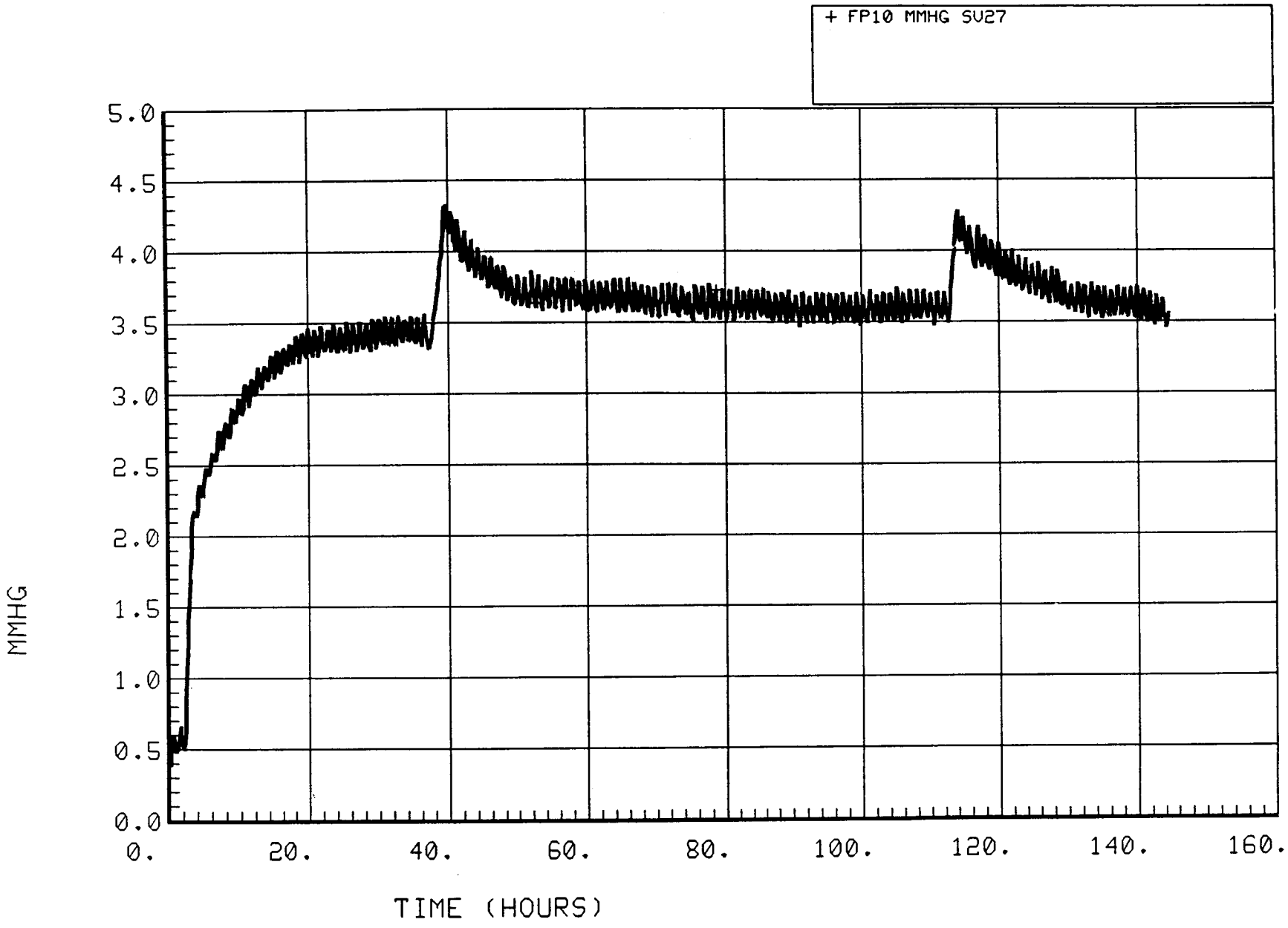

Figure 6-6. Simulator CO_2 partial pressure (FP10).

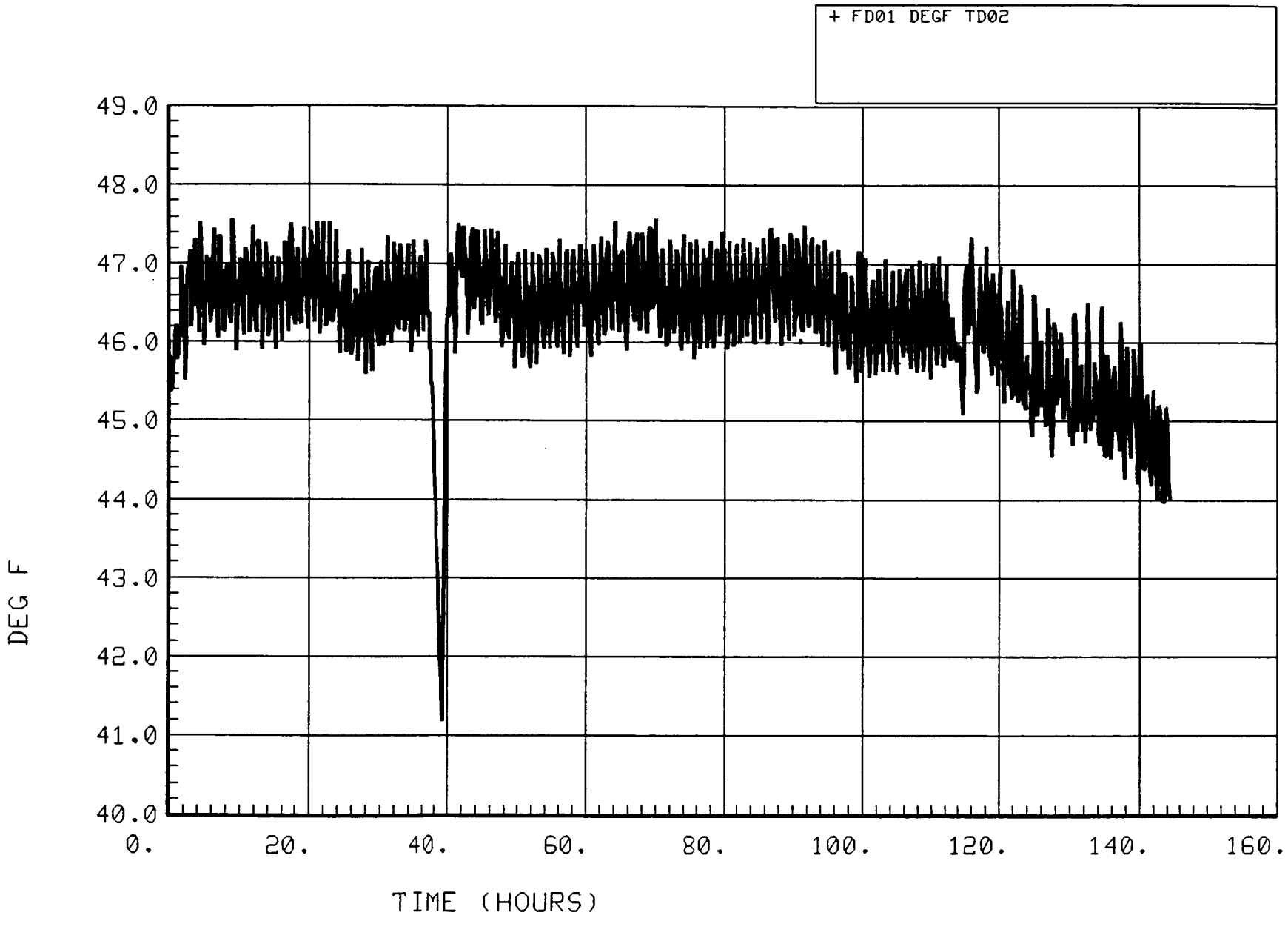

Figure 6-7. Simulator dewpoint (FD01).

7.0 SYSTEM POWER

Neither the phase II ECLS system or subsystems were specifically instrumented to measure power consumption. However, it is possible from the EMCT data to make several observations about system and subsystem power consumption. Discussions regarding total system heat rejection, SFE efficiency, and TIMES TER power are contained in the following sections.

7.1 ECLS Heat Load

Plots of the total module simulator heat load and the total heat load minus any contribution from the ventilation fans are given in Figure 7-1. These loads were computed from temperature measurements located upstream and downstream of the fan/HX packages and an assumed air flow rate obtained from vendor data on the ventilation fans. As seen in both plots, the total airborne heat load ranged from approximately 4200 W to 6200 W. The fan contribution was small and averaged several hundred watts throughout the test. The load is assumed to be predominately sensible since no moisture was added during the EMCT and, aside from Molecular Sieve anomalies, the dewpoint was steady state. The large undulations in the heat load are due to day/night variations of the coolant supply temperature to the simulator heat exchangers. The higher frequency, almost hourly, variations are caused by heat leak from the Molecular Sieve desorption cycles when heater power and a partial vacuum is applied to the carbon dioxide sorbent beds. No other subsystem or equipment item in the simulator would have a cyclic heat rejection profile of this magnitude.

7.2 SFE Power

The power efficiency of an electrolysis process is the product of the current efficiency and the voltage efficiency. Current efficiency is the ratio of the theoretical current required to produce a given amount of oxygen (as determined by Faraday's law) to the actual current required. The SFE operates at a relatively low delta pressure across its H_2/O_2 membrane providing little driving force for either the hydrogen or oxygen to diffuse across the membrane and recombine into water. If much recombination takes place, the overall efficiency of the process is lowered since the recombined water must be "re-electrolyzed" into hydrogen and oxygen. Based upon the low delta pressure and an operating pressure of 180 psia, it is assumed that the SFE current efficiency is 100 percent. From Faraday's law it can be calculated that the current required to produce 5.5 lbm/day of O_2 is 348 A.

The voltage efficiency is the ratio of the thermal neutral voltage (that voltage at which electrolysis occurs with no waste heat generation) to the actual cell voltage. The average cell voltage for the SFE during the EMCT was 1.65 V. The voltage efficiency and the overall power efficiency (current efficiency = 100 percent) would be equal to 1.48/1.65 or 89.7 percent. The average power required for the electrolysis during the EMCT was 348 A x 1.65 V or 574.2 W. The theoretical power requirement would be 348 A x 1.48 V or 515.0 W.

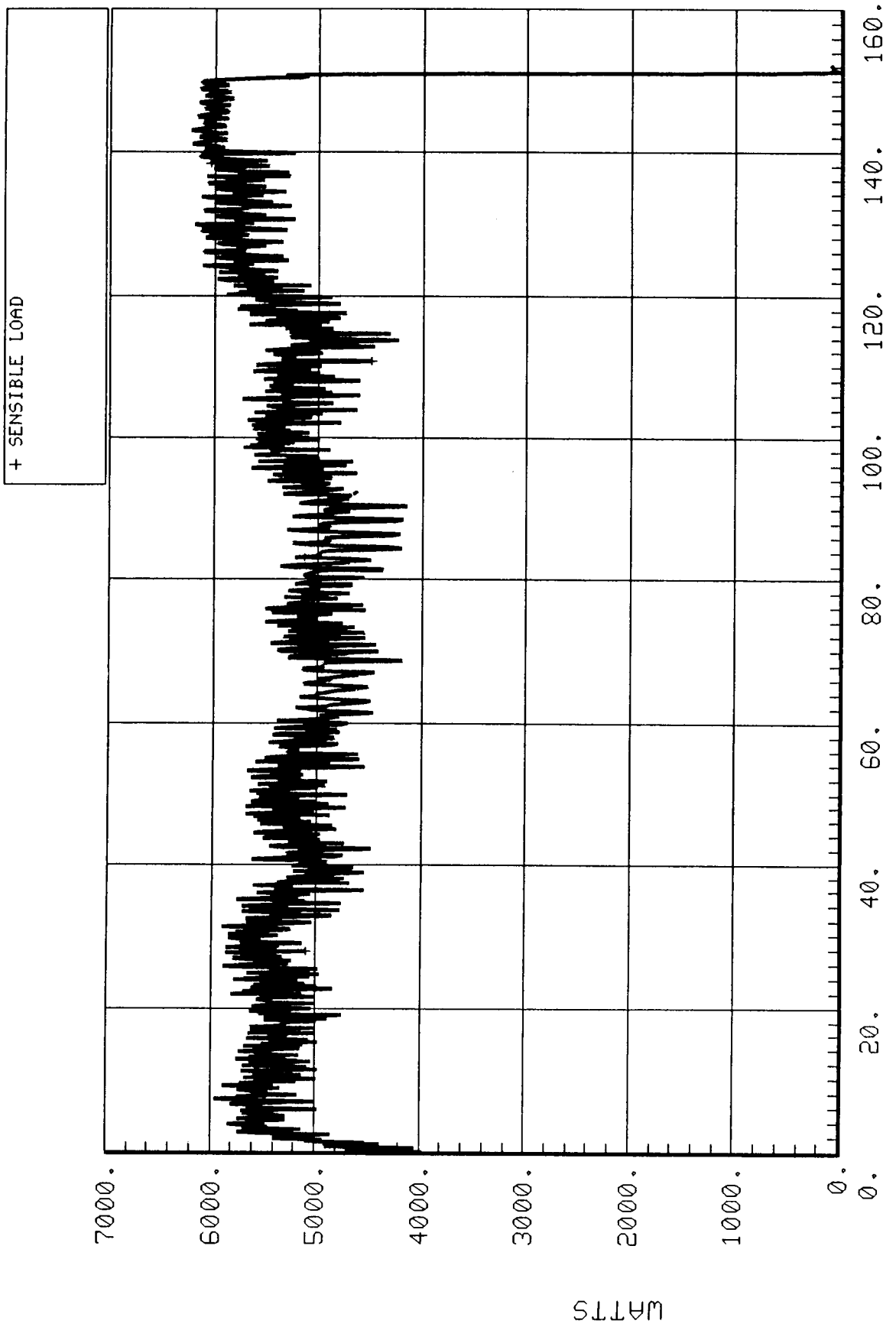

Figure 7-1. Module simulator heat load.

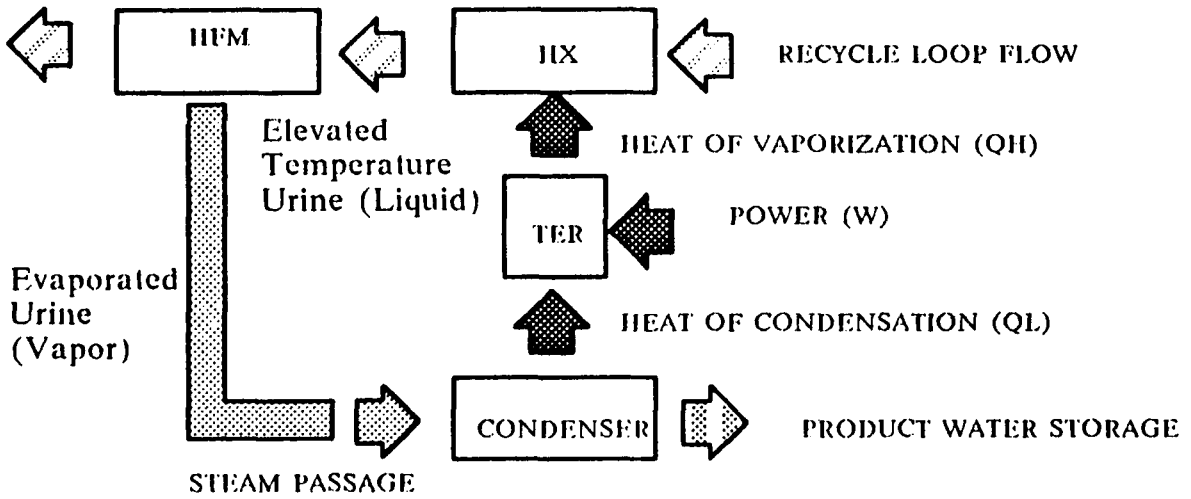

Figure 7-3.1. TIMES process diagram.

7.3 TIMES TER Power

The TIMES Thermoelectric Regenerator (TER) is a classical heat pump device, requiring a power input to pump heat from a low temperature source to a higher temperature source (Fig. 7.3-1). In this application, the cold side of the thermoelectric devices is the TIMES steam passage where evaporated urine is condensed as product water. Since the evaporated urine is releasing only the heat of condensation, the temperature of the cold side of the thermoelectrics is set by the steam reference pressure (usually 1.8 to 2.0 psia). The recovered heat is used to elevate the temperature of the urine recycle loop prior to evaporation of the urine in a downstream component (HFM). During EMCT, TER power was not measured directly, but has been computed from available voltage and current measurements made on the TER. Also, the TIMES was operated in a batch mode, processing urine for only 3 to 4 hr of each 24-hr period. A plot of the computed TER power is provided in Figure 7.3-2. The plot is for the first TIMES cycle of the test which corresponds with the first 3.4 hr of the test. As shown in the plot, the TER input power ranged between 190 and 230 W. The transient from 192 W to 227 W during the interval from 0.9 hr to 1.2 hr is assumed to be a startup transient as recycle loop temperatures had not yet reached nominal values and the steam reference pressure had not yet stabilized.

A useful indicator of the TIMES performance is the specific energy which is defined as the ratio of power input to water produced and is often expressed in W-hr/lbm. Using data after the transient, the TER power input averaged 225 W. Also, during the period from 1.2 to 3.35 hr (after the transient), the TIMES processed 7.20 lb of urine which translates to an average processing rate of 3.35 lbm/hr [7.20/(3.35 to 1.2)]. Using the average TER power input and processing rate, the average specific energy for the TIMES (TER power only) during the first operational cycle was computed to be 67.2 W-hr/lbm. For comparison, the theoretical specific energy of a distillation process operating at the same pressure as the TIMES with no recovery of the heat of condensation would be 300 W-hr/lbm (heat of vaporization of water at 1.9 psia is 300 W-hr/lbm) clearly showing the advantage gained by waste heat recovery. It should be noted that the specific energy computed for the TIMES in this case was based only on the TER input power and not the total subsystem power.

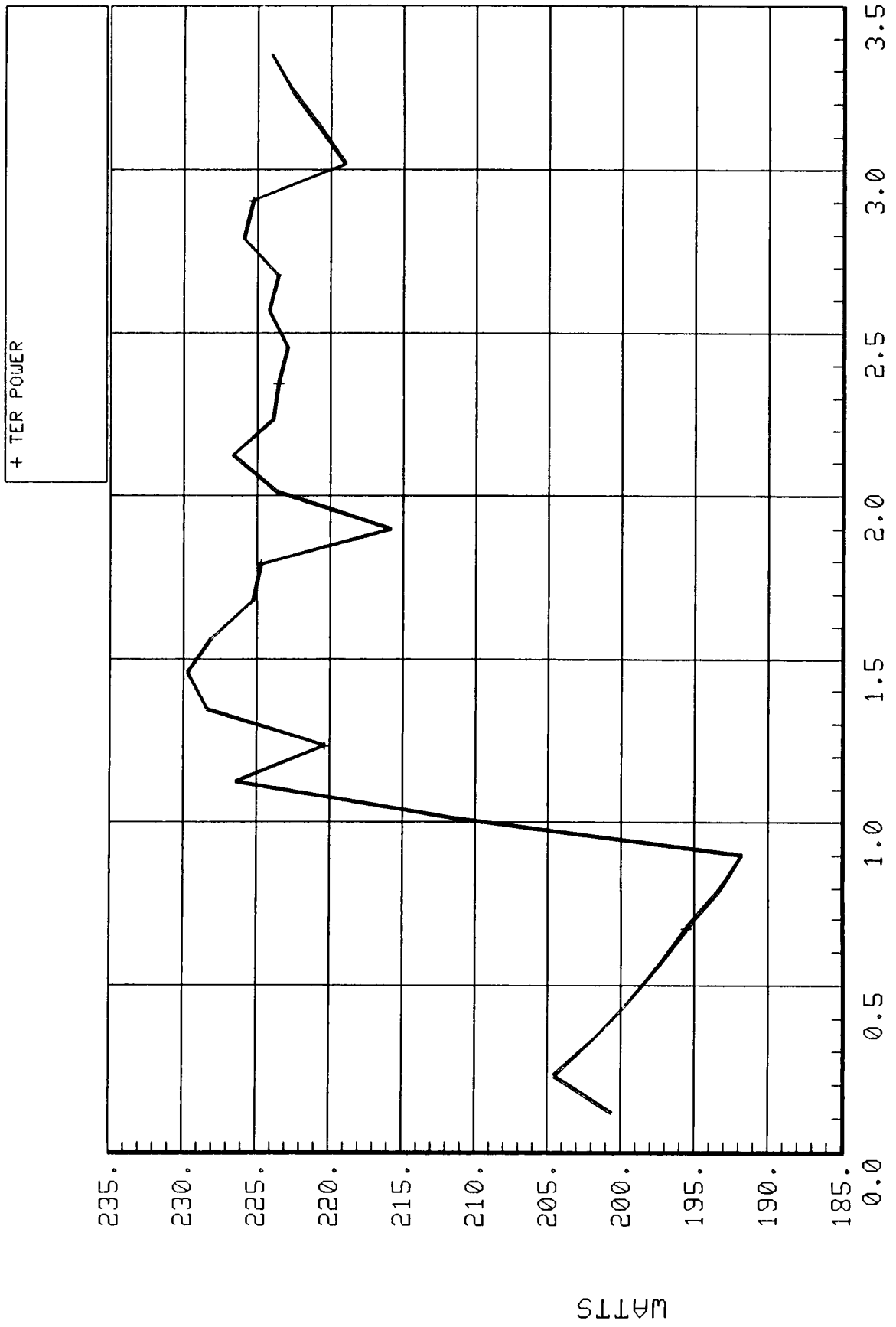

Figure 7-3.2. ThermoElec regen power (computed).

8.0 SYSTEM MASS BALANCE

A system level mass balance for the EMCT was reconstructed using various system flow and dewpoint measurements, tank scales, and lab analyses. The mass balance is shown in Figure 8-1. It was possible to estimate the total mass flow in and out of each subsystem except the SFE where no measurement of water usage was made. In each case, the mass flow into the subsystem was greater than the mass flow out, leaving a certain percentage unaccounted for. The Molecular Sieve subsystem balanced the best, with 6.5 percent of the input mass unaccounted, while the Sabatier subsystem balanced the worst, with 8.6 percent of the input mass unaccounted for. Explanations for each subsystem are in the sections that follow.

8.1 TIMES

The TIMES process a total of 83.50 lb of pretreated urine/deionized water mixture during the EMCT. A total of 89.17 lb of the input mixture was actually provided, but 5.67 lb of this was required for sampling. A total of 76.89 lb of the input mixture was accounted for leaving 6.61 lb or 7.9 percent of the total input unaccounted. Shortly after the test began, the data link between the data acquisition computer and the TIMES product water and brine tanks failed. This could be a source of error as the scale data was taken manually for the remainedr of the test. As Figure 8-1 shows, approximately 9.64 lb of brine was collected, 29.58 lb of product water was diverted to the SFE, 0.166 lb of water was collected in the vacuum moisture trap, 27.04 lb was used for sampling, and a delta of 10.46 lb of product water was left in the product tank (the tank was partially full at the beginning of the test).

8.2 Molecular Sieve

Approximately 40.88 lb of carbon dioxide was injected into the simulator with 39.10 lb of this processed by the Molecular Sieve and the additional 1.78 lb remaining in the simulator at the conclusion of the test. The Molecular Sieve concentrated 36.56 lb of carbon dioxide during the EMCT with a net of 0.12 lb remaining in the accumulator. The amounts of nitrogen and oxygen in the product stream were computed from flow measurements and post test gas analyses. All but 6.5 percent of the Molecular Sieve input carbon dioxide was accounted for. Some of the unaccounted mass was used in sampling.

8.3 SFE

A complete mass balance was not possible on the SFE since no measurement was made of the input water electrolyzed. From the TIMES measurements it was possible to determine that approximately 29.58 lb of water was transferred to the SFE/TSA input water tank. However, this tank was charged with water from a previous TIMES run at the beginning of the EMCT making it impossible to determine how much was actually electrolyzed. Both the SFE hydrogen and oxygen output streams contained water vapor. The mass of water vapor in each stream was calculated from dewpoint sensors located in the product lines. The mass of oxygen to hydrogen electrolyzed was computed to be 7.19 which is not stoichiometric (stoichiometric = 8.0).

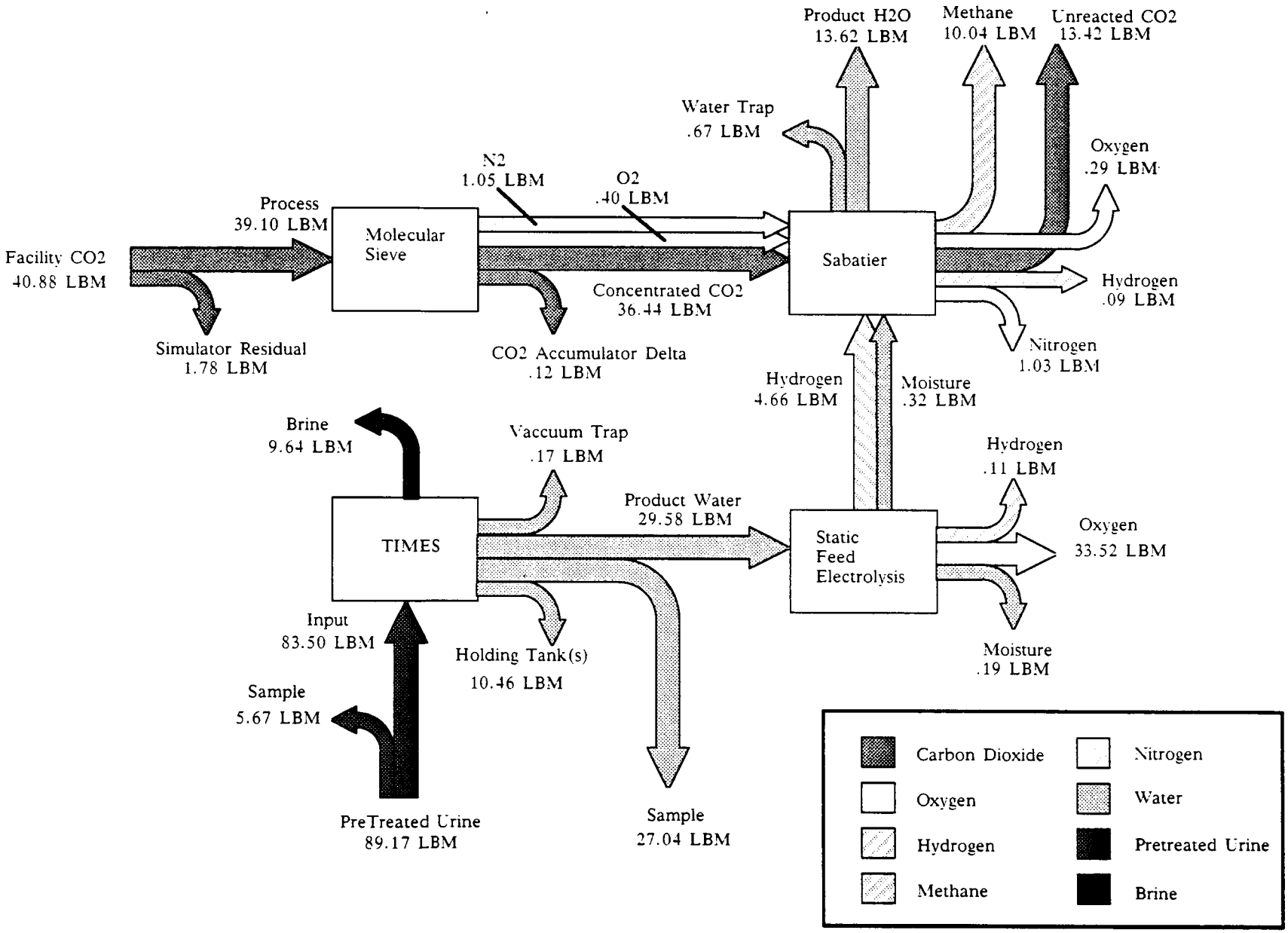

Figure 8-1. EMCT mass balance.

8.4 Sabatier

As shown in Figure 8-1, the Sabatier subsystem processed a total of 42.87 lb of carbon dioxide and hydrogen with trace amounts of nitrogen, oxygen, and water. This mixture was reacted into approximately 39.16 lb of methane, water, carbon dioxide (unreacted), and small amounts of oxygen, nitrogen, and hydrogen with 8.6 percent of the input mass unaccounted for. The Sabatier gas composition was found by applying the results of a post test volumetric lab analysis to the Sabatier vent flow measurement. The actual composition of gases in the Sabatier product stream probably varied throughout the test and since the lab analysis was at a fixed point in time during the test, this could account for much of the error. It is interesting to note that the estimated mass of nitrogen into the Sabatier (1.05 lb) is approximately equal to the mass of nitrogen out (1.03 lb), indicating that the nitrogen passed through essentially unreacted. A decrease in mass of oxygen across the Sabatier was also noted, which may indicate that some of the oxygen in the Molecular Sieve product carbon dioxide stream was reduced to water.

9.0 TGA AND GAS SAMPLING RESULTS

The TCCS was intentionally not operated during the test so that any contaminants generated would be allowed to accumulate without removal. An analytical device, the TGA, was operated daily in hopes of monitoring any contaminant buildup inside the module. A sample of the chamber environment was pulled each day of the test and run through the gas chromatograph/mass spectrometer TGA for analysis. No contaminants were detected by the TGA for any day of the test. This was a reasonable result considering the large volume of the module, the virtually all-metal composition of the subsystems, and the near ambient temperature and pressure of the chamber environment. In addition, a grab sample was taken of the chamber inside air near the end of the test and results of its analysis indicated no detectable levels of contaminants as well (see Table 9-1).

Grab samples of subsystem process gases were taken about 110 to 115 hr into the test using 5-ply, 15-liter collection bags. Samples were taken of the 4BMS product carbon dioxide, the SFE product hydrogen and oxygen, the Sabatier vent gas, and the internal chamber air. Results of analysis of these samples are presented in Table 9-1. Each of the sample results are discussed further as applicable in the individual subsystem sections.

For the EMCT, a new method involving a Draeger tube device was used to analyze for water vapor in the samples. Previously, no method had been available to quantify water vapor in a grab-type sample. The levels, however, should have been in the percentage, rather than ppm range. It is felt that any method used for a grab sample probably will not be accurate because of condensation in the bag, and different temperatures at sampling and analysis. For future testing, an in-line real-time measurement will be used to quantify water vapor in product gases.

TABLE 9-1
GAS SAMPLE RESULTS
EXTENDED METABOLIC CONTROL TEST

Sample	%CO_2	%O_2	%N_2	%H_2	%CH_4	%H_2O
4BMS CO_2	92.7	1.4	4.2			6 ppm
SFE H_2		2.8	3.4	88.9		28 ppm
SFE O_2		96.1	1.9	0.6		70 ppm
Sabatier Vent	29.9	0.9	3.6	4.1	61.5	34 ppm
Chamber air	no detectable organics					

10.0 WATER SAMPLING RESULTS

Water quality analyses were conducted by two independent laboratories: the Environmental Laboratories of Boeing Aerospace Company in Huntsville, Alabama, and the Quality Evaluation Laboratory of Martin Marietta Space Systems in New Orleans, Louisiana. Laboratory quality control and sampling techniques were the same as those reported for the ECLSS Simplified Integrated Test. Analytical methodologies used by each laboratory are listed in Table 10-1.

Each laboratory conducted physical, chemical, and microbiological analyses of five different process liquids: pretreated urine, non-post-treated TIMES distillate, post-treated TIMES distillate, TIMES brine, and Sabatier product water. As described in Section 5.1.3.3, all samples, except those of the post-treated distillate, represent aggregate samples taken from the respective facility tanks. Post-treated distillate samples were collected directly from the post-treatment module effluent. Results from each laboratory for the five fluids are listed in Tables 10-2 through 10-4. All samples were collected on the morning of November 23, the second to last day of the test.

Comparison of the data from each laboratory shows that the agreement between respective data points was generally fair. Disagreement was generally the greatest in the comparative data for the TIMES brine which is understandable considering the extremely heterogeneous nature of that fluid. However, there was also a degree of disagreement in the comparative analyses of non-post-treated and post-treated distillates and Sabatier water. In general, the level of data agreement in these fluids was expected to be high given their relatively dilute and homogeneous nature.

Of particular interest are the comparative analyses of conductivity and total organic carbon (TOC) since those two parameters are widely used as general indicators of water quality. Conductivity results were consistently and significantly higher in the samples analyzed by Martin Marietta. The discrepancies are assumed not to be the result of differences due to methodology since

TABLE 10-1 ANALYTICAL METHODS

PARAMETER	BOEING Method Ref.	BOEING Method Description	MARTIN Method Ref.	MARTIN Method Description
PHYSICAL				
pH	EPA 150.1	Electrochemical	EPA 150.1	Electrochemical
Color	EPA 110.2	Colorimetric	EPA 110.2	Colorimetric
Turbidity	EPA 180.1	Spectrometric	EPA 180.1	Spectrometric
Conductivity	EPA 120.1	Electrochemical	EPA 120.1	Electrochemical
Total Solids	EPA 160.3	Gravimetric	EPA 160.3	Gravimetric
Total Sus Solids	EPA 160.1	Gravimetric	EPA 160.1	Gravimetric
Total Dis Solids	EPA 160.2	Gravimetric	EPA 160.2	Gravimetric
ELEMENTS				
Arsenic	EPA 200.7	ICP	EPA 206.3	AAS/Hydride
Barium	EPA 200.7	ICP	EPA 200.7	ICP
Cadmium	EPA 200.7	ICP	EPA 200.7	ICP
Calcium	EPA 200.7	ICP	EPA 200.7	ICP
Copper	EPA 200.7	ICP	EPA 200.7	ICP
Iron	EPA 200.7	ICP	EPA 200.7	ICP
Lead	EPA 200.7	ICP	EPA 200.7	ICP
Magnesium	EPA 200.7	ICP	EPA 200.7	ICP
Manganese	EPA 200.7	ICP	EPA 200.7	ICP
Mercury	EPA 245.1	AAS/Cold Vapor	EPA 245.1	AAS/Cold Vapor
Molybdenum	EPA 200.7	ICP	EPA 200.7	ICP
Nickel	EPA 200.7	ICP	EPA 200.7	ICP
Potassium	EPA 200.7	IC	EPA 200.7	ICP
Selenium	EPA 200.7	ICP	EPA 270.3	AAS/Hydride
Silver	EPA 200.7	ICP	EPA 200.7	ICP
Sodium	EPA 200.7	IC	EPA 200.7	ICP
Zinc	EPA 200.7	ICP	EPA 200.7	ICP
IONS				
Chloride	EPA 300.0	IC	EPA 300.0	IC
Fluoride	EPA 300.0	IC	EPA 300.0	IC
Nitrate	EPA 300.0	IC	EPA 300.0	IC
Sulfate	EPA 300.0	IC	EPA 300.0	IC
Ammonia	EPA 300.7	IC	SM 417.8	Colorimetric
Cyanide	HACH	Colorimetic	EPA 335.3	Colorimetric
Iodine	NA	NA	SM 415	Colorimetric
Phosphate	EPA 300.0	IC	NA	NA

TABLE 10-1 ANALYTICAL METHODS (CONT'D)

PARAMETER	BOEING Method Ref.	BOEING Method Description	MARTIN Method Ref.	MARTIN Method Description
ORGANICS				
TOC	EPA 415.2	UV&persulfate/IR	EPA 415.2	UV&persulfate/IR
TOA	NA	NA	SM 504.A	Titration
Urea	In-House	IC	Sig 640	Colorimetric
Chloroform	NA	NA	EPA 624	GC/MS
Acetone	NA	NA	in-house	HS/GC/FID
Ethanol	NA	NA	in-house	HS/GC/FID
Isopropanol	NA	NA	in-house	HS/GC/FID
Methanol	NA	NA	in-house	HS/GC/FID
Total Phenols	SM 510	Colorimetric	EPA 420	Colorimetric
MICROBIOLOGICALS				
Total Bacteria	NA	NA	SM 900	NA
Total Anaerobes	NA	NA	SM 900	NA
Total Yeast/Mold	NA	NA	SM 900	NA
Gram +	NA	NA	SM 900	NA
Gram -	NA	NA	SM 900	NA
Heterotrophs	SM	PCA	NA	NA
Heterotrophs	SM	R2A	NA	NA

NA-Not Applicable, specified analysis was not conducted

both laboratories used the same standardized method (EPA 120.1). The discrepancies also do not appear to be the result of clear differences in the chemical composition of the samples analyzed by the respective laboratories. Conductivity is generally proportional to the concentration of total solids which itself is a general measure of overall chemical composition. Comparison of the analyses does not reveal discrepancies in the total solids results (and hence, overall chemical composition) of sufficient magnitude to account for the noted discrepancies in conductivities.

Discrepancies in the comparative data for TOC may be attributable to different performance capabilities of the laboratory instruments used. Martin Marietta used a Dohrman model DC-80 analyzer, whereas Boeing used an Astro model 2001. Both analyzers incorporate UV-enhanced persulfate oxidation and infrared detection.

One of the difficulties in comparing two sets of analyses from different laboratories is that there is often not enough data to clearly show which, if either, of the data sets is closer to the actual data. With only two analyses there is no third independent measurement which may be used to gain

TABLE 10-2 RESULTS OF TIMES PRODUCT WATER

Sample date 11-23-87
MM-Martin Marietta Corp.
B-Boeing Aerospace Comp.

		TIMES RAW Distillate		TIMES (Post-Treated) Distillate	
Physical		MM	B	MM	B
pH	(pH)	3.4	3.24	4.4	4.16
Color	(Pt/Co)	3.0	0	0	0
Turbidity	(NTU)	0.58	0.34	0.37	0.34
Conductivity	(umho/cm)	153	17.8	115	19.3
Total Solids	(ppm)	61	21	90	92
Total Sus. Solids	(ppm)	46	21	2	<1
Total Dis. Solids	(ppm)	15	<1	88	92
ELEMENTS					
Arsenic	(ppb)	<5.0	<23	<5.0	<23
Barium	(ppm)	<0.02	0.004	<0.02	<0.002
Cadmium	(ppm)	0.02	0.002	0.03	<0.001
Calcium	(ppm)	0.10	0.235	0.11	0.425
Chromium	(ppm)	<0.025	0.01	<0.025	<0.005
Copper	(ppm)	0.05	0.041	0.05	0.150
Iron	(ppm)	0.35	0.345	0.49	0.759
Lead	(ppm)	0.19	0.013	0.20	0.035
Magnesium	(ppm)	0.06	0.058	0.15	0.044
Manganese	(ppm)	0.13	0.003	0.12	0.006
Mercury	(ppb)	<5.0	<0.4	<5.0	<0.4
Molybdenum	(ppm)	<0.02	<0.008	0.02	<0.001
Nickel	(ppm)	0.06	0.062	<0.02	<0.014
Potassium	(ppm)	1.27	1.94	0.10	1.18
Selenium	(ppb)	<5.0	<14	<5.0	<14
Silver	(ppm)	<0.02	<0.016	<0.02	<0.016
Sodium	(ppm)	1.19	2.64	20.4	34.16
Zinc	(ppm)	<0.03	0.043	1.30	0.747
IONS					
Chloride	(ppm)	3.24	3.17	32.4	28.9
Fluoride	(ppm)	9.0	.1605	13.9	<0.025
Nitrate	(ppm)	<0.5	<.125	<0.5	<0.125
Sulfate	(ppm)	2.95	2.66	<0.5	2.18
Ammonia	(ppm)	<0.25	2.47	<0.25	<0.050
Cyanide	(ppm)	<0.02	0.038	<0.02	0.067
Iodine	(ppm)	<0.5	----	<0.5	----
ORGANICS					
TOC	(ppm)	106	59.3	76	27.3
TOA	(ppm)	--	----	--	----
Urea	(ppm)	<150	----	<150	----
Volatiles					
Chloroform	(ppb)	15	----	15	----
Miscellaneous					
Acetone	(ppm)	<1.0	----	<1.0	----
Ethanol	(ppm)	10.2	----	22.0	----
Isopropanol	(ppm)	<1.0	----	<1.0	----
Methanol	(ppm)	<5.0	----	<5.0	----
Total Phenols	(ppb)	110	678	<5.0	11
MICROBIOLOGICALS					
Tot.Bacteria	(CFU)	4/ml	----	2000/ml	----
Tot.Anaerobic	(CFU)	<1/10ml	----	28/ml	----
Tot.Yeast/Mold	(CFU)	<1/10ml	----	<1/10ml	----
Gram Negative	(CFU)	3/ml	----	----	----
Gram Positive	(CFU)	1/ml	----	2000/ml	----
Heterotrophs	(CFU/ML)	----	1.20x10e2/ 10ml	----	4.65x10 e3/ml

TABLE 10-3 RESULTS OF TIMES BRINE & PRETREATED URINE

Sample Date 11-23-87
MM-Martin Marietta Corp.
B-Boeing Aerospace Comp.

		TIMES BRINE		TIMES PRETREAT-URINE	
Physical		MM	B	MM	B
pH	(pH)	2.8	2.89		
Color	(Pt/Co)	3250	4500		
Turbidity	(NTU)	276	106.8		
Conductivity	(umho/cm)	>20,000	28200	10,500	----
Total Solids	(ppm)	71,394	60324	21,604	17,548
Total Sus. Solids	(ppm)	282	34	92	52
Total Dis. Solids	(ppm)	71,112	60290	21,512	17,496
ELEMENTS					
Arsenic	(ppb)	<5.0	3100		
Barium	(ppm)	0.08	<0.002		
Cadmium	(ppm)	0.23	0.025		
Calcium	(ppm)	372	65.05		
Chromium	(ppm)	0.59	0.3		
Copper	(ppm)	1.31	1		
Iron	(ppm)	1.14	3.05		
Lead	(ppm)	2.21	9.4		
Magnesium	(ppm)	257	49.17		
Manganese	(ppm)	0.85	<0.001		
Mercury	(ppb)	<5.0	10.7		
Molybdenum	(ppm)	0.36	<0.001		
Nickel	(ppm)	1.14	1.275		
Potassium	(ppm)	6612	<.1		
Selenium	(ppb)	<5.0	29250		
Silver	(ppm)	<0.02	<0.016		
Sodium	(ppm)	5951	2.77		
Zinc	(ppm)	1.20	1.525		
IONS					
Chloride	(ppm)	12400	14.51		
Fluoride	(ppm)	<500	<.025		
Nitrate	(ppm)	<500	<.125		
Sulfate	(ppm)	18000	6.95		
Ammonia	(ppm)	730	171		
Cyanide	(ppm)	0.05	----		
Iodine	(ppm)	----	----		
ORGANICS					
TOC	(ppm)	17685	----		
TOA	(ppm)	----	----		
Urea	(ppm)	1710	----		
Volatiles					
Chloroform	(ppb)	70	----		
Miscellaneous					
Acetone	(ppm)	<1.0	----		
Ethanol	(ppm)	1.5	----		
Isopropanol	(ppm)	<1.0	----		
Methanol	(ppm)	<5.0	----		
Total Phenols	(ppb)	8140	----		
MICROBIOLOGICALS					
Tot.Bacteria	(CFU)	<1/ml	----		
Tot.Anaerobic	(CFU)	<1/10ml	----		
Tot.Yeast/Mold	(CFU)	<1/10ml	----		
Gram Negative	(CFU)	<1/ml	----		
Gram Positive	(CFU)	<1/ml	----		
Heterotrophs	(CFU/ML)	----	----		

TABLE 10-4 RESULTS OF SABATIER WATER

Sample date 11-23-87
MM-Martin Marietta Corp.
B-Boeing Aerospace Comp.

		SABATIER WATER	
Physical		MM	B
pH	(pH)	6.6	7.06
Color	(Pt/Co)	0	0
Turbidity	(NTU)	6.6	7.1
Conductivity	(umho/cm)	250	18.5
Total Solids	(ppm)	35	25
Total Sus. Solids	(ppm)	3	<1
Total Dis. Solids	(ppm)	32	25
ELEMENTS			
Aluminium	(ppm)	0.01	0.037
Arsenic	(ppb)	----	----
Barium	(ppm)	----	----
Cadmium	(ppm)	0.02	0.003
Calcium	(ppm)	----	----
Chromium	(ppm)	<0.01	0.008
Copper	(ppm)	0.04	0.502
Iron	(ppm)	0.30	0.416
Lead	(ppm)	----	----
Magnesium	(ppm)	0.01	0.418
Manganese	(ppm)	----	----
Mercury	(ppb)	----	----
Molybdenum	(ppm)	0.03	0.013
Nickel	(ppm)	0.05	0.053
Potassium	(ppm)	----	1.28
Ruthenium	(ppm)	<0.04	----
Selenium	(ppb)	----	----
Silver	(ppm)	----	----
Sodium	(ppm)	----	2.97
Zinc	(ppm)	10.3	2.165
IONS			
Chloride	(ppm)	0.65	14.43
Fluoride	(ppm)	<0.5	0.246
Nitrate	(ppm)	<0.5	<.125
Sulfate	(ppm)	<0.5	1830
Ammonia	(ppm)	29.7	3.52
Cyanide	(ppm)	----	----
Iodine	(ppm)	<0.5	----
ORGANICS			
TOC	(ppm)	14	18
TOA	(ppm)	----	----
Urea	(ppm)	----	----
Volatiles			
Chloroform	(ppb)	----	----
Miscellaneous			
Acetone	(ppm)	----	----
Ethanol	(ppm)	----	----
Isopropanol	(ppm)	----	----
Methanol	(ppm)	----	----
Total Phenols	(ppb)	----	----
MICROBIOLOGICALS			
Tot.Bacteria	(CFU)	350/ml	----
Tot.Anaerobic	(CFU)	----	----
Tot.Yeast/Mold	(CFU)	----	----
Gram Negative	(CFU)	----	----
Gram Positive	(CFU)	----	----
Heterotrophs	(CFU/ML)	----	2.05x10e3/ml

insight relative to which analysis is more representative of the true sample. In situations such as this, it is somewhat useful to evaluate the consistency of any one set of data against itself. Several techniques exist for checking the internal consistency of data obtained from analyses conducted on a given sample of water (reference Standard Methods for the Examination of Water and Wastewater, 17th edition, currently in preparation). These checks include: (1) anion-cation balance, and (2) calculation of total dissolved solids and comparison of the result to the measured value. In addition, calculation of total organic carbon and comparison of the result to the measured TOC provides an indication of the level of organics that are present in the sample but which have not been identified. Each of these internal checks are discussed in the following sections. Since the checks are most valid for dilute solutions they will be used to evaluate the internal consistency of the non-post-treated and post-treated distillates and of Sabatier water.

10.1 Anion – Cation Balance

In an electrically neutral solution, the anion and cation sums (expressed as milliequivalents per liter) must balance. Sums which are not balanced usually indicate that one or more of the elemental analyses is not correct or that additional ionic contaminants are present in the solution but have not been otherwise detected. The balance is checked by the following relation:

$$\% \text{ difference} = 100 \times \frac{\Sigma \text{ cations} - \Sigma \text{ anions}}{\Sigma \text{ cations} + \Sigma \text{ anions}} \qquad (10.1)$$

Acceptability is determined according to the following criteria:

anion sum (meq/l)	acceptable % difference
0 - 3.0	+/– 0.2
3.0 - 10.0	+/– 2
20.0 - 800	+/– 5

Table 10-5 summarizes the balances calculated for each of the three waters checked. For elements with more than one oxidation state, the state used to calculate the corresponding equivalent weight is listed under the comments.

Inspection of Table 10-5 shows that none of the six analyses conducted by the two laboratories combined yielded data for which an acceptable ionic balance could be calculated. In addition, in five of the six analyses the anion sum was signficantly greater than the cation sum. It is also important to note that analyses for carbonate and bicarbonate anions were not conducted on these water samples, yet such anions are most likely present in these solutions due to normal absorption of carbon dioxide from the atmosphere and, in the case of the Sabatier, the relatively high concentrations of carbon dioxide existing in the process. Carbonates and bicarbonates would increase the discrepancies between anion and cation sums beyond that indicated in Table 10-5. Organic acids (which were also not analyzed for in these samples) would also have the same effect.

TABLE 10-5: Anion-Cation Balances of Water Samples

Ions	eq.wt.	NON-POST TREATED DISTILLATE				POST TREATED DISTILLLATE				SABATIER PRODUCT WATER				comments
		BAC		MMC		BAC		MMC		BAC		MMC		
		mg/l	meq/l	mg/l	meq/l	mg/l	meq/l	mg/l	meq/l	mg/l	meq/l	mg/l	meq/l	
Anions														
ammonia	17.0	2.47	0.145	ND	0	ND	0	ND	0	3.52	0.207	29.7	1.747	
chloride	35.5	3.17	0.089	3.24	.0.91	28.9	0.814	32.4	0.913	14.43	0.406	0.65	0.018	
cyanide	26.0	0.038	0.001	ND	0	0.067	0.003	ND	0	NA	–	NA	–	
fluoride	19.0	0.1605	0.008	9.0	0.474	ND	0	13.9	0.732	0.246	0.013	ND	0	
iodide	126.9	ND	0	ND	0	ND	0	ND	0	NA	–	ND	0	
nitrate	20.6	ND	0	ND	0	ND	0	ND	0	ND	0	ND	0	
sulfate	24.0	2.66	0.111	2.95	0.123	2.18	0.091	ND	0	1830	76.25	ND	0	
Subtotal		8.499	0.354	15.190	0.688	31.147	0.908	46.3	1.645	1848	76.876	30.35	1.765	
Cations														
aluminum	9.0	NA	–	NA	–	NA	–	NA	–	0.037	0.004	0.01	0.001	
arsenic	15.0	ND	0	ND	0	ND	0	ND	0	NA	–	NA	–	As (IV)
barium	68.6	0.004	<0.001	ND	0	ND	0	ND	0	NA	–	NA	–	
cadmium	56.2	0.002	<0.001	0.02	<0.001	ND	0	0.03	0.001	0.003	<0.001	0.02	<0.001	
calcium	20.0	0.235	0.012	0.10	0.005	0.425	0.021	0.11	0.006	NA	–	NA	–	
chromium	17.3	0.01	0.001	ND	0	ND	0	ND	0	0.008	<0.001	ND	0	Cr (III)
copper	31.8	0.041	0.001	0.05	0.002	0.150	0.005	0.05	0.002	0.502	0.016	0.04	0.001	Cu (II)
iron	18.6	0.345	0.019	0.35	0.019	0.759	0.041	0.49	0.026	0.416	0.022	0.30	0.016	Fe (III)
lead	51.8	0.013	<0.001	0.19	0.004	0.035	0.001	0.20	0.004	NA	–	NA	–	Pb (III)
magnesium	17.2	0.058	0.003	0.06	0.003	0.044	0.003	0.15	0.009	0.418	0.024	0.01	0.001	Mn (IV)
manganese	13.7	0.003	<0.001	0.13	0.009	0.006	<0.001	0.12	0.009	NA	–	NA	–	Hg (II)
mercury	100.3	ND	0	ND	0	ND	0	ND	0	NA	–	NA	–	Mo (IV)
molybenum	24.0	ND	0	ND	0	ND	0	0.02	0.001	0.013	0.001	0.03	0.001	Ni (II)
nickel	29.4	0.062	0.002	0.06	0.002	ND	0	ND	0	0.053	0.002	0.05	0.002	
potassium	39.1	1.94	0.050	1.27	0.032	1.18	0.030	0.10	0.003	1.28	0.033	NA	–	Se (IV)
ruthenium	50.5	NA	–	NA	–	NA	–	NA	–	NA	–	ND	0	
selenium	19.7	ND	0	ND	0	ND	0	ND	0	NA	–	NA	–	
silver	107.9	ND	0	ND	0	ND	0	ND	0	NA	–	NA	–	
sodium	23.0	2.64	0.115	1.19	0.052	34.16	1.485	20.4	0.887	2.97	0.129	NA	–	
zinc	32.7	0.043	0.001	ND	0	0.747	0.023	1.3	0.040	2.165	0.066	10.3	0.315	
Subtotal		5.396	0.204	3.42	0.128	37.506	1.609	22.970	0.988	7.865	0.297	10.76	0.337	
% difference			-26.9		-67.6		27.8		-25.0		-99.2		-67.9	per equation 10.1
acceptable % difference			+/- 0.2		+/- 0.2		+/- 0.2		+/- 0.2		+/- 2.0		+/- 0.2	

ND = NONE DETECTED NA = NOT ANALYZED

There are three possible causes for the discrepancies: (1) one or more of the anions may have been consistently measured too high by both laboratories; (2) one or more of the cations may have been consistently measured too low by both laboratories; or, (3) there may have been one or more cations present in solution that were not otherwise identified.

One probable cation is the hydrogen ion which was not included in the calculations of Table 10-5. In the case of the non-post-treated TIMES distillate, MMC measured a pH of 3.4 which corresponds to a hydrogen ion concentration of 0.398 meq/l. The calculated ion balance for the MMC analysis would then result in a percentage difference of -13.3 percent. Similar adjustments to the other five analyses also fail to bring the corresponding balances into the range of acceptability.

10.2 Comparison of Measured Versus Calculated Total Dissolved Solids

A second check for internal consistency is the comparison of the total dissolved solids (TDS) concentrations measured in the laboratories to those calculated from the individual contaminant measurements made on the same sample. The criteria for acceptability is generally given by:

$$1.0 < \frac{\text{measured TDS}}{\text{calculated TDS}} < 1.2 \qquad (10.2)$$

The TDS concentration is typically calculated from the concentrations of individual ionic contaminants. Table 10-6 shows the resulting comparison. The calculated TDS values were obtained from the appropriate subtotals in Table 10-5, expressed in mg/l. Inspection of Table 10-6 shows that none of the six analyses satisfies the acceptability criteria.

Several points are worth noting. First, this method accounts only for the ionic contaminants listed in Table 10-5. The contributions to the calculated TDS of the various nonionic contaminants, predominantly organic, are not included. Secondly, it is typically expected that the measured TDS will exceed the calculated TDS due to the likelihood of the presence of dissolved contaminants which are not identified and, therefore, are not included in the calculated TDS. However, Table 10-6 shows that in three of the four analyses conducted, the opposite occurred; i.e., the calculated TDS exceeds the meaured TDS. It is likely that this discrepancy is attributable to the difficulty in obtaining accurate TDS measurements, especially in the low ranges of concentrations seen here. Accurate measurements of low TDS concentrations will typically require larger sample volumes than were possible to use in this test. And finally, it is believed that the extremely high sulfate concentration leading to the similarly high calculated TDS for Sabatier water represents an undetermined error.

10.3 Comparison of Measured Versus Calculated TOC

Comparison of the total organic carbon determined by oxidation of the organics and quantification of the byproduct carbon dioxide to that calculated by summing up the carbon contribution of each of the individual organics identified can be used as an indication of the extent of organic contamination that is of essentially unknown identity. For the non-post-treated and post-treated TIMES

TABLE 10-6: TOTAL DISSOLVED SOLIDS (TDS) COMPARISONS

	NON-POST TREATED DISTILLATE		POST TREATED DISTILLATE		SABATIER WATER	
	BAC	MMC	BAC	MMC	BAC	MMC
MEASURED (TDSm)	ND	15	92	88	25	32
CALCULATED (TDSc)	13.895	18.610	68.65	69.27	1856	41.11
RATIO (TDSm/TDSc)	-	0.806	1.34	1.27	0.013	0.78

Acceptability criteria : 1.0 < ratio <1.2

distillates and TIMES brine (the only three fluids for which detailed organic analyses were conducted), only 5.02 percent, 15.09 percent,and less than 1 percent of the total organic carbon is accounted for. The extent of unaccounted organics highlights the need for the development and application of specialized analytical methodologies for the analysis of these and similar ECLSS waste and product streams. Traditional standard methods optimized for the identification of priority pollutants, industrial by-produts, etc., are not suitable for complete assessment of ECLSS waters.

11.0 CONCLUSIONS

The space station ECLSS EMCT was the final test of the ECLS phase II system test program. Two previous phase II tests, the SIT and the MCT, were conducted primarily to verify proper system operation. The EMCT was designed to build upon the previous tests in that it was to be longer in duration allowing observations about system operation under steady state conditions and to provide an opportunity for a system level mass balance. The SIT and EMCT were each approximately 50 hr in duration with the EMCT about three times as long.

Based upon the results of the previous system tests, the goal of achieving stable system operation for six to seven days was an ambitious one. Each of the previous tests had been aborted during startup attempts and experienced potentially serious anomalies during operation. However, the EMCT system test configuration reflected six months of refinement from the original configuration tested under the SIT, including several major subsystem improvements. The Molecular Sieve, for instance, had undergone a major rework with a complete redesign and replacement of the sorbent bed control valves. The refinements worked as over 147 hr of integrated operation were accumulated during the EMCT. Due to several Molecular Sieve controller anomalies, this did not represent 147 continuous hours of integrated operation, but the results were nonetheless encouraging. The other three ECLS subsystems operated over the duration of the test with only minor anomalies reported. Within 24 hr after the start of the test, several key measurements, such as the simulator partial pressure of carbon dioxide and the simulator dewpoint, reached steady state. These were important indicators as they reflected the performane of the Molecular Sieve's desiccant and CO_2 sorbent beds and aside from operating the TIMES in a batch processing mode, the Molecular Sieve was the only cyclic subsystem

in the EMCT test configuration. Both of these measurements were "upset" by the two previously documented Molecular Sieve failures at 39 hr and 116 hr. The CO_2 partial pressure required approximately the same time constant (~20 hrs) to return to steady state after each failure while the simulator dewpoint had a much quicker response time. Other measurements, such as the bulk simulator temperature and pressure, required several 24-hr cycles before a determination of stability could be made. Measurements like the bulk simulator temperature and pressure appeared to be influenced greatly by factors external to the simulator, such as the chiller supply temperature to the simulator heat exchanger and the simulator external temperature and barometric presure. One way to improve the stability of the simulation is to reduce the impact of transient non-flight-like boundary conditions upon the test configuration. The EMCT stability data should provide excellent background data for future longer duration tests or tests where transient metabolic loads are imposed.

Another goal of the EMCT was to determine a system level mass balance. It was necessary to operate the system for an extended period of time in order to conduct the mass balance under boundary conditions that were as realistic as possible. A mass balance was conducted on each of the ECLS subsystems using available flow measurements, weight scale readings, and post-test laboratory determinations. The results varied between subsystems with 6 to 9 percent of a subsystem's input mass unaccounted for in the output streams. There are several explanations for the mass balance discrepancies. In the case of the TIMES, it was necessary to reconstruct weight scale information from data recorded manually during the test as the link between the scales and the data acquisition system failed early in the test. As the scale data was manually recorded once every hour, this led to some assumptions and interpretations about the actual tank mass during the numerous tank refills, brine dumps, and samplings. To improve the system level mass balance it will be essential to provide real time measurement of fluids contained in waste and product water tanks. For each of the air revitalization subsystems, total mass flow in or out of a gas was omputed by integrating the appropriate flow measurement over the duration of the test. The actual composition of many of the gas streams was assumed to be constant over the duration of the test as composition data was available only at a fixed point in time (the time when samples were taken). In several cases, when a real time composition measurement was available in a stream, there was disagreement with the laboratory analysis. Mass balance determination is one facet of the CMIF test program that will require improvement in future test phases. A verifiable mass balance will become increasingly important as more flight-like systems are tested and evaluated.

The CMIF ECLS test program is oriented to evolving to a flight-like ECLS simulation. The EMCT represented several milestones along the path to this goal. First of all, the EMCT provided the first experience with extended-duration ECLS testing. This test demonstrated that it is possible to operate and maintain an integrated ECLS system, even through anomalies and failures, for an extended period of time. Secondly, the EMCT provided much baseline data about the stability of an ECLS system that will be used in preparation for future long-duration tests and tests with transient metabolic loads imposed. The EMCT data will also provide insight about the dynamic response time of an ECLS system. Finally, the EMCT pointed out what developments and improvements are needed to conduct future integrated tests with a verifiable system level mass balance.

APPENDIX A

EXTENDED DURATION METABOLIC CONTROL TEST LOG

Wednesday 11/18/87

Elapsed Time	*Real Time*	*Person*	*Entry*
00.00	1:00 pm	Schunk	SCATS is on (Data Base = Z111813.A03)
00:05	1:05 pm	Schunk	SFE PDU on line and recording
00:10	1:10 pm	Schunk	TIMES on
00:17	1:17 pm	Schunk	SFE on
00:18	1:18 pm	Schunk	Molecular Sieve on
00:41	1:41 pm	Schunk	Sabatier on
02:25	3:25 pm	Schunk	Simulator door closed
02:26	3:26 pm	Schunk	Sabatier operating on SFE hydrogen
02:27	3:27 pm	Schunk	SFE O2 output switch from vent to internal simulator
02:28	3:28 pm	Schunk	Bunn Oxygen Concentrator on
02:30	3:30 pm	Schunk	CO2 input switched from Molecular Sieve inlet to simulator
02:32	3:32 pm	Schunk	CO2 flow increased to 9 man level, FF15 set to 1.5 lb/day
02:50	3:50 pm	Davis	Erratic behavior on ST03
03:30	4:30 pm	Davis	TIMES shutdown (planned)
04:00	5:00 pm	Davis	Simulator ppO2 at 22.53%
05:00	6:00 pm	Davis	Simulator ppO2 at 22.54%, Low CO2 holding tank pressure (15.24 psig), TIMES brine dump (FS03=.06 lb) *(NOT CONFIRMED)*
07:40	8:40 pm	Davis	Bunn O2 removal rate increased to 7 lb/day to match O2 removal
08:01	9:01 pm	Davis	FF05 (SFE O2 flow) reading is increasing
09:10	10:10 pm	Davis	FF05 trending back down

Thursday 11/19/87

Elapsed Time	*Real Time*	*Person*	*Entry*
13:10	2:10 am	Wilkes	FH07 continues to read high at 6000 ppm
14:00	3:00 am	Wilkes	Data plotting terminal "locked up"
18:50	7:50 am	Schunk	CO2 inlet flow reduced to 6.356 lb/day, Bunn removal rate reduced
19:00	8:00 am	Schunk	TIMES powered up
23:41	12:41 pm	Schunk	TIMES shut down
24:12	1:12 pm	Schunk	Bunn removal rate at 5.8 lb/day
24:27	1:27 pm	Schunk	Opened valve to take TGA sample
25:55	2:55 pm	Davis	Bunn removal rate reduced to 5.6 lb/day
28:05	5:05 pm	Davis	Simulator PPO2 seems to be balancing better
30:11	7:11 pm	Davis	Simulator PPO2 holding at 21.86%
31:18	8:18 pm	Davis	Simulator dewpoint approx equals Molecular Sieve coolant temp

Friday 11/20/87

Elapsed Time	*Real Time*	*Person*	*Entry*
37:42	2:45 am	Wilkes	Gauge shows simulator pressure slightly less than ambient

39:10	4:10 am	Wilkes	Molecular Sieve holding tank pressure low at 6.474 psig, Sabatier CO2 inlet flow is low at 2.38 lb/day, and Sabatier bed temperatures are low
39:19	4:19 am	Wilkes	Molecular Sieve appears to have been "stuck" in mode 2, it was manually advanced to mode 3A. The CO2 holding tank pressure is now increasing. The chamber to ambient delta pressure now postive.
40:15	5:15 am	Wilkes	Molecular Sieve is still not changing modes automatically. It was just manually advanced to mode 1A.
43:03	8:03 am	Holder	TIMES on, all subsystems operating nominally with exception of Mo lecular Sieve which is being manually cycled
43:45	8:45 am	Wieland	Molecular Sieve is not cycling automatically. Still being manually advanced through cycle modes. Chamber ppCO2 had increased to approx 4.3 mm Hg, CO2 accumulator pressure and CO2 flow to Sabatier both decreased (to 5.5 psig and 2.1 lb/day, respectively). Mostly recovered within 4 hours. Chamber ppCO2 still high at 3.8 mm Hg and decreasing.
47:23	12:23 pm	Schunk	TIMES scheduled shut down/heater on (standby mode)
48:08	1:08 pm	Schunk	Simulator air sample via TCCS inlet hand valve
48:16	1:16 pm	Schunk	Drained 60 ml water from Sabatier methane vent trap
48:30	1:30 pm	Schunk	Simulator air sample completed
57:08	9:08 pm	Davis	High Simulator to ambient delta pressure 2.13 torr

Saturday 11/21/87

Elapsed Time	*Real Time*	*Person*	*Entry*
67:08	8:08 am	Schunk	TIMES started, unintentional brine dump
67:32	8:32 am	Schunk	50 ml water drained from Sabatier vent trap
69:32	10:34 am	Schunk	Sabatier temperature sensor seems "flaky"
70:42	11:42 am	Schunk	TCCS inlet sample port valve opened for TGA sample
71:00	12:00 pm	Schunk	Bulk air sample completed
71:35	12:35 pm	Schunk	TIMES scheduled shut down
71:45	12:45 pm	Schunk	Drained 30 ml out of TIMES vacuum trap
77:00	6:00 pm	Davis	Sabatier ST03 jumped approx 40 deg F, ST04 remained level
78:00	7:00 pm	Davis	ST03 still high
79:00	8:00 pm	Davis	ST03 lower (800 deg F), simulator temperature (FT16) trending downward
81:00	10:00 pm	Davis	ST03 lower (757 deg F),ST04 holding steady

Sunday 11/22/87

Elapsed Time	*Real Time*	*Person*	*Entry*
86:00	3:00 am	Wilkes	Sabatier moisture trap emptied (63 ml)
91:02	8:02 am	Schunk	TIMES powered up
93:10	10:10 am	Schunk	Add water to SFE TSA from TIMES (conductivity=96 mmho/cm)
95:34	12:34 am	Schunk	TIMES powered down
101:00	6:00 pm	Davis	Simulator bulk air temperature and ppO2 both increasing slightly
101:58	6:58 pm	Davis	SFE O2/H2 delta pressure 1.9 psia, alarm at 2.5 psia

104:05	9:05 pm	Davis	SFE O2/H2 delta pressure 2.0 psia, bulk ppO2 dropping (21.14%)
105:15	10:15 pm	Davis	SFE outlet dewpoint increased to 50 deg F

Monday 11/23/87

Elapsed Time	*Real Time*	*Person*	*Entry*
113:35	6:35 am	Wilkes	Moisture trap ahead of FF03 was drained (63 ml)
113:50	6:50 am	Schunk	Molecular Sieve heater current failure, the unit was powered off and restarted, problem seems to have cleared up
114:55	7:55 am	Schunk	Bunn unit outlet flow reduced from 5.5 lb/day to 5.25 lb/day
114:58	7:58 am	Schunk	TIMES started
115:50	8:50 am	Schunk	Bunn unit flow reduced to 5.22 lb/day
116:40	9:40 am	Schunk	Molecular Sieve timer failure, return to manual cycling operation
119:30	12:30 pm	Schunk	Begin TGA sample
120:00	1:00 pm	Schunk	TIMES scheduled shut down
121:15	2:15 pm	Schunk	Reduce Bunn Flow from 5.25 to 4.75 lb/day
121:20	2:20 pm	Schunk	Reduce GN2 makeup from 1.6 to 1.5 ld/day
121:55	2:55 pm	Davis	Review test log, briefed by Schunk, watch ppO2 and Molecular Sieve parameters
124:03	5:03 pm	Davis	ST03 reading high, 896 deg F
126:05	7:05 pm	Davis	Bulk temperature rising
129:00	10:00 pm	Davis	Sabatier CO2 flow slightly high, seems to be due to high Molecular Sieve accumulator pressure
130:00	11:00 pm	Wilkes	Replaced Davis

Tuesday 11/24/87

Elapsed Time	*Real Time*	*Person*	*Entry*
137:23	6:23 am	Schunk	70 ml of water drained from Sabatier vent
138:40	7:40 am	Schunk	50 ml of water drained from TIMES vacuum trap
138:55	7:55 am	Schunk	TIMES powered up
139:00	8:00 am	Schunk	TIMES warning, HFM evaporation rate low
144:05	1:05 pm	Schunk	TIMES scheduled shut down
148:53	5:53 pm	Davis	T-1 HOUR TO SHUT DOWN!
150:02	7:02 pm	Davis	Begin shut down sequence

7:02 pm Sabatier shut down
7:02 pm SFE shut down
7:13 pm Molecular Sieve shut down

FINAL SCALE READINGS

TIMES product water	64.92 lbs
TIMES waster water	67.70 lbs
TIMES brine	.14 lbs
Sabatier product water	11.28 lbs

150:17	7:17 pm	Davis	Simulator doors opened

APPROVAL

SPACE STATION CMIF EXTENDED DURATION METABOLIC CONTROL TEST FINAL REPORT

By Richard G. Schunk, Robert M. Bagdigian, Robyn L. Carrasquillo, Kathyrn Y. Ogle, and Paul O. Wieland

The information in this report has been reviewed for technical content. Review of any information concerning Department of Defense or nuclear energy activities or programs has been made by the MSFC Security Classification Officer. This report, in its entirety, has been determined to be unclassified.

For JAMES C. BLAIR
Director, Structures and Dynamics Laboratory

☆ U.S. GOVERNMENT PRINTING OFFICE 1989—631-056/00084